

**THE KINETICS OF STEAM GASIFICATION
OF SOUTH AFRICAN COALS.**

by

Rodger Keith Riley (B.Sc.Eng.(Natal, 1982))

Submitted in partial fulfillment of the requirements for the degree
of Doctor of Philosophy in the Department of Chemical Engineering at
the University of Natal, Durban, South Africa.

February 1990.

ABSTRACT.

The prime objective of a current research project at the University of Natal is to develop a novel autothermal fluidised bed coal gasifier which is capable of efficiently producing synthesis quality gas (rich in hydrogen and carbon monoxide) from discard of duff coal resources using air and steam as the reactant gases.

The development of this gasifier was initially motivated to utilise the ever increasing supply of discard coal in South Africa which represents a significant potential source of energy and currently poses severe environmental pollution hazards caused by spontaneous combustion and wind erosion of the discard coal dumps. Recently, however, the gasifier has been considered for the conversion of more general coal resources in an Integrated Coal Gasification Combined Cycle process (IGCC) for the production of electricity.

The knowledge of the kinetics of steam gasification of local coal resources is of vital importance to the design of this gasifier. However, no such kinetic data are available of which the author is aware.

This thesis presents the following contributions to the overall knowledge of the gasifier :

- (a) The development of a microreactor to measure the rate of reaction of the steam gasification of coal-char at

(ii)

temperatures of up to 1000°C and pressures up to 5 bar absolute;

- (b) Kinetic studies using the microreactor on the steam gasification of coal-chars derived from Bosjesspruit and Transvaal Navigation coal samples.

The following principal results were obtained with Bosjesspruit coal-char :

- The rate of steam-char gasification is very sensitive to variations in the temperature of reaction in the range 840°C to 920°C.
- Neither the rate of steam-char gasification nor the product gas composition are affected by the steam partial pressure in the range 1.8 to 4.8 bar absolute;
- The concentrations of the H₂ and CH₄ components of the product gas stream rapidly approached their respective equilibrium compositions, whereas the concentrations of CO and CO₂ gradually approach their respective equilibrium compositions during gasification at a rate which is typical of the stoichiometry of the Boudouard reaction.
- The average product gas composition is independent of the temperature of reaction in the range 840°C to 920°C and is approximately 49% H₂, 32% CO, 17% CO₂ and 2% CH₄ on a molar basis;
- The steam gasification kinetic data are well described by a fundamental Arrhenius-type volumetric reaction model at

(iii)

temperatures of up to 920°C. The value of the activation energy for the reaction is 146 kJ/gmol, which indicates that the gasification kinetics are controlled by the rates of the chemical reactions (ie. $C + H_2O = CO + H_2$ and $C + CO_2 = 2CO$) at temperatures up to 920°C;

- There are no major differences between the kinetics measured for Bosjesspruit coal-char and those reported in the literature for foreign coal-chars.

The experimental results obtained for the steam gasification of char derived from Transvaal Navigation coal show that the concentrations of both the H_2 and the CH_4 in the product gas stream rapidly attain their respective equilibrium values and remain approximately constant throughout gasification, whereas the concentrations of CO and CO_2 gradually approach their respective equilibrium values during the course of gasification and almost attain equilibrium concentrations as the conversion of carbon nears completion. The rate of steam gasification of this char is therefore also controlled by the rate of the Boudouard reaction.

- (c) The mathematical development of a steady-state, one-dimensional compartment model of the gasifier. The model is also presented in the form of a Fortran 77 computer program which is designed to run on a personal computer. The program is capable of simultaneously solving the overall material and energy balances of the gasifier to a tolerance of 1% within 15 minutes when using a microprocessor which operates at 10 Mhz.

- (d) The gasifier simulation program is currently being used in the design of a pilot scale gasifier which is intended to demonstrate the capability of the process on a continuous basis of operation.

- (e) Experimentation on the air-steam gasification of Bosjesspruit coal using a mini-pilot scale gasifier. These experiments have successfully demonstrated the feasibility of the production of a gas stream which is rich in hydrogen and carbon monoxide. The composition of the product gas stream compares well with the predictions of the simulation model of the gasifier.

DECLARATION.

I declare that the entire contents of this thesis represents my own original work, with the exception of those particular cases which are acknowledged accordingly in the text of the thesis. I also declare that this thesis has not been submitted to any other educational institution for the purpose of the awarding of an academic qualification.

A handwritten signature in blue ink, appearing to read 'R.K. Riley', with a horizontal line underneath the name.

R.K. Riley.

(vi)

DEDICATION.

To Hazel, with all my love.

ACKNOWLEDGEMENTS.

The undertaking of the research work reported in this thesis and the compilation of the thesis itself has been greatly assisted by the generous support of many people. It has indeed been an immense privilege for me to have had the opportunity to work on this project. I am sincerely grateful for the invaluable contributions made by the following people towards this work :

- Professor Robin Judd for his enthusiastic promotion of the gasifier research project, his talented scientific advice, his warm encouragement and his thorough supervision;
- Mr Dave Wright for much advice regarding the design of the microreactor, the analysis of the kinetic results and the approach to the mathematical modelling of the gasifier;
- Mr Chris Brouckaert for advice during the troubleshooting of the gasifier simulator computer program;
- Mr Doug Penn for his supervision of the fabrication of the microreactor and of modifications to the mini-pilot scale gasifier;
- Messrs 'Clarry' Clarence, Ken Jack and the late Ian Truter for their expert fabrication and modification of the microreactor and its peripheral components;
- My dear wife, Hazel, for carefully tracing the drawings contained in this thesis from my original sketches, for patiently typing the thesis and for providing me with moral support throughout the course of the project;

- My Father, Mother and Grandmother for their prayers and encouragement;
- My good friend, Mike Baudin, for the loan of his personal computer which was employed extensively in the compilation of this thesis;
- Mr Andrew Holmes and Miss Marie Hetherington for conducting numerous replicate experiments of my work and for conducting some original experiments using the microreactor, under my supervision;
- Mr Ian Henderson for the loan of his mini-fluidised bed in the preparation of char samples;
- SASOL, for the supply of a sample of Bosjesspruit coal;
- The Division of Energy Technology, CSIR, for the supply of a sample of Transvaal Navigation coal;
- AECI, for the use of the non-linear, least squares regression computer software 'SIMPLEX';
- Mr Chris Buckley of the Water Research Commission at the University of Natal for the loan of his computer facilities which enabled the generation of the graphical plots contained in this thesis.

INDEX.

CONTENTS	PAGE
ABSTRACT	i
DECLARATION	v
DEDICATION	vi
ACKNOWLEDGEMENTS	vii
1. INTRODUCTION	1.1
2. LITERATURE SURVEY	2.1
3. THE DESIGN AND TECHNIQUE OF OPERATION OF THE MICROREACTOR FOR THE MEASUREMENT OF THE STEAM GASIFICATION KINETICS OF COAL CHAR	3.1
4. STEAM-CHAR GASIFICATION STUDIES	4.1
5. THE APPLICATION OF THE MEASURED KINETIC DATA FOR STEAM-CHAR GASIFICATION TO THE SIMULATION OF THE JUDD CIRCULATING FLUIDISED BED COAL GASIFIER	5.1
6. RESULTS OF GASIFICATION EXPERIMENTS WITH BOSJESSPRUIT COAL USING THE MINI-PILOT SCALE JUDD GASIFIER AND OF CASE STUDIES OF COMPUTER SIMULATIONS OF THE JUDD GASIFIER	6.1
7. CONCLUSIONS AND RECOMMENDATIONS	7.1
REFERENCES	

CONTENTS

PAGE

APPENDICES :

A	THE TECHNIQUE OF OPERATION OF THE EXPERIMENTAL APPARATUS FOR THE MEASUREMENT OF THE KINETICS OF STEAM-CHAR GASIFICATION	A.1
B	EXPERIMENTAL INPUT DATA SET REQUIRED BY THE PROGRAM 'RATES' FOR THE COMPUTATION OF THE KINETIC RESULTS OF RUN # 42	B.1
	G.C. CALIBRATION FACTORS	B.5
C	PROGRAM LISTING OF THE COMPUTER CODE 'RATES'	C.1
D	THERMODYNAMIC ANALYSIS OF PRODUCT GAS COMPOSITIONS	D.1
E	THE DERIVATION OF THE MATERIAL AND ENERGY BALANCE EQUATIONS FOR THE SIMULATION OF THE JUDD CIRCULATING FLUIDISED BED COAL GASIFIER	E.1
F	A DISCUSSION OF THE STRUCTURE OF THE SIMULATOR CODE	F.1
G	THE LISTING OF THE SIMULATOR CODE	G.1
H	TYPICAL INPUT DATA REQUIRED FOR SIMULATOR CODE	H.1
I	GEOMETRICAL RELATIONSHIPS OF THE GASIFIER	I.1

(1.1)

CHAPTER 1.

INTRODUCTION.

South Africa is blessed with an abundant supply of indigenous coal which is exploited for use in both the local and export markets. Some of the coal reserves in the country contain a relatively high proportion of ash (more than 25%). This grade of coal is not in popular demand for the following reasons :

- the utilisation of high-ash coal involves the expense of ash handling facilities and the problem of the disposal of the resultant ash stream; and
- the conversion of high-ash coal in most existing chemical plant (eg. power stations) presents process engineering problems related to the potential melting and agglomeration of ash in the reactor and the promotion of advanced rates of corrosion and erosion of the internal components of the reactor by the ash.

The mechanical mining techniques employed in the mining industry tend to generate large quantities of coal with a relatively small particle size. The processing of this fine material, or duff coal, is not ideally suited to conventional fluidised bed technology because of the intrinsic problem associated with this technology, namely the elutriation of fine material from the reactor. In practice most vendors overcome this problem by recycling the elutriated fine material back into the process feed stream.

(1.2)

In view of the history of the lack of a popular demand for high-ash and duff coal resources, the coal mining industry in South Africa has practised the stockpiling of so-called 'discard' coal for a number of years. This practice is intended to conserve the potential energy supply associated with the discard coal until such time as an efficient process for the utilisation of such a resource arises. The current reserves of discard coal in South Africa amount to approximately 500 million tons and are accumulating at the rate of approximately 50 million tons per annum (Draft White Paper, 1985). Unfortunately these discard coal dumps pose severe environmental pollution hazards caused by spontaneous combustion and wind erosion of the coal dumps.

The availability of the discard coal resources in South Africa provided the initial motivation for the local development of a novel fluidised bed coal gasifier which produces synthesis gas (a mixture of hydrogen and carbon monoxide). The inherent advantages of fluidised bed technology, namely favourable conditions for material and energy transfer, favourable mixing, flexibility of turndown etc., provided the motivation for the development of a fluidised bed reactor. The principal novelty demanded by the new process, however, is the capability of the process to efficiently utilise discard coal resources. The production of synthesis gas from the discard coal resources is motivated by the following reasons :

- South Africa (S.A.) lacks natural hydrocarbon fuel resources and currently imports crude oil, which is refined to satisfy the demand of the local market. Synthesis gas may be

(1.3)

converted into hydrocarbon fuels by employing established technology such as that which is currently practised on an industrial scale at SASOL;

- synthesis gas has widespread application as a feedstock in the production of chemical products such as ammonia, methanol, hydrogen, carbon monoxide, ethylene, ethanol etc.;
- synthesis gas may be employed as a fuel for domestic heating purposes.
- synthesis gas may also be used as a fuel for the gas turbine cycle of an Integrated Coal Gasification Combined Cycle process (IGCC) for the generation of electricity. The IGCC process features the combination of two thermodynamic cycles; the Brayton cycle incorporates a gas turbine and operates between two rather high temperatures (eg. 1500/600°C), whilst the Rankine steam cycle acts as the heat sink for the Brayton cycle. Since the efficiency of a thermodynamic cycle depends directly on the difference in temperature between the heat source and the heat sink, the IGCC is theoretically capable of generating electricity more efficiently than the conventional Rankine (steam) cycle (eg. 45% vs 40%). The IGCC concept is also reputed to generate less environmental pollution than traditional fossil fuel based power generating technologies (Knizia and Weinzier, 1987). The results of the operation of the world's first commercial-scale IGCC plant at Cool Water, California, USA, have demonstrated that IGCC is a highly efficient, ultra clean process for the production of electrical energy from coal (Grover and Page, 1986; Clark and Shorter, 1986).

The development of the fluidised bed coal gasifier was initiated in the Department of Chemical Engineering at the University of Natal in January 1978. The project has been directed to date by Professor M.R. Judd. The financial support of the project has been provided by the Foundation for Research Development (FRD) of the Council for Scientific and Industrial Research (CSIR) of the Republic of South Africa, with minor contributions from Industry.

The development of the gasifier began with the exploitation by Judd of a peculiar fluidisation phenomenon, namely that a significant degree of circulation of solid material can be achieved within a gas-solid fluidised bed by the inclusion of an open-ended vertical 'draft tube' on the central vertical axis of the vessel (Judd, 1983). By directing separate gas streams to the base of the draft tube and the surrounding annular region of the vessel one is able to operate the draft tube as a slugging fluidised bed and the annular region (hereafter referred to as 'the annulus') at close to incipient fluidising conditions. This causes solid material to circulate within the vessel by moving up the draft tube and down the annulus. The partition of the fluidising gases between the draft tube and the annulus is determined by the equalisation of the pressure drop across these two gas paths.

It is feasible that a certain fraction of the fluidising gas which is intended to rise up the draft tube actually rises up the annulus. This condition is referred to in this text as 'crossflow' of the fluidising gas. It is also feasible that crossflow may occur in the

(1.5)

reverse direction, ie. the flow of fluidising gas from the annulus region to the draft tube region. Under certain conditions of the vessel geometry and of the separate fluidising gas flowrates, the time averaged extent of crossflow in the vessel is found to approach zero (Pillay, 1986).

The simultaneous division of the volume of a vessel which contains a draft tube into two separate coaxial regions and the circulation of solid material between these two zones without the significant crossflow of the separate fluidising gases of the respective zones has provided the incentive for the development of an allothermal⁺⁺ coal gasifier which is capable of producing a synthesis gas stream using air and steam as the reactant fluidising gases. The division of the volume of the vessel into two separate regions allows one to restrict the occurrence of the exothermic coal-char combustion reactions to the interior of the draft tube region, and the occurrence of the steam-char gasification reactions to the annulus region of the gasifier by directing air and steam to the draft tube and annulus regions of the gasifier, respectively. The separation of the 'waste gas' product stream of the draft tube region from the synthesis gas product stream of the annulus is achieved by the inclusion of a cylindrical hood over the draft tube, without interrupting the circulation of solid material in the reactor.

⁺⁺ An allothermal reactor is defined in this text as one in which a material stream circulates between the energy liberating and energy demanding regions of the reactor, thereby providing the mechanism for the transfer of energy between the respective regions. In the case of this gasifier, the fluidised solid material acts as the allothermal agent.

(1.6)

The attraction of the separation of the volume of the gasifier into two distinct reaction zones with the concomitant separation of the reactant and product gas streams of the gasifier lies in the advantage of utilising air as the oxidant stream for the char combustion reactions without contaminating the desired synthesis gas product with nitrogen, under conditions of zero crossflow. This feature of the gasifier avoids the necessity on an oxygen plant as a peripheral component of the gasifier.

The energy liberated by the combustion of char in the draft tube is transferred to the steam-char gasification zone in the annulus by means of the circulating solid material in the gasifier.

The design of the circulating fluidised bed coal gasifier discussed above has become generally known as the Judd gasifier, the configuration of which is shown in Figure 1.

The nature of the solids circulation pattern which prevails in the gasifier is such that solid material is propelled up the draft tube by gas at relatively high interstitial velocities after which the dense phase expands at the top of the draft tube in the shape of mushrooms and collapse gently into the top of the annulus region. The solids then move down the annulus in slip-stick fashion until they are drawn into the vicinity of the base of the draft tube. The expansion of a 'plug' of solid material at the top of the draft tube is accompanied by a fluctuation in the gas differential pressure drop across the draft tube which momentarily upsets the pressure

(1.7)

balance between the draft tube and annulus gas paths in the reactor. These pressure fluctuations are a function of the fluidising gas velocity in the draft tube and are probably not significantly affected by the total pressure of the system.

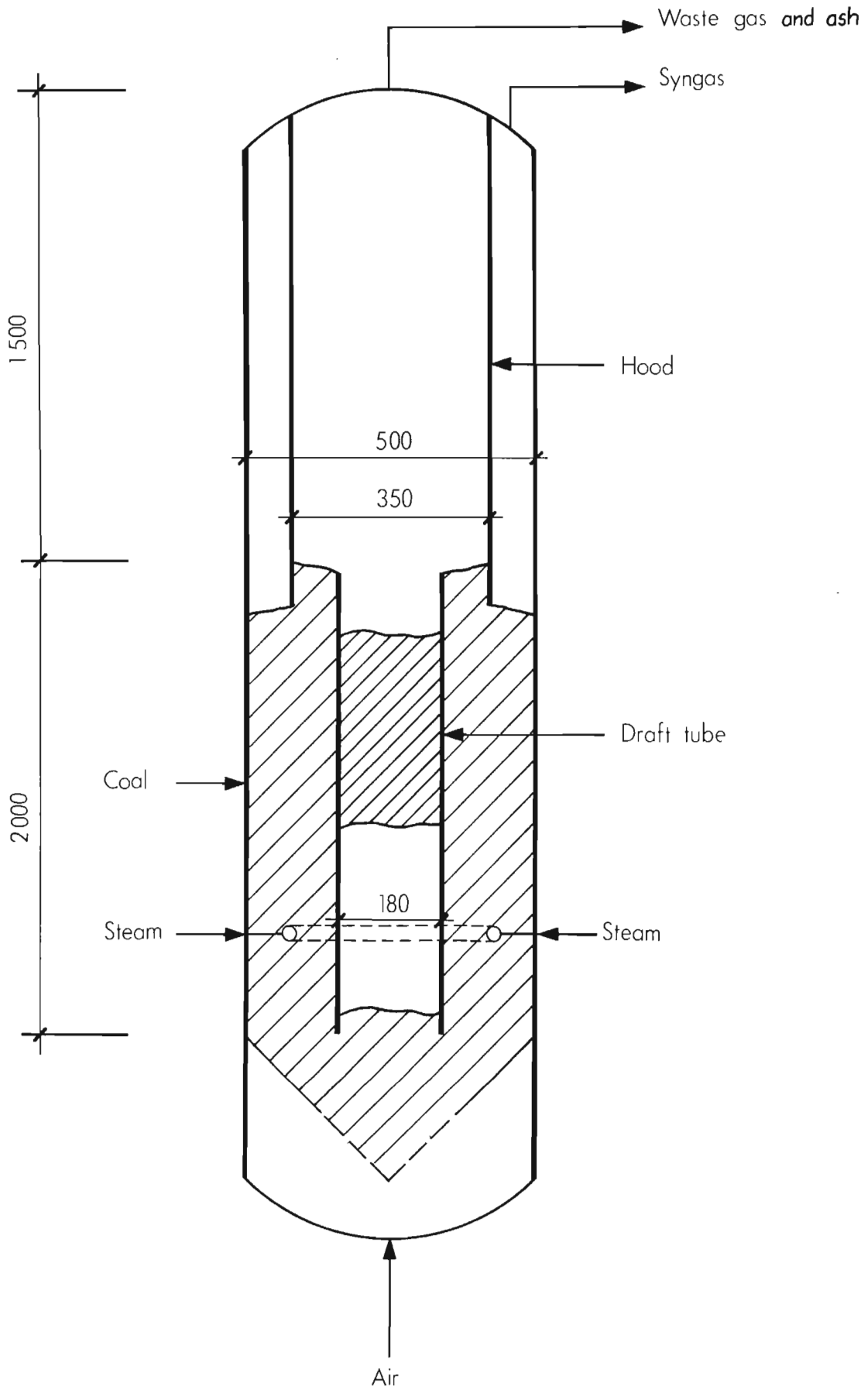


FIGURE 1 Pilot plant gasifier

It is the opinion of the author that the principle of operation of the Judd gasifier is therefore well suited to operation at elevated pressures in that the magnitude of the pressure fluctuations across the draft tube relative to the total pressure of the system become less pronounced as one increases the pressure of operation. This effect is expected to result in a more stable state of circulation of solid material at elevated pressures of operation, with a corresponding simplification in the control of the extent of crossflow in the gasifier.

In the original development of this gasifier, the char combustion reactions and the steam-char gasification reactions were confined to the annulus and draft tube regions of the gasifier, respectively. In response to a proposal by the author, the relative location of the reaction zones in the gasifier have subsequently been reversed. The motivation for the reversal of the locations of the reaction zones lies in the relative order of magnitude of the kinetics of the combustion and gasification reactions. This issue is discussed below.

It is well established that the kinetics of steam gasification of coal-derived char are controlled by the rates of the chemical reactions at temperatures of up to 1000°C, and that the kinetics of char combustion are limited by the rates of mass transfer of gaseous species to or from the char at temperatures above about 500°C (Schmal et al., 1982). Thus for temperatures between 500°C and

1000°C, the steam gasification kinetics are sensitive to temperature and the combustion kinetics depend on the nature of the gas-solids contacting pattern which prevails. It is also known that the reaction rates of steam-char gasification are typically 2 to 3 orders of magnitude lower than the rates of char combustion (Wen and Dutta, 1979).

Because of the much larger volume occupied by solid material in the annular region of a fluidised gasifier with a draft tube, the annulus is the preferred location of the gasification zone. Here, the solids move downwards in a slip-stick fashion, and char gasification occurs essentially under packed bed conditions. In the slugging fluidisation regime the dense phase interstitial gas velocity is relatively high, which results in very good gas-solid contacting. Therefore the draft tube, which operates as a slugging bed, is particularly suited to accommodating the combustion reactions.

The evolution of the Judd gasifier began in 1978 with the construction of a mini-pilot scale gasifier. The overall dimensions of this gasifier were as follows : overall height = 3.5m; draft tube length = 1.5m; draft tube diameter = 0.15m; outer diameter of annulus = 0.5m. The initial experimental program involved studying the operation of the reactor exclusively as a coal combustor, ie. air was employed to fluidise both the draft tube and annulus regions of the unit. The significant results of this study, which have been adopted in the gasifier process to date, are as follows (Meihack, 1982) :

(1.11)

(1) The bulk of the solids inventory of the reactor (about 90 - 95% by mass, with a d_p of about 0.750mm) is refractory grade silica sand which is selected for the following reasons :

- on entering the reactor, coal is well dispersed by the sand which prevents the coal from sintering and/or agglomerating;
- the typical temperature of operation of the gasifier is 1000°C, which is well below the melting point of the sand (approximately 1300°C);
- the sand is readily fluidised by a gas and is able to flow easily in the slip-stick fashion down the annulus;
- the sand is chemically inert to the coal gasification process; and
- by employing a vast excess of silica in the reactor, the circulation of solid material in the reactor is not sensitive to the particle size and density of the coal feed.

It is the opinion of the author, however, that the selection of silica sand as the fluidised solid material in the gasifier may present a significant restriction on the coal processing capacity of the gasifier in view of the performance of the sand as the allothermal agent in the reactor. Silica has an extremely low thermal conductivity which may impede the rate of transfer of energy between the separate reaction zones of the reactor. In the event of this phenomenon occurring, one should identify a more suitable allothermal agent for use in the Judd gasifier (eg Aluminium spheres).

- (2) A principal feature of the nature of the circulation of solids in the reactor is that the elutriation rate of fine coal particles from the reactor is very low. This arises since coal is fed into the annular region of the gasifier, below the level of the solid material in the bed, which causes the coal to be entrained into the downward flowing solid material in the annulus. This effectively increases the residence time of fine coal-char particles in the reactor which allows such particles to reach a much higher level conversion than would be attained in a conventional fluidised bed (Judd et al., 1983). The gentle nature of the expansion of the dense phase at the top of the draft tube is unlike the surface of a vigorously fluidised bed from which fine particles are readily elutriated with the outlet gas stream. A favourable property of the circulation pattern of solid material in the Judd gasifier is therefore the efficient retention and utilisation of fine coal particles. In an experiment conducted by Meihack and Judd (1983) the carbon utilisation efficiency of a stream of flyash feed material of $d_p = 0.050\text{mm}$ was 95%.

On entering the gasifier, the coal feed is mixed with the vast mass of silica sand and is rapidly heated to the local temperature of the gasifier. The heating of the coal causes major structural changes to occur to the coal. This process is generally referred to as thermal pyrolysis, carbonisation, or devolatilisation and is accompanied by the evolution of volatile matter (H_2 , CO_2 , H_2O , SO_2 , H_2S , CH_4 and light hydrocarbons) from the coal. The ultimate

(1.13)

composition of the solid residue derived from the pyrolysis of coal consists of fixed carbon and mineral matter (SiO_2 , Al_2O_3 , Fe_2O_3 , CaO etc). This solid residue is generally referred to as coal-char , or merely char.

Pyrolysis of the coal feed to the Judd gasifier is expected to occur fairly rapidly because of the large proportion of allothermal agent relative to the coal feed in the gasifier. Subsequent to pyrolysis, the resultant coal-char participates as the solid carbonaceous reactant in the combustion and steam gasification zones of the reactor. The allothermal agent circulates the char between the respective reaction zones until complete conversion of the fixed carbon content of the char is achieved.

During the steady state operation of the gasifier, the oxygen content of the air supplied to the draft tube is completely consumed in the char combustion reactions (ie. partial combustion of carbon occurs in the draft tube). The carbon inventory of the gasifier is therefore maintained in excess of the stoichiometric amount required for combustion, and steam gasification of the excess char proceeds in the region above the steam spargers in the annulus. The successful operation of the Judd gasifier as a synthesis gas producer requires that suitable material and energy balances exist under the conditions at which stable circulation of solid material is established in the reactor and at which the amount of crossflow of the fluidising gases between the reaction zones is very low.

Pillay (1986) conducted research into the hydrodynamic behavior of the Judd gasifier using the mini-pilot plant scale apparatus. The principal results of the research conducted by Pillay are as follows :

- (1) Good circulation of solid material in the gasifier was observed for fluidising gas velocities to the draft tube reanging from 6 to 10 times the incipient fluidising velocity (u_{mf}), and for fluidising gas velocities to the annulus ranging from 0.6 to $1 u_{mf}$.
- (2) The time averaged extent of crossflow of the fluidising gases between the separate reaction zones of the gasifier approaches zero for certain combinations of the respective fluidising gas velocities in the ranges mentioned above and for a fixed specification of the geometry of the gasifier.

The above results are valid for operating temperatures up to 1000°C.

In order to achieve suitable material and energy balances for the gasifier within the regime of conditions required for stable circulation of solid material and for low amounts of crossflow of the reactant gases between the different reaction zones, one requires a knowledge of the kinetics of steam gasification of the coal-char to be employed in the gasifier.

This thesis addresses the following aspects of coal gasification which pertain to advancing the development of the Judd gasifier :

- (1) The development of a microreactor to measure the kinetics of steam gasification of coal-char;
- (2) The measurement of the kinetics of steam gasification of two local coal-chars by use of the microreactor mentioned above;
- (3) The identification of a fundamental chemical engineering model which may be used to describe the steam gasification kinetics of char derived from a significant local coal resource, namely Bosjesspruit;
- (4) The mathematical development of a steady-state, one-dimensional compartment model of the entire Judd gasifier;
- (5) The incorporation of the kinetic model for Bosjesspruit coal-char in the simulation of the Judd gasifier using the one-dimensional model mentioned above. These simulations are conducted by running a Fortran 77 computer program based on the model of the Judd gasifier.
- (6) Experimentation on the air-steam gasification of Bosjesspruit coal using the mini-pilot scale Judd gasifier

CHAPTER 2.

LITERATURE SURVEY.

The principal results and conclusions of numerous researchers in the field of coal gasification are presented in this chapter. For the sake of brevity, the survey of the literature has been restricted to the following aspects of coal gasification :

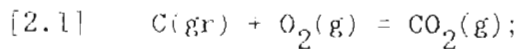
- thermodynamic characteristics,
- effects of coal pyrolysis,
- characteristics of reaction kinetics,
- catalysis, and
- gasifier models.

2.1 THERMODYNAMIC CHARACTERISTICS OF COAL GASIFICATION.

Bastick et al. (1986) have produced a comprehensive review of the general characteristics of coal gasification. Their approach is to consider coal gasification to occur in two stages; a principal carbon-gas reaction (eg. $C + H_2O = CO + H_2$), followed by secondary reactions between carbon and the products of the principal reaction, as well as gas phase reactions. The analysis of the apparently complicated reaction system thus reduces to the consideration of a few relatively simple reactions.

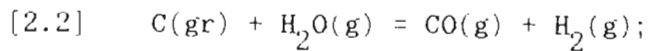
In the selection of a system of chemical reactions to represent coal gasification, Bastick et al. support Johnson (1979) and Schilling et al. (1981) in the use of the chemical properties of carbon (graphite) to represent the carbonaceous content of coal.

The set of equilibria imposed upon each principal coal gasification system (ie. oxy-, steam-, carboxy- or hydro-gasification) may be studied by considering the thermodynamic characteristics of each primary reaction associated with the four gasification systems. The four principal reactions of coal gasification are as follows, in which C(gr) represents carbon graphite :



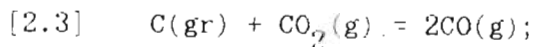
$$\Delta H_{298\text{K}}^{\circ} = -393.6 \text{kJ/gmol}$$

$$\Delta G_{1000\text{K}}^{\circ} = -396.0 \text{kJ/gmol}$$



$$\Delta H_{298\text{K}}^{\circ} = +131.3 \text{kJ/gmol}$$

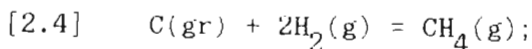
$$\Delta G_{1200\text{K}}^{\circ} = -36.3 \text{kJ/gmol}$$



$$\Delta H_{298\text{K}}^{\circ} = +172.4 \text{kJ/gmol}$$

$$\Delta G_{1000\text{K}}^{\circ} = -4.6 \text{kJ/gmol}$$

$$\Delta G_{1200\text{K}}^{\circ} = -39.4 \text{kJ/gmol}$$



$$\Delta H_{298\text{K}}^{\circ} = -74.9 \text{kJ/gmol}$$

$$\Delta G_{298\text{K}}^{\circ} = -50.8 \text{kJ/gmol}$$

$$\Delta G_{1200\text{K}}^{\circ} = +41.3 \text{kJ/gmol}$$

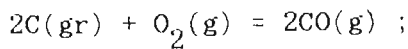
Reaction [2.3] is known as the Boudouard reaction.

(2.3)

2.1.1 REACTIONS OF OXYGEN WITH CARBON.

Reaction [2.1] represents the complete combustion of carbon which is strongly exothermic and is therefore favoured by low temperatures (below 700K). In oxygasification, CO is sought according to the following reaction :

[2.5] = [2.1] + [2.3] :

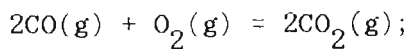


$$\Delta H_{298\text{K}}^{\circ} = -221.2\text{kJ/gmol}$$

$$\Delta G_{1000\text{K}}^{\circ} = -400.6\text{kJ/gmol}$$

It is of interest to note that CO may also arise from the decomposition of CO_2 , according to the following homogeneous reaction :

[2.6] = [2.1] - [2.3] :



$$\Delta H_{298\text{K}}^{\circ} = -566.0\text{kJ/gmol}$$

$$\Delta G_{1000\text{K}}^{\circ} = -391.4\text{kJ/gmol}$$

The value of the equilibrium constant of reaction [2.6] declines rapidly with increasing temperature (Bastick et al., 1986), whilst the effect of temperature on the equilibrium constant of reaction [2.5] is not nearly as severe. The Boudouard reaction is the only truly reversible reaction in the carbon-oxygen system between 700K and 1300K. The formation of CO is thus favoured by high temperatures (above 1300K).

(2.4)

2.1.2 REACTIONS OF STEAM WITH CARBON.

In general, the following two reactions must also be considered to occur in the steam gasification system :

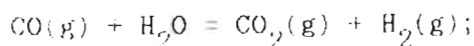
[2.7] = 2[2.2] - [2.3] :



$$\Delta H_{298\text{K}}^{\circ} = +90.2\text{kJ/gmol}$$

$$\Delta G_{1200\text{K}}^{\circ} = -33.2\text{kJ/gmol}$$

[2.8] = [2.2] - [2.3] :



$$\Delta H_{298\text{K}}^{\circ} = -41.1\text{kJ/gmol}$$

$$\Delta G_{1200\text{K}}^{\circ} = +3.1\text{kJ/gmol}$$

Reaction [2.8] is known as the water-gas shift reaction.

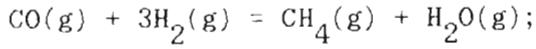
The values of ΔG° at 1200K for reactions [2.7] and [2.8] indicate that the respective reactions are at equilibrium within the range of general operating conditions.

When operating with pure steam as the reactant gas, the gas phase at equilibrium may contain CO, CO₂, H₂, CH₄ and H₂O. At a total pressure of one atmosphere, the H₂ and CO contents of the gas phase increase monotonically with temperature. This trend is to be expected, since reactions [2.2], [2.3] and [2.7] are endothermic. At 1000K, H₂O is effectively decomposed into an equimolar mixture of H₂ and CO, in accordance with reaction [2.2].

(2.5)

The hydrogen content of the gas phase may react with carbon to form methane, according to the reactions of methane synthesis [2.4] and methanation [2.9] :

$$[2.9] = [2.4] - [2.2]$$



$$\Delta H_{298\text{K}}^{\circ} = -206.2\text{kJ/gmol}$$

$$\Delta G_{1200\text{K}}^{\circ} = +77.7\text{kJ/gmol}$$

Since these two reactions are exothermic, the presence of methane at equilibrium is favoured by a reduction of the temperature. CH_4 production is also favoured by an elevation of the pressure of the gas phase. This condition also favours the formation of CO_2 .

To summarise, the gas phase equilibrium composition of the steam-carbon system contains high concentrations of H_2 and CO at high temperatures and low pressures, whilst high concentrations of CH_4 and CO_2 prevail at low temperatures and high pressures.

2.2 THE EFFECTS OF COAL PYROLYSIS ON CHAR GASIFICATION.

Thermal pyrolysis is an important aspect of coal behaviour since it occurs as the primary step in all major coal conversion processes, eg. carbonization, gasification, liquification and combustion.

Pyrolysis occurs as a result of the exposure of coal to high temperatures and results in the breaking of certain structural bonds within the coal matrix, which in turn results in the evolution of gaseous products and the production of a porous, carbon-rich residue known as char. The conditions under which char is formed have a great impact on its internal surface structure, elemental composition and reactivity (Solomon and Beer, 1987; Radovic et al., 1985). The subsequent reactivity of the char towards a gasifying agent (eg. H_2O , O_2 , H_2) is dependent on the nature of the intraparticle structure (porosity) of the char and the concentration of active reaction sites (heteroatoms). The main parameters of the pyrolysis process which affect the reactivity of char are the final temperature and the residence time (van Heek and Muhlen, 1987).

The general effect of pyrolysis on the reactivity of char is detrimental because pyrolysis destroys heteroatoms and dislocations in the crystalline structure which are believed to provide the active sites for surface reactions.

Radovic et al. (1985) conducted experiments to ascertain the effect of pyrolysis temperature and residence time on the air reactivity of lignite char at 1 bar. Their results indicate a significant decrease in char reactivity with increasing severity of pyrolysis conditions (higher temperatures and/or longer residence times). The char which was pyrolysed at 1200°C showed a considerable loss in reactivity compared with char prepared at 700°C; no significant difference in reactivity was observed for chars pyrolysed above 1000°C. This effect on reactivity has been attributed to the fact that high temperatures promote orderly orientation of the coal layer planes, thus reducing the concentration of active reaction sites (Laurendeau).

The effect of coal heating rate (or residence time during pyrolysis) was determined at a coal pyrolysis temperature of 1000°C. After 3 seconds at this temperature, the char reactivity had declined considerably; after 5 minutes the char reactivity had reached its lowest value and had not declined any further after a residence time of one hour. These effects were also observed in CO₂ and H₂O reactivity tests. Plausible explanations of the effects of pyrolysis residence time are provided by Ashu et al. (1978) and Howard et al. (1981) who suggest that the significant fragmentation of char particles at rapid heating rates (low residence times) caused by the violent release of volatile matter, leads to the production of fractured char particles and thus a relatively high concentration of active sites. The decrease in reactivity with increasing residence time is attributed to thermal annealing, which promotes deactivation of the char due to realignment of the coal layer planes.

van Heek and Muhlen (1987) emphasize that there seems to be a characteristic pyrolysis temperature (typically above 800°C) for each char at which the reactivity of the char is drastically reduced within a relatively short residence time.

Toda et al. (1970), Razouk et al. (1968) and Chiche et al. (1976) have investigated changes in surface areas of coals during pyrolysis. They observe that the specific surface area increased with increasing pyrolysis temperature, passed through a maximum in the vicinity of 750°C and decreased thereafter.

Johnson (1975) and Chin et al. (1983) have succeeded in generating fairly good correlations between the total surface areas and the reactivities of chars towards steam/hydrogen mixtures and pure steam, respectively. However, chars with large original surface areas, such as those derived from high volatile bituminous coals exhibit poor correlations between surface area and reactivity (Juntgen, 1981).

Radovic et al. (1985) claim that because of 'the presence of inorganic impurities in coal chars, their gasification should be regarded as potentially catalytic gas-solid reactions.' This approach suggests that the reactivity of a char depends on the inherent activity of the catalytic components of char and on the concentration of the active carbon sites. The catalytic activity of a char depends only on the composition of the mineral matter in the coal, whereas active site concentration depends also on the

conditions of pyrolysis. Radovic, Walker and Jenkins (1983) demonstrated that both the concentration of carbon active sites (carbon active surface area, which is measured by O_2 adsorption) and the concentration of catalyst sites (catalyst dispersion) decreases with increasing severity of pyrolysis.

Smith (1978) reported a wide range of carbon gasification reactivities using the same coal precursor by varying the conditions of its pyrolysis and pretreatment. However, the observed activation energies were similar in all cases (125 - 135 kJ/gmol, which is typical of the regime in which chemical reaction rates control overall kinetics (van Heek and Muhlen, 1985)), thus suggesting that the variations in gasification rate were due to changes in the concentration of active sites (and not due to lack of accessibility of reactants). Radovic et al. (1983) have successfully correlated the reactivity of chars in air with the carbon active surface areas of the chars.

Radovic et al. (1985) therefore conclude that the active surface area (either of carbon or catalyst) of a char is a decisive factor in determining the reactivity of a char during gasification, and that severely high pyrolysis temperatures or residence times destroy active surface area, thereby reducing char reactivity.

2.3 CHARACTERISTICS OF CHAR GASIFICATION REACTION KINETICS.

Although a knowledge of the thermodynamic characteristics of carbon gasification reactions is essential in determining the feasibility of transformation, the overall rate of gasification is determined by the nature of the kinetics of the particular reactions.

The kinetics of coal gasification are influenced by such factors as :

- the chemical composition of the coal;
- the physical structure and texture of the coal;
- the thermal history of the coal-char (pyrolysis conditions);
- and
- the effects of catalysts/inhibitors, (Bastick et al., 1986).

Char-gas reactions may be classified into two distinct categories, namely, volumetric reactions and surface reactions (Wen and Dutta, 1979). In a volumetric reaction the reacting gas diffuses into the interior of the char particles and reaction occurs throughout the internal surface of the char. This type of reaction is typical of cases in which the chemical reaction rates are relatively low (eg. char-H₂O, char-H₂, char-CO₂ reactions) and represent the rate-controlling step of gasification (van Heek and Muhlen, 1987). In a surface reaction, however, the gaseous reactant hardly penetrates the interior surfaces of the char and the reaction is confined to exterior surface of the 'shrinking core of unreacted solid'.

In

general, surface reactions occur when the chemical reaction is extremely fast, as in char combustion, and when diffusion is the rate controlling step.

Many studies are reported in the literature in which the kinetics of steam gasification of various foreign coal-derived chars have been investigated. Most of these studies have involved differential conversion of the reactant gas in order to simplify the interpretation of kinetic data. Experiments which have employed differential reactors were conducted either thermogravimetrically or by product gas analysis.

Investigations by Jensen (1975), Klei et al. (1975), Kayembe and Pulsifer (1976), Schmal et al. (1982), van Heek et al. (1985) and Kasaoka et al. (1985) have demonstrated that the kinetics of steam-char gasification are chemical reaction rate controlled for small char particles (< 500 microns) at temperatures up to about 1000 - 1200°C. The carbon-steam reaction occurs uniformly throughout the interior of the char particles under these conditions. van Heek and Muhlen (1985) have reported activation energies of between 130 and 200 kJ/gmol for the steam-char gasification reaction when chemical reaction rates are controlling. They have also observed that the activation energy for the reaction approximately halves when mass transfer rates control the overall kinetics.

(2.12)

Two distinct approaches have been adopted by authors to mathematically describe the kinetics of char gasification. One approach has been to correlate the fractional conversion of the char, X , with a dimensionless time group, τ , where $\tau = t/t_{X=0,5}$. Here, t represents the time taken for the char to reach a fractional conversion of X , and $t_{X=0,5}$ represents the time taken for the char to reach a fractional conversion of 0,5. The motivation for this approach is that general char gasification data may be represented by one equation and that $t_{X=0,5}$ may be used as a parameter to describe the relative reactivity of a char. This approach has been used by Walker et al.(1977) and Kasaoka et al.(1985).

The other modelling approach which has been adopted describes the rate of carbon gasification directly. Johnson (1974), Miura et al.(1986) and Guo and Zhang (1986) have followed this approach.

Walker et al.(1977) conducted steam-char gasification experiments with 13 different coal chars at a temperature of 910°C and a steam partial pressure of 0,022 atm. They then correlated X with τ using various arbitrary polynomial equation forms. The correlation which yielded the best fit was found to be :

$$X = a_W \tau + b_W \tau^2 + c_W \tau^3 \quad [2.10]$$

where $a_W = 0,375$; $b_W = 0,276$ and $c_W = -0,148$. However, this correlation is limited by their experimental data to values of $X < 0.7$.

(2.13)

Kasaoka et al.(1983; 1985) conducted thermogravimetric steam-char gasification experiments with 23 different coal-chars of widely varied compositions at temperatures from 800°C to 1400°C and steam partial pressures from 0,16 to 0,41 atm.. They correlated their results using the expression :

$$X = 1 - \exp (-a\tau^b) \quad [2.11]$$

which is based on the volumetric model for the reaction (Doraiswamy, L.K. and Sharma, M.M., 1984). This correlation is able to describe the sigmoidal shape of some $X - t$ plots which is attributed to a maximum rate occurring at some time during the course of the reaction other than at $t = 0$. For these conditions $b > 1$ in equation [2.11]. When $0 < b \leq 1$, the rate of gasification is at a maximum at the beginning of the reaction and decreases monotonically as gasification progresses, which conforms to most $X - t$ curves (Kasaoka, 1983). When $b = 1$ in equation [2.11], the reaction kinetics are described by the volumetric model and are controlled by the chemical reaction rates (Doraiswamy, L.K. and Sharma, M.M, 1984). The data of Kasaoka et al., are well described by equation [2.11] with $a = 0,675$ and $b = 1,340$.

Wen and Dutta (1979) have compiled a comprehensive review of the char gasification literature. They report that, despite many inconsistencies in earlier works regarding the mechanism of the char-steam reaction, it is now established that H_2 and CO are the principal products of the reaction and that hydrogen has a strong retarding effect on the reaction (Johnstone et al., 1952; Klei et al., 1975)

(2.14)

A popular approach among earlier investigators has been the use of Langmuir-Hinshelwood type adsorption equations to express the rate of the char-steam reaction. This approach is based on the concepts of adsorption and desorption of gases on solid surfaces. Walker et al. (1959) proposed the following mechanism and rate equation for the carbon-steam reaction :



$$\text{Rate} = \frac{k_8 (H_2O)}{1 + \frac{k_8}{k_{10}} (H_2O) + \frac{k_9}{k_{10}} (H_2)} \quad [2.14]$$

in which,

C_f = Free active sites on carbon surface.

k_8, k_9, k_{10} = Rate constants for reactions [2.12] and [2.13].

$(H_2O), (H_2)$ = Concentrations of H_2O and H_2 , respectively.

Equation [2.14] accounts for the inhibiting effect of H_2 on the char- H_2O reaction.

Ergun and Mentser (1965) extended the mechanism of Walker et al. by including the following reaction step :



(2.15)

This leads to the following expression for the rate of char-steam gasification :

$$\text{Rate} = \frac{k_8 (\text{H}_2\text{O}) + k_{11} (\text{CO}_2)}{1 + \frac{k_8}{k_{10}} (\text{H}_2\text{O}) + \frac{k_9}{k_{10}} (\text{H}_2) + \frac{k_{12}}{k_{11}} (\text{CO})} \quad [2.16]$$

Equation [2.15] introduces an inhibiting effect on the gasification rate caused by the presence of CO.

The use of rate equations based on adsorption mechanisms is attractive if such mechanisms are indeed representative of the true mechanism and the effects of the various gases are significant. However, Wen and Dutta (1979) advise that 'the direct applicabilities of most of these equations for design purposes are limited because of the requirement of more than one arbitrary rate constant'. They also state that the 'determination of these rate constants is extremely difficult, and the validity of these mechanisms is often questionable'. Though attempts have been made by many researchers to determine the rate constants of adsorption type mechanistic equations, Wen and Dutta (1979) state that wide variations are observed in the reported values.

(2.16)

Wen (1972) proposed the following simplified equation based on a collection of rate data :

$$\frac{dX}{dt} = k_v \left[C_{H_2O} - \frac{C_{H_2} C_{CO} RT}{K} \right] (1 - X) \quad [2.17]$$

in which,

k_v = the rate constant, and

K = the equilibrium constant of the reaction

C_{H_2O} etc. = concentration of gaseous species, gmol/m³.

Equation [2.17] has been shown by Wen and Dutta (1979) to represent the rate data of several investigators (Feldkirchner and Linden (1963), Feldkirchner and Herbler (1965), Johnson (1974) and Jensen (1975)). Arrhenius plots of this collection of data suggest that an average activation energy of 146kJ/gmol is typical of the char-steam reaction.

Wen and Dutta (1979) cite Walker et al. (1959) by reporting that the kinetics of steam-char gasification are first order with respect to the steam partial pressure for partial pressures up to atmospheric pressure, but approach zero order as the partial pressure of steam increases above atmospheric pressure. Chin et al. (1983) have confirmed this finding at sub-atmospheric steam partial pressures. Kasaoka et al.(1985) have found the order of the char-steam reaction to be 0.43 with respect to steam partial pressure for Illinois #6 coal-char and two other coal types at a temperature of 900°C and at steam partial pressures from 0.16 to

(2.17)

0.41 atmospheres. Johnson (1974) has developed a correlation to describe the kinetics of char gasification based on thermogravimetric results obtained with a variety of bituminous coal chars which were gasified in $\text{CO-CO}_2\text{-H}_2\text{-H}_2\text{O-CH}_4$ mixtures at temperatures from 800°C to 1100°C and total pressures from 1 to 70 atmospheres. For gasification in pure steam, Johnson's correlation predicts that the order of the reaction with respect to steam partial pressure becomes zero at 10 atmospheres.

According to the volumetric reaction model, the rate of the char- H_2O reaction may be expressed as follows :

$$\frac{dX}{dt} = k_v C_{\text{H}_2\text{O}} (1 - X) \quad [2.18]$$

in which,

k_v = the rate constant;

$C_{\text{H}_2\text{O}}$ = the concentration of H_2O , gmol/m^3 ;

X = the fractional conversion of carbon content of char.

(Wen and Dutta (1979))

Johnson (1974) has proposed a model for the rate of gasification of coal-derived char in mixed gas environments which has a fundamental nature in that it contains exponential temperature terms and a mass action term which is identical to that used by the shrinking core

(2.18)

model. Some empiricism is introduced, however, by including a 'relative reactivity factor' in the model. For a pure steam environment, Johnson's correlation reduces to :

$$\frac{dX}{dt} = f_R K_T (1-X)^{2/3} \quad [2.19]$$

where
$$K_T = \frac{\exp(9,0201-12\,910/T)}{[1+(1/P_{H_2O})\exp(-22,216+24\,882/T)]^2} \quad [2.20]$$

and

X = carbon conversion expressed as a fraction of the amount of carbon initially present; gmol/gmol carbon initially present.

t = time; minutes.

f_R = relative reactivity factor, which depends on the char type and char thermal history, where $0,3 \leq f_R \leq 10$.

K_T = kinetic parameter, or rate constant.

T = reaction temperature; Kelvin.

P_{H_2O} = partial pressure of steam, atmospheres(absolute).

Recently, Miura et al.(1986) and Guo and Zhang (1986) have considered a more general fundamental model to describe steam-char

(2.19)

gasification kinetics. The form of this model is :

$$-r_C = \frac{dX}{dt} = K(1-X)^n \quad [2.21]$$

where K represents the classical Arrhenius-type rate constant ($K = k \exp(-E/RT)$) and n is a constant. The above authors state that when the homogeneous or volumetric reaction model applies, $n = 1$ in equation [2.22], and when the shrinking core model is applicable, $n = 2/3$.

Miura et al. (1986) investigated the effects of different alkaline and alkaline-earth metal catalysts on the kinetics of steam gasification of carbon at 835°C and at a steam partial pressure of 1 atmosphere. They found that the volumetric reaction model ($n = 1$ in equation [2.21]) applied for carbon samples which contained Ca or Fe, and that the shrinking core model (with chemical reaction rate controlling) applied for samples which contained Ni.

Guo and Zhang (1986) studied the kinetics of steam gasification of 5 different coal-chars at temperatures from 850°C to 950°C and at a steam partial pressure of 30 atmospheres using a packed bed microreactor. Their results were well described by equation [2.21] with $n = 1$.

2.4 CATALYSIS OF CHAR GASIFICATION.

The use of catalysis during coal gasification offers many advantages, some of which are listed below (Penner and Wiesenhahn, 1987) :

- Increased gasification rates;
- Reduced operating temperatures, pressures, residence times and/or component sizes; and
- Easier gas clean-up

Although most catalysts are deliberately added to the coal feed stream of a gasifier, it is well established that certain inorganic elements that occur naturally in coal deposits have significant effects on the rates of coal gasification reactions (Wen and Dutta, 1979).

The catalytic effects on char gasification introduced by inherent mineral matter may influence both gas-solid and gas phase reactions during gasification. The gas phase reactions are predominantly affected by ash particles, whereas the primary char-gas reactions are affected by the minerals dispersed in the carbon-rich char (Wen and Dutta, 1979).

The catalytic activity of a chemical species is dependent upon the identity of the reactant gas (eg. O_2 , CO_2 , H_2O , H_2) (Bastick et al., 1986). In general the alkali, alkaline earth and transition

metals have been found to be the most effective catalysts (Wen and Dutta, 1979).

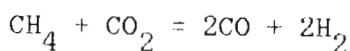
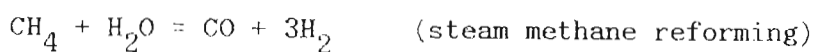
Bastick et al. (1986), Miura et al. (1986), Liu and Zhu (1986) and Linares-Solano et al. (1986) report that the steam-char reaction is well catalysed by the carbonate salts of the alkaline and alkaline-earth metals and by the oxides and salts of the metals from the families of iron and platinum. Wen and Dutta (1979) note that 'among the oxides of iron and other transition metals, the stoichiometrically deficient oxides are believed to be better catalysts in C-CO₂ and C-H₂O reactions. Thus FeO or Fe₃O₄ is a better catalyst than Fe₂O₃ in such reactions. Among the salts of these metals, the organic salts like oxalates, acetates and citrates show catalytic effects superior to those of the inorganic salts. This is due to the fact that the former group of salts yield finer subdivision and dispersion of the metal ions inside the body of the reacting solid particles. The catalytic activity decreases with the increase in size of the dispersed catalyst particles'.

Although it is believed that CO and H₂ are inhibitors of C-CO₂ and C-H₂O reactions, this may only be true if the reactions are not catalysed. In the case of catalysed reactions, particularly by the oxides of Ni, Co or Fe, CO and H₂ may actually promote the reactions by reducing the metallic oxides into the more active metal states (Wen and Dutta, 1979). The most effective catalysts for the char-steam reaction are reported to be K, Na, and Ni, and those for the char-carbon dioxide reaction are reported to be K, Na, Li, Ni, Co, Fe and Ca (Wen and Dutta).

Ohlsuka and Tomita (1986) investigated the calcium catalysed steam gasification of an Australian Brown coal. (Calcium is inherently present with carboxyl functional groups of low rank coals, and exchangeable calcium cations are reputed to promote steam gasification (Takarada et al., 1985)). Their results show that calcium hydroxide, carbonate, nitrate and chloride all exhibited similar catalytic activity. The steam-char gasification rate increased lineally with increasing calcium content, and at a concentration of 5%(m/m) complete gasification was attained within 25 minutes at 973K.

Linares-Solano et al. (1986) investigated the catalytic activity of calcium for lignite char gasification in various atmospheres. Their results show that gasification rates increase rectilinearly with increase in calcium loading and that the activation energies for reaction in air, steam and CO₂ atmospheres are 130, 170 and 200 kJ/gmol, respectively.

Chen et al. (1987) investigated the catalytic activity of coal ash with a high Fe₂O₃ content on the following three reaction :



Their results show that the extents of both the water-gas shift and the steam methane reforming reactions were appreciable, though the

reaction of methane and carbon dioxide was not significant up to 900°C. The rates of the former two reactions were found to be several times greater than the corresponding non-catalytic reactions.

Huttlinger et al. (1986) and Miura et al. (1986) have investigated the catalytic activity of potassium in the carbon monoxide shift reaction (water-gas shift). Their results demonstrate that potassium is an active catalyst for the shift reaction. In particular, high concentrations of H_2 and CO_2 are observed during steam gasification.

2.5 GASIFIER MODELS.

The steam-char gasification zone (annulus region) of the Judd gasifier behaves almost like a classical moving bed reactor, with a packed bed of solids (or incipiently fluidised solids) descending in slip-stick flow, countercurrent to the rising gas stream in plug flow. In order to develop a simple model of the Judd gasifier, it is therefore appropriate to consider the approaches adopted in the literature to model moving bed coal gasifiers.

Models of coal gasifiers may be classified according to the level of sophistication employed in their formulation, as follows :

- (1) Equilibrium models.
- (2) One dimensional, steady state kinetic models.
- (3) Two or three dimensional, steady state kinetic models.
- (4) Two or three dimensional, dynamic kinetic models.

The basic difference between models of levels (2), (3) and (4) is the number of spatial co-ordinates employed in the equations used to describe the model. Hill (1977) explains that one-dimensional models take into account variations in composition and temperature along the length of the reactor, while two-dimensional models also allow for variations in these properties in the radial direction. Hill also comments that 'the one dimensional model is used most often in preliminary design calculations because it provides a good

approximation to the desired result with limited consumption of computer time, and it can be used to determine the effect of changes in design parameters and operating conditions on effluent conditions. The two-dimensional model is more complex, but provides essential information about radial temperature profiles within the bed.'

One may also regard the inventory of a reactor as being either 'pseudo homogeneous' or heterogeneous. Pseudo homogeneous models assume that the local properties of the reactor may be characterized by a given bulk temperature, pressure and composition and that these quantities vary continuously with position in the reactor. In heterogeneous models, however, fluid and solid phases are explicitly treated as separate entities, with separate material and energy balance equations for each phase. Hill (1977) mentions that pseudo homogeneous models of fixed bed reactors are widely employed in reactor design calculations, where the prediction of the bulk properties of the reactor are adequate.

In 1978, Yoon et al. developed a one-dimensional, pseudo homogeneous steady state model of the Lurgi type moving bed reactor. The model considered the gasifier as consisting of distinct reaction zones situated along the axis of the reactor, ie. zones of coal drying, pyrolysis, gasification and combustion. The results of this model were reported to be in reasonable agreement with the published experimental data.

In 1981, Cho and Joseph extended the model of Yoon et al. by introducing heterogeneous effects. A major assumption of their model was that the heat capacity of the solid phase was insignificant by comparison with the heats of the prevailing reactions. The results of this model were also reported to compare well with the experimental data.

In 1978, Amundson and Arri developed a steady state two-dimensional pseudo homogeneous model of the Lurgi type moving bed reactor. The reactor was conceptually divided into two distinct reaction zones, the gasification and combustion zones. No account was made for coal pyrolysis. Their model employed the Johnson (1974) kinetic expressions and assumed the water-gas shift reaction to be at equilibrium throughout the gasification zone. Numerous studies were made of the effects of the various input parameters on the behaviour of the gasifier. In particular, this model was able to predict the location and magnitude of excessive temperatures ('hot spots') in the combustion zone. The results of the model were not compared with any experimental data, however.

Bhattacharya et al. (1986) developed a fixed bed experimental apparatus in order to validate proposed gasifier models. They compared experimental char gasification data with the results of a model similar to that of Yoon (1978) and Cho (1981). Their model was a two-dimensional, radial dispersion model in which radial dispersion of mass was neglected but that of energy was included. The model showed good agreement with experimental data in the

initial stages of gasification. They attribute the discrepancy between the model and experimental data at later stages of gasification to inaccurate kinetic data for char gasification.

It is interesting to note the popular use of constant heat capacities for both gaseous and solid phases in the literature on gasifier models. All of the abovementioned models employed constant heat capacity terms in the formulation of the respective energy balances, excepting that of Yoon et al. (1978). It is assumed that this approach was adopted to simplify the mathematics involved in the solution of the models and may be justified, especially for the less sophisticated one-dimensional models, by noting that the effects on the overall energy balances of the heat capacity terms are far less significant than those of the heats of reaction. This argument is elaborated upon later in the development of the one-dimensional, psuedo homogeneous model of the Judd gasifier.

In 1967, Froment compared the predictions of the classical one-dimensional, psuedo homogeneous model of a fixed bed reactor with those of an improved two-dimensional model. Each model assumed constant heat capacities. He concluded that the one-dimensional model would continue to be used for exploratory purposes, though the two-dimensional model may be favoured for final calculations.

Numerous texts exist in which the modelling of moving bed or fixed bed reactors is treated. Westerterp et al. (1984) claim that the usual assumptions for moving bed reactors are :

- plug flow of both gas and solid phases;
- no radial mass gradients;
- often, isothermicity of the particles and constant heat capacities.

Wakao and Kaguei (1982) employ constant heat capacities in a two-dimensional model of a packed bed heat exchanger.

Rase, in his popular text on chemical reactor design, presents energy balance equations for both one and two-dimensional models of packed beds. Each case employs constant heat capacities.

Smoot and Smith (1985) have compiled a comprehensive chapter which features highlights of models of coal processes in general.

CHAPTER 3.

THE DESIGN AND TECHNIQUE OF OPERATION OF THE MICROREACTOR FOR THE
MEASUREMENT OF THE STEAM GASIFICATION KINETICS OF COAL-CHAR.

3.1 INTRODUCTION.

A packed bed microreactor has been developed at the University of Natal to measure the kinetics of char gasification in a pure steam environment at temperatures up to 1000°C and at pressures up to 5 bar absolute. The kinetics of the steam-char gasification reaction are obtained by measuring the flowrate and composition of the gaseous products of gasification at various time intervals after the start of the reaction, whilst maintaining the char sample at a constant temperature and pressure. The design of the experimental apparatus and the technique of measuring the steam-char gasification kinetics are motivated by the following arguments :

- (1) The principal reaction which occurs in the gasification zone of the gasifier is that of carbon-steam gasification, ie.



It is well established that the kinetics of steam-char gasification are controlled by the rates of the chemical reactions at temperatures below 1000°C and that the order of magnitude of the rate of reaction is relatively low (Schmal et al., 1982; van Heek et al., 1985; and Kasaoka et al., 1985). It is therefore likely that the prevailing steam concentration

in the gas environment of the annulus region of the gasifier is relatively high. Consequently, the gasification experiments in this study have been conducted in a pure steam environment.

- (2). The principle of operation of a microreactor involves the differential conversion of at least one reactant species by supplying an excess quantity of the appropriate reactant. This enables the conditions of the reaction to be maintained approximately steady with respect to the excess reactant. In this study a relatively high flowrate of steam is supplied to the microreactor, which contains a small packed bed of char (with a capacity of approximately 5g). The char sample is therefore maintained in essentially a pure steam environment during the course of its conversion.
- (3) During steam-char gasification, the water-gas shift reaction is known to be promoted by various components of the mineral matter content of char (Huttinger, K.H., 1986; Miura et al., 1986). As a result, the dry product gas stream consists of a mixture of H_2 , CO and CO_2 . A small quantity of CH_4 is also expected to be present in the product gas stream. The rates of steam-char gasification may be obtained by mass balance after measuring the composition and the rate of production of the products of gasification. Gas chromatography has been employed to analyse the product gas stream in this study. An alternative technique which may be employed to measure reaction rates in a microreactor is that of thermogravimetric analysis, in which the rate of mass loss of the solid reactant

is monitored. The product gas analysis technique was selected in this study because of the lower capital investment involved in this technique.

- (4) Johnson (1974) has conducted a vast quantity of research into the steam gasification kinetics of various foreign coal chars under a variety of experimental conditions. A principal result of his findings is that the rate of steam-char gasification increased with increasing partial pressure of steam up to 10 bar absolute, above which no further increase in the rate of reaction was observed. Consequently, the microreactor developed for this study has been designed to operate at pressures of up to 5 bar absolute (this limitation is imposed by the steam generator which was available for use in this study); the microreactor is, however, designed to operate at 10 bar absolute. In view of the fact that steam-char gasification kinetics are known to be sensitive to reaction temperatures up to 1000°C, the microreactor has been designed to operate at this temperature.

3.2 A BRIEF DESCRIPTION OF THE PROCESS FLOWSHEET.

The process flow and instrumentation diagram of the complete apparatus is shown in Figure 2. A laboratory scale electric boiler supplies steam to the microreactor within which the steam is preheated to the desired reaction temperature before encountering the char sample. A differential amount of conversion of the reactant steam occurs as a result of steam gasification of the char

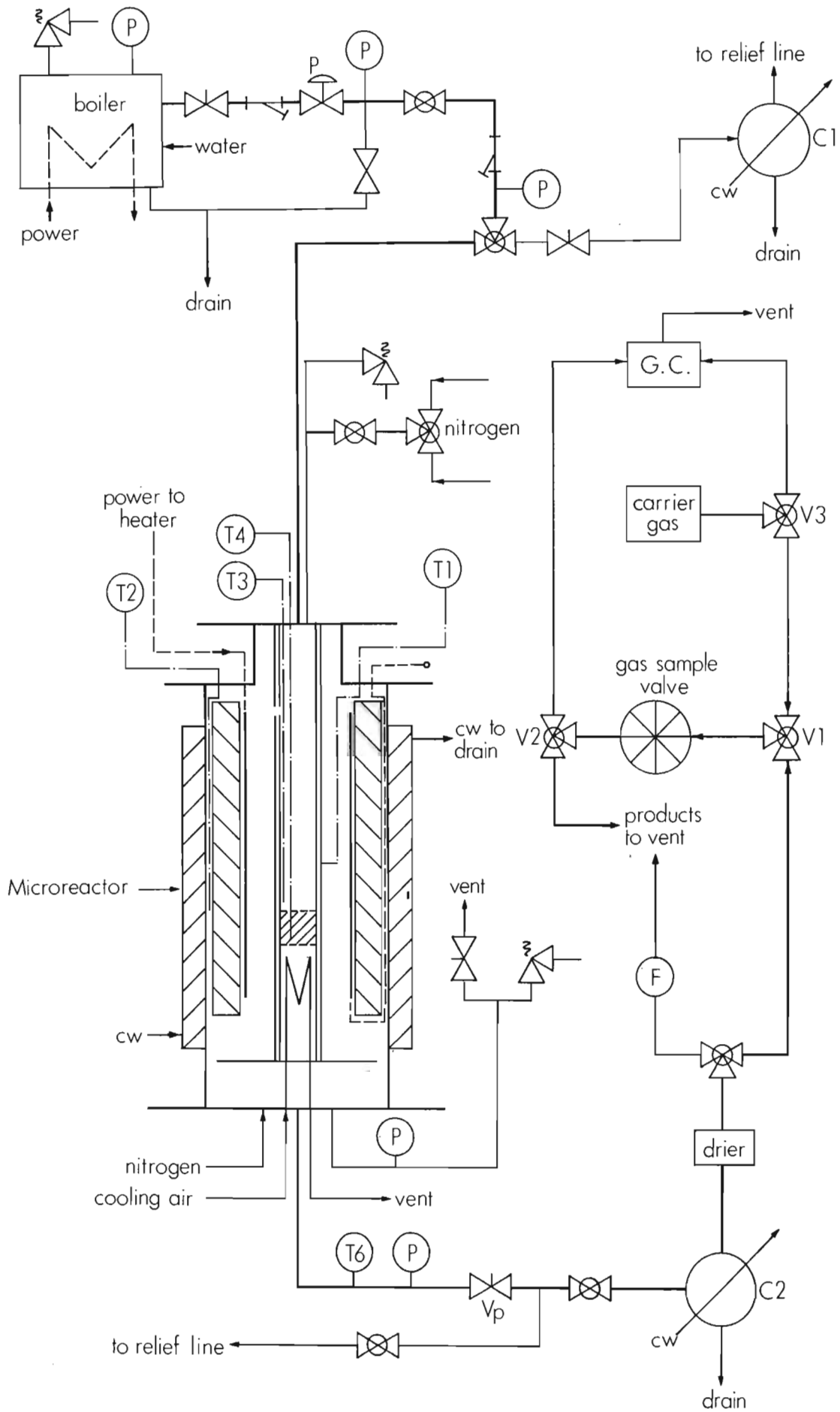


FIGURE 2 Process flow and instrumentation diagram

(3.4)

sample in the sample basket. The products of gasification and the excess steam are then cooled before leaving the microreactor.

Thereafter, the excess steam is totally condensed by condenser C2, after which the products of gasification are dried and then either sampled or passed through a rotameter.

The product gas samples are stored in the sample loops of a 16-loop sampling valve during the course of an experiment and are later recalled for analysis by gas chromatography (GC).

A more detailed discussion of the process flow diagram is contained in Appendix A1. The purpose of Appendix A1 is to assist an operator of the microreactor in identifying the various components of the apparatus and in understanding the functions of the respective components.

The design details of the microreactor and of the peripheral components of the apparatus are contained in the eighteen pages which follow the flowsheet, shown overleaf. Should the reader wish to bypass this material, without any significant loss in continuity, he may continue from page (3.14).

3.3 MICROREACTOR CONFIGURATION.

The general configuration of the microreactor is shown in Figure 3, overleaf. The microreactor comprises a system of two coaxial reactor tubes which support the sample basket (A) and are surrounded by a coaxial tubular silicon carbide heating element (D). In order to investigate the effect of pressure on the kinetics of gasification, the reactor tubes and heater are contained within a cylindrical pressure vessel. Nitrogen is employed to pressurise the pressure vessel during operation at elevated pressures. A layer of thermal insulation (E) shields the outer vessel from the electric heater. The heater is supported by insulating discs which are attached to the outer reactor tube.

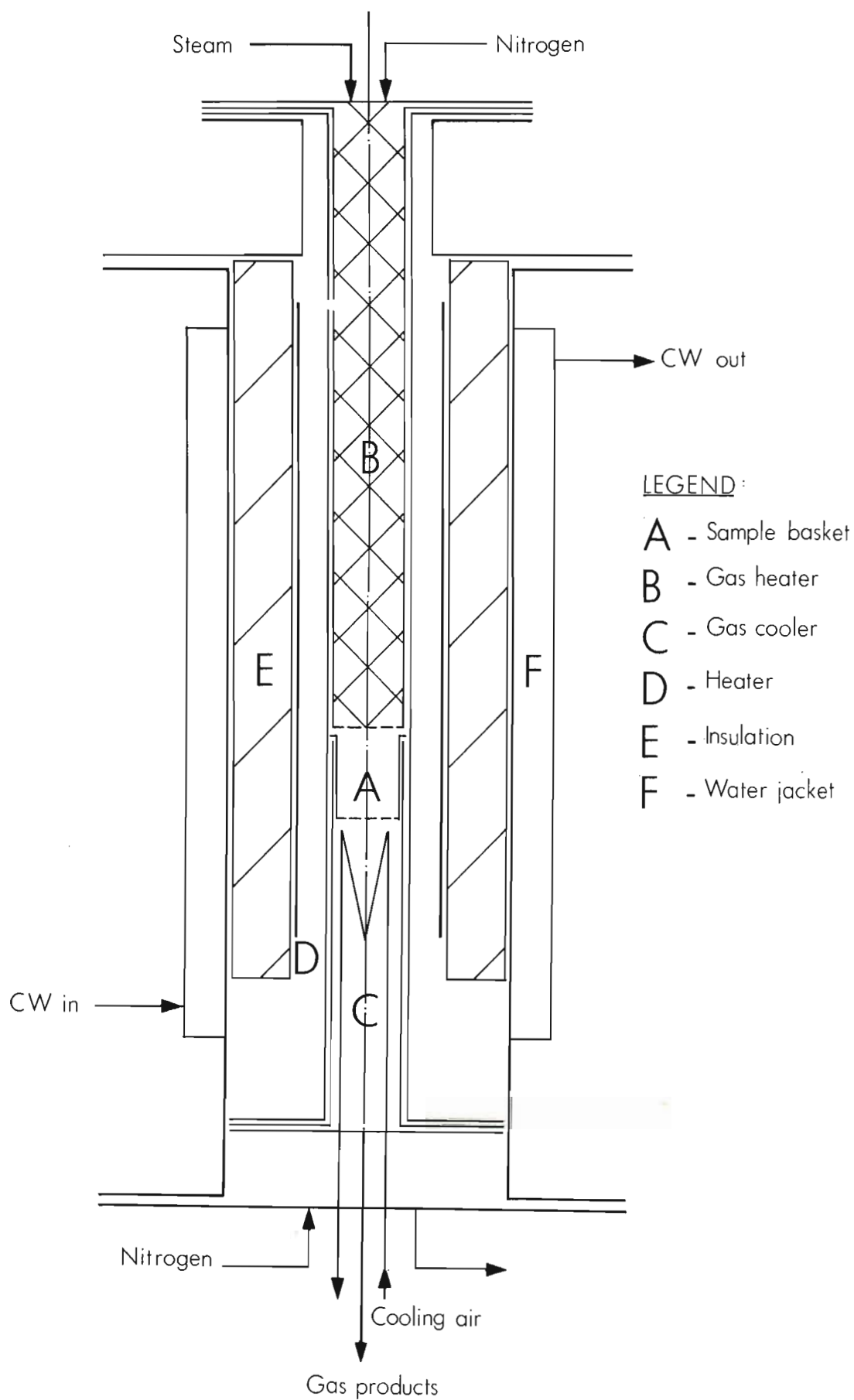


FIGURE 3 Section through the microreactor showing the location of components

(3.6)

The system of coaxial reactor tubes comprises a single outer tube within which the sample basket is sealed between two inner tubes. The upper inner tube is packed with stainless steel pellets and serves as the steam preheating tube in the microreactor. The lower inner tube contains two passes of air cooled stainless steel tubes and serves as the product gas cooling tube (C). The product gas cooling tube is joined to the lower end of the outer tube by means of a flange assembly. Similarly, the reactant steam preheating tube is joined to the upper end of the outer tube. Figures 4 and 5 show the axial and radial dimensions of the principal components of the microreactor, respectively.

The design of the sample basket is shown in detail in Figure 6. This diagram also shows the interface of the steam preheating tube with the upper face of the sample basket. When the sample basket is installed in the microreactor, the lower end of the basket slides into the top end of the product gas cooling tube until the sample basket interfaces with the plane top edge of the gas cooling tube. The seals between the sample basket and reactor tubes are achieved by the compression of gaskets which are designed to operate successfully up to 1000°C. The sample basket is accessed by removing the steam preheating tube and locating the two internal mounting pins of the basket (see Figure 6) with a special tool.

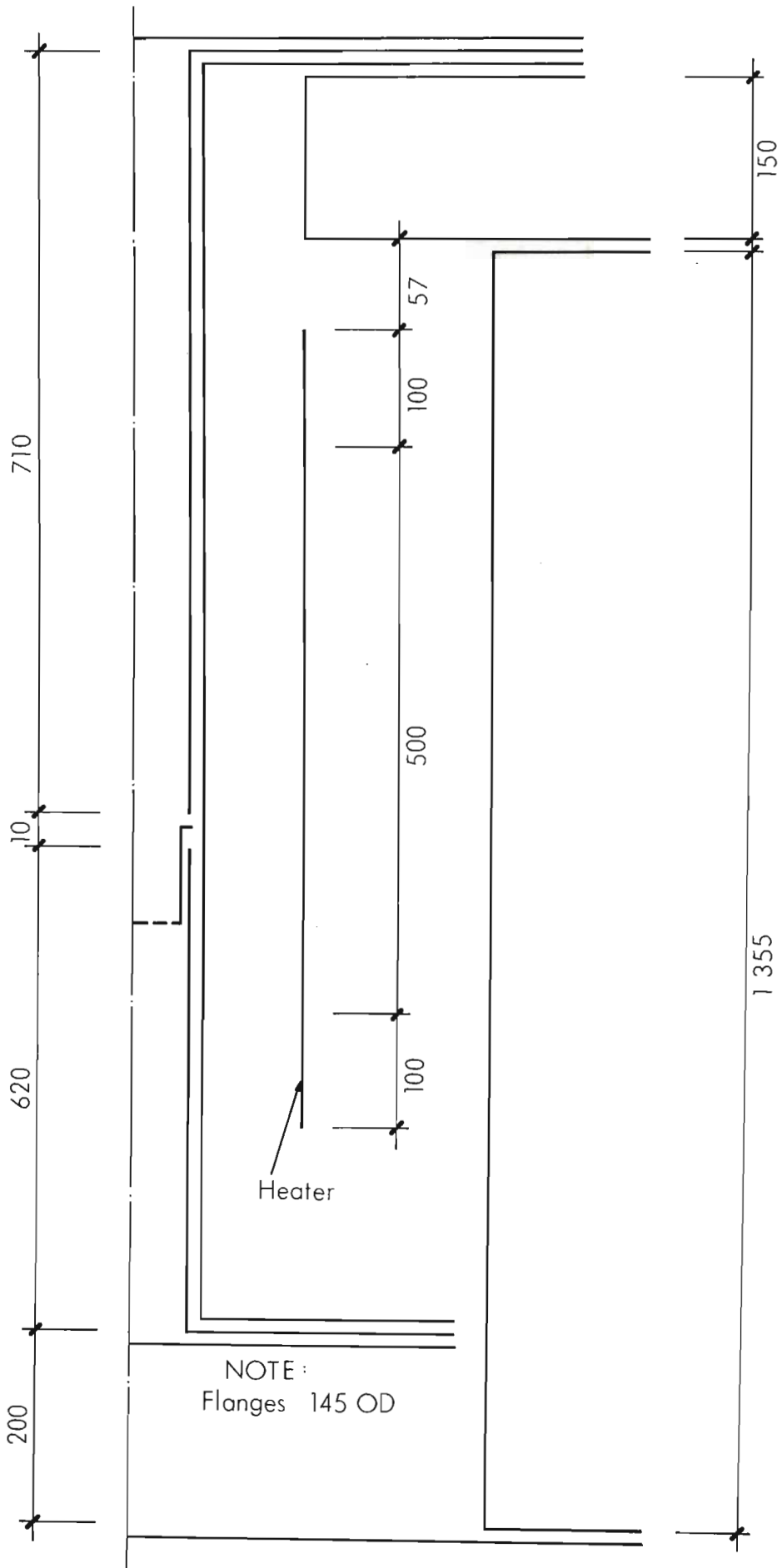


FIGURE 4 Axial dimensions of the microreactor

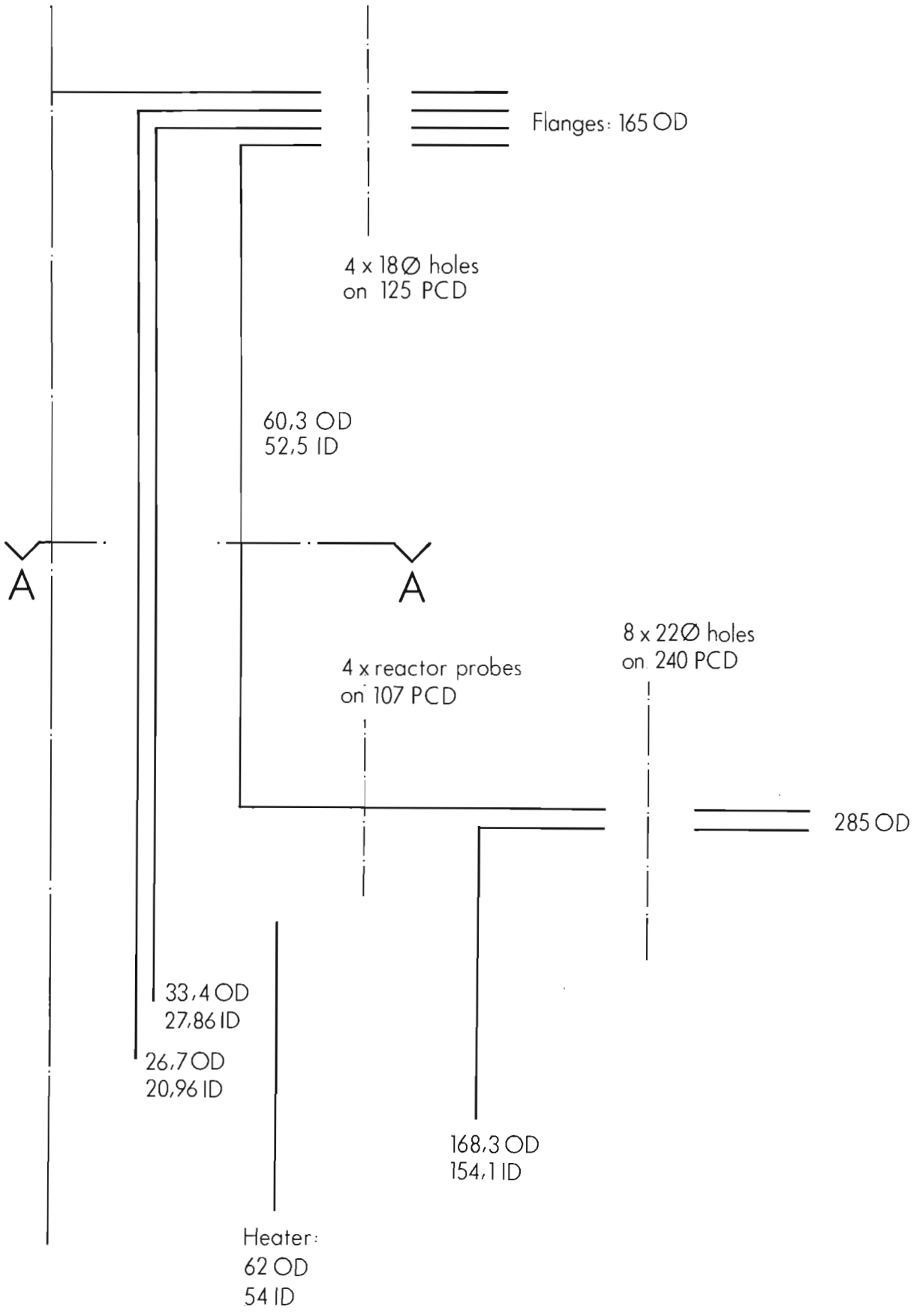
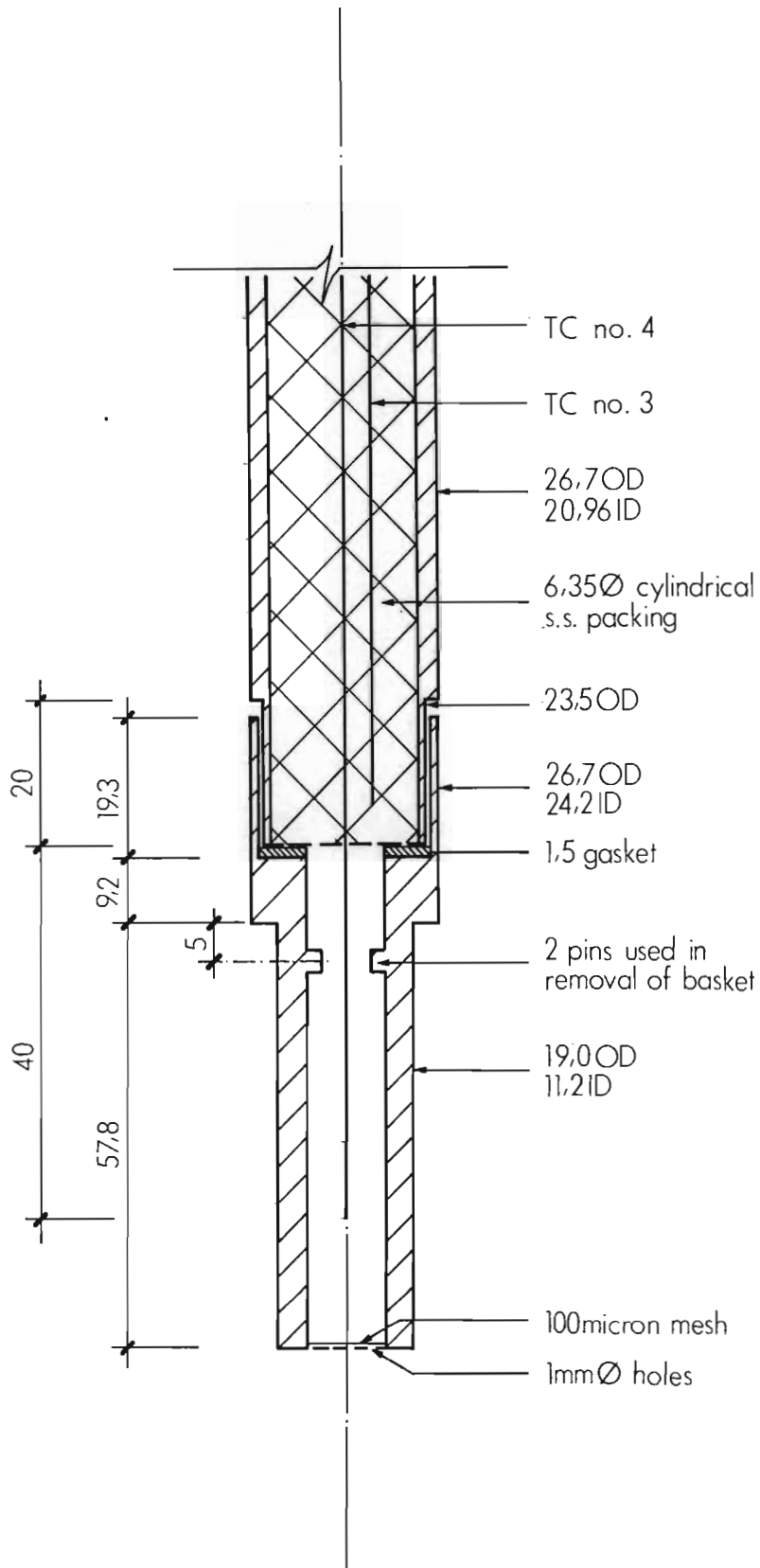
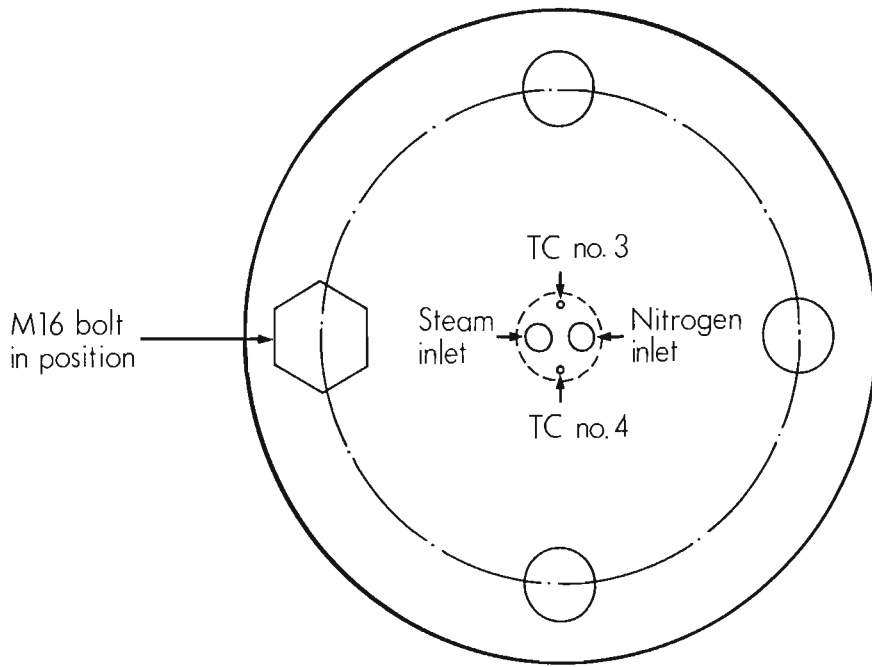


FIGURE 5 Radial dimensions of the microreactor



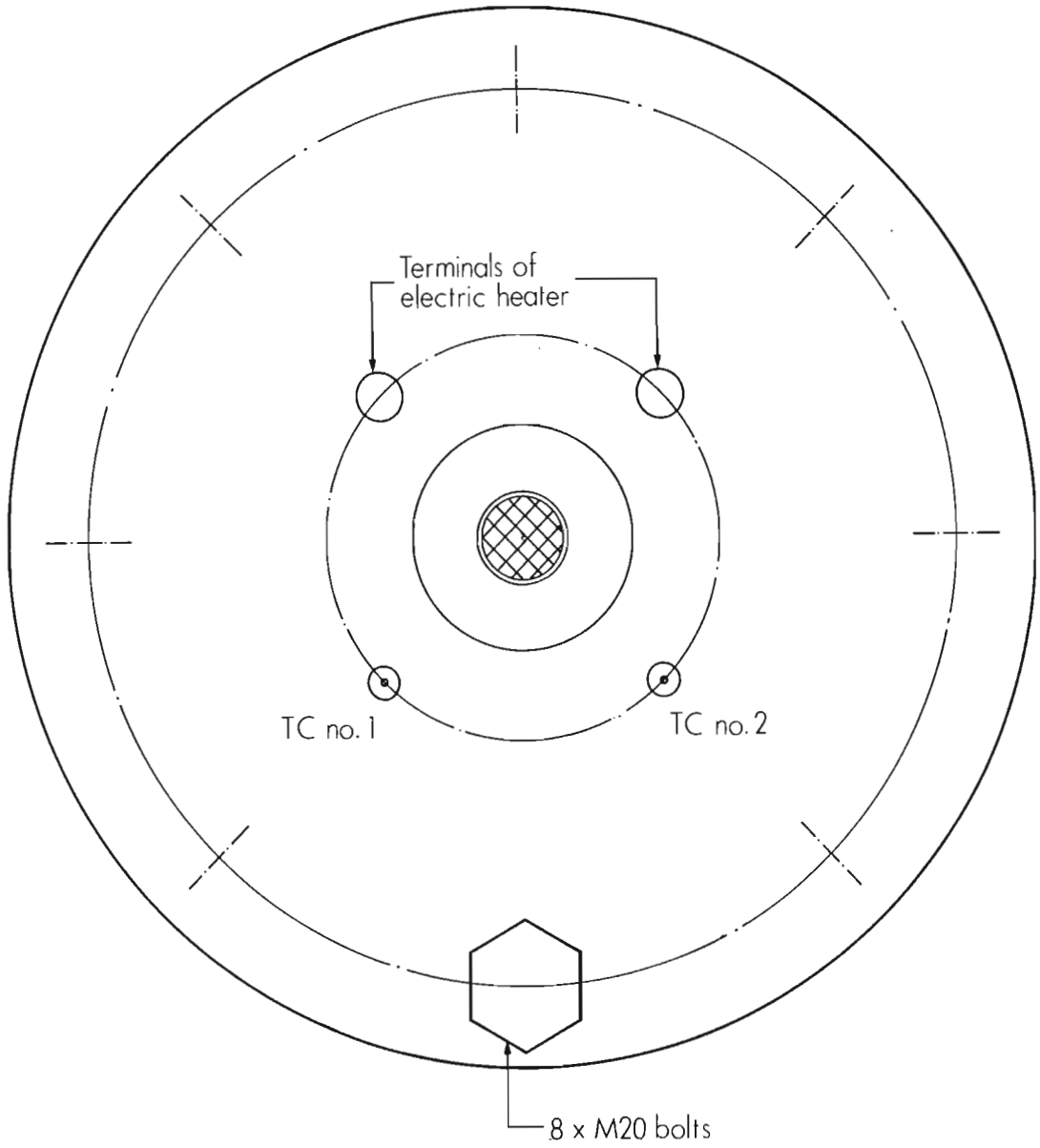
SCALE : 1:1

FIGURE 6 Detailed section through sample basket and lower end of gas heating tube



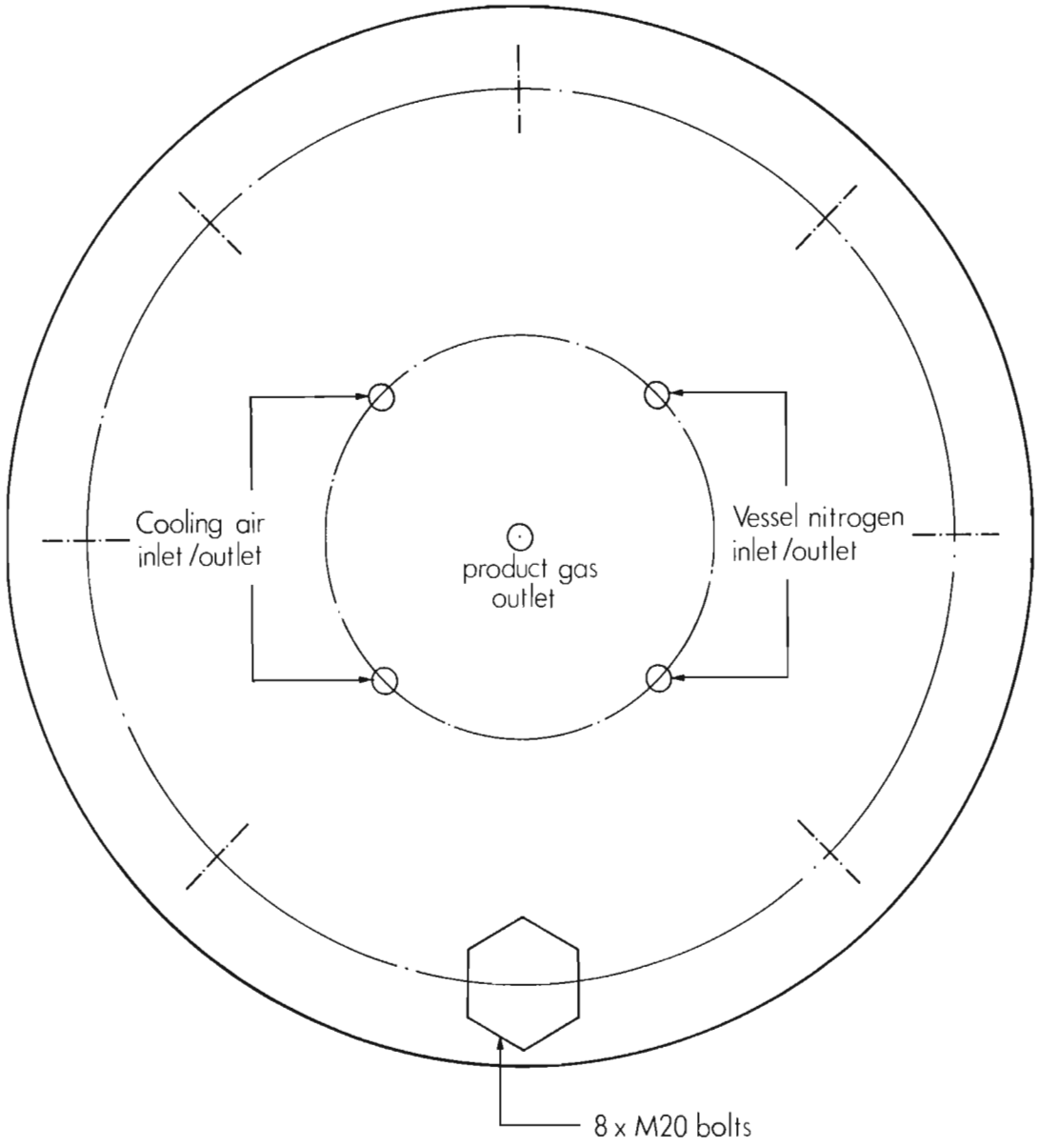
SCALE : 1:2

FIGURE 7 Top view of upper flange assembly



SCALE: 1:2

FIGURE 8 Sectional top view on plane A - A
(see Figure 5)



SCALE : 1:2

FIGURE 9 Bottom view of base flange

(3.7)

The removal of the steam preheating tube from the microreactor is assisted by a counter-weight which supports the mass of the tube. This counter-weight is connected via two pulleys and a cable to a point on the central axis of the steam preheating tube.

The vertical location of the electrical heater in the microreactor is such that the hot zone of the heater is directly exposed to the position of the steam heating tube and the sample basket.

A novel feature is included in the design of the microreactor to prevent the unlikely occurrence of a major imbalance of pressure across the reactor tube walls during operation. This feature involves the inclusion of a natural pressure relief system in the form of a 1mm diameter hole drilled through the upper end of the inner and outer reactor tube walls (see Figure 3).

3.4 THE TEMPERATURE CONTROL SYSTEM OF THE MICROREACTOR.

The microreactor is equipped with four type K thermocouples in order to measure the following temperatures (see Figure 2) :

- (1) The outer surface temperature of the outer reactor tube in the centre of the hot zone of the heater (T1). The tip of this thermocouple is made to contact the outer tube wall by fastening the lower end of the thermocouple to the outer tube with four loops of 1.5mm stainless steel wire;
- (2) The inner wall temperature of the pressure vessel at the elevation of the hot zone of the reactor (T2);

(3.8)

- (3) The outlet temperature of the steam preheating tube (T3). This thermocouple is contained within the steam preheating tube; and
- (4) The sample temperature (T4). This thermocouple is also contained in the steam preheating tube and protrudes from a central hole in the perforated plate on the lower end of the tube, as is shown in Figure 6.

Thermocouples T3 and T4 penetrate the top flange of the upper flange assembly of the microreactor, and thereby enter the steam preheating tube. The locations of these points of penetration are shown in Figure 7. In view of the restricted area available for this purpose, thermocouples T3 and T4 are sealed into the top flange by means of silver solder. Thermocouples T1 and T2 penetrate the top flange of the pressure vessel at the locations shown in Figure 8.

The temperatures T1 and T2 of the microreactor are displayed on channels 1 and 2, respectively, of a Fluke 2190A digital thermometer which is situated adjacent to the microreactor. Thermocouples T3 and T4 are employed to control the temperature of the microreactor. The philosophy of the temperature control system of the microreactor is discussed below.

The electrical circuit diagram of the microreactor is illustrated schematically in Figure 10. The temperature of the sample within the sample basket (T4) is controlled by a 'Eurotherm' model 070 PID temperature controller which regulates the electrical power supply

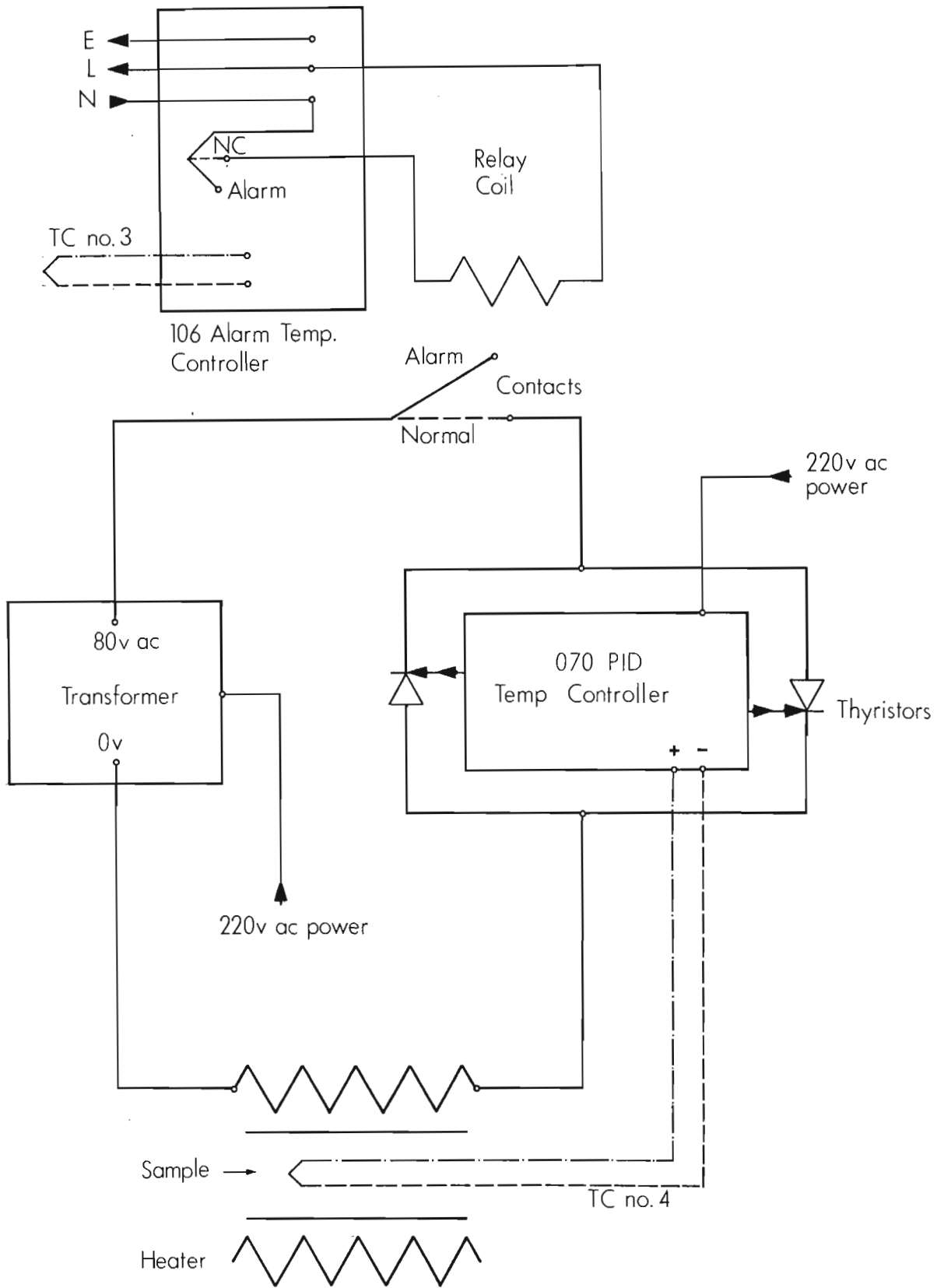


FIGURE 10 Electrical circuit diagram of the microreactor

(3.9)

to the heater of the microreactor. The operation of the temperature controller involves phase angle firing of a pair of thyristors which are rated to operate at a maximum of 25A. For this reason, the voltage supplied to the 070 temperature controller is limited to 80v a.c. by a voltage transformer, since the nominal resistance of the electric heater is 3.2 ohms.

A 'Eurotherm' model 106 alarm type temperature controller is included in the electrical circuit in order to prevent the temperature of the reactor from rising above the pre-set limit. This temperature controller monitors T3 and trips the contacts of the relay which supplies power to the microreactor heater in the event of T3 rising above the set-point of the 106 controller. This action is also taken in the event of the failure (open-circuit) of thermocouple T3. During the operation of the microreactor, the set-point of the temperature alarm controller is typically set at a value of 50°C above that of the sample temperature controller.

The technique of operation of the electrical circuitry of the microreactor is discussed in detail in Appendix A2.

3.5 MATERIALS OF CONSTRUCTION OF THE MICROREACTOR.

The inner and outer reactor tubes are constructed of Inconel Alloy 600. This selection was based on the favourable mechanical and chemical properties of the material in nitrogen and reducing gas atmospheres at temperatures of up to 1100°C (Wiggin, 1971).

The sample basket was fabricated by machining a solid rod of SS310 material.

The flanges employed to seal the reactor tubes are constructed of 12mm thick SS316. These seals are not exposed to high temperatures and are achieved by compressing standard 3.2mm full face asbestos gaskets. The gaskets employed in the sealing of the sample basket are composed of 1.5mm 'Durbla' material (stable up to 1000°C).

The thermocouples which are contained in the microreactor are sheathed in 1.5mm diameter SS316 tubing. The general connecting tubing of the entire apparatus is 6.35mm OD SS304 tubing. The 'Swagelok' system of tube fittings is employed on the apparatus.

The pressure vessel is constructed from a length of seamless, mild steel, API schedule 40 pipe with a nominal diameter of 150mm. The flanges of the pressure vessel are also fabricated from mild steel and are 18mm thick.

(3.11)

The seals between the pressure vessel and the surrounding atmosphere at the points of penetration of the various probes of the vessel are achieved by standard stuffing box arrangements with square-sectioned teflon packing material. Figure 9 shows the locations of the probes which penetrate the base flange of the pressure vessel.

The seals for the electrical connections to the heater and for the thermocouples which penetrate the pressure vessel are terminated by teflon male studs in order to provide added protection.

3.6 DESIGN DETAILS OF THE PERIPHERAL COMPONENTS OF THE APPARATUS.

3.6.1 THE BOILER.

The steam required for gasification is generated by an electrically heated 'Hot Shot' laboratory boiler. The maximum capacity of the boiler is 2kg/hour and the maximum attainable steam pressure is 5 bar gauge. A 'Bailey's' G4 pressure regulator is installed downstream of the boiler to enable a steady steam pressure to be supplied to the reactor.

The technique of operation of the boiler is discussed in detail in Appendix A3.

The reactant steam is carried to the point of the second strainer downstream of the boiler, shown in Figure 2, by regular 12.5mm

(3.12)

diameter steam piping, after which the steam is carried to the microreactor by 6.35mm diameter stainless steel tubing. The piping and tubing which carry steam in the apparatus are electrically heated by an outer layer of insulated nichrome wire in order to prevent condensation of steam in the respective lines. The fabrication of these heating tapes involves wrapping a single layer of insulation tape around the relevant tube, followed by a spiral of nichrome wire and ultimately two further layers of insulation tape. The insulation tape employed for this purpose is adhesive 'Refrasil' material of width 50mm and thickness 1.5mm. The tape is applied to the tubing by laterally wrapping precut lengths onto the various sections of tubing. A spacing of about 20mm is employed between the spirals of nichrome wire which are terminated by securing the wire tightly to the ends of the insulated tube length and by consecutive doubling back of the ends of the wire to create a low resistance path for electricity. The entire apparatus contains three sets of independent heating tapes which are powered by separate variable transformers.

3.6.2 THE STEAM CONDENSERS.

Two identical steam condensers are included in Figure 2, namely C1 and C2. C1 is employed to allow steam to bypass the microreactor in order to develop steady conditions in the steam line upstream of the reactor whilst the reactor is being heated to the desired operating temperature of an experiment. C2 is employed to totally condense the steam content of the product gas stream during char gasification experiments.

(3.13)

The design of the condensers is shown in Figure 11. Steam condenses in the annular region between two coaxial, vertical stainless steel pipes. Cooling is effected by water flowing within a helical copper coil which is wrapped around the inner vertical condenser pipe. The steam laden product gas stream enters the condenser at the base of the annular region, and the products of gasification exit at the top of the condenser.

A condensate accumulator is located below the condenser. During steady operation of the apparatus, the level of the condensate in the accumulator, which is displayed in a sight glass, is maintained at a steady position by adjusting the position of the needle valve downstream of the accumulator. At steady state, the flowrate of condensate from C2 equals the flowrate of steam entering the microreactor.

3.6.3 THE PRODUCT GAS DRIER.

The product gas stream is dried downstream of condenser C2, before proceeding to the gas analysis system. The drier comprises a 25.4mm stainless steel tube which holds a packed bed of approximately 10 grams of anhydrous magnesium perchlorate. The product gas stream flows downward through the drier. Anhydrous magnesium perchlorate is widely employed in chemical laboratories for the quantitative extraction of moisture from gases (Vogel, 1961).

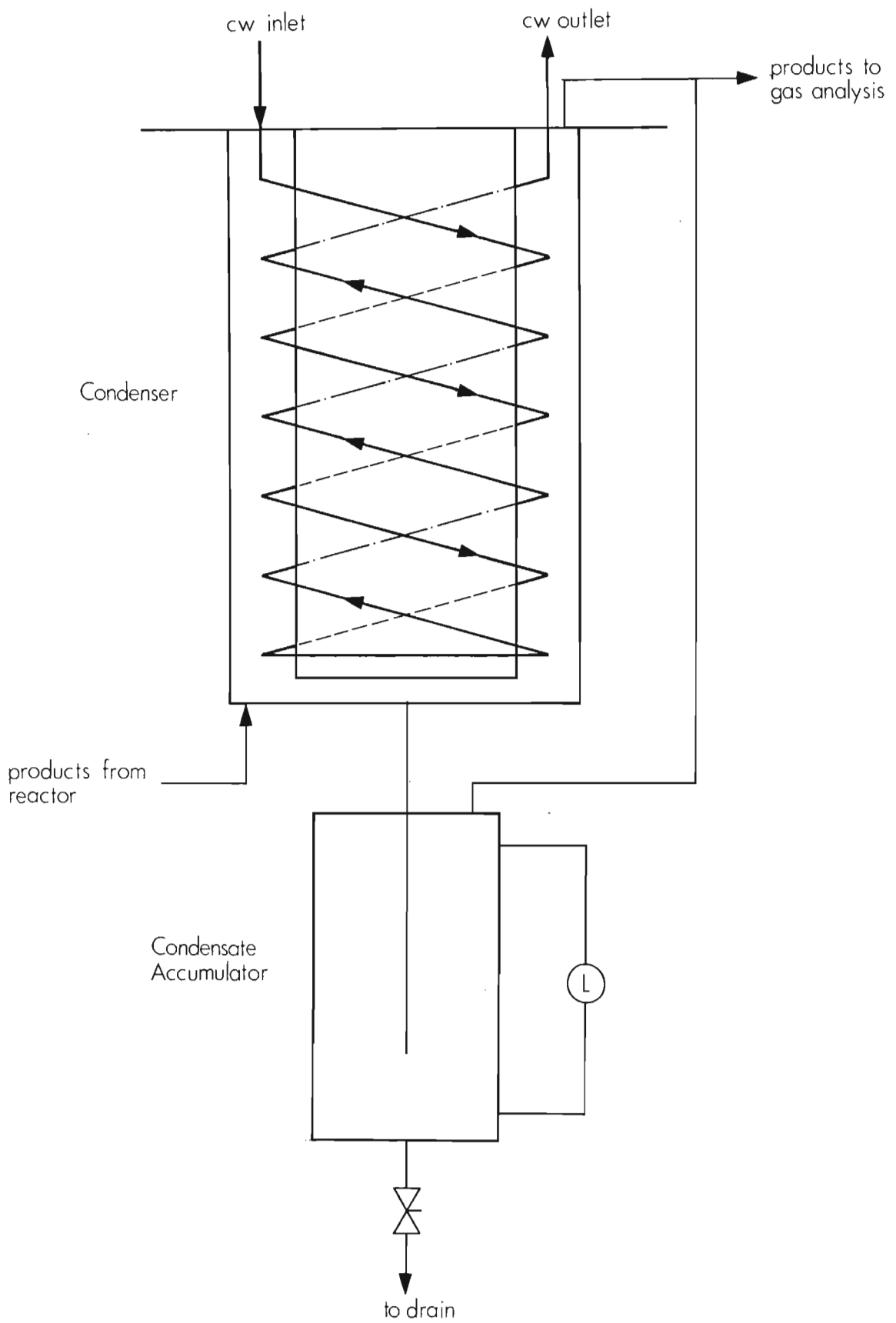


FIGURE 11 Detailed section through steam condenser arrangement

3.6.4 THE PRODUCT GAS ANALYSIS SYSTEM.

3.6.4.1 THE GAS SAMPLING SYSTEM.

Samples of the product gas stream are stored in a 16 loop 'Valco' gas sampling valve which is located downstream of the gas drier. The valve comprises an inlet and an outlet stream which may be internally connected to any one of the 16 sample loops by rotating the central shaft of the valve. The position of the valve is adjusted pneumatically and displayed by a remote control box. The sample loops consist of 3.175mm O.D stainless steel tubing which contain an internal volume of approximately 0.5ml.

At the beginning of an experiment loop no. 2 of the sample valve is selected. As the experiment proceeds, gas samples are stored sequentially in the respective loops by advancing the valve to the following position. Loop no. 1 is employed in the flushing of the analysis system between the sampling and the analysing of the product gas stream.

3.6.4.2 THE GAS ANALYSIS TECHNIQUE.

The compositions of the samples of the product gas stream are determined by gas chromatography by employing a temperature programmed analysis on a Varian 3300 GC. The GC is installed with a single 3m x 3.175mm Carbosieve SII packed column and a thermal

(3.15)

conductivity detector. This technique is capable of resolving H_2 in high concentrations, O_2 , N_2 , CO , CH_4 , and CO_2 under the following operating conditions :

- (1) Column temperature program :
 - Initial temperature = $35^{\circ}C$;
 - Holding time at initial temperature = 7minutes;
 - Heating rate = $32^{\circ}C$ /minute;
 - Final temperature = $225^{\circ}C$;
 - Holding time at final temperature = 10minutes.
- (2) TCD filament current = 136mA.
- (3) The TCD polarity reverses after 4 minutes of analysis. This allows one to record the response from the GC during the entire analysis, since the relative thermal conductivity of H_2 is opposite in polarity to the thermal conductivities of the other components of the product gas.
- (4) Carrier gas composition = 10% H_2 in He. This composition of carrier gas is known to have the lowest thermal conductivity of H_2 - He mixtures, which allows one to resolve H_2 more readily than with a pure Helium carrier gas, since the thermal conductivities of H_2 - He mixtures with more than 10% H_2 are all higher than that of the 10% H_2 in He gas.
- (5) Carrier gas flowrate = 30ml/min.
- (6) Gas sample volume = 0.5ml.

During an analysis, the response from the GC is recorded on a Varian 4270 Integrator. On completion of a chromatogram, the integrator reports the areas between the recorded signal and the baseline for each of the distinct components of the sample. A typical chromatogram is shown in Figure 37.

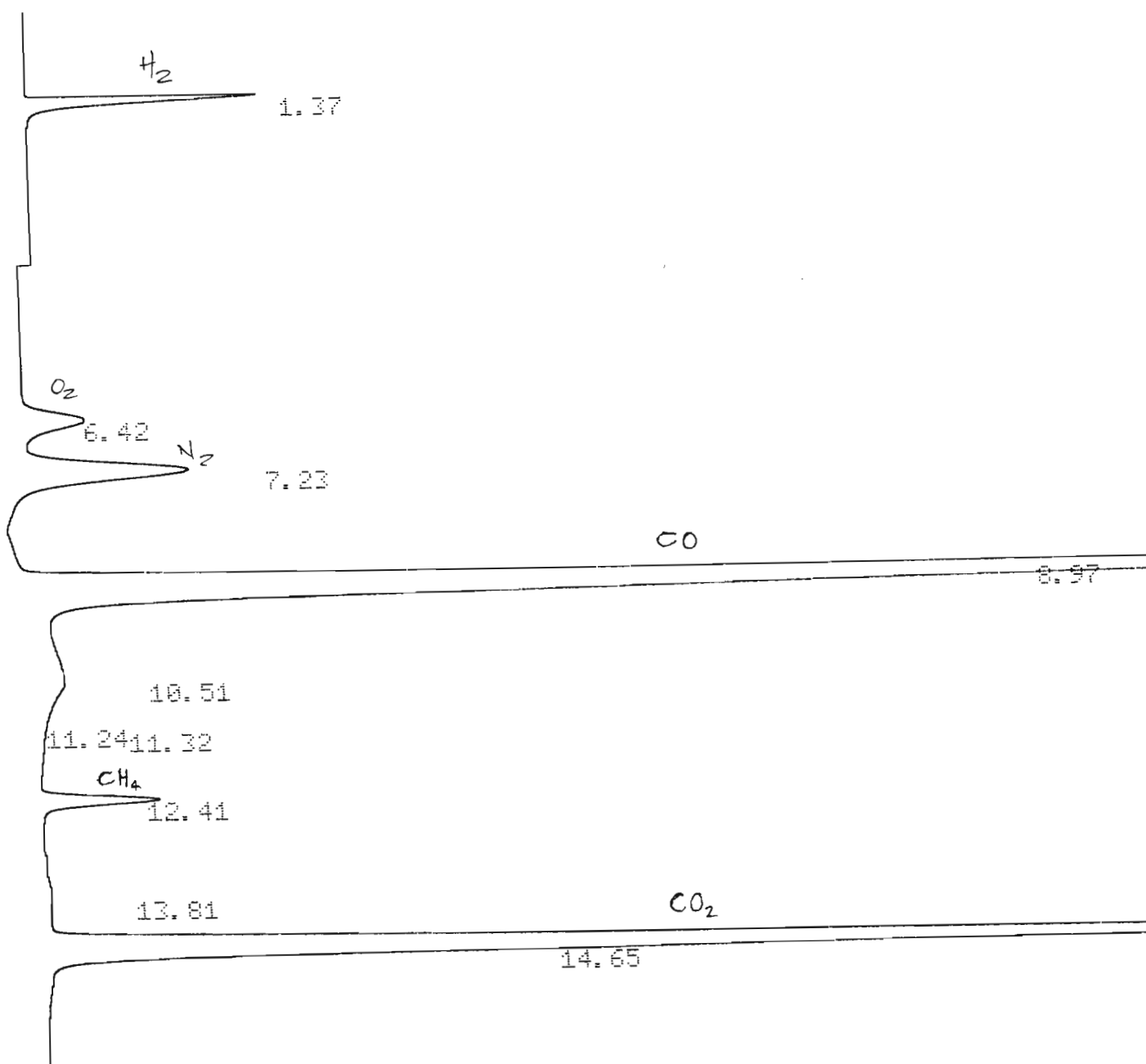


FIGURE 37 A typical chromatogram obtained during the analysis of a sample of the product gas stream from the microreactor.

(3.16)

3.6.4.3 PRODUCT GAS FLOWMETER.

A 'Schutte Koerting' SK-1/8-15-G-5 rotameter was employed with a spherical black glass float to measure the flowrate of the product gas stream from the microreactor.

3.7 ILLUSTRATIONS OF THE EXPERIMENTAL APPARATUS.

Plates 1 to 6, which are contained on the following three pages, illustrate the appearance and the scale of the experimental apparatus employed in this kinetic study.

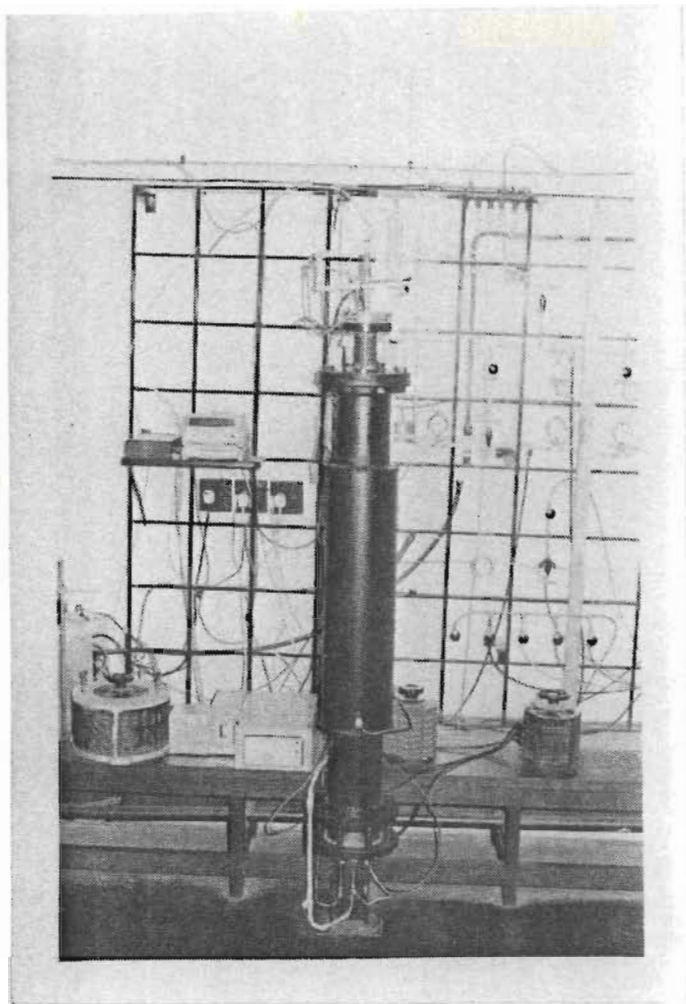


PLATE 1. The front view of the microreactor.

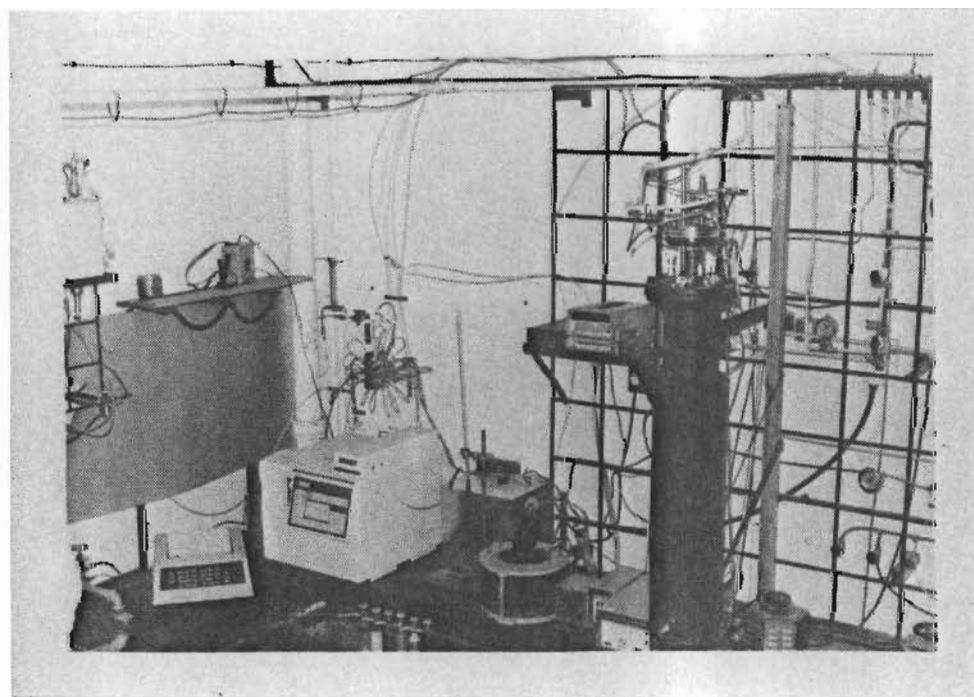


PLATE 2. The gas analysis system alongside the microreactor.

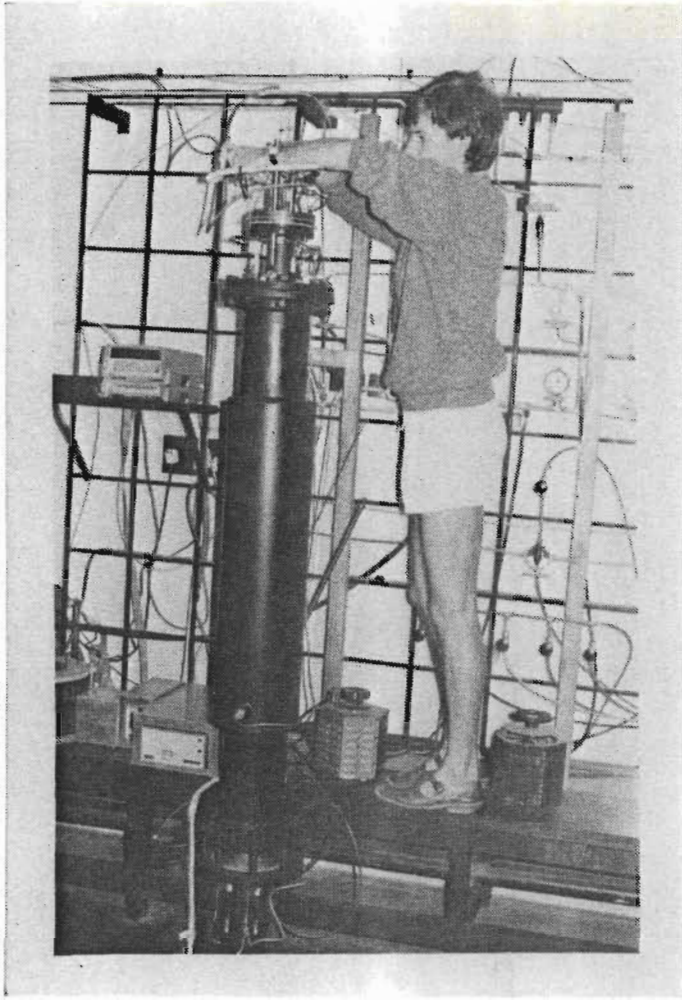


PLATE 3. The position adopted to seal the top flange assembly.

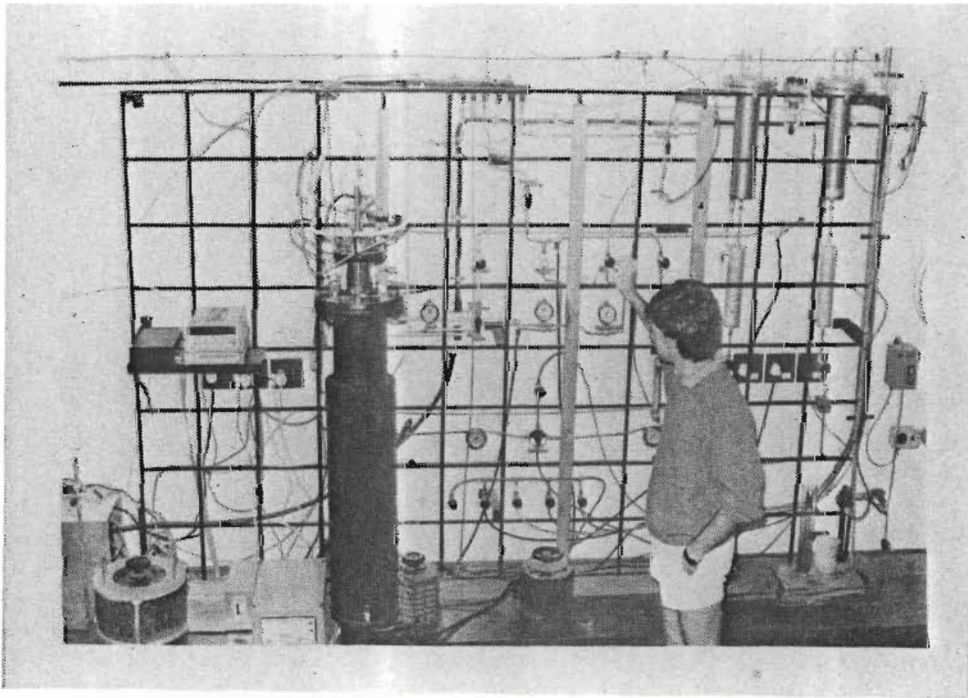


PLATE 4. The control panel of the apparatus.

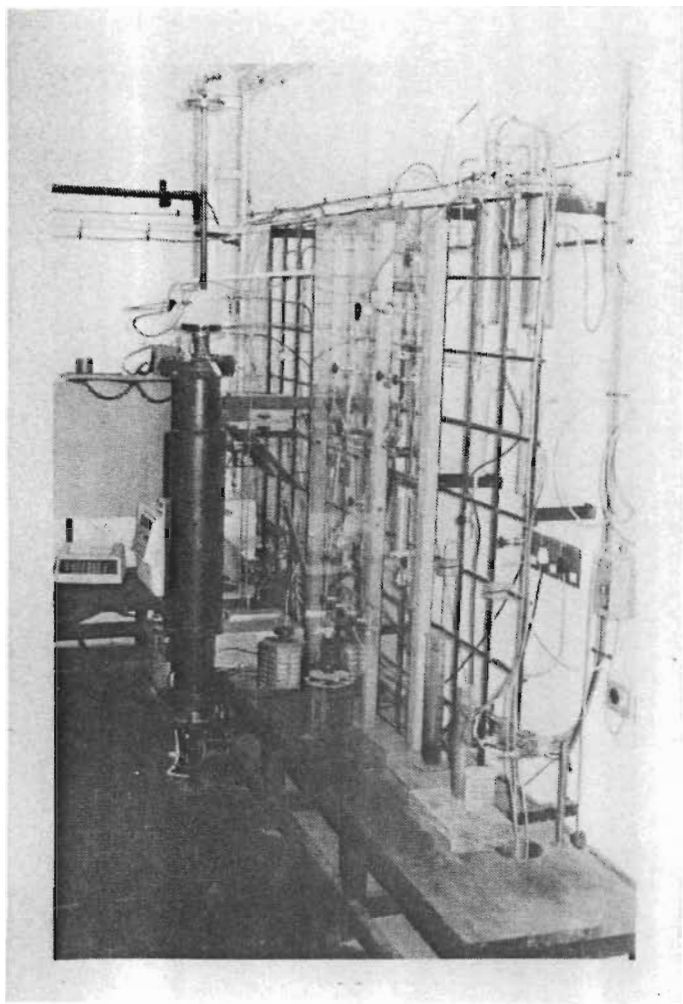


PLATE 5. The right side view of the microreactor with the gas preheating tube removed.

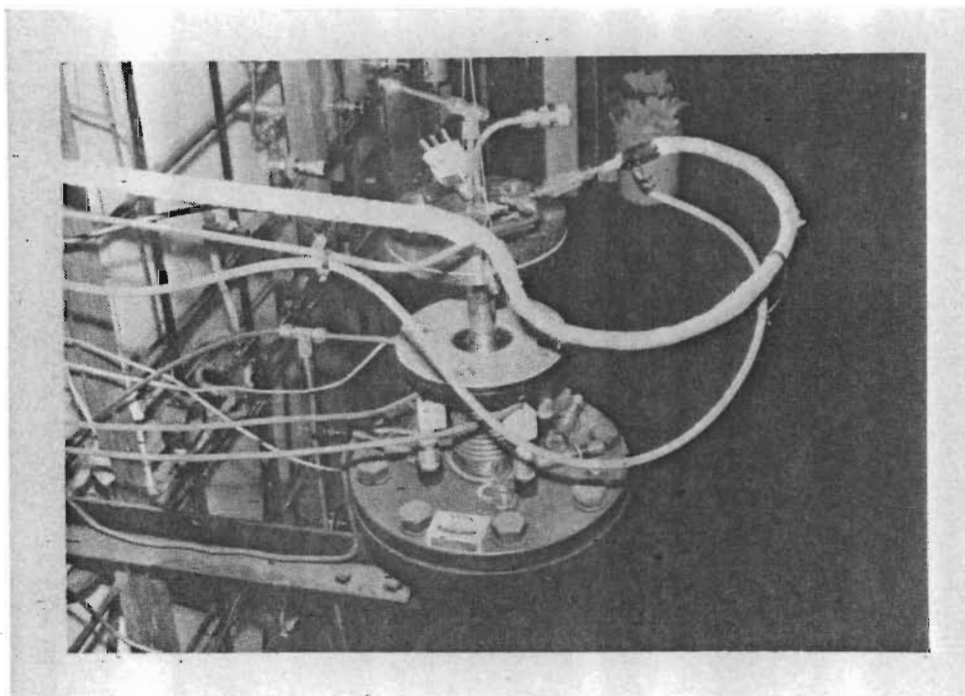


PLATE 6. A close-up view of the upper flange assembly.

(4.1)

CHAPTER 4.

STEAM-CHAR GASIFICATION KINETIC STUDIES.

4.1 EXPERIMENTAL TECHNIQUE.

The experimental approach employed in this study is that of product gas analysis using the microreactor apparatus described in Chapter 3. The experimental procedure involves heating a coal-char sample contained within the microreactor to the desired reaction temperature in a nitrogen atmosphere, after which steam is directed to the char sample in order to initiate steam-char gasification. During gasification of the char sample, the temperature of the sample is controlled at a constant value whilst the sample is exposed to an isobaric steam environment.

Samples of the gaseous products of gasification are collected in a multiple loop gas sampling valve downstream of the microreactor at various time intervals after the start of gasification. The composition of these gas samples are determined by gas chromatography after the gasification experiment has been completed. The flowrate of the product gas stream is also recorded at various time intervals after the start of gasification, at the position of the gas sampling valve.

The experimental procedure and the technique of operation of the experimental apparatus are reported comprehensively in Appendix A.

*Substrate
to sample*

4.2 TECHNIQUE OF PREPARATION OF COAL-CHAR SAMPLES.

The char samples employed in the experimental program of this study were derived from representative samples of two South African coal resources, namely Bosjesspruit and Transvaal Navigation coal. The reasons for considering Bosjesspruit coal in this study are as follows :

- Bosjesspruit coal is mined from one of the largest collieries in S.A. and is currently employed in the Lurgi gasifiers at the Secunda plant of SASOL. The kinetic results are therefore of interest to SASOL.
- A large quantity of duff coal is generated at the colliery. This coal is unsuitable for use in the Lurgi gasifiers and may be employed in the Judd gasifier.

The composition of Transvaal Navigation coal differs somewhat with respect to the composition and the content of ash and also with respect to the content of volatile matter, compared to that of Bosjesspruit coal, and has been principally employed in this study to compare the effects of these differences on the kinetics of steam gasification. The properties of these coal resources are shown in Tables 4.1 to 4.4 respectively. The technique employed to withdraw samples from the bulk samples of the respective coals was according to that specified by the S.A.B.S. After sampling, the coal samples were crushed to a particle size of less than 0.45mm. The samples were then classified by separating the material of $d_p < 0.15\text{mm}$. The

(4.3)

larger size fraction of each coal sample, namely $0.15\text{mm} < d_p < 0.45\text{mm}$, was then divided by riffle splitting into 20g samples. These samples were then employed to generate samples of coal-char for use in the steam gasification experiments.

(4.4)

Proximate Analysis	Ultimate Analysis	Size range	Mass fraction
(Air dry basis)	(ADB)	/ mm	
H ₂ O 3,9 %	H ₂ O 3,9 %	> 6,30	-
Ash 20,9	Ash 20,9	4,75 to 6,30	0,054
VM 21,9	C 60,4	3,35 to 4,75	0,101
FC 53,3	H 3,2	2,63 to 3,35	0,121
CV 31,0 MJ/kg	O 9,8	1,70 to 2,63	0,117
	N 1,6	1,18 to 1,70	0,148
	S 0,2	0,85 to 1,18	0,115
		0,425 to 0,85	0,189
		< 0,425	0,155

TABLE 4.1 Properties of Bosjesspruit coal.

	C o m p o n e n t									
	SiO ₂	Al ₂ O ₃	Fe ₂ O ₃	P ₂ O ₅	TiO ₂	CaO	MgO	K ₂ O	Na ₂ O	SO ₃
Mass % in Mineral Matter	43,6	26,3	6,47	1,43	1,43	11,8	3,64	0,57	0,60	4,06

TABLE 4.2 Mineral matter composition of Bosjesspruit coal.

(4.5)

Proximate Analysis		Ultimate Analysis	
(Air dry basis)		(ADB)	
H ₂ O	2.7 %	H ₂ O	2.7 %
Ash	15.1	Ash	15.1
VM	28.0	C	68.2
FC	53.5	H	4.2
CV	27.5 MJ/kg	O	7.4
		N	1.7
		S	0.8

TABLE 4.3 Properties of Transvaal Navigation coal.

	C o m p o n e n t									
	SiO ₂	Al ₂ O ₃	Fe ₂ O ₃	P ₂ O ₅	TiO ₂	CaO	MgO	K ₂ O	Na ₂ O	SO ₃
Mass % in Mineral Matter	48.0	34.7	6.18	0.56	1.76	3.26	1.44	0.58	0.13	2.59

TABLE 4.4 Mineral matter composition of Transvaal Navigation coal.

(4.6)

Coal-char samples were prepared by pyrolysing each of the respective 20g samples of coal at 800°C in a nitrogen atmosphere to prevent oxidation of the fixed carbon content of the coal. The char samples were prepared at 800°C for the following reasons :

- This temperature was chosen as the base-case temperature of the steam-char gasification experiments, it being the lowest temperature at which significant rates of reaction were measured during the experimental program. The chars which were gasified at higher temperatures were pyrolysed in situ while the microreactor was being preheated to the reaction temperature;
- It is reported by van Heek and Muhlen (1987) that a characteristic pyrolysis temperature (typically above 800°C) seems to exist for all chars at which the reactivity of the char concerned is drastically reduced within a relatively short residence time.

Two different techniques were employed in the preparation of the char samples.

The first technique involves top-feeding a sample of coal into an electrically heated mini-fluidised bed at 800°C. The fluidised bed contains 200g of silica particles of $d_p < 0.15\text{mm}$. This technique was designed to simulate the conditions of coal pyrolysis in the Judd gasifier as closely as possible by generating char at a relatively rapid heating rate, which is typical of fluidised bed coal gasifiers. After loading the coal sample into the

(4.7)

mini-fluidised bed, the temperature of the bed is maintained at 800°C for 3 minutes, after which the bed is cooled to room temperature in a nitrogen atmosphere. The char is then separated from the bed inventory by size classification.

The second technique employed in the preparation of char samples in this study involves the use of a horizontal tubular furnace which contains a stainless steel tube divided into a nitrogen heating region and a sample holding region. The nitrogen heating region contains a packed bed of 6.35mm stainless steel pellets whilst the sample holder consists of a smaller diameter tube which slides coaxially into the outer tube and seals against the one end of the outer tube. The technique employed to generate char in the horizontal furnace involves heating the furnace to 800°C in a nitrogen atmosphere after which one loads the coal sample into the reactor tube. The coal sample is then heated to 800°C at a relatively slow rate. The procedure employed in this study is to hold the furnace at 800°C for one hour, after which no significant change in the mass of the sample is observed. Thereafter one allows the char to cool to room temperature in a nitrogen atmosphere.

Although the latter technique of char preparation does not appear to simulate the pyrolysis conditions in a fluidised bed gasifier, it was decided to employ the tubular furnace for the preparation of most of the char samples used in this study for the following reasons :

- The tubular furnace technique is a more convenient method of

preparing char because of the simplicity of the apparatus and the elimination of any size classification of produced char;

- It was suspected that very little difference (if any) would be realized in the steam reactivity of the char samples prepared using either the fluidised bed or the tubular furnace techniques. This is suggested by Radovic et al.(1985) who studied the effect of residence time at a pyrolysis temperature of 1000°C on the reactivity of a lignite char in H₂O and CO₂. Their results showed that the char reactivity had declined considerably after pyrolysis for 3 seconds; after 5 minutes the char reactivity had reached its lowest value and had not declined further after a residence time of 1 hour. Certainly, the reactivities of chars prepared in a drop-tube furnace (with very rapid heating rates similar to those which prevail in an entrained bed gasifier) would be expected to be greater than those prepared in either of the techniques employed in this study;
- It was also suspected that the reactivity of the char samples may be affected by the preheating of the microreactor to the desired reaction temperature. Ashu et al. (1978) and Howard et al. (1981) claim that the decrease in reactivity in char with increasing residence time of pyrolysis may be attributed to thermal annealing, which promotes deactivation of the char due to realignment of the coal layer planes. This effect is expected to occur to the char sample contained in the microreactor during the period of initial heating (approximately 30 minutes). It is the opinion of the author,

(4.9)

however, that because of the large volume of the annulus zone of the Judd gasifier, the residence time of char in the pyrolysis and gasification zones of the annulus is relatively high (in the region of 5 - 10 minutes, for average geometries) which results in the promotion of thermal annealing of the char structure. It is therefore highly probable that the reaction rates measured in the microreactor are representative of those which occur in the gasification zone of the Judd gasifier.

(4.10)

The compositions of the char samples employed in the experimental program are shown in Table 4.5, below. These compositions were determined by combusting samples of the char at 800°C in a muffle oven for one hour. Note that the fraction of the char which combusts under these conditions has been assumed to represent the fixed carbon content of the char, ie. it is assumed in this study that the char comprises a negligible quantity of volatile matter after having been pyrolysed at 800°C.

Sample number	Coal ⁺⁺ source	Preparation ^{**} technique	Composition / mass%	
			Ash	Fixed carbon
B1	B	FB	29.06	70.94
B2	B	FB	32.24	67.76
B3	B	FB	29.52	70.48
B4	B	FB	30.27	69.73
B5	B	TF	30.27	69.73
T6	T	TF	14.43	85.57

TABLE 4.5 Compositions of char samples employed in the experimental program.

⁺⁺ B = Bosjesspruit coal

T = Transvaal Navigation coal

^{**} FB = Pyrolysis at 800°C in a fluidised bed

TF = Pyrolysis at 800°C in a tubular furnace

4.3 EXPERIMENTAL CONDITIONS.

In view of the kinetic results reported by other authors in the steam-char gasification literature, numerous experiments have been conducted in this study at temperatures from 800°C to 920°C and at steam pressures of 1.8; 3.3 and 4.8 bar absolute using char derived from Bosjesspruit coal. These experiments have been conducted in order to investigate the effects of temperature and pressure on the steam-char gasification kinetics under conditions in which the kinetics are likely to be controlled by the rates of the chemical reactions. The pressure of operation during an experiment is limited by the maximum delivery pressure of the boiler, namely 5 bar gauge (The microreactor is, however designed to operate at 10 bar gauge). Experiments have also been conducted at temperatures between 840°C and 920°C with a steam pressure of 1.8 bar absolute using char derived from Transvaal Navigation coal.

The conditions under which the various experiments were conducted are summarized in Table 4.6, below. Note that the first 25 experiments were required to successfully develop the overall design of the apparatus and the experimental technique which is currently employed.

Run no.	Char sample no.	Reaction temp. °C	Steam pressure/ bar abs.	Sample mass/ g	Steam flowrate/ g/min.
26	B1	800	1.8	2.86	9.50
27	B1	840	1.8	2.06	9.64
30	B1	880	1.8	1.91	9.61
34	B2	840	3.2	2.30	13.34
35	B2	880	3.2	2.71	9.81
36	B1	920	1.8	1.99	9.42
37	B2	920	3.2	3.09	7.07
38	B3	840	4.6	1.59	8.34
40	B3	880	4.6	3.07	9.56
42	B3	880	4.6	3.04	14.00
45 ^{R27}	B4	850	1.8	3.37	8.83
47	B5	880	1.8	2.39	4.74
50	T6	850	1.8	3.59	7.65
51 ^{R30}	B4	880	1.8	3.46	8.41
53 ^{R30}	B4	880	1.8	3.00	8.68
54 ^{R36}	B4	920	1.8	2.49	8.99
56	T6	920	1.8	2.89	6.00

TABLE 4.6 Experimental conditions for the measurement of the kinetics of steam-char gasification.

Note : Runs superscripted with R denote replicate experiments.

4.4 TECHNIQUE OF INTERPRETATION OF EXPERIMENTAL DATA.

The principle of operation of the microreactor employed in this study involves the differential conversion of the reactant steam stream during the gasification of the char sample. This feature allows char gasification to be studied in a gas environment of essentially pure steam; (the maximum conversion of steam observed in this study was approximately 2.5%). The existing microreactor is not, however, limited to a pure steam environment, and different mixtures of reactant gas may also be employed. During the course of an experiment the level of conversion of the fixed carbon content of the char increases with time as carbon is consumed in the steam gasification reaction.

This study employs the product gas analysis approach, in which the rates of production of gaseous products of the steam-char gasification reaction are obtained directly from the measurement of the composition and flowrate of the products of gasification, downstream of the reactor. The rate of consumption of carbon in the steam-char gasification reactions is calculated by summing the rates of appearance of carbon in the product gas stream in the form of CO, CH₄, and CO₂. It is assumed in this study that no other carbonaceous products (ie. light hydrocarbons, tars and oils) are formed during gasification under the experimental conditions investigated. In order to detect the presence of the products of gasification at the gas sampling system, the outlet of the product rotameter is directed at an instrument (Warnex alarm) which is

(4.14)

sensitive to the presence of inflammable gases. This technique is employed to signal the time at which the initial products of gasification reach the gas sampling system. This moment is regarded as the gasification-time reference of the experiment, or the time-zero of the duration of steam-char gasification during the experiment.

The kinetic results are reported as a function of the fractional fixed carbon conversion (or fractional conversion) of the char sample by calculating the cumulative amount of carbon which passes the gas sampling system after the time-zero of the steam-char gasification, relative to the amount of carbon initially present in the char sample.

A computer program has been written to determine the results of an experiment. The program is written in BASIC and runs on an IBM compatible personal computer. A listing of the program is contained in Appendix C1.

The program begins by prompting the user for the data gathered during an experiment. This data includes details of the operating conditions of the experiment and the experimental results. The following experimental results are required by the program :

- (1) The product gas flowrates and the corresponding run-times at which these were recorded.
- (2) The identity of the gas samples and the corresponding run-times at which these were recorded.

- (3) The characteristic chromatogram areas of each of the product gas samples collected during an experiment.
- (4) The steady steam flowrate which passed through the microreactor during an experiment. This result is employed qualitatively to check the level of conversion of the reactant steam which occurred during an experiment.

Note that the product gas flowrates are recorded at slightly different time intervals after the initiation of char gasification than the time intervals at which samples of the product gas stream are captured. This is because the product gas rotameter and the sampling valve are arranged in parallel downstream of the microreactor (see Figure 2). The reason for this arrangement is that the pressure drop across the gas sampling valve varies slightly as one varies the position of the sampling valve. This occurs because the various sampling loops consist of physically separate lengths of tubing which inevitably possess slightly varied dimensions. The pressure drop across the rotameter route is caused to be equal to the nominal pressure drop across the gas sampling valve by the inclusion of a restriction in the line upstream of the rotameter. This feature prevents the occurrence of major pressure surges in the product gas stream and allows the product gas stream to flow through a path of constant resistance for the purposes of measuring the flowrate of the gas products, throughout the duration of an experiment.

In this study, the time elapsed during an experiment is termed the

(4.16)

run-time. The initiation of the experiment per se is defined as the moment at which power is first supplied to the electrical heater, at the beginning of the reactor heating phase. The gasification-time of the experiment is defined as the time elapsed since the gasification-time reference point, which was defined earlier. The convention employed in this study to represent an arbitrary run-time involves the use of a decimal number with four decimal places. The digit which precedes the decimal point represents the hourly component of the run-time; the first two decimal digits represent the 'minutes' component of the run-time; whilst the last two decimal digits represent the 'seconds' component of the run-time.

A typical set of experimental data (input data) gathered during a run is contained in Appendix B1. This data set appears in the exact sequence in which the computer program prompts one for input data.

Having prompted one for the experimental input data the computer program ('Rates') then stores the input data on disk after which it proceeds with the computation of the reaction rates. The following computations are executed in the process of the calculation of the kinetic results :

- (1) The compositions of the product gas samples are determined by employing the relevant G.C. calibration factors for the various components of the gas samples. The G.C. calibration factors for the respective components of the products of gasification are contained in Appendix B2. Note that three sets of calibration factors are reported : one set for each

separate supply of carrier gas employed in the study. The technique of calibration of the G.C. is reported at the end of Appendix A5.

- (2) The compositions of the product gas stream at each of the gasification-times at which the flowrate of the product stream was measured are then determined by cubic spline interpolation of the gas sample composition-time data.
- (3) The actual volumetric flowrates of the product gas stream are then determined by employing the calibration factors of the rotameter for air and by including the relevant conversion factors to account for the differing densities of the product gas stream.
- (4) The molar rates of production of the various components of the product gas stream are then computed, assuming that ideal gas behaviour is displayed by the product gas stream.
- (5) The molar rates of gasification of carbon are then computed at the gasification-times of the measurement of the product gas flowrates by summing the contributions by carbon to the various component flowrates of the product gas stream.
- (6) The fractional fixed carbon conversion of the char is then computed at each of the gasification-times at which the flowrate of the product gas stream was measured. It is assumed in these computations that the rate of carbon gasification is steadily maintained at the value corresponding to the previous product gas flowrate during the time interval between gas flowrate measurements. This assumption is based on the frequency with which product gas flowrates are

(4.18)

measured, ie. during an experiment one records the flowrate as frequently as a reasonably significant change in the flowrate occurs (eg. every 0.1 unit on the scale 0 - 10).

'Rates' then stores the results of the computations in three different files on a magnetic disk. The results are stored in the form of a comprehensive report of the run; the compositions of the product gas stream as a function of the fractional conversion of char are stored in separate file, as are the rates of appearance of the products of gasification and the rate of gasification of carbon at the corresponding fractional conversions of the char sample. The file containing the report of a run may be printed after having been stored, or alternately the program is designed to read and print any report at a later stage. The program is also designed to cater for the editing of the input data set. The composition and reaction rate results of an experiment are stored in matrix form in ASCII files which are readily imported by the 'Lotus' spreadsheet software package. This package is conveniently employed to graphically present the results of the experimental program.

4.5 EXPERIMENTAL RESULTS.

The results of the experiments conducted on the kinetics of the steam gasification of the coal-char samples employed in this study are presented graphically in Figures 13a to 30b inclusive. These Figures appear in chronological order below and are arranged in sets of two Figures per experiment.

Part 'a' of each set contains rate data of the run, ie. the rates of appearance of each component of the product gas stream and the rate of gasification of carbon. These results are presented as a function of $(1 - \text{the fractional conversion of the char})$, which is equivalent to the representation of the rate data as a function of the fraction of fixed carbon present in the char. This convention has been employed to illustrate the relationship between the rate data and the concentration of carbon in the char sample.

Part 'b' of each set of results illustrates the molar composition of the dry product gas stream from the microreactor as a function of the fractional conversion of the char sample. Note that the product gas stream typically contains some nitrogen which originates from the outer vessel side of the reactor during an experiment (N_2 is not a gasification product per se; furthermore, the presence of N_2 in the product gas stream does not detrimentally affect the computation of the kinetic results in that only the products of gasification are considered.)

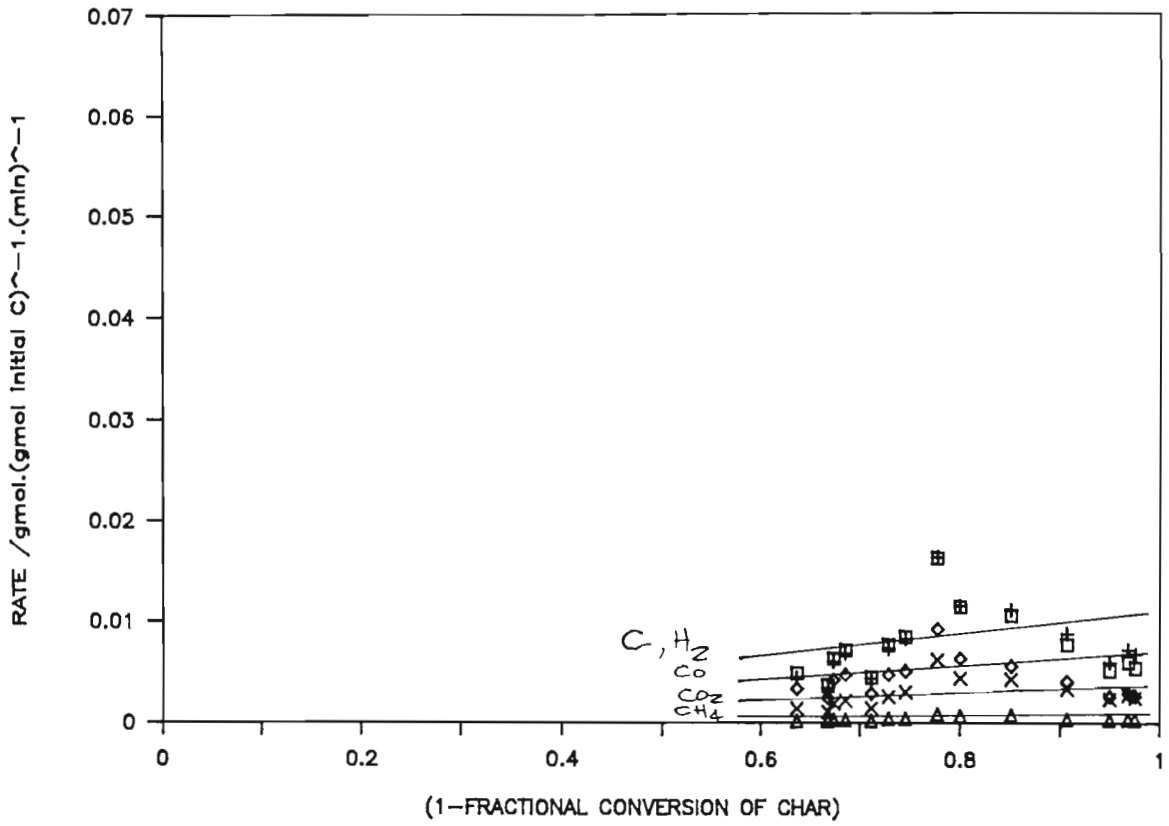


FIGURE 13a Kinetic results of Run 26 (T = 800°C; P = 1.8 bar abs.)

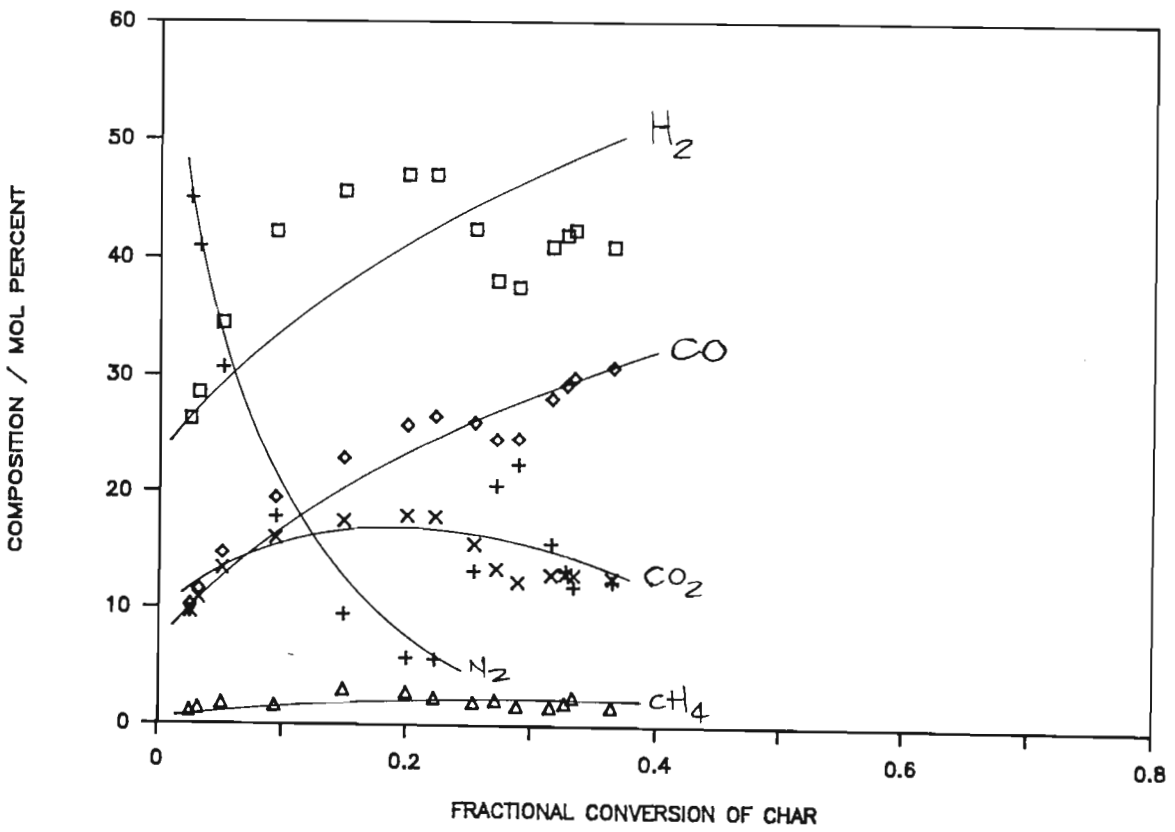


FIGURE 13b Product gas compositions of Run 26

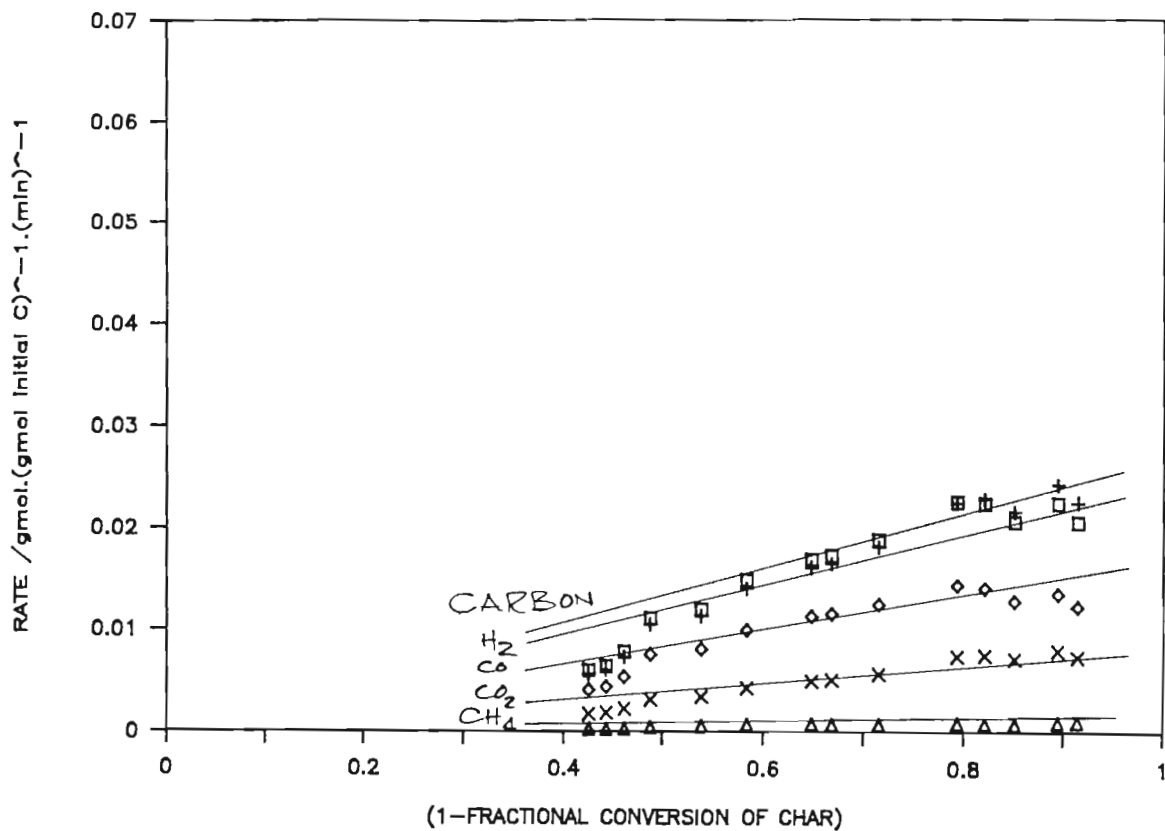


FIGURE 14a Kinetic results of Run 27 (T = 840°C, P = 1.8 bar abs)

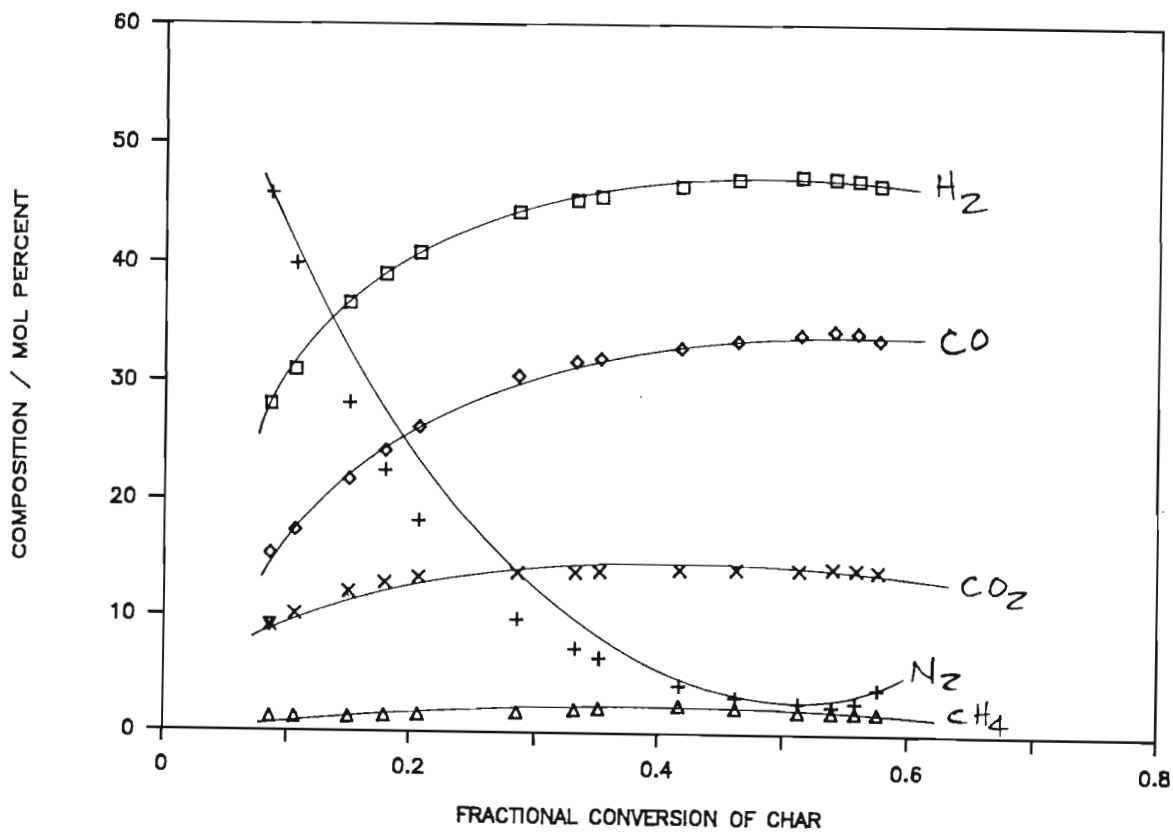


FIGURE 14b Product gas compositions of Run 27

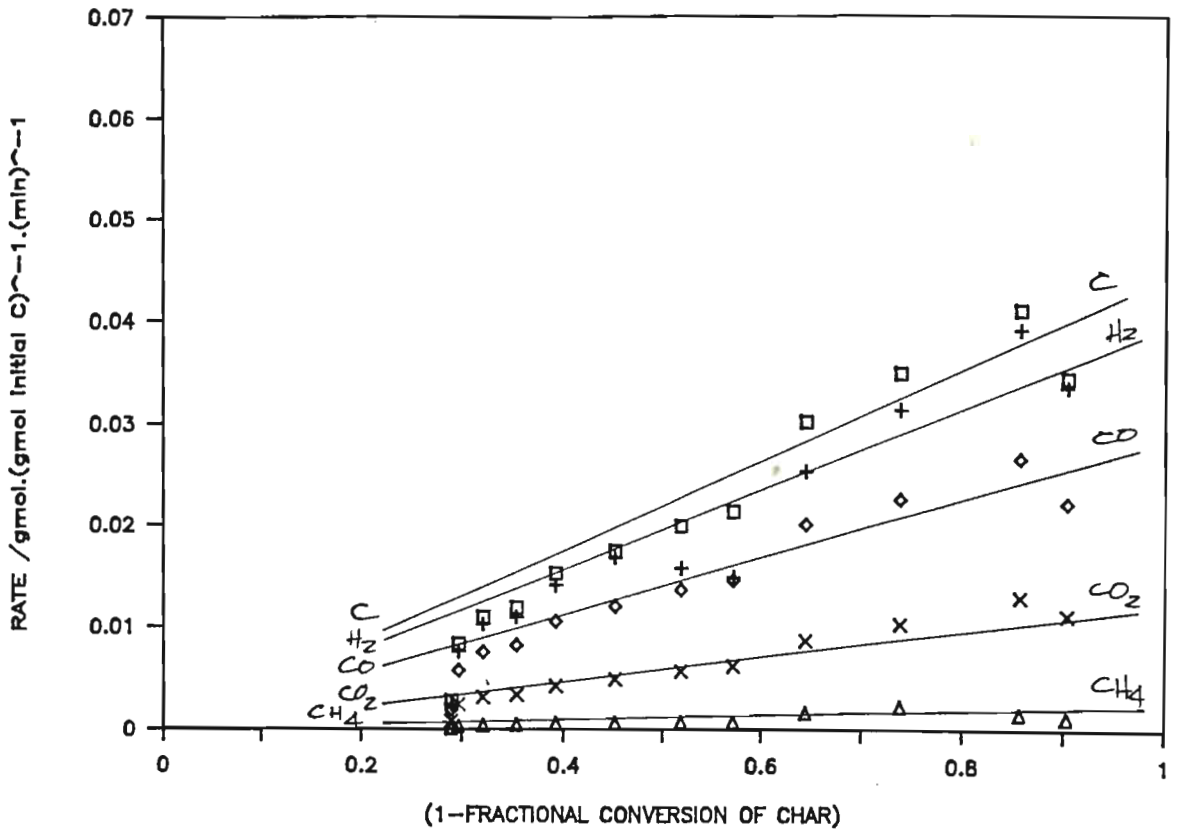


FIGURE 15a Kinetic results of Run 30 (T=880°C, P = 1.8 bar abs)

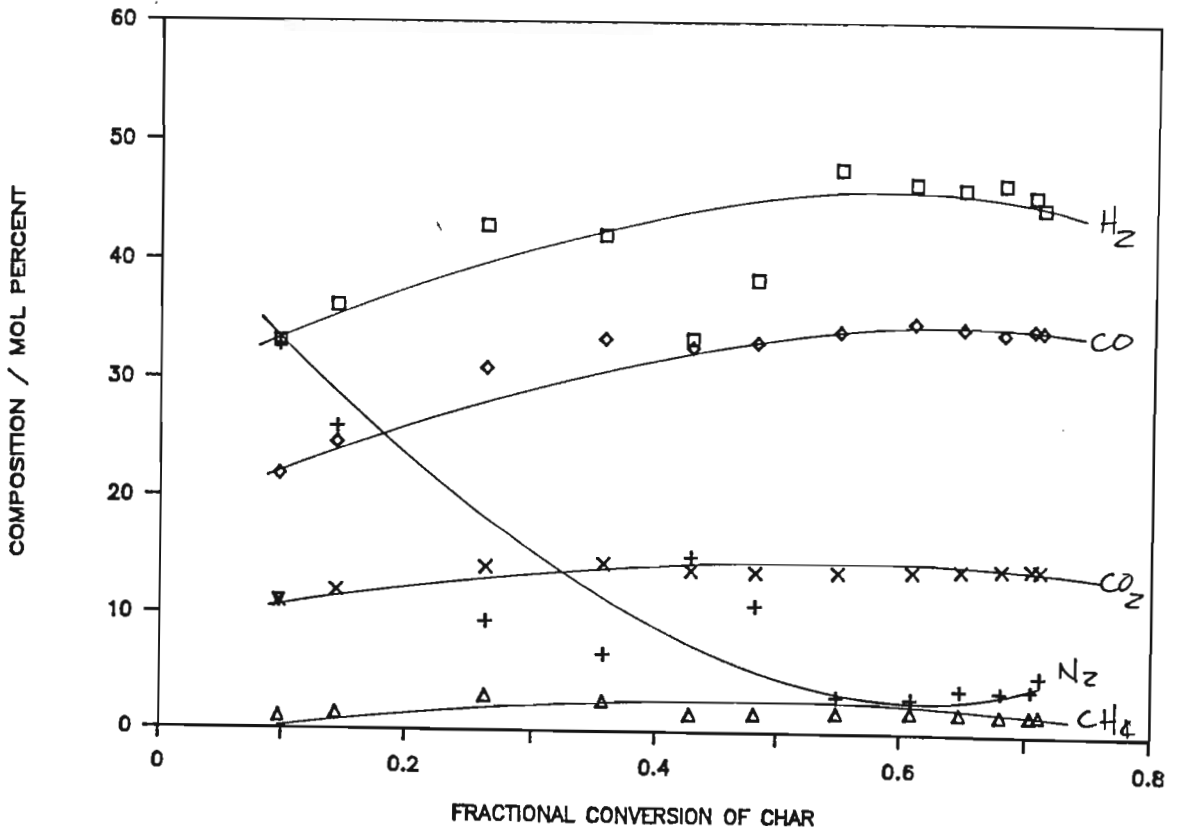


FIGURE 15b Product gas compositions of Run 30

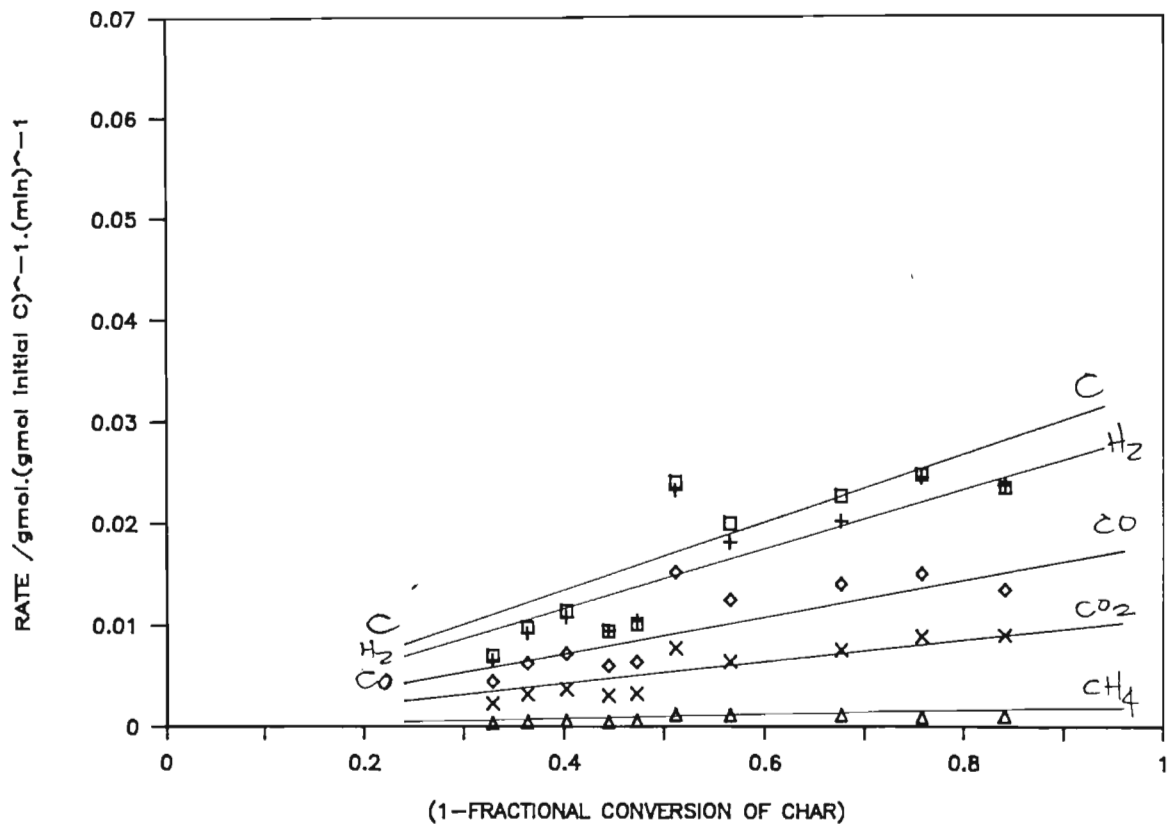


FIGURE 16a Kinetic results of Run 34 (T = 840°C, P = 1.8 bar abs)

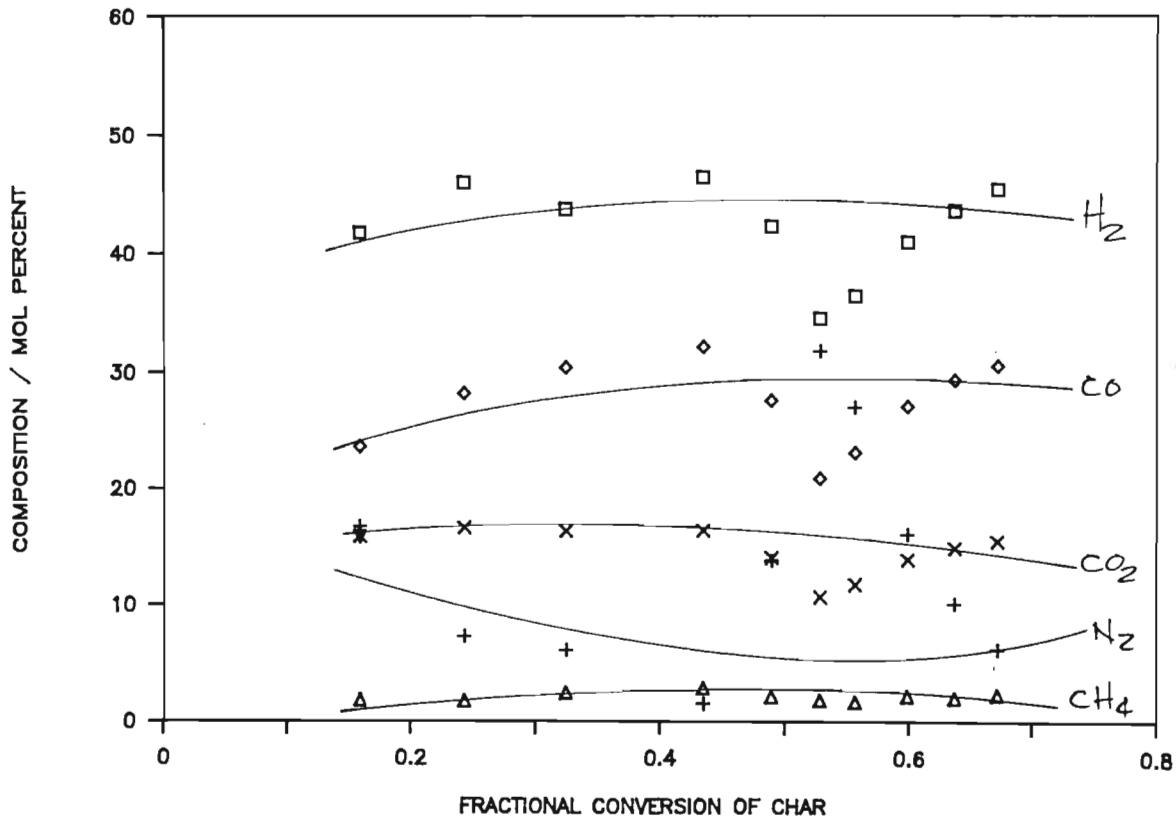


FIGURE 16b Product gas compositions of Run 34

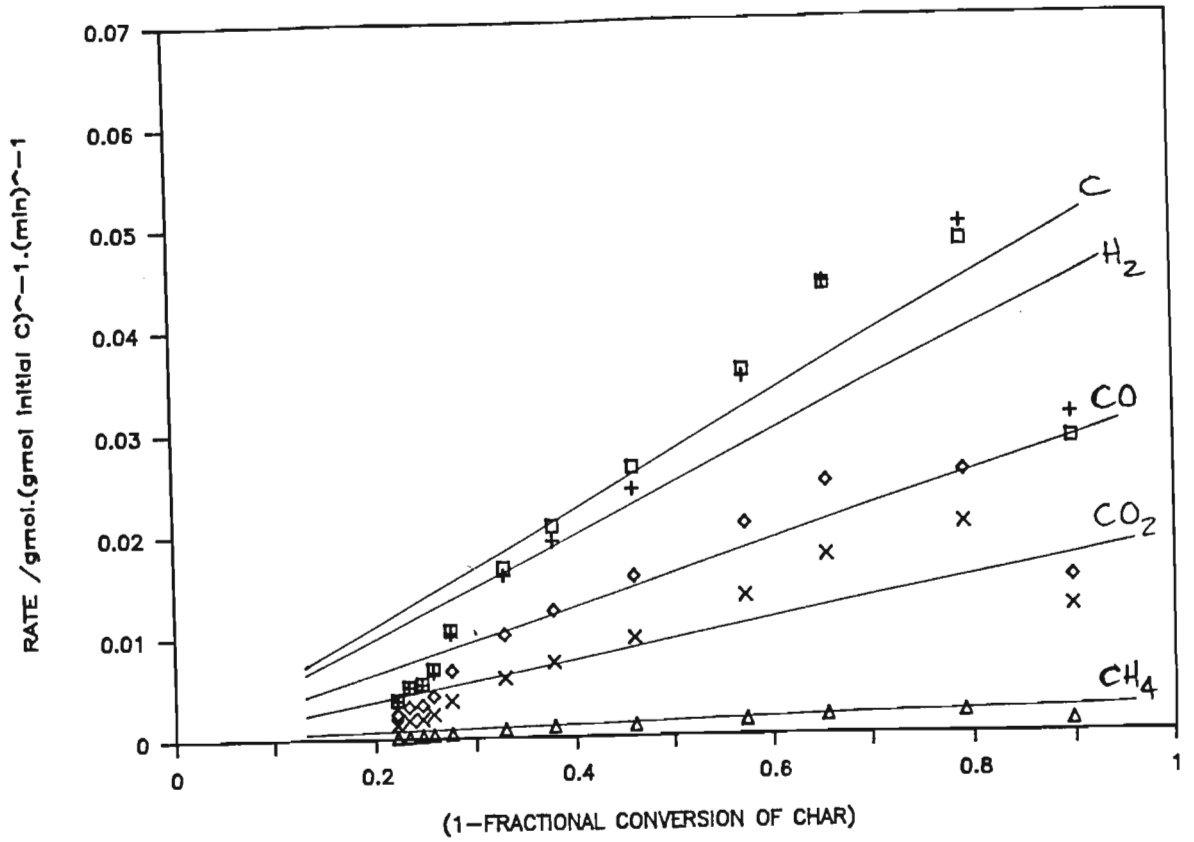


FIGURE 17a Kinetic results of Run 35 (T = 880°C; P = 3.2 bar abs)

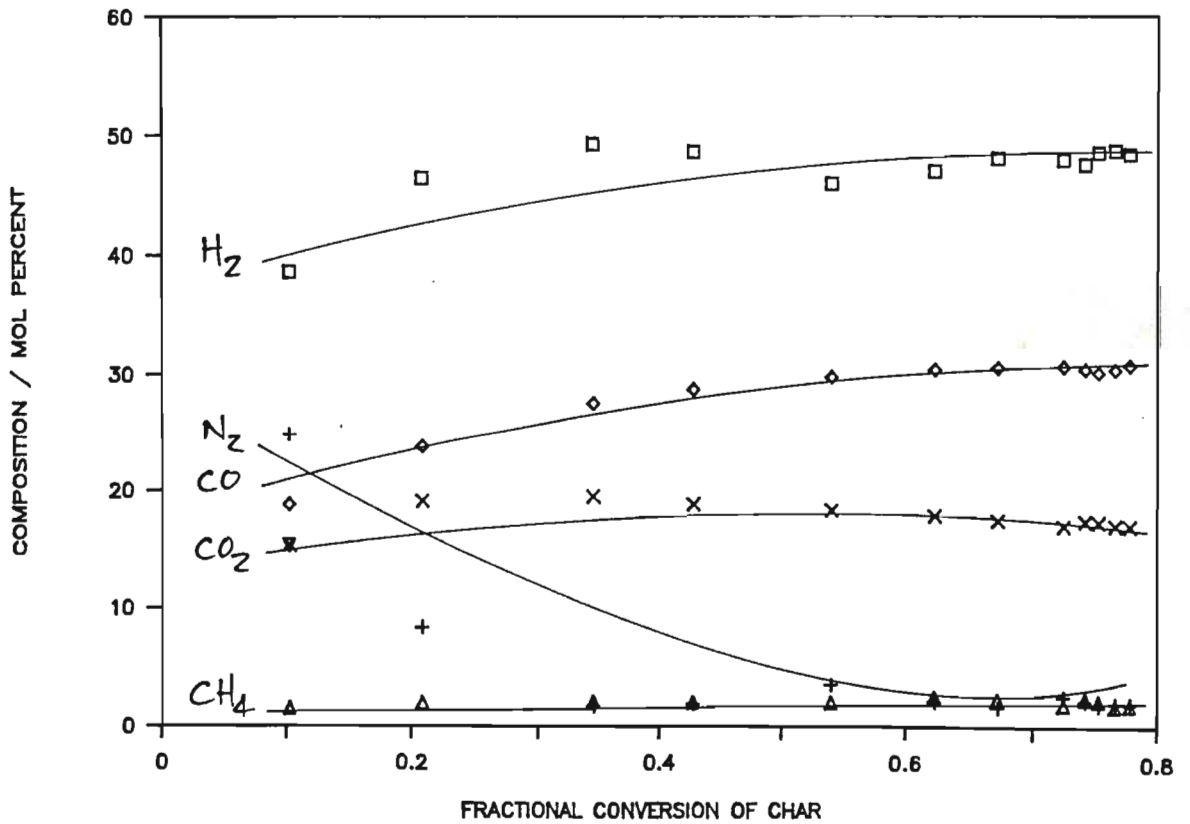


FIGURE 17b product gas compositions of Run 35

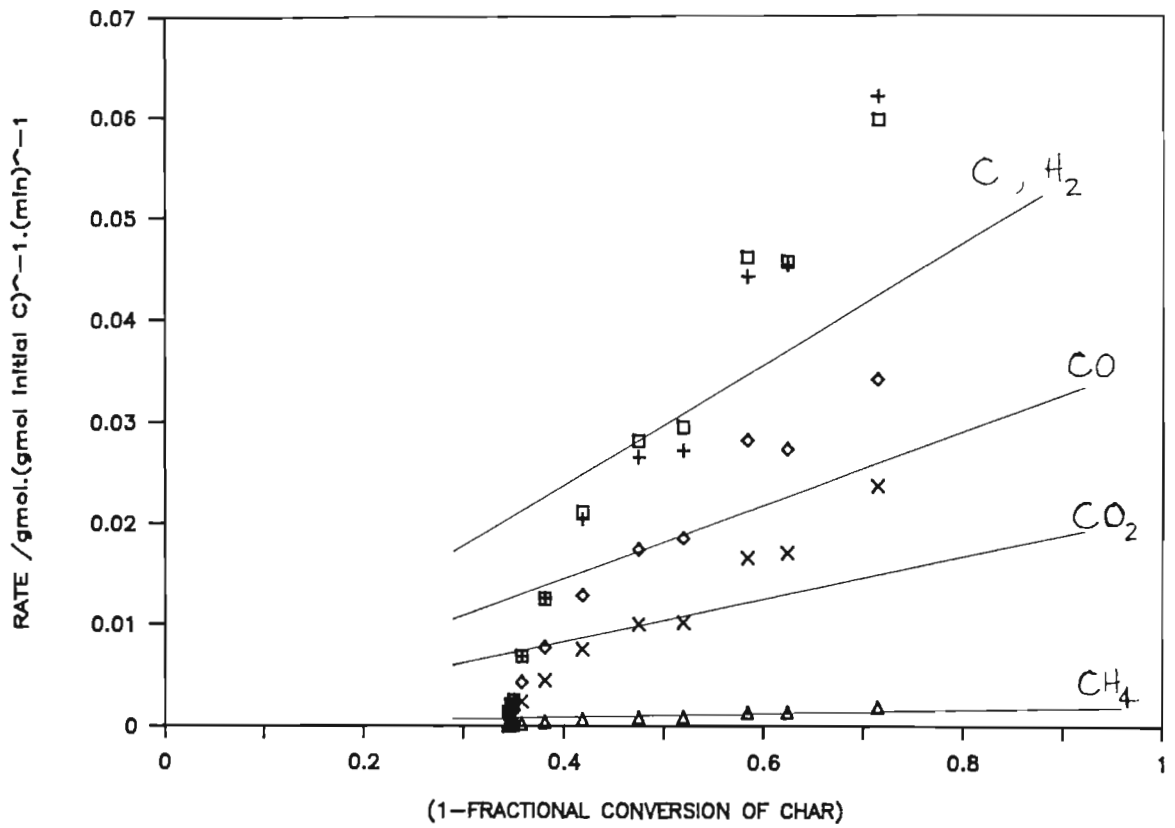


FIGURE 18a Kinetic results of Run 36 (T = 920°C, P = 1.8 bar abs)

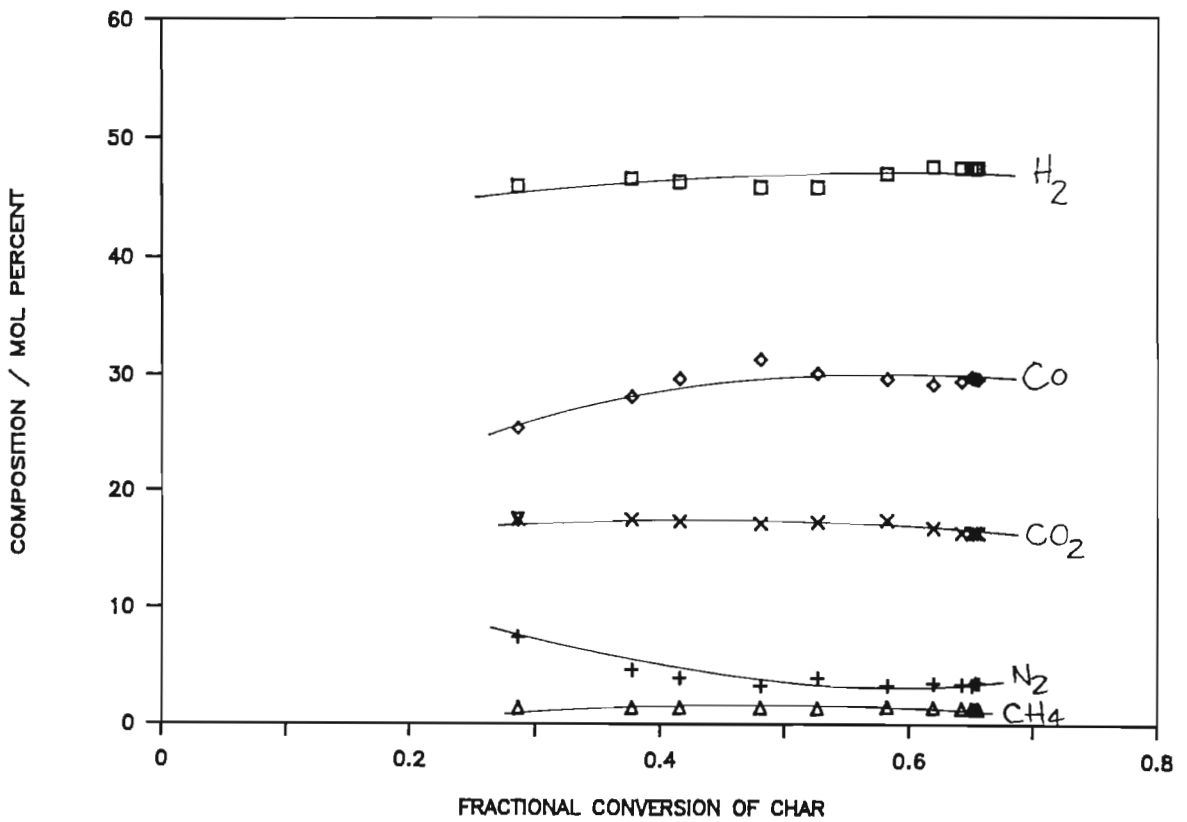


FIGURE 18b Product gas compositions of Run 36

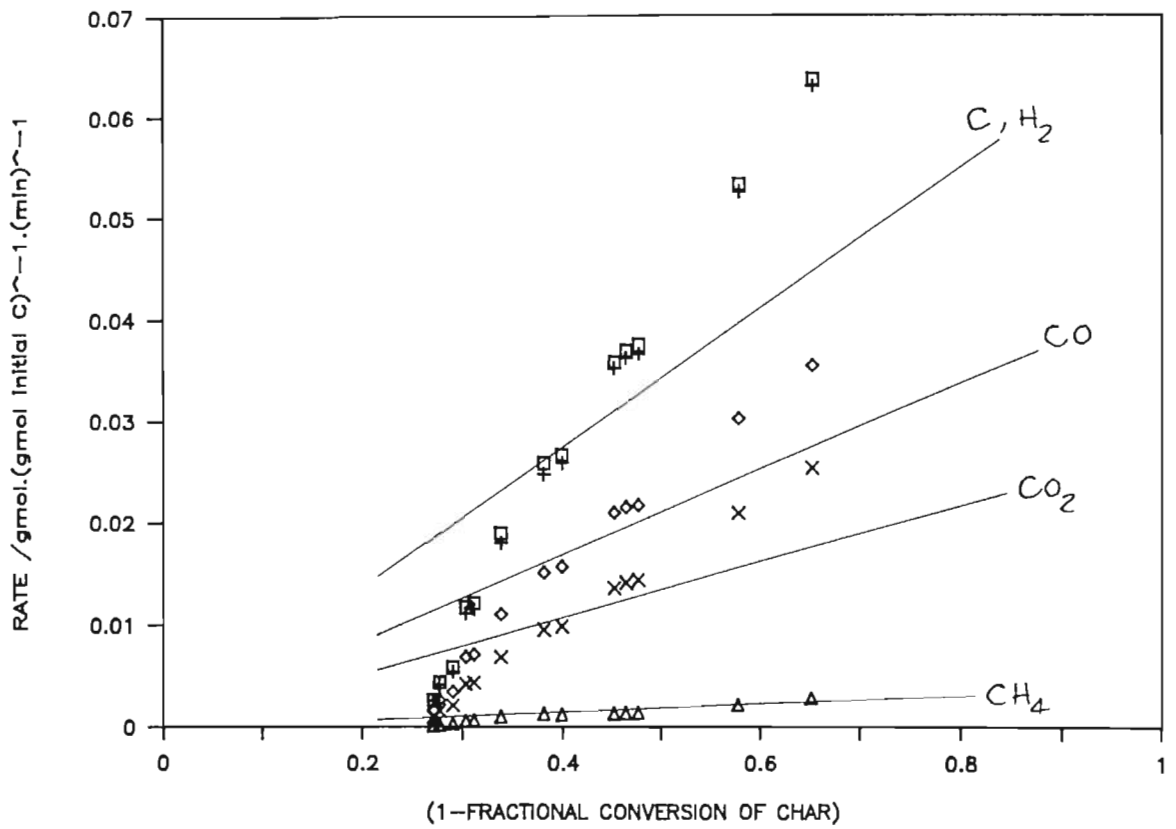


FIGURE 19a Kinetic results of Run 37 (T = 920°C; P = 3.2 bar abs)

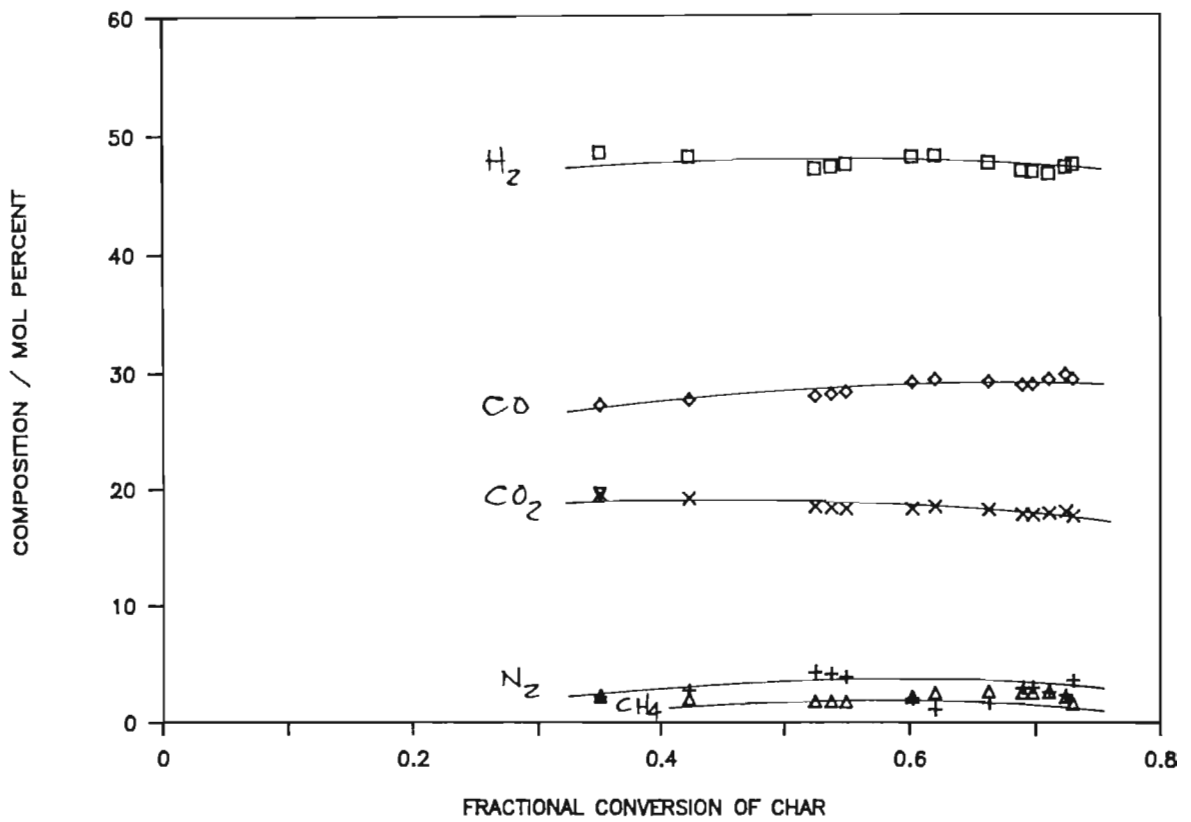


FIGURE 19b Product gas compositions of Run 37

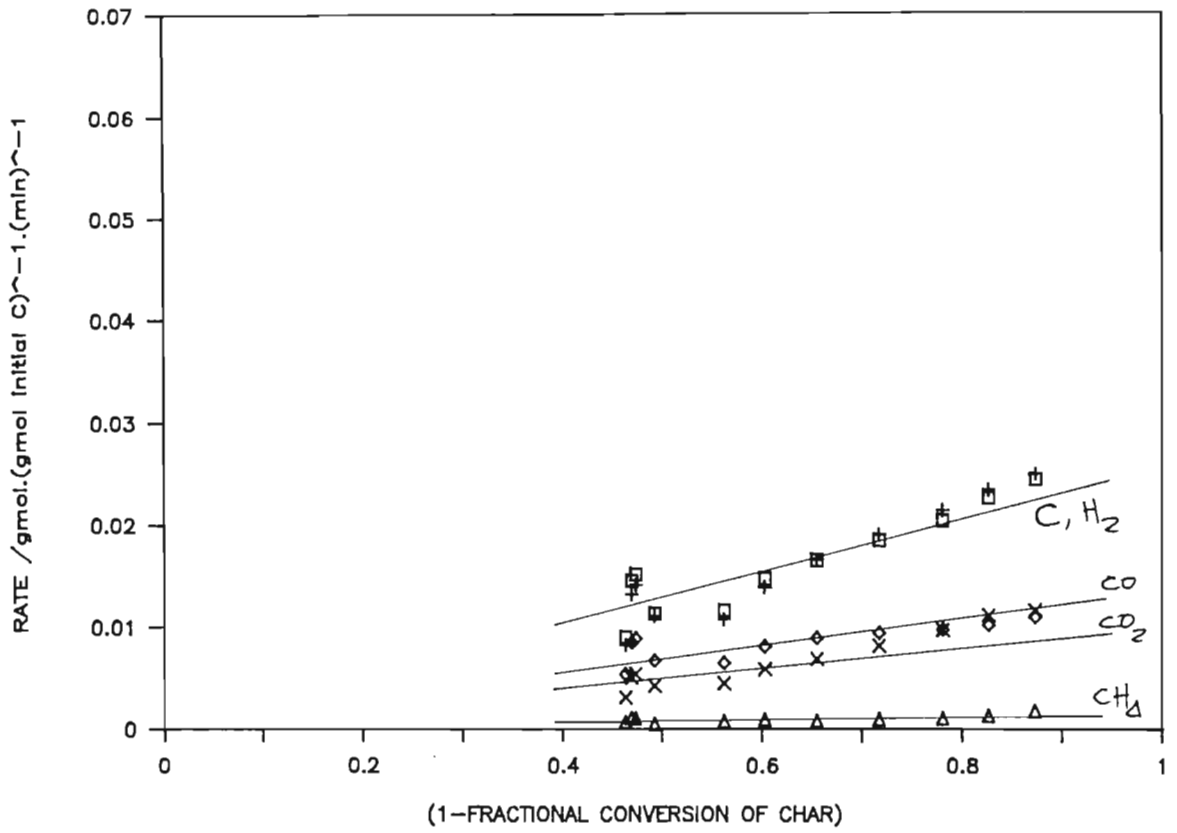


FIGURE 20a Kinetic results of Run 38 (T = 840°C, P = 4.8 bar abs)

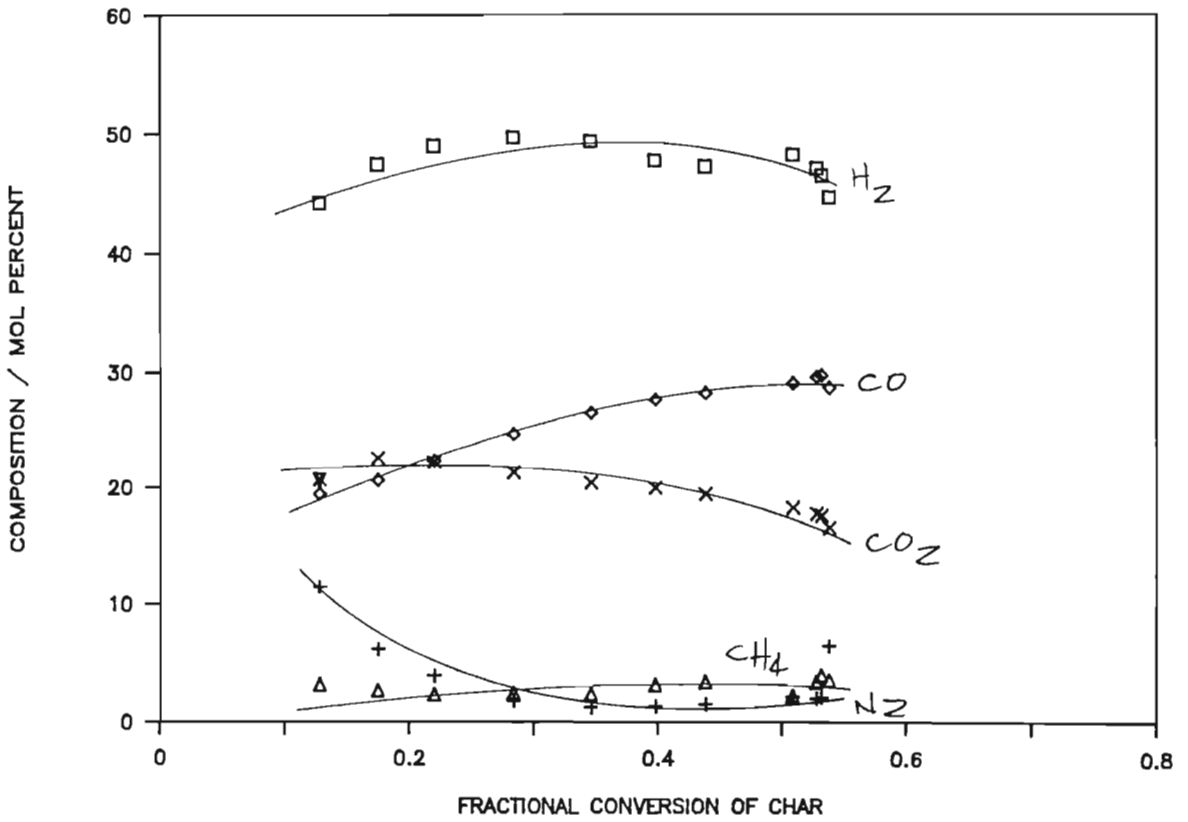


FIGURE 20b product gas compositions of Run 38

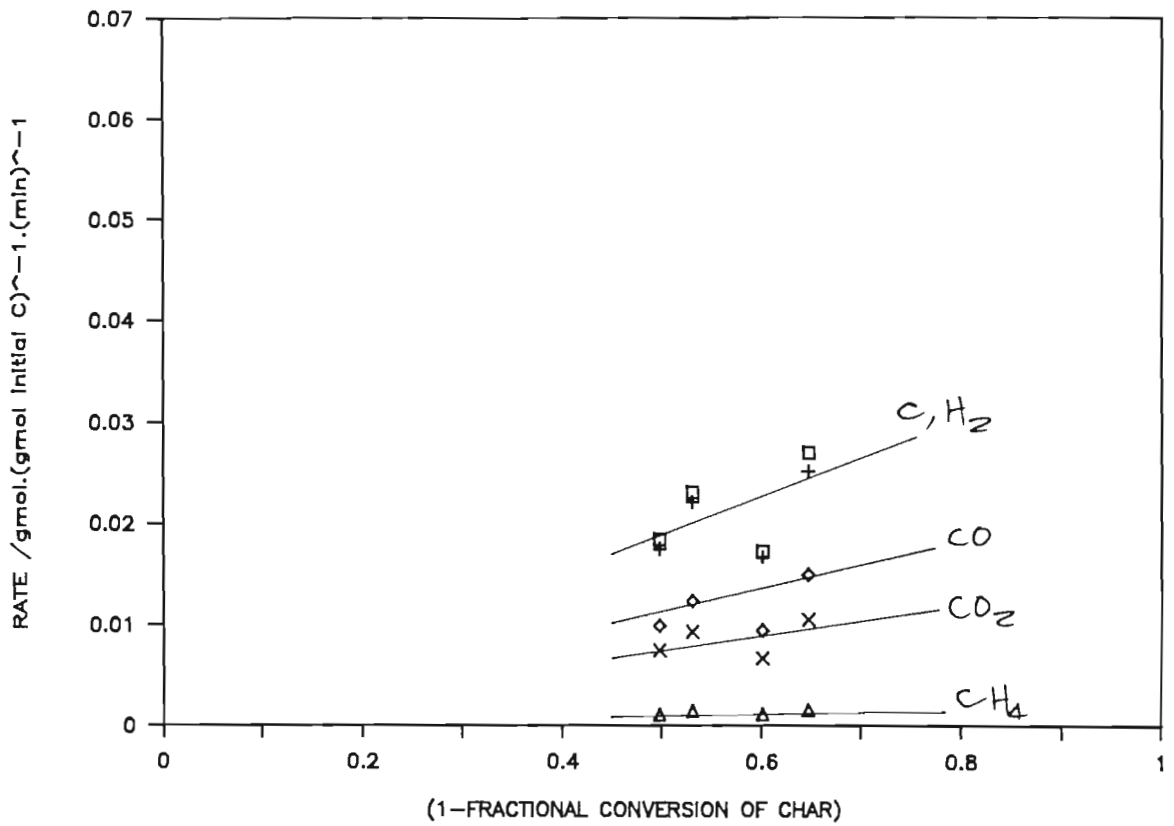


FIGURE 21a Kinetic results of run 40 (T = 880°C; P = 4.8 bar abs)

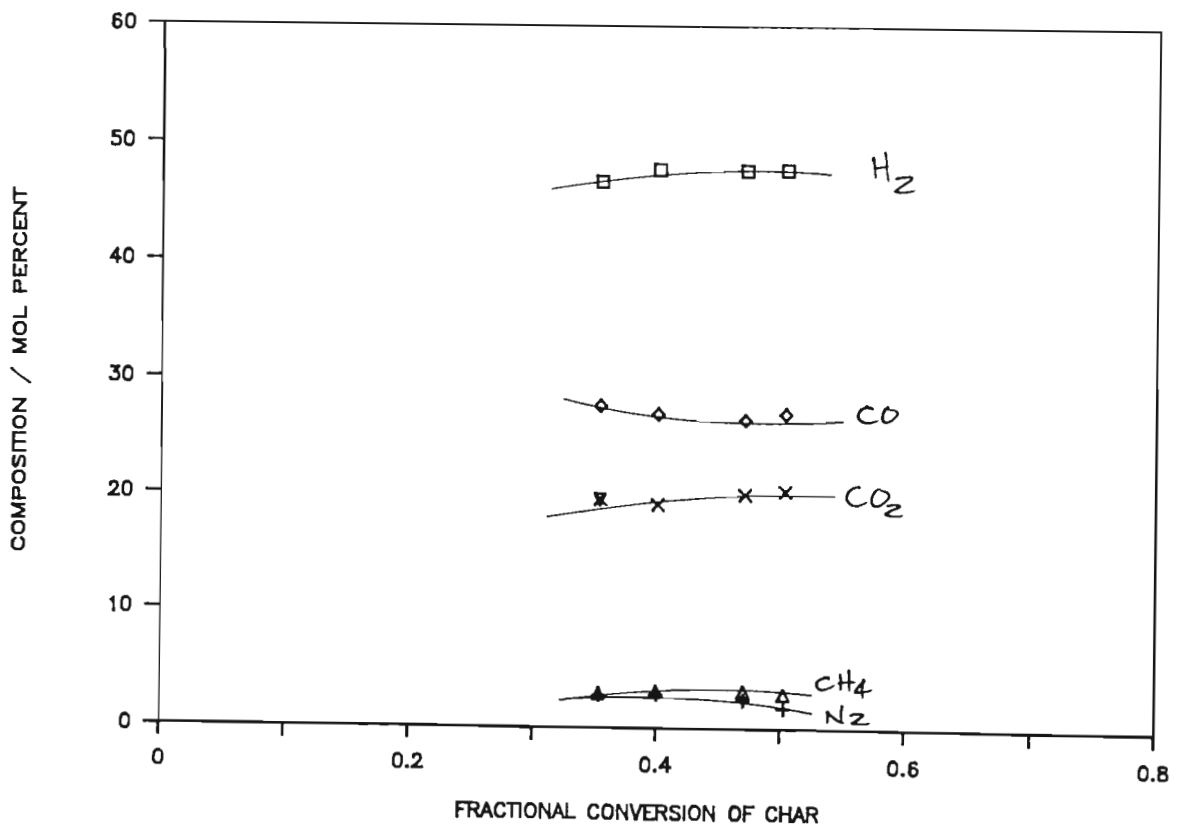


FIGURE 21b Product gas compositions of Run 40

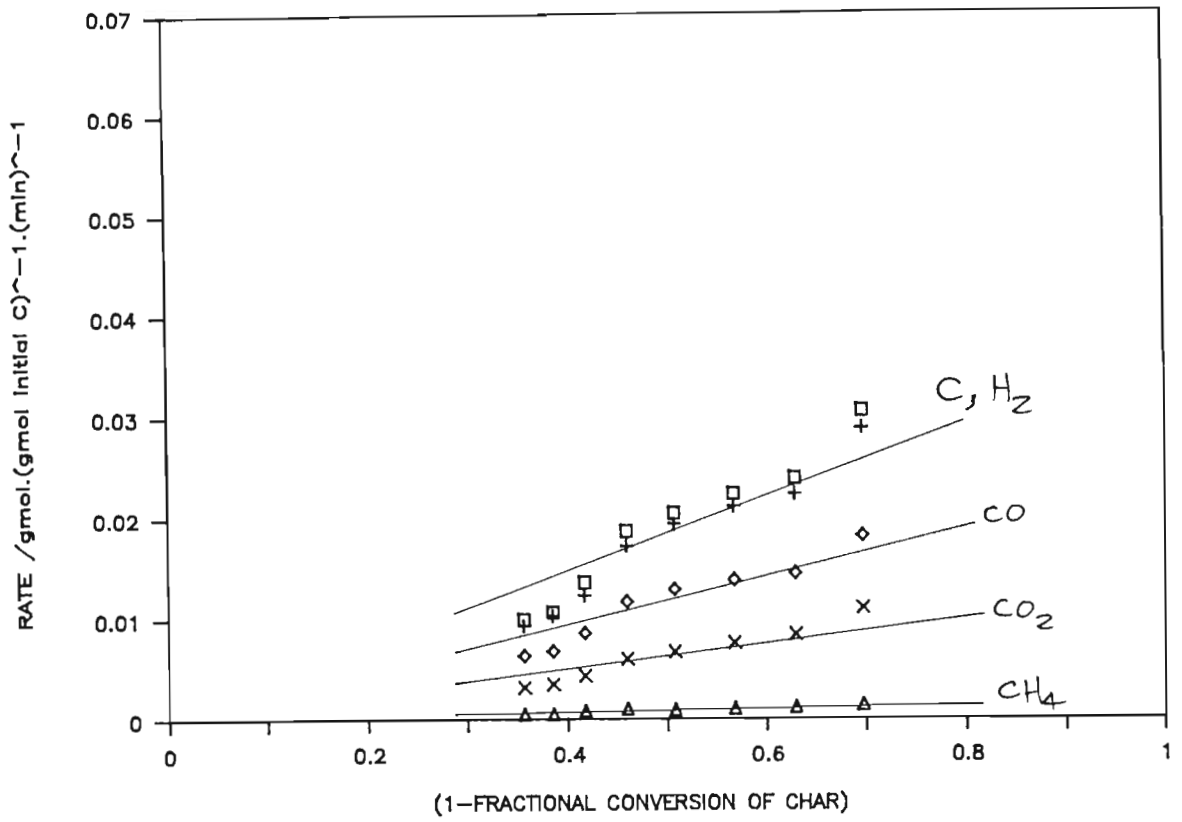


FIGURE 22a Kinetic results of Run 42 (T = 880°C, P = 4.8 bar abs)

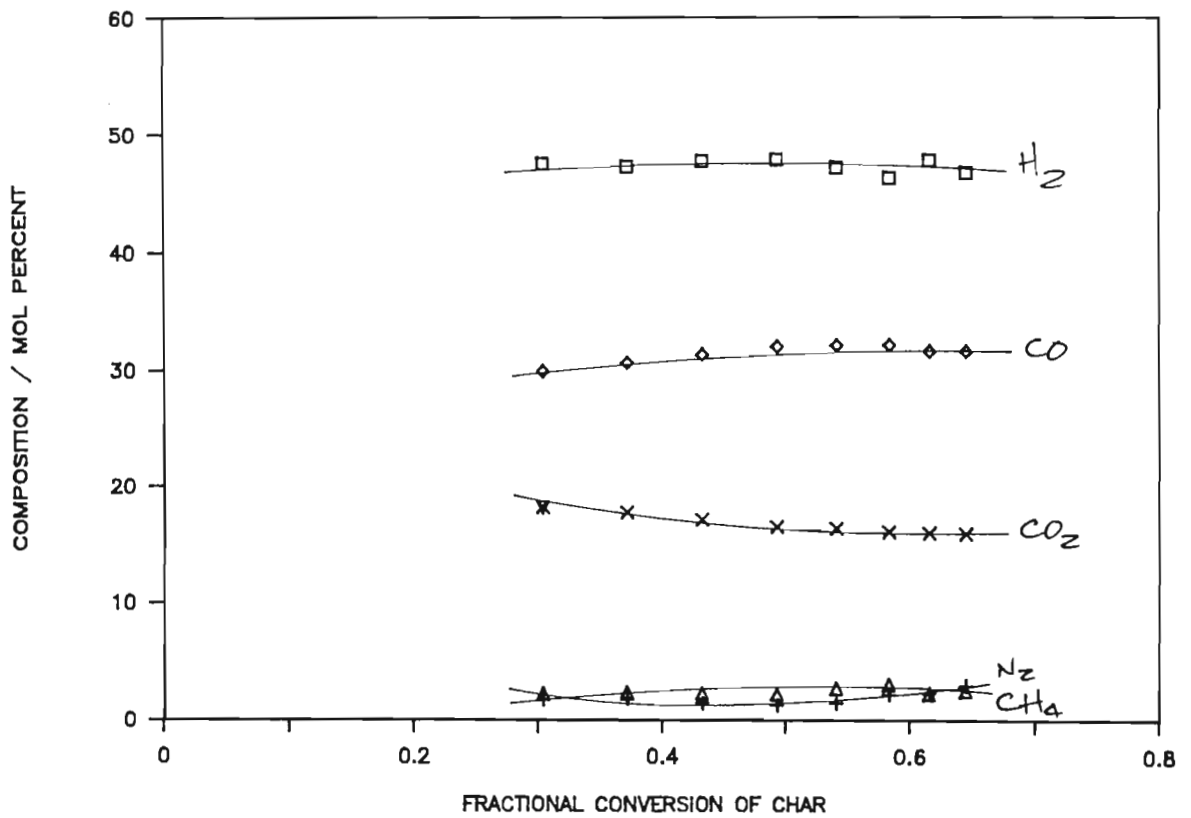


FIGURE 22b Product gas compositions of Run 42

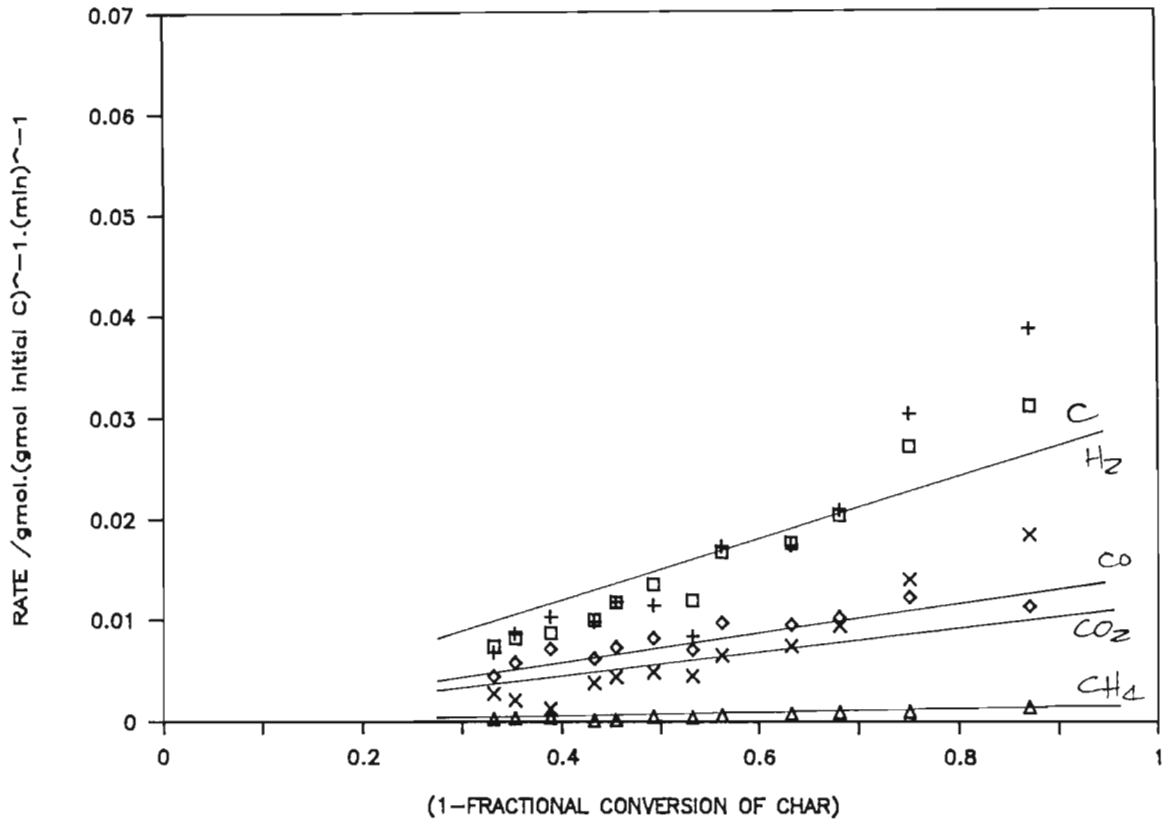


FIGURE 23a Kinetic results of Run 45 (T = 850°C; P = 1.8 bar abs)

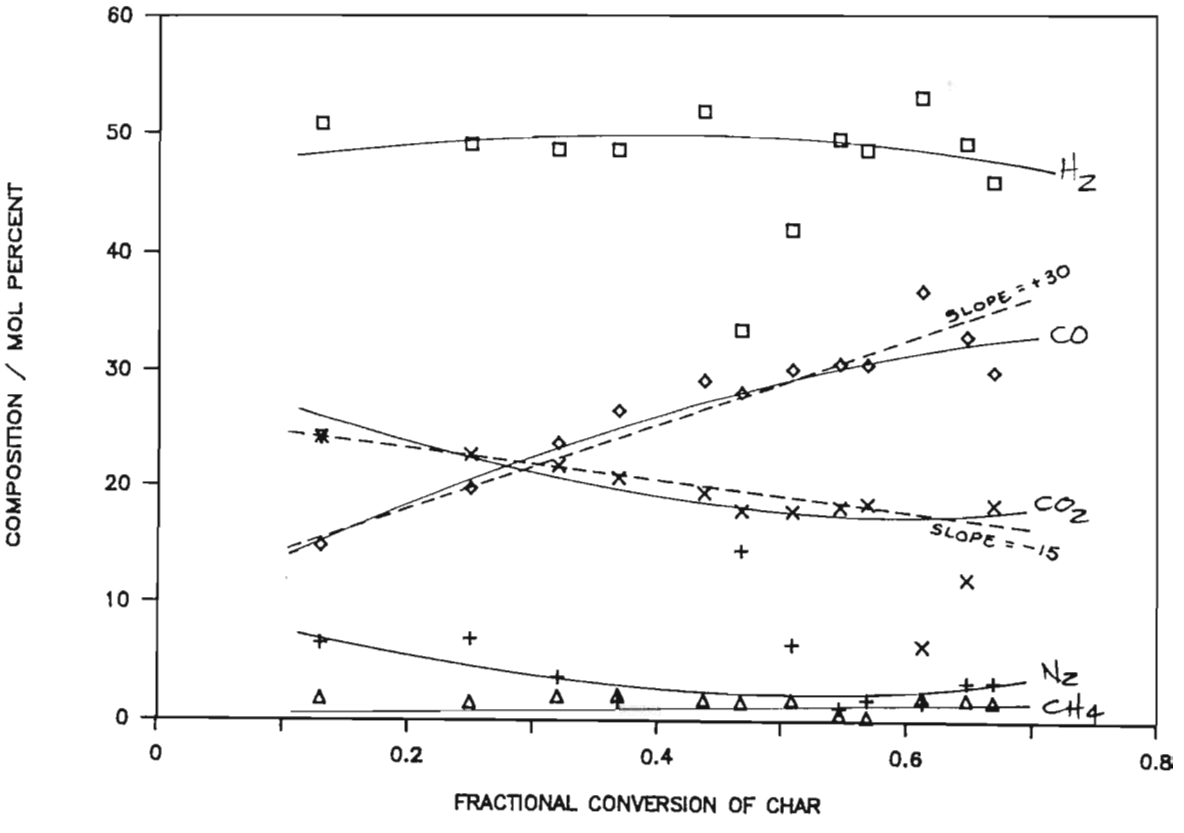


FIGURE 23b Product gas compositions of Run 45

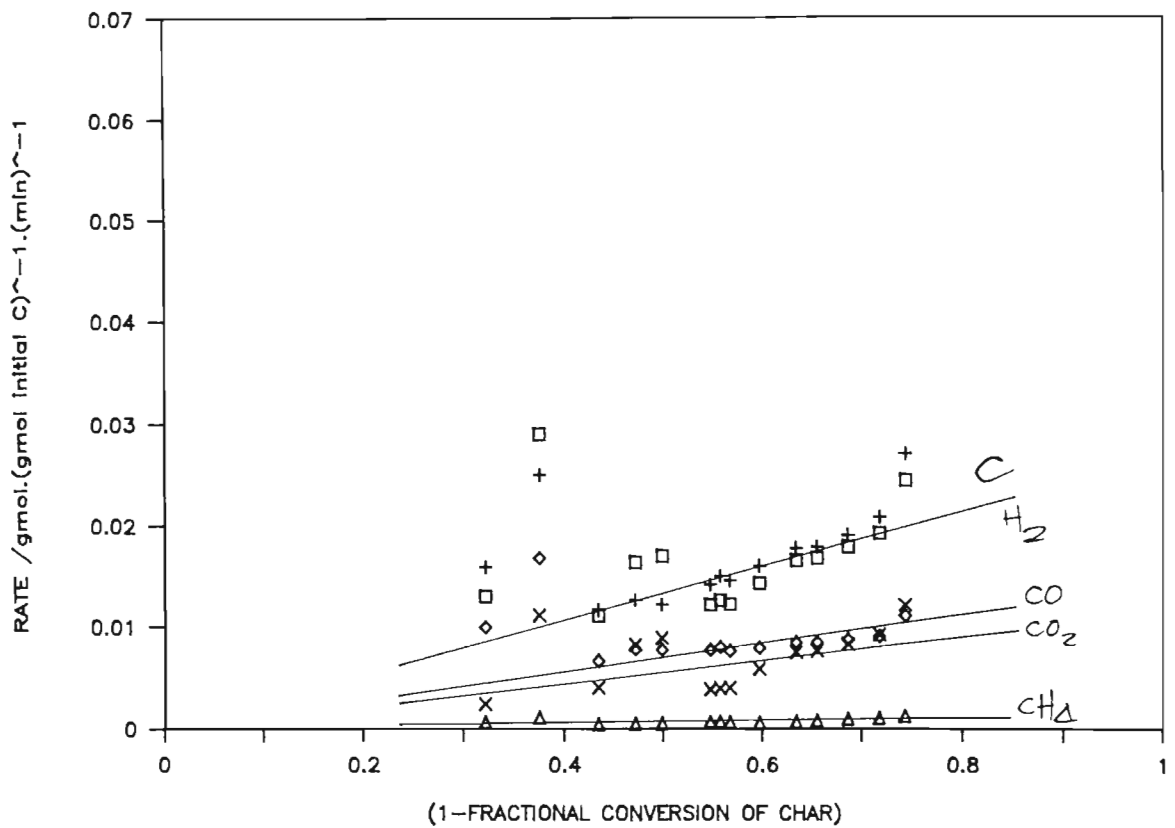


FIGURE 24a Kinetic results of Run 47 (T = 880°C; P = 1.8 bar abs)

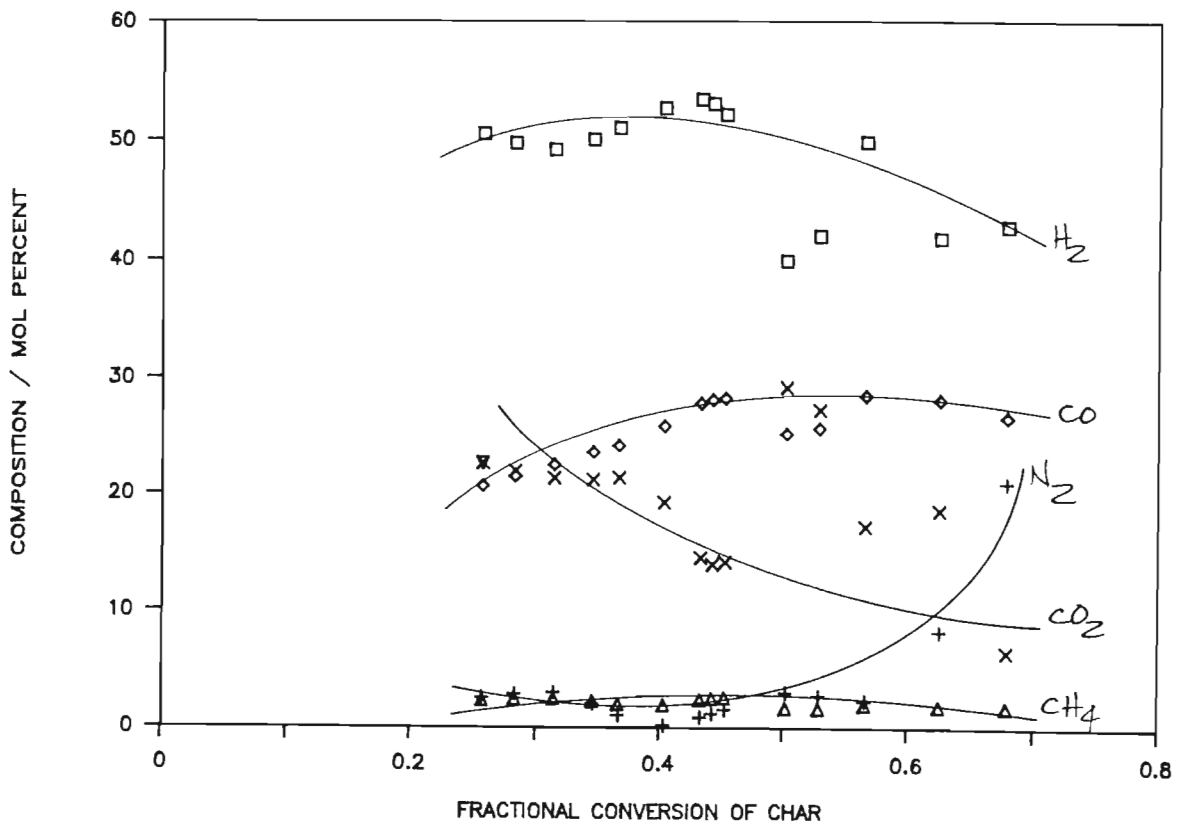


FIGURE 24b Product gas compositions of Run 47

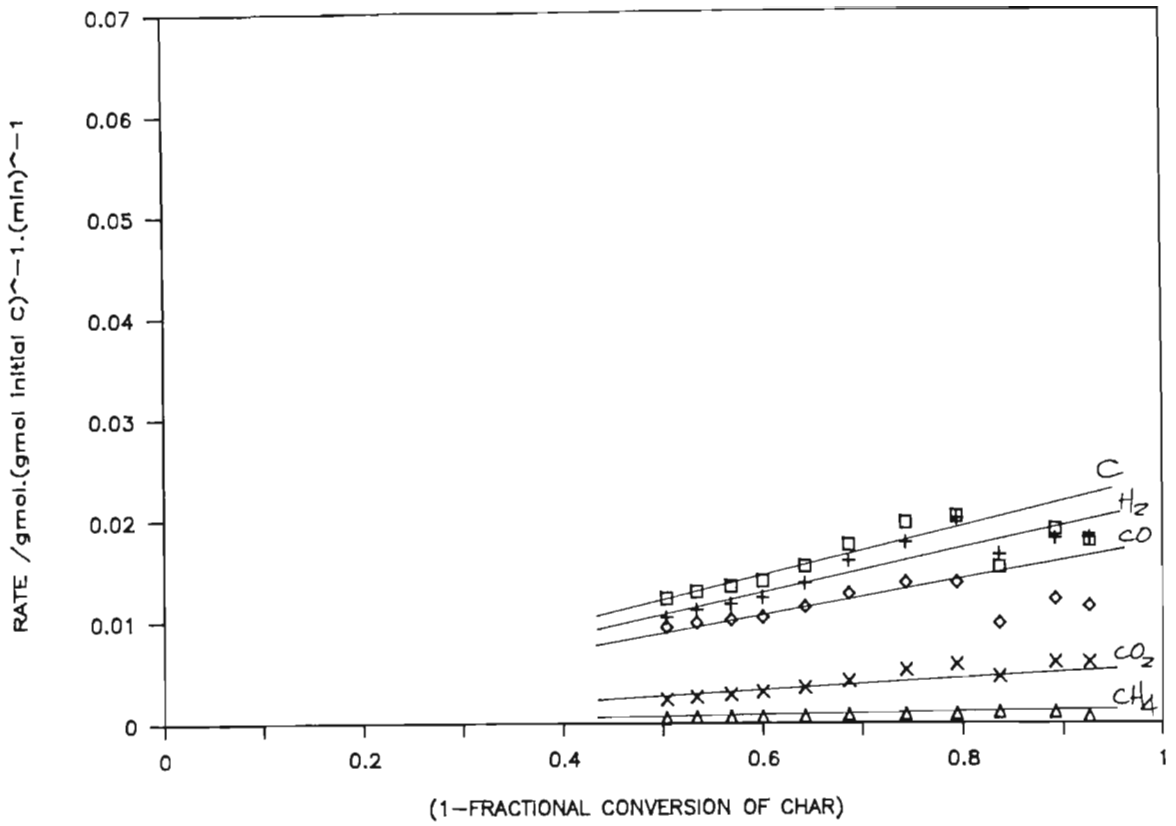


FIGURE 25a Kinetic results of Run 50 (T = 850°C; P = 1.8 bar abs)

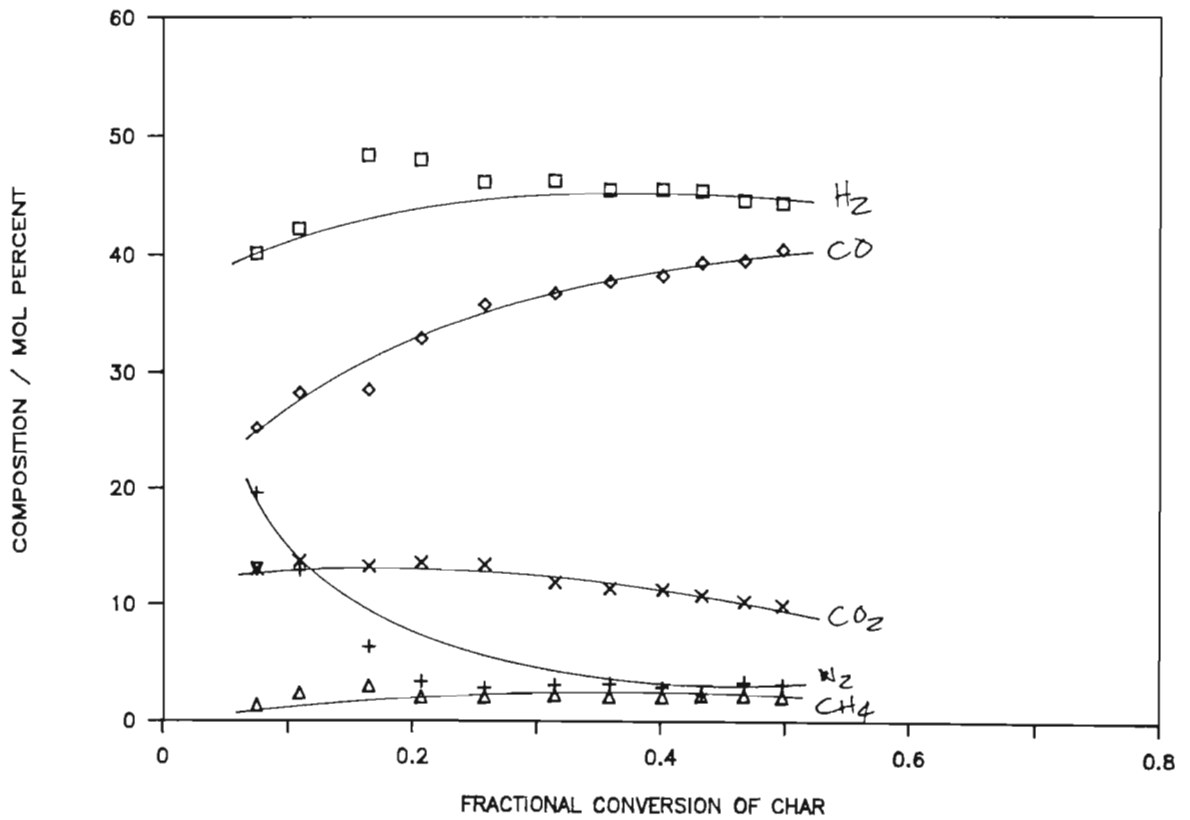


FIGURE 25b Product gas compositions of Run 50

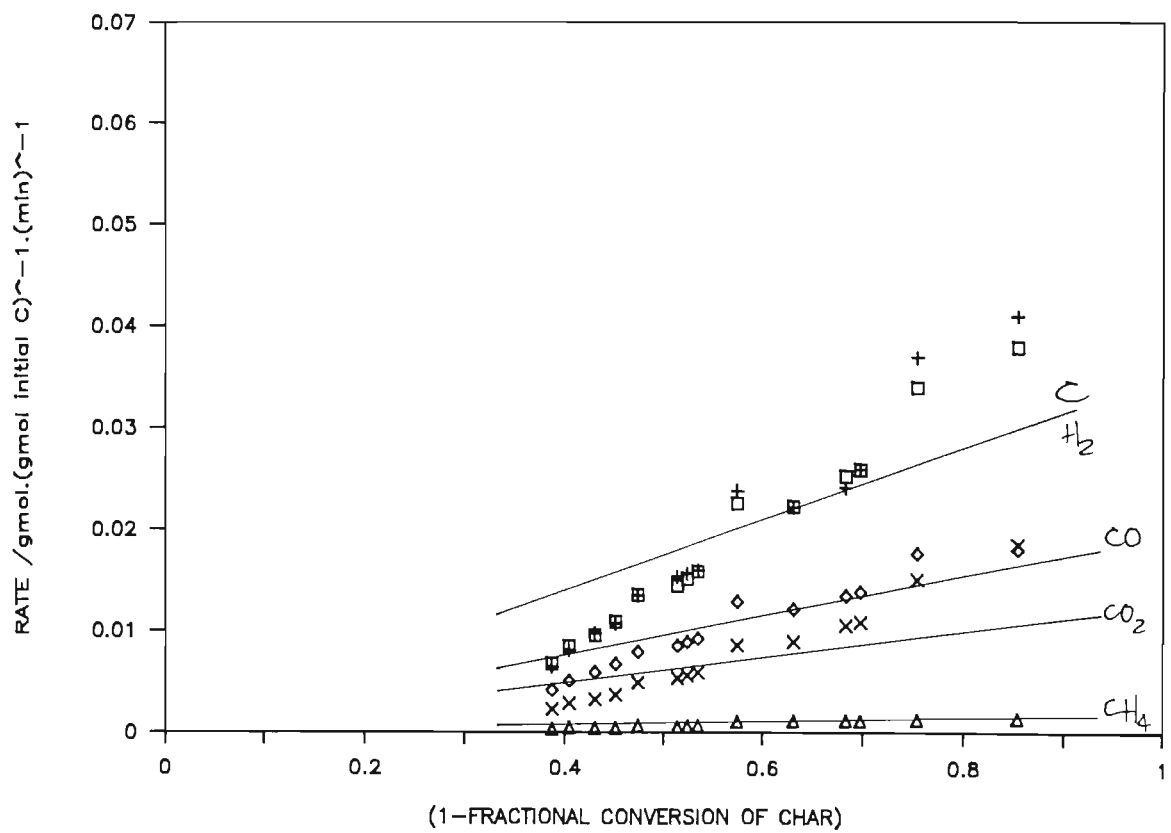


FIGURE 26a Kinetic results of Run 51 (T = 880°C, P = 1.8 bar abs)

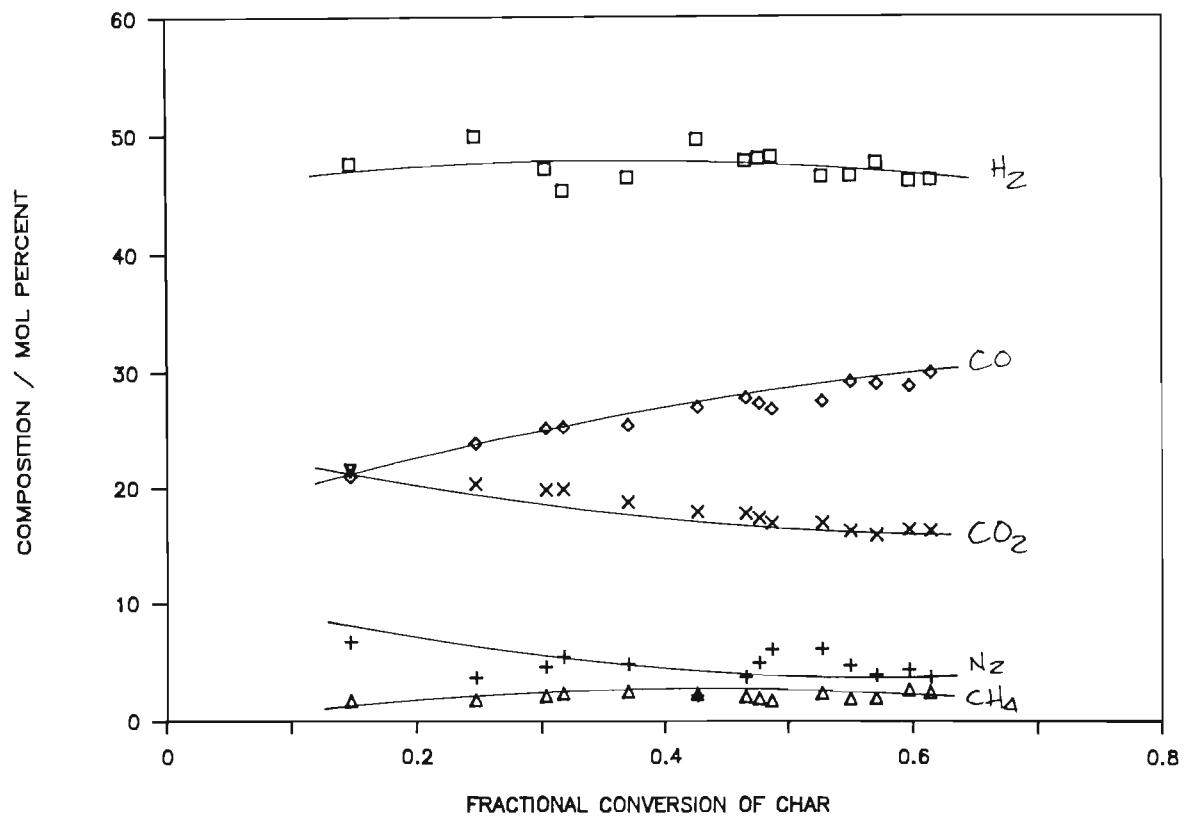


FIGURE 26b Product gas compositions of Run 51

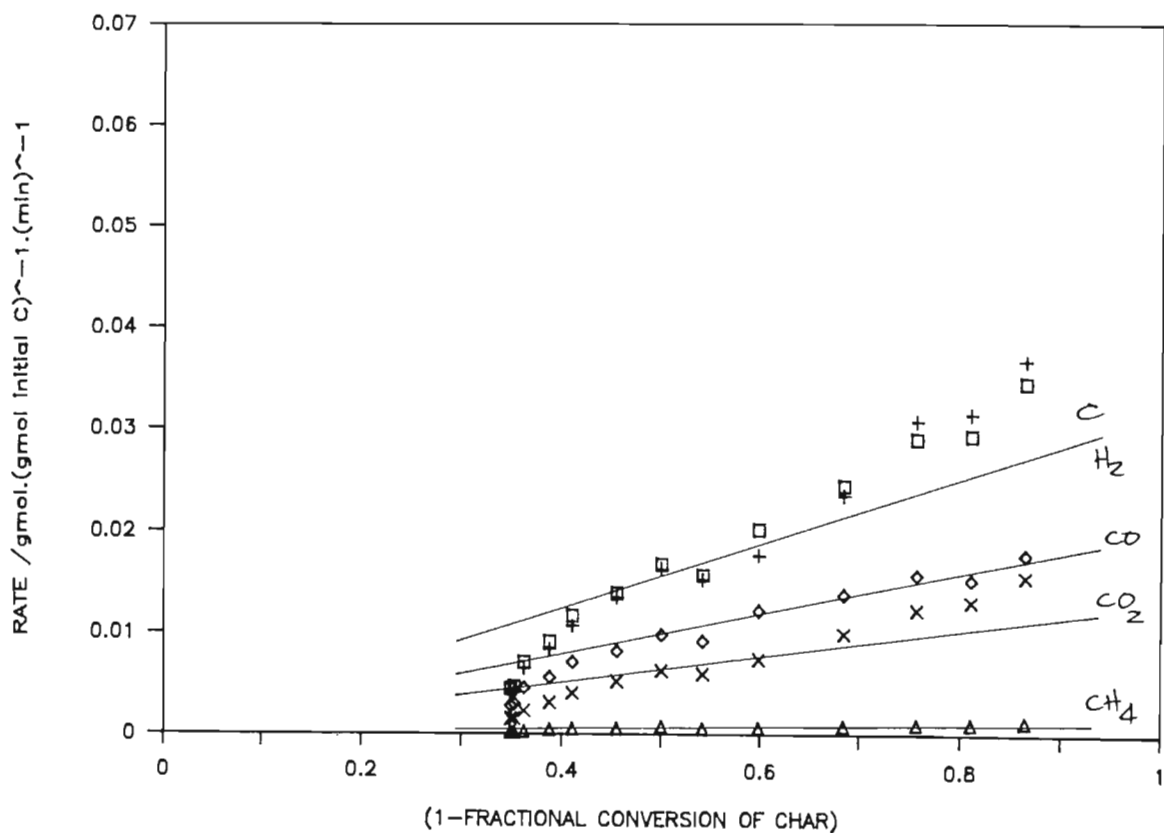


FIGURE 27a Kinetic results of Run 53 (T = 880°C; P = 1.8 bar abs)

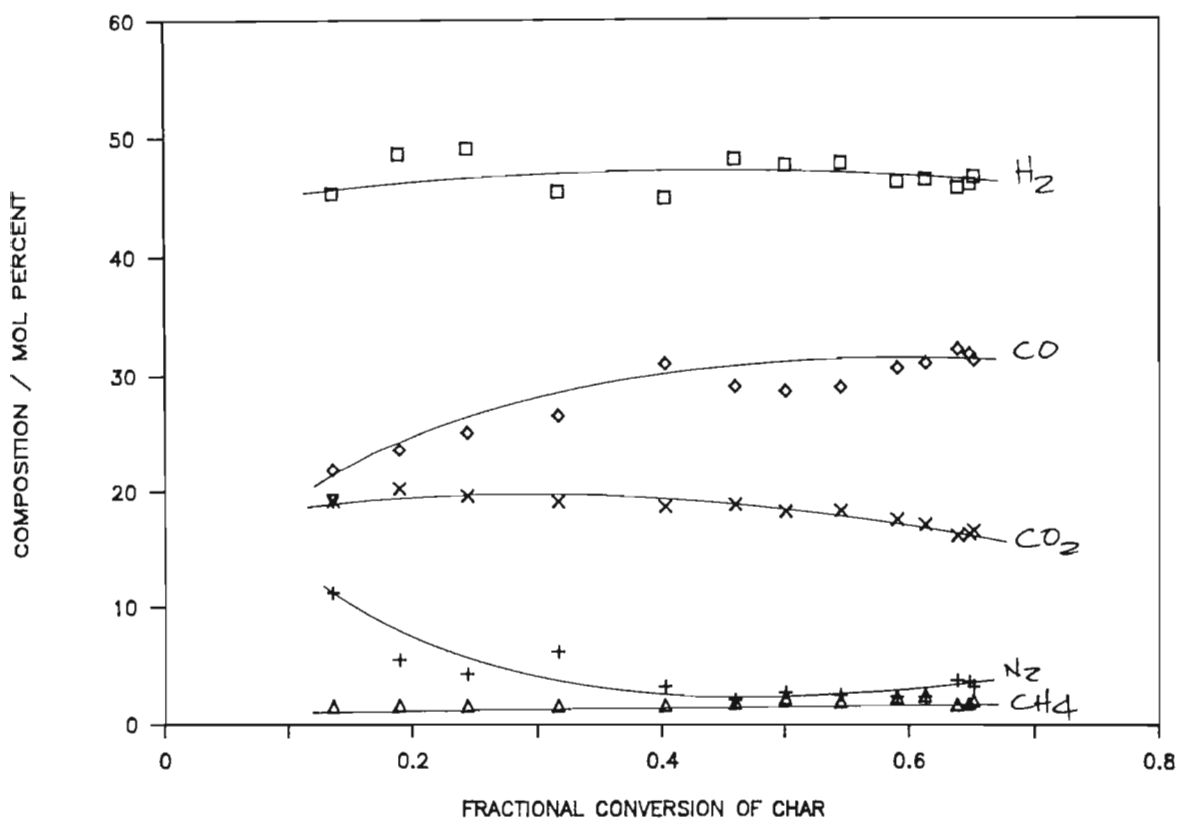


FIGURE 27b Product gas compositions of Run 53

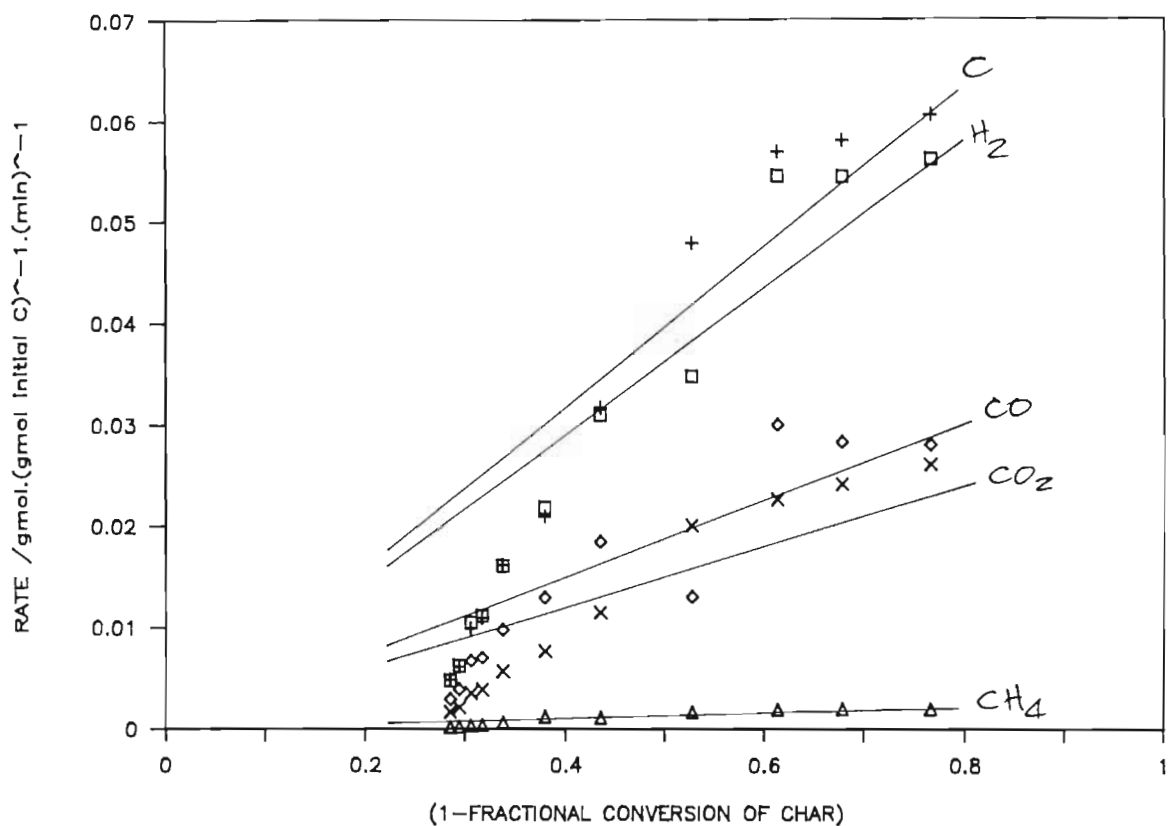


FIGURE 28a Kinetic results of Run 54 (T = 920°C; P = 1.8 bar abs)

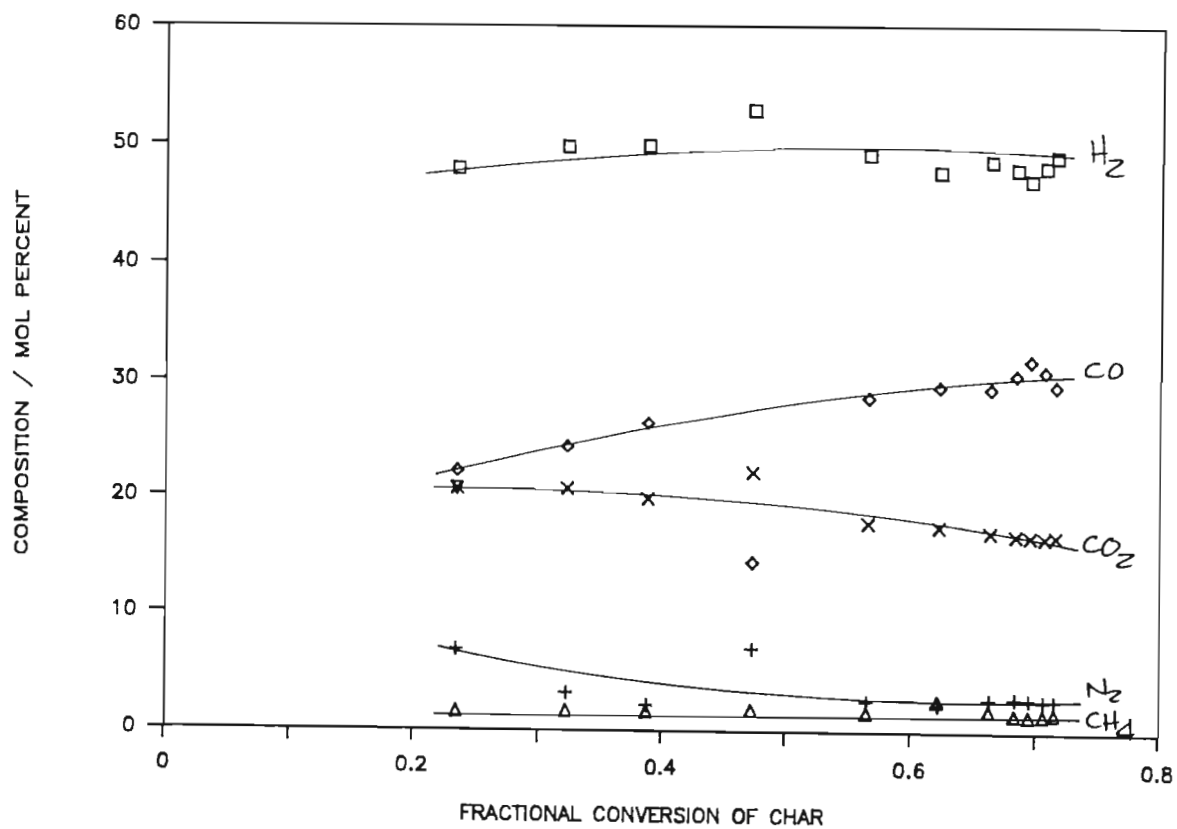


FIGURE 28b Product gas compositions of Run 54

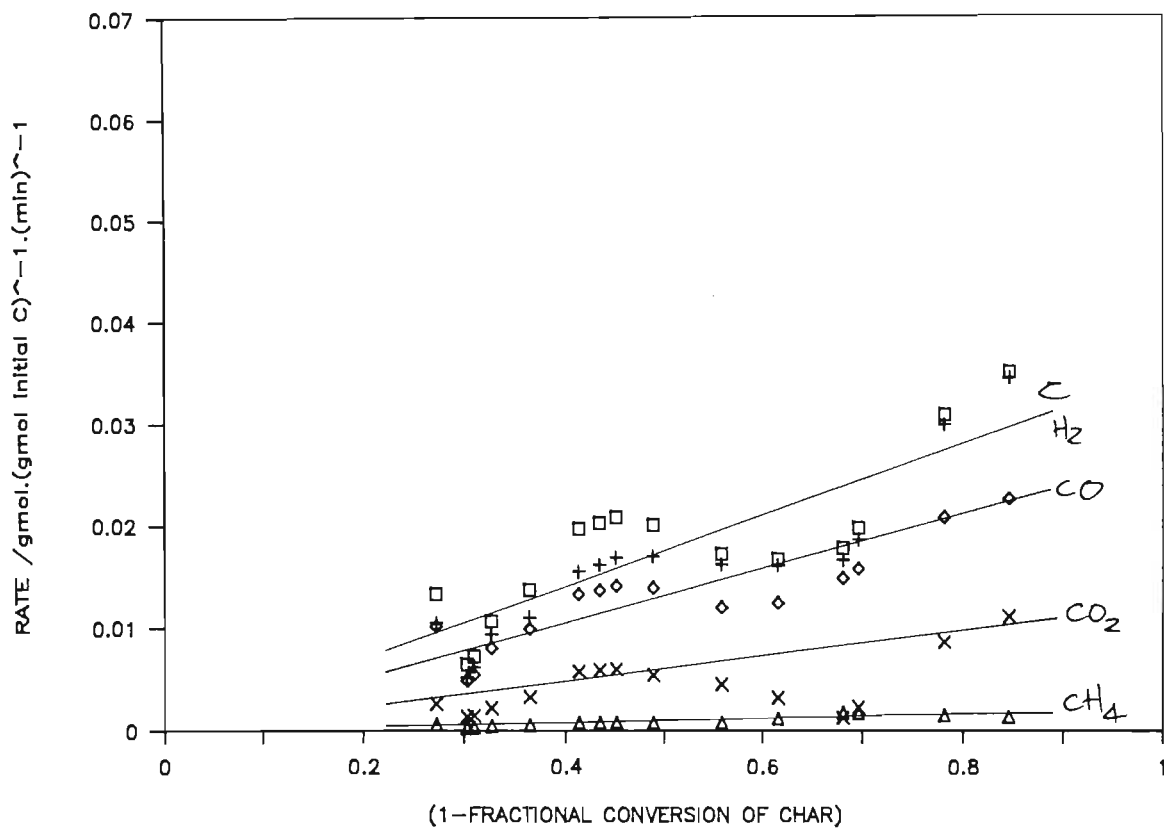


FIGURE 29a Kinetic results of run 55 (T = 880°C; P = 1.8 bar abs)

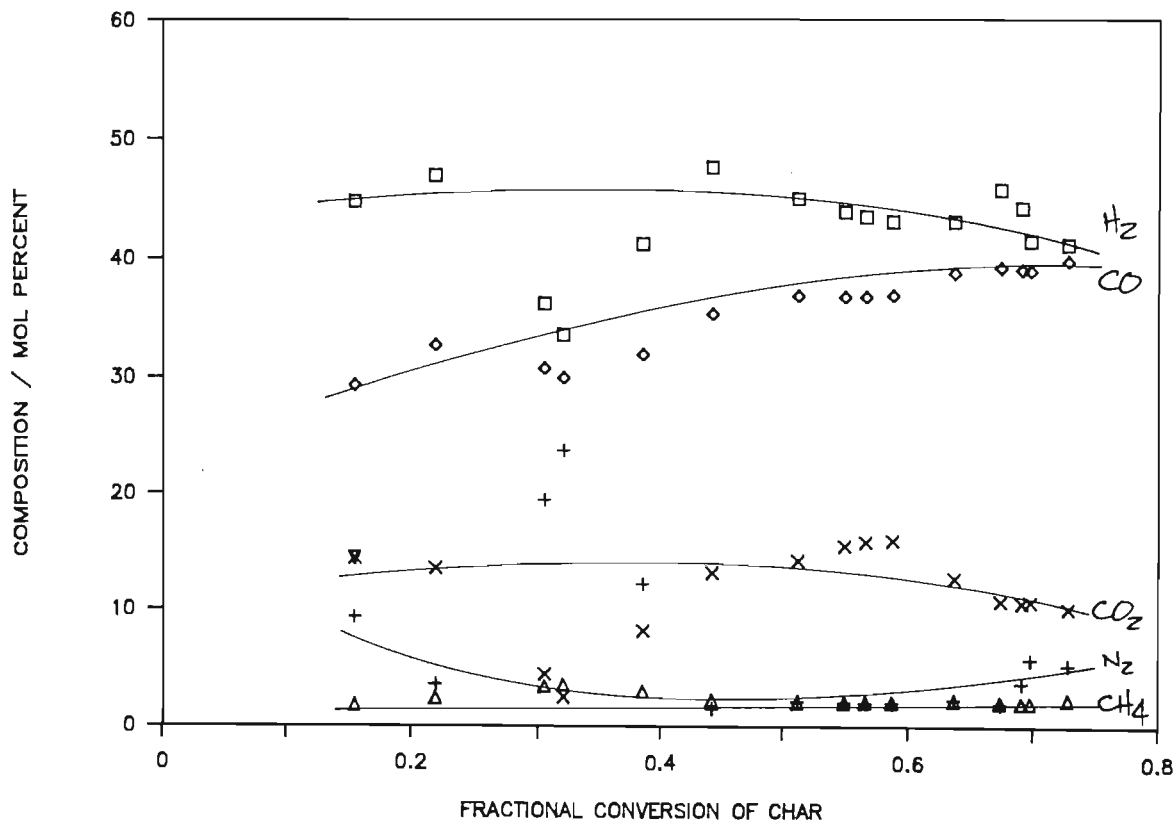


FIGURE 29b Product gas compositions of Run 55

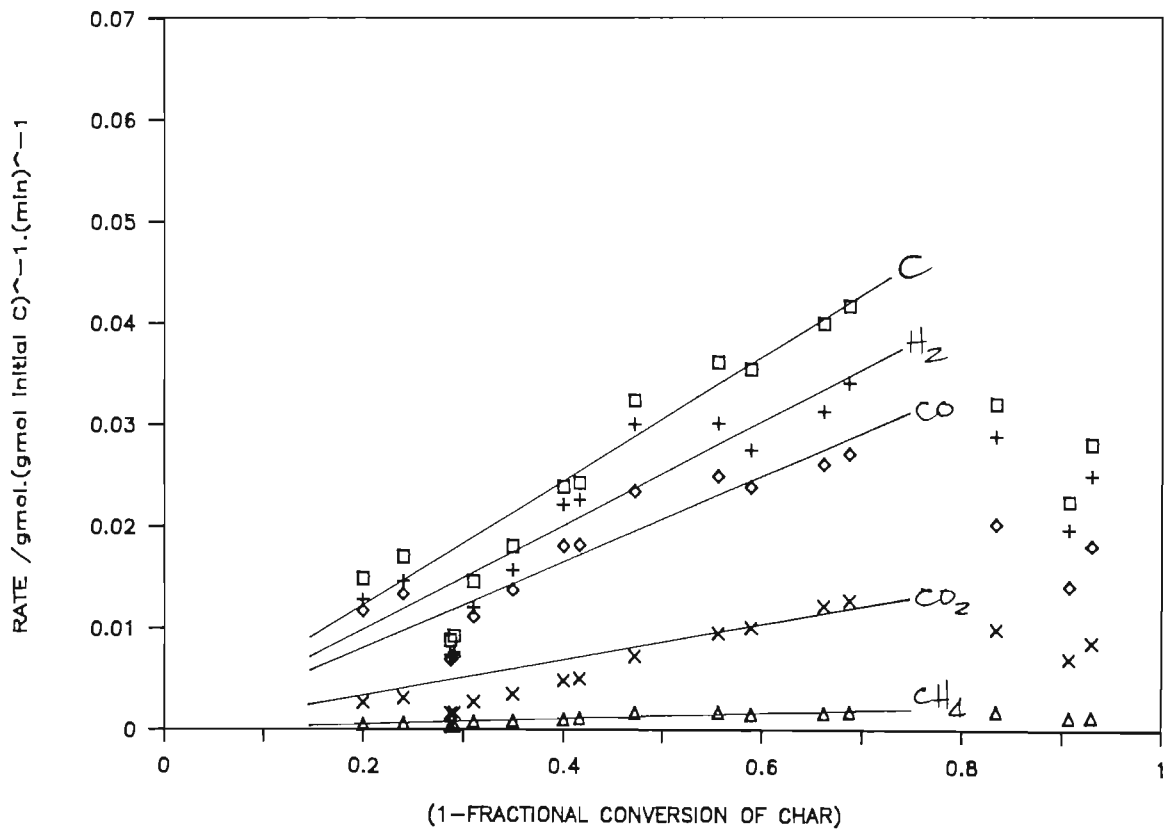


FIGURE 30a Kinetic results of Run 56 (T = 920°C; P = 1.8 bar abs)

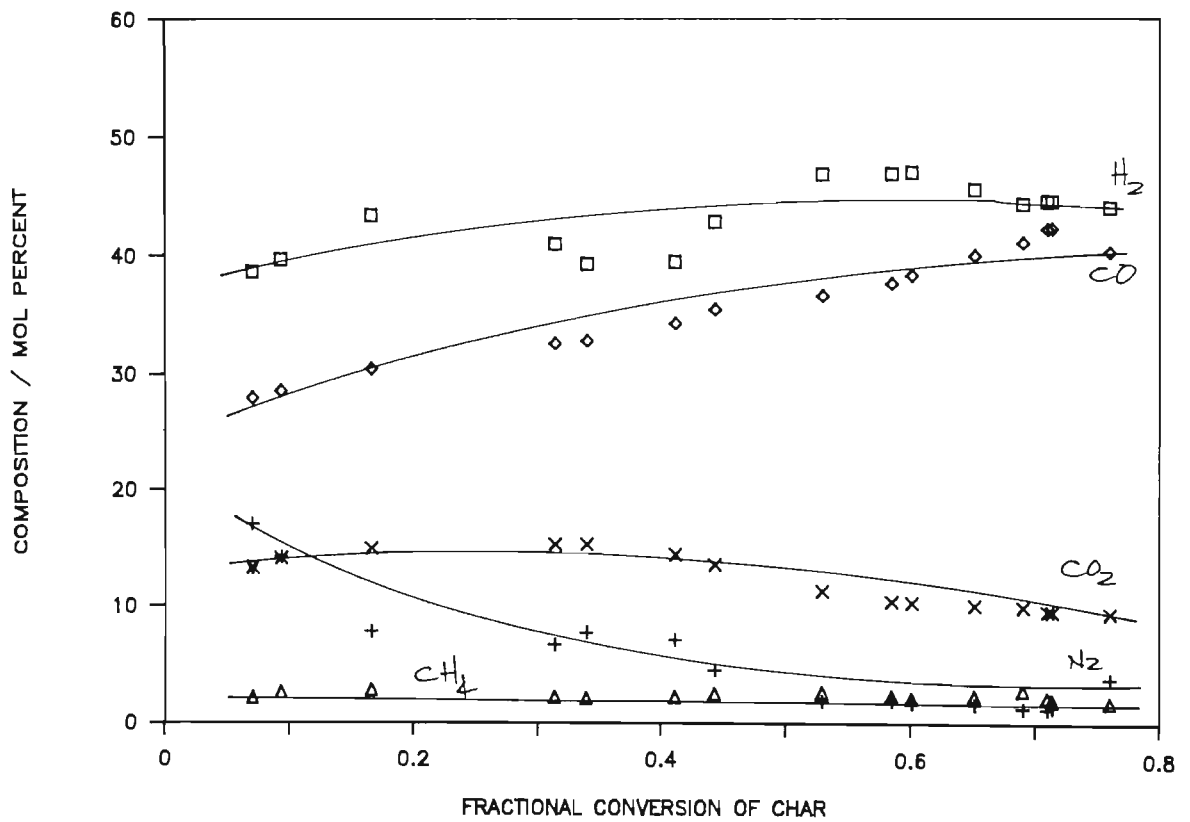


FIGURE 30b Product gas compositions of Run 56

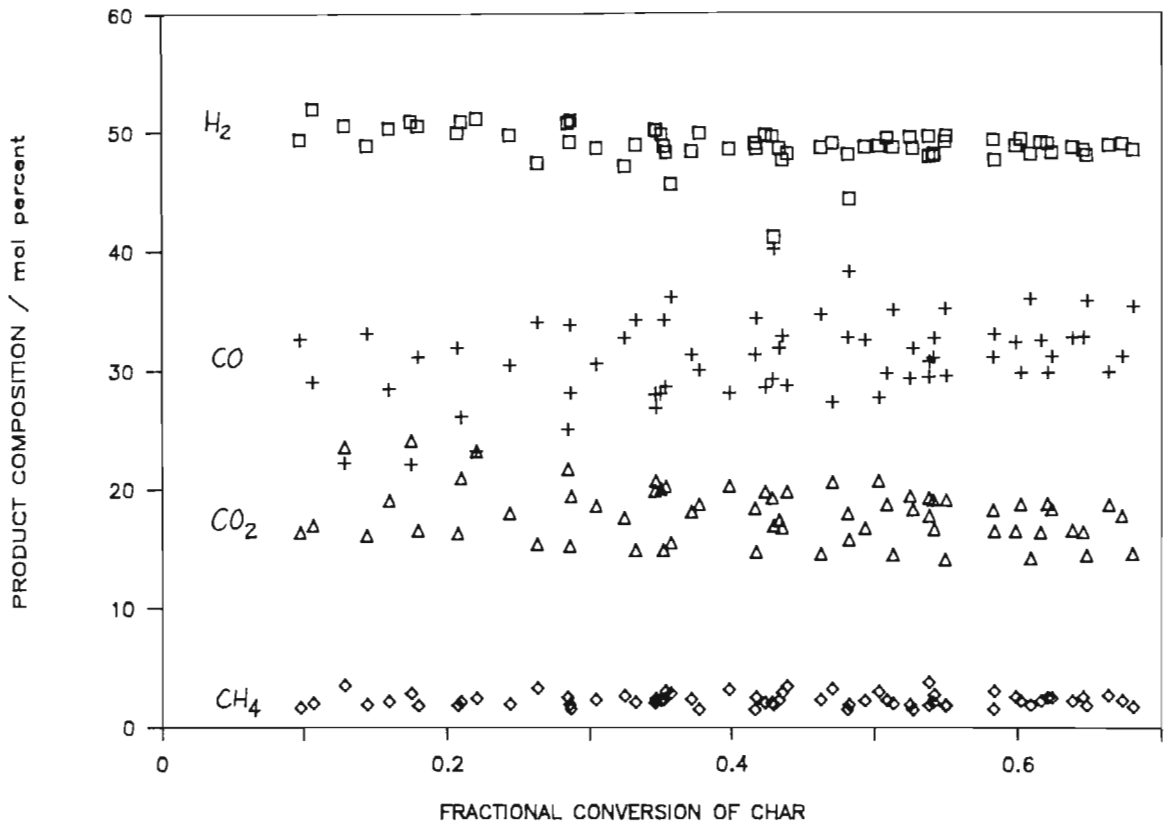


Figure 31. Compositions of gasification products for the set of data employed in the mathematical modelling exercise for Bossjespruit coal char.

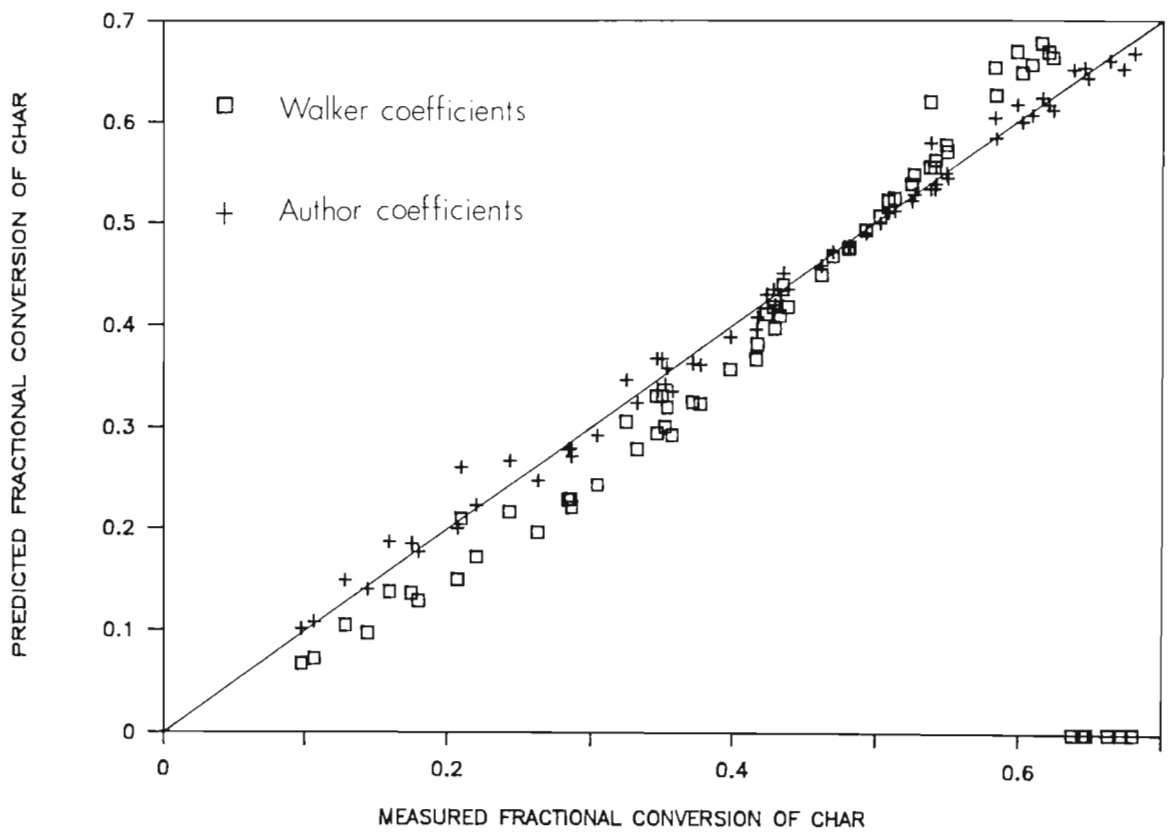


Figure 32. Predictions of the Walker model (eqn(2.10)) compared with the measured data contained in Table 4.7.

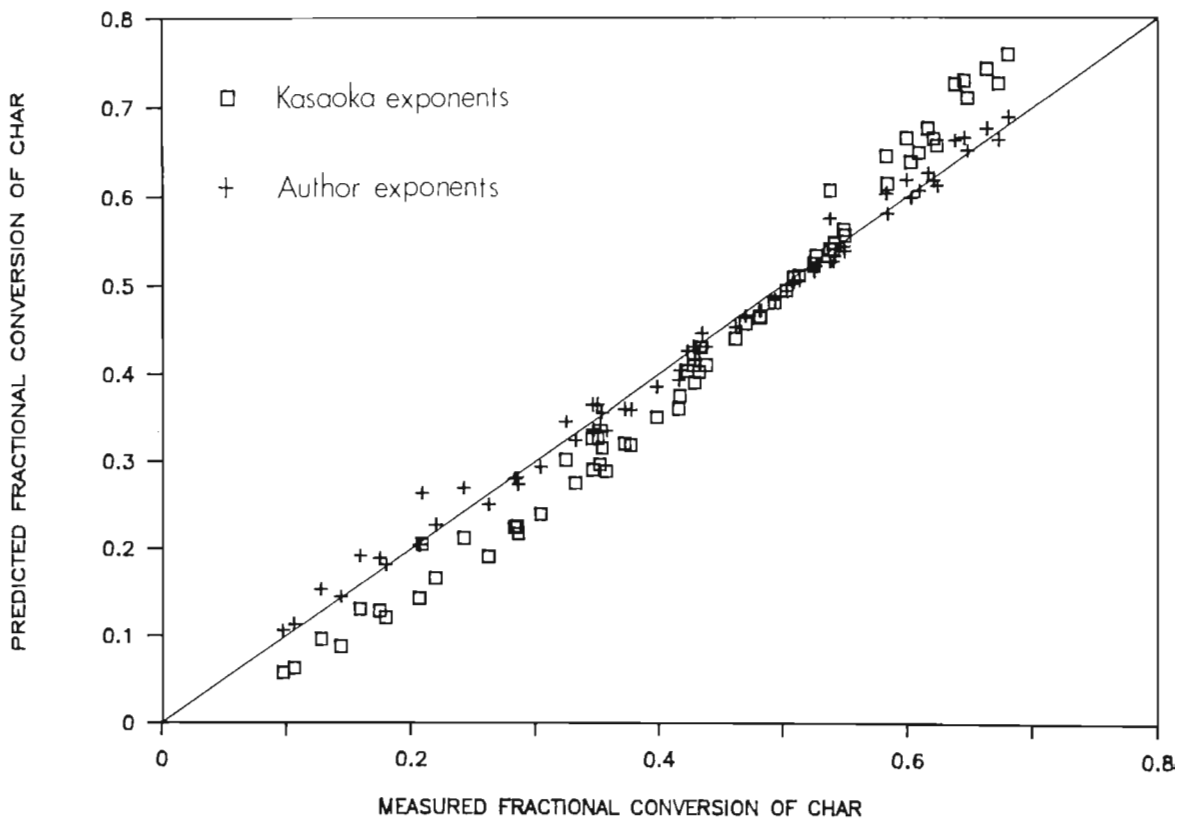


Figure 33. Predictions of the Kasaoka model (eqn(2.11)) compared with the measured data contained in Table 4.7.

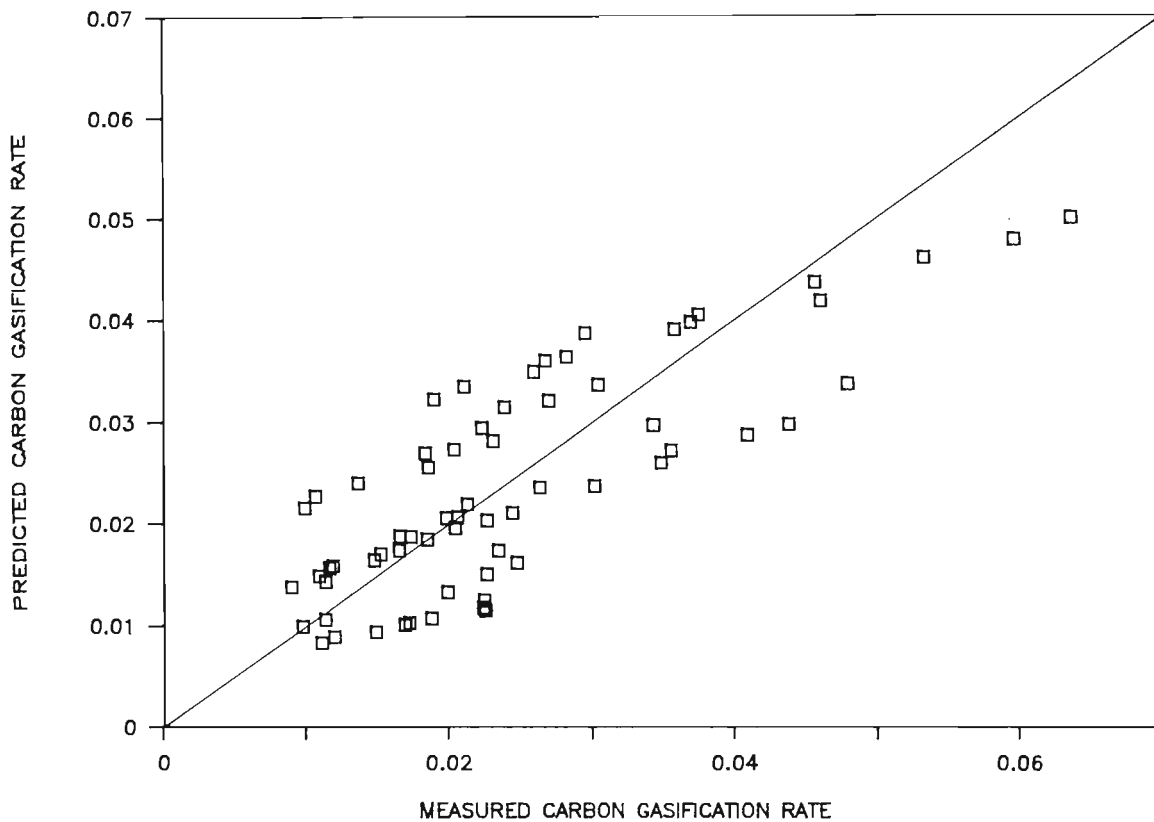


Figure 34. Predictions of the Johnson model (eqn(2.19)) compared with the measured data contained in Table 4.7.

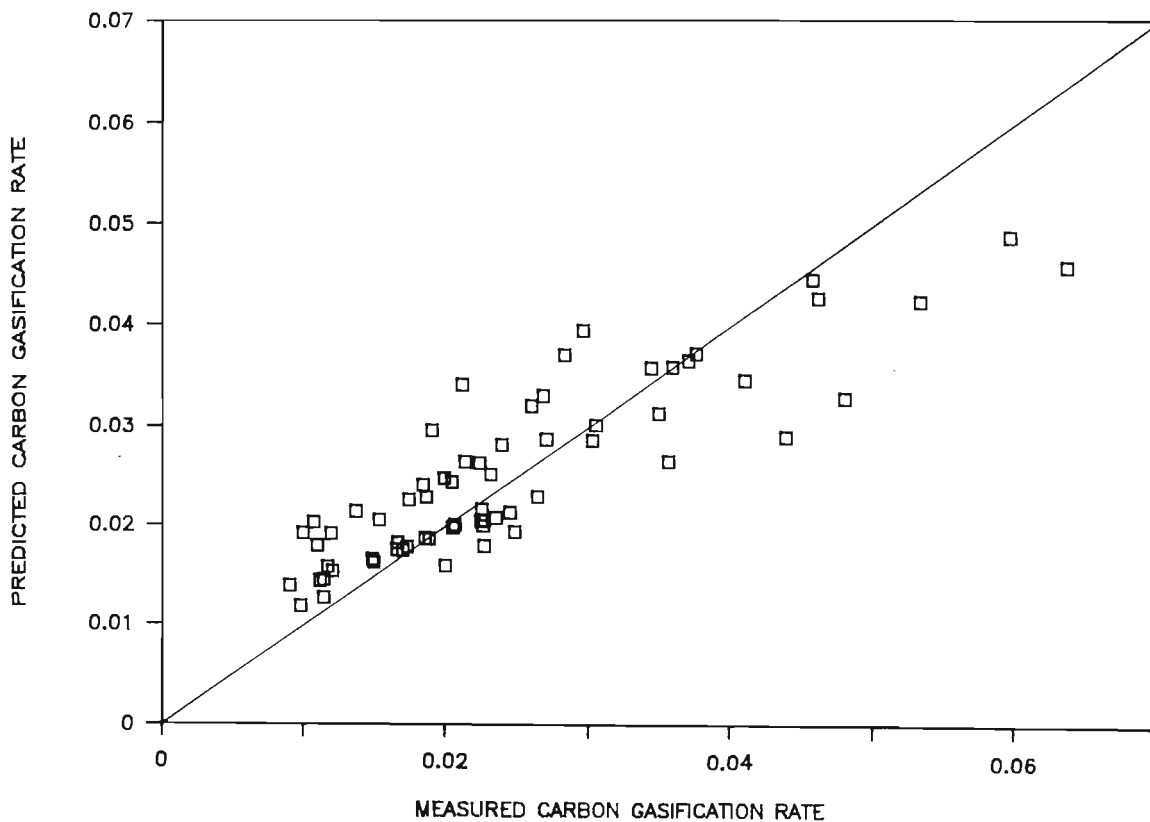


Figure 35. Predictions of Model 1 (eqn(2.21) with $n=2/3$) compared with the measured data contained in Table 4.7.

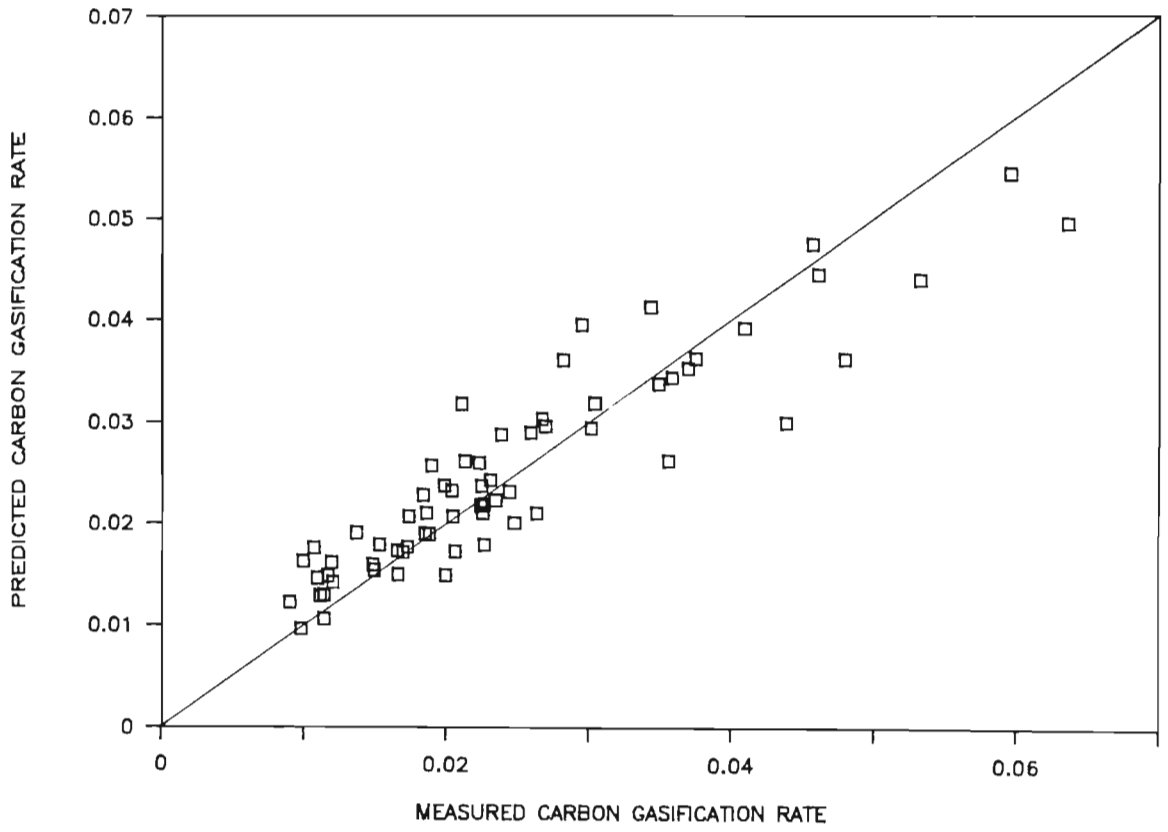


Figure 36. Predictions of the Model 2 (eqn(2.21) with $n=1$) compared with the measured data contained in Table 4.7.

4.5.1 ANALYSIS OF RESULTS.

4.5.1.1 THERMODYMANIC ANALYSIS.

The gas phase composition of a steam-char gasification process, in which the gaseous products are H_2 , CO , CO_2 and CH_4 , is dictated by the relative extents of the following set of three independent reactions :

(a) THE BOUDOUARD REACTION



(b) THE WATER-GAS SHIFT REACTION



(c) THE METHANE FORMATION REACTION



Note that the steam-carbon gasification reaction, $C + H_2O = CO + H_2$ is derived by combining equations [D.1] and [D.2].

The equilibrium compositions of the gas phase during steam-char gasification under the various conditions of temperature and pressure investigated in this study are computed in Appendix D and illustrated in Figures D.1 - D.3, below :

It is evident from Figures D.1 - D.3 that the equilibrium compositions of H_2 and CO increase very gradually between $800^\circ C$ and $920^\circ C$ and that the equilibrium compositions of CO_2 and CH_4 decrease even more gradually in the same temperature interval. It is also

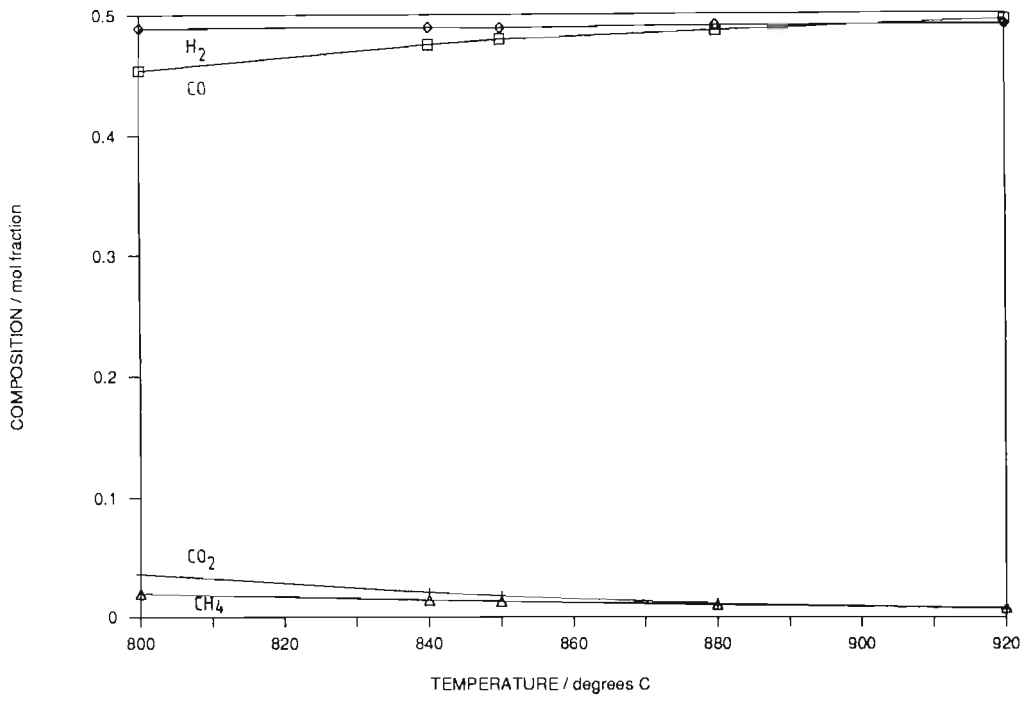


Figure D.1 The effect of temperature on the equilibrium composition (dry) of synthesis gas at a total pressure of 1.78 bar(abs.).

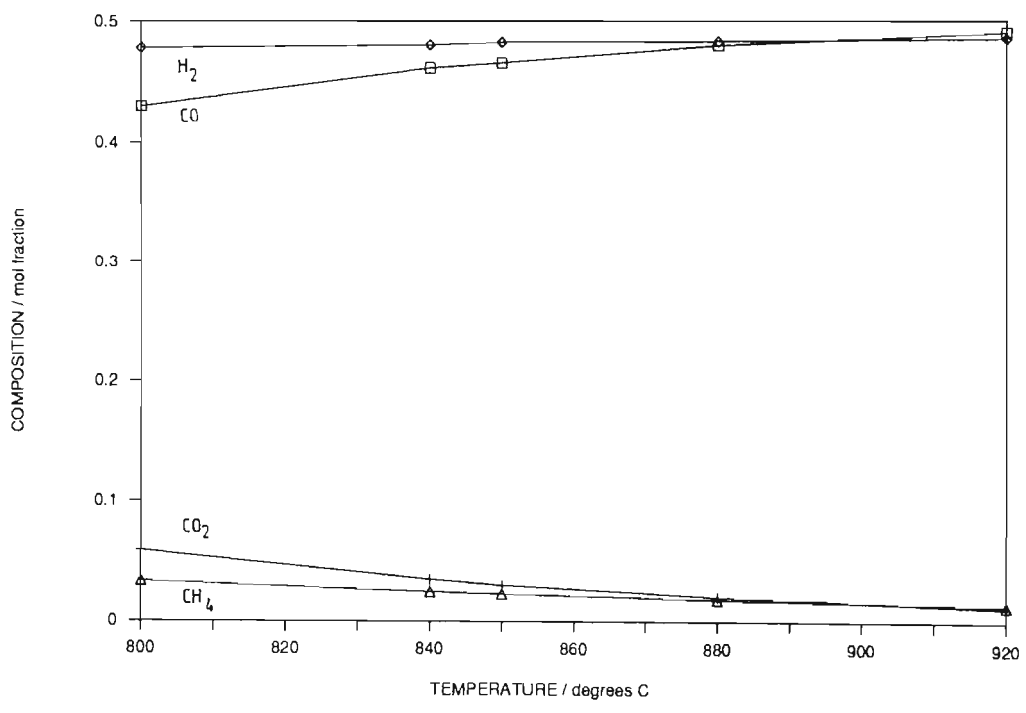


Figure D.2 The effect of temperature on the equilibrium composition (dry) of synthesis gas at a total pressure of 3.16 bar(abs.).

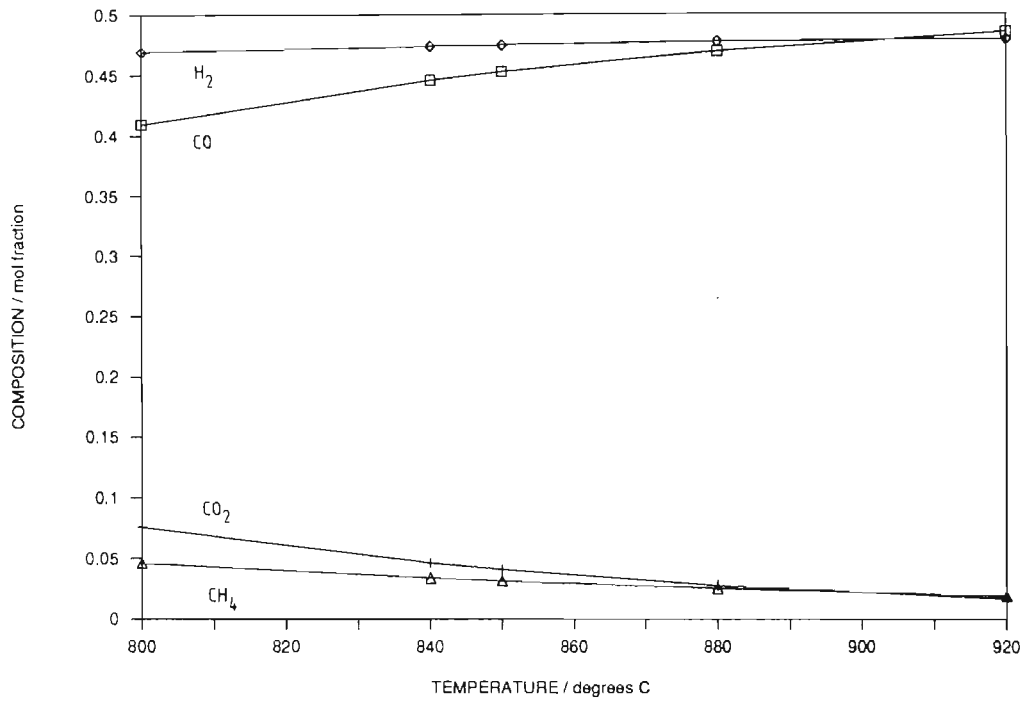


Figure D.3 The effect of temperature on the equilibrium composition (dry) of synthesis gas at a total pressure of 4.78 bar(abs.).

(4.21)

clear that the equilibrium compositions, generally, are marginally lower at higher steam partial pressures.

The following results are evident when one compares the gas phase compositions measured in the experimental program with the equilibrium compositions of the gas phase :

- The H_2 concentrations rapidly approached the equilibrium values and subsequently remained almost constant. This result is to be expected, since the homogeneous watergas shift reaction is relatively fast (compared to the rate of the heterogeneous Boudouard reaction or the $C + H_2O$ reaction) and is known to be at equilibrium within the range of general gasifier operating conditions ($\Delta G_{1200K}^{\circ} = +3.1 \text{ kJ/gmol}$, see p (2.4)).
- The measured CH_4 concentrations rapidly approached the relatively low equilibrium values, and remained fairly constant throughout the course of gasification.
- The effect of the Boudouard reaction on the measured product gas compositions was remarkably evident. Although this reaction is reversible in the temperature range 700k - 1300k ($\Delta G_{1000K}^{\circ} = -4.6 \text{ kJ/gmol}$; $\Delta G_{1200K}^{\circ} = -39.4 \text{ kJ/gmol}$), the measured CO and CO_2 compositions hardly attained equilibrium values during the course of gasification. This indicates that the rate of the Boudouard reaction is relatively slow and is therefore certainly significant in controlling the overall gasification kinetics. Figure 23b shows that the rate at which the CO concentration increases to approach its

(4.22)

equilibrium value is approximately twice the rate at which the CO_2 concentration decreases to approach its equilibrium value. (The approximate slope of the CO curve is +30 mol % per unit of fractional char conversion and that of the CO_2 curve is -15 mol % per unit of fractional char conversion). This reaction stoichiometry can only be described by the Boudouard reaction ($\text{C} + \text{CO}_2 = \text{CO}$).

In summary, the nitrogen-free compositions of the product gas streams are found to be remarkably uniform throughout the course of the reaction (Approximately 49% H_2 , 32% CO, 17% CO_2 and 2% CH_4 on a molar basis) and are independent of both the reaction temperature in the range 800°C to at least 920°C and the steam pressure in the range 1.8 to at least 4.8 bar absolute.

4.5.1 ANALYSIS OF RATE DATA FOR BOSJESSPRUIT CHAR.

The majority of the experiments conducted in this study have involved Bosjesspruit char, for which the following results are evident :

- The rates of carbon-steam gasification are independent of the steam pressure in the range 1.8 to at least 4.8 bar absolute. Compare Figure 19a with Fig. 28a and Fig. 22a with Fig. 27a. These results are supported by Walker et al. (1959), Johnson (1974), Chin et al. (1983) and Kasaoka et al. (1985), all of whom report that the reaction rates of steam-char gasification approach zero order with respect to steam partial pressure as

(4.23)

the partial pressure of steam increases above atmospheric pressure.

- The rate data are particularly sensitive to temperature; an increase in the temperature of gasification in the range 800°C - 920°C typically results in a drastic increase in reaction rate. This behaviour is characteristic of a reaction for which the kinetics are controlled by the rates of the chemical reactions and has been demonstrated by Jensen (1975), Klei et al. (1975), Kayembe and Pulsifer (1976), Schmal et al. (1982), van Heek et al. (1985) and Kasaoka (1985) for the steam-char gasification of small char particles (< 0,5mm) at temperatures up to 1000°C. These investigators claim that the carbon-steam reaction occurs uniformly throughout the interior of the char particles under these conditions.
- The carbon gasification rates are first order with respect to the carbon concentration of the char, ie. (1-fractional conversion of the char). This result is evident from the linearity of the plots of the rate data versus fractional conversion of char (see Figures 13a - 30a) and is consistent with the results obtained by Miura et al. (1986) for the steam gasification of carbon at 835°C and at a steam partial pressure of 1 atmosphere. The fact that the measured rate data are first order with respect to the fraction of carbon remaining in the char and are not dependent on the partial pressure of steam, suggests that the volumetric reaction model may be employed to describe the nature of the steam gasification of Bosjesspruit coal char at temperatures between

(4.24)

800°C and 920°C and steam pressures from 1.8 bar absolute to at least 4.8 bar absolute (Wen and Dutta (1979)).

- The different char preparation techniques employed in this study, namely, a fairly rapid heating rate in a fluidised bed and a slower heating rate in a tubular furnace, have no effect on the subsequent steam-char gasification kinetics. This result may be explained by the observation made by Radovic et al. (1985), that after 5 minutes of the pyrolysis of a lignite char at 1000°C, the reactivity of the char towards steam had reached its lowest value and had not declined any further after a residence time of 1 hour. Ashu et al. (1978) and Howard et al. (1981) attribute the decreased reactivity of chars after a relatively short pyrolysis residence time to thermal annealing, which promotes deactivation of the char due to realignment of the coal layer planes. It is the opinoin of the author that thermal annealing of the chars employed in this study during pyrolysis and during the preheating of the microreactor before a steam gasification experiment played a significant role in determining the reactivity of the respective chars. This effect, however, is also likely to occur in the pyrolysis and gasification zones of the Judd gasifier.

4.5.2 REPRODUCIBILITY OF EXPERIMENTAL RESULTS.

The degree of reproducibility of the experimental results was found to be very good for each of the conditions of reaction temperature investigated, as is evident from the similarity of the results contained in Figures 14a, 16a, 20a, and 23a (for which $T=840^{\circ}\text{C}$); Figures 15a, 17a, 21a, 22a, 24a, 26a, and 27a (for which $T=880^{\circ}\text{C}$) and Figures 18a, 19a and 28a (for which $T=920^{\circ}\text{C}$). Note that the degree of reproducibility of results with different operators was also very good.

4.5.3 ANALYSIS OF RESULTS FOR TRANSVAAL NAVIGATION CHAR.

The experimental results obtained for the steam gasification of char derived from Transvaal Navigation coal show that the product gas stream contains very high concentrations of H_2 and CO and relatively low concentrations of CO_2 and CH_4 (approximately 50% H_2 , 42% CO , 6.5% CO_2 and 1.5% CH_4 on a N_2 free basis at a carbon conversion of $X=0.5$) at both 850°C and 920°C . The levels of both the H_2 and the CH_4 concentrations rapidly attain their respective equilibrium values and remain approximately constant throughout gasification, whereas the concentrations of CO and CO_2 gradually approach their respective equilibrium values during the course of gasification and almost attain equilibrium concentrations as the conversion of carbon nears completion. The rate of steam gasification of this char is therefore also controlled by the rate of the Boudouard reaction.

(4.26)

This product gas composition may be explained by the moderately rapid rate of the steam-carbon reaction (compared with the rate of the Boudouard reaction). During gasification, an equimolar mixture of H_2 and CO which is close to that of the equilibrium composition is generated by the steam-carbon reaction. In addition, the water gas shift reaction rapidly acts to draw the H_2 concentration closer to equilibrium and to produce some CO_2 , at the expense of CO and H_2O . The CO_2 is then converted to CO by the Boudouard reaction at a relatively low rate. The net rate of increase of the CO concentration of the product gas stream during gasification is found to be twice the rate of decrease of the CO_2 concentration, which indicates that the rate of steam-char gasification is essentially controlled by the rate of the Boudouard reaction.

The results of the experiments conducted in this study show that the magnitudes of the steam gasification kinetics of Transvaal Navigation coal-char are comparable with those of Bosjesspruit coal-char; this may be attributed to the fact that the rate of gasification of each char is controlled by the rate of the Boudouard reaction, despite the fact that the steam-carbon reaction is promoted at a slightly lower rate during the gasification of Bosjesspruit char, as is evident from the differing product gas spectrums of the two chars. It is strongly suspected, however, that the differing reaction rates displayed by the carbon-steam reaction for each of the two chars investigated in this study were as a result of the catalytic effects of certain inherent components of the chars, although no specific tests of this nature were conducted.

4.5.4 MATHEMATICAL MODELLING OF THE EXPERIMENTAL RESULTS.

The kinetic results of Runs 27 to 42 inclusive have been employed in an exercise in which the steam gasification kinetics of Bosjesspruit coal-char have been mathematically modelled. Runs 45, 51, 53 and 54 were conducted subsequent to the modelling exercise as replicate runs of previous experiments. These replicate experiments were conducted by Mr. A. Holmes and Miss M. Hetherington under the supervision of the author. Although the results of the replicate runs have not been included in the modelling exercise, it is intended that this be done in the near future. The mathematical modelling exercise involved the regression of the following mathematical models on the relevant experimental data :

Johnson's model :

$$\frac{dX}{dt} = f_R K_T (1-X)^{2/3} \quad [2.19]$$

$$\text{where } K_T = \frac{\exp(9,0201-12\,910/T)}{[1+(1/P_{H_2O})\exp(-22,216+24\,882/T)]^2} \quad [2.20]$$

and

X = carbon conversion expressed as a fraction of the amount of carbon initially present; gmol/gmol carbon initially present.

t = time; minutes.

(4.28)

- f_R = relative reactivity factor, which depends on the char type and char thermal history, where $0,3 \leq f_R \leq 10$.
- K_T = kinetic parameter, or rate constant.
- T = reaction temperature; Kelvin.
- P_{H_2O} = partial pressure of steam, atmospheres(absolute).

Despite the indication by the rate data that the behaviour of the steam gasification of Bosjesspruit char may be represented by the volumetric reaction model, Johnson's model was considered in this study as a reference case in which the applicability of a model with a 'shrinking core' type mass action term $((1 - X)^{2/3})$ and a steam partial pressure effect was tested.

Thereafter, the model proposed by Muira et al. (1986) and Guo and Zhang (1986) was considered. The general form of this model is :

$$-r_C = \frac{dX}{dt} = K(1-X)^n \quad [2.21]$$

in which

X = the fractional conversion of carbon, and

K = an Arrhenius-type rate constant.

This model is more fundamental than that of Johnson's in that it contains the classical Arrhenius-type rate constant which accounts for the exponential effect of temperature on the reaction rate. Guo and Zhang claim that this expression represents the volumetric reaction model when $n = 1$ and the shrinking core model when $n = 2/3$.

(4.29)

Equation [2.21], with $n = 1$, is identical to that proposed by Wen and Dutta (1979) for the volumetric reaction model with a zero order steam partial pressure term. Equation [2.21] with $n = 2/3$ is referred to in this text as Model 1; the case of equation [2.21] with $n = 1$ is referred to as Model 2. These cases are reflected below :

$$\text{Model 1 :} \quad -r_C = \frac{dX}{dt} = K(1-X)^{2/3}$$

$$\text{Model 2 :} \quad -r_C = \frac{dX}{dt} = K(1-X)$$

Based on the nature of the rate data measured in this study, it is hypothesized that the volumetric reaction model, as described by Model 2, is an appropriate model for the steam gasification of Bosjesspruit char at temperatures from 800°C to 920°C and at steam pressures of 1.8 bar absolute to at least 4.8 bar absolute.

A non-linear least-squares regression computer package called 'Simplex' was employed in the mathematical modelling exercise. The resultant expressions of the models contain coefficients and exponents which allow the respective models to predict the experimental results with the least possible variance.

The experimental data employed in the modelling exercise excluded such data which was regarded by the author as being completely inconsistent with the general trend of the data. This philosophy was employed to exclude the effect of any gross experimental error on the overall results.

(4.30)

The complete set of experimental data included in the mathematical modelling exercise are contained in Table 4.7, below, together with the corresponding predictions of the kinetic models considered, namely Johnson's model and two Arrhenius-type models, Model 1 and Model 2. The significance of the various models is discussed after the presentation of Table 4.7, in which the experimental data set employed in the mathematical modelling exercise together with the predictions of the kinetic models are presented. Table 4.7 is contained in the following three pages.

Run no.	Temp. °C	X	Carbon gasification rate / gmol / (gmol C initially present . min)			
			Measured rate	Predicted rates		
				Model 1	Model 2	Johnson
27	840	.1061	.02241457	.02156871	.02370338	.01245716
		.1796	.02237541	.02037021	.02175541	.01176496
		.2070	.02252959	.01991391	.02102854	.01150142
		.2853	.01877939	.01857759	.01894778	.01072962
		.3321	.01725770	.01776091	.01771217	.01025794
		.3518	.01692483	.01740913	.01718857	.01005477
		.4168	.01487822	.01622549	.01546575	.00937115
		.4617	.01198991	.01538048	.01427345	.00888311
		.5127	.01109043	.01439384	.01292228	.00831327
30	880	.0972	.03432329	.03575909	.04134177	.02964974
		.1436	.04092080	.03452365	.03921791	.02862537
		.2626	.03482926	.03124637	.03376827	.02590801
		.3569	.03011751	.02852009	.02944664	.02364750
		.4289	.02126573	.02635080	.02615172	.02184884
		.4818	.01983299	.02469762	.02372969	.02047810
		.5487	.01737468	.02252350	.02066633	.01867542
		.6084	.01522533	.02049282	.01793543	.01699167
		.6473	.01187421	.01910919	.01615001	.01584443
.6799	.01091472	.01791402	.01465881	.01485345		
34	840	.1589	.02344826	.02071148	.02230442	.01735119
		.2430	.02473089	.01930625	.02007341	.01617395
		.3242	.02262049	.01789998	.01792062	.01499583
		.4348	.01992165	.01588955	.01498793	.01331158
		.5983	.01136356	.01265339	.01065085	.01060047
		.6373	.00976075	.01182123	.00961763	.00990332

(4.32)

Run no.	Temp. °C	X	Carbon gasification rate / gmol / (gmol C initially present . min)			
			Measured rate	Predicted rates		
				Model 1	Model 2	Johnson
35	880	.2091	.04794710	.03274163	.03622095	.03368192
		.3456	.04378692	.02885714	.02997017	.02968587
		.4279	.03554889	.02638236	.02619870	.02714002
		.5403	.02626396	.02280372	.02105320	.02345861
		.6229	.02060233	.01998280	.01727006	.02055668
		.6722	.01657935	.01819873	.01500966	.01872137
36	920	.2857	.05959222	.04872645	.05445984	.04785908
		.3769	.04560889	.04448442	.04750520	.04369257
		.4161	.04604223	.04260165	.04452141	.04184331
		.4809	.02945972	.03938807	.03958004	.03868693
		.52663	.02812918	.03705288	.03611288	.03639331
		.5825	.02106323	.03406359	.03183207	.03345723
37	920	.3494	.06357291	.04578414	.04960231	.04993597
		.4229	.05318097	.04226416	.04399341	.04609679
		.5245	.03746772	.03714603	.03624915	.04051454
		.5375	.03692998	.03646971	.03526369	.03977688
		.5494	.03577165	.03584022	.03435462	.03909030
		.6018	.02665716	.03300338	.03035756	.03599622
		.6199	.02585428	.03199559	.02897774	.03489704
		.6628	.01894101	.02954040	.02570714	.03221920

(4.33)

Run no.	Temp. °C	X	Carbon gasification rate / gmol / (gmol C initially present . min)			
			Measured rate	Predicted rates		
				Model 1	Model 2	Johnson
38	840	.1277	.02440702	.02122113	.02313272	.02100627
		.1748	.02260419	.02044974	.02188295	.02024269
		.2203	.02042533	.01969062	.02067585	.01949126
		.2837	.01849973	.01860835	.01899486	.01841995
		.3463	.01653917	.01750829	.01733563	.01733102
		.3980	.01478637	.01657237	.01596435	.01640458
		.4383	.01163102	.01582231	.01489289	.01566211
		.50084	.01136699	.01447843	.01303636	.01433185
		.5377	.00899946	.01389786	.01226016	.01375715
40	880	.3529	.02694494	.02864011	.02963271	.03205885
		.4698	.02305088	.02507907	.02428155	.02807273
		.5025	.01835940	.02403572	.02278217	.02690485
42	880	.3036	.03042534	.03007762	.03189147	.03366796
		.3716	.02380939	.02808715	.02877868	.03143989
		.4325	.02227451	.02624016	.02598717	.02937242
		.4929	.02036686	.02434502	.02322333	.02725106
		.5412	.01858770	.02277109	.02100802	.02548926
		.5833	.01361822	.02135704	.01908187	.02390641
		.6154	.01065405	.02024750	.01761434	.02266442
		.6447	.00991278	.01920336	.01626954	.02149565

(4.34)

Figure 31 shows the relationship between the composition of the products of gasification and the fractional conversion of the char for each of the data points in the above table.

The experimental char conversion data are compared with the predictions of Walker's model (equation [2.10]) in Figure 32. Figure 32 also contains the predictions of the Walker model with coefficients which were derived by non-linear least squares regression of the model on the experimental data. The values of these coefficients were found to be $a_W = 0,654$; $b_W = -0,160$; and $c_W = 0,0025$, which have little mechanistic significance though, as the Walker model has no fundamental basis. It is interesting to note, however, that the predictions of the original Walker model are reasonably similar to the measured data.

The experimental char conversion data are compared with the predictions of Kasaoka's model (equation [2.11]) in Figure 33. Figure 33 also contains the predictions of the Kasaoka model with exponents which were obtained by regression of the model on the experimental data. The regressed exponents were found to be $a = 0,675$; and $b = 0,984$. This value of a is identical to that obtained by Kasaoka et al., whilst the value of b is significant in indicating that the reaction follows the volumetric reaction model with the chemical reaction rates controlling the overall kinetics. This result is consistent with that reported by Miura et al.(1986) for chars which contain Ca or Fe.

(4.35)

The experimental carbon gasification rate data are compared with the predictions of Johnson's model (equation [2.19]) in Figure 34. The value of f_R in this model was obtained by regression of the model on the experimental data, and was found to be 0,47. This model yielded the worst fit to the measured rate data, which is not surprising when one considers that the measured rate data were found to be of zero order with respect to steam pressure, whereas the Johnson's model includes the partial pressure of steam as a parameter.

Figure 35 compares the measured kinetic data with the predictions of the Arrhenius-type model of equation [2.21] in which $n = 2/3$ (Model 1). This model was considered in order to test the shrinking core mechanism for this reaction, as suggested by Johnson's model. Model 1 contains Arrhenius factors which were obtained by regression and found to be $k_1 = 41\ 064$ gmol carbon gasified / (gmol carbon initially present . minute) and $E_1 = 133$ kJ / gmol.

Figure 36 also compares the measured kinetic data with the predictions of the Arrhenius-type model of equation [2.21]. In this case $n = 1$ (Model 2) and the frequency factors and activation energy, which were found by regression, are $k_2 = 183\ 707$ gmol carbon gasified / (gmol carbon initially present . minute) and $E_2 = 146$ kJ / gmol respectively. Model 2 was considered in order to test the validity of the volumetric mechanism for this reaction. This mechanism is suggested by the results obtained by applying the Kasaoka model (Figure 33) to the data and by the composition of the mineral matter of the char.

(4.36)

The complete expression of the volumetric reaction model for the steam gasification of Bosjesspruit char at temperatures of 800°C to 920°C and at steam pressures of 1.8 bar absolute to at least 4.8 bar absolute, is as follows :

$$-r_C = k_1 \exp(-E_1/RT) (1-X)$$

in which,

$-r_C$ = the rate of steam gasification of carbon,
gmol/(gmol carbon initially present.min);

k_1 = 183 707 gmol carbon gasified / (gmol carbon
initially present.min), the frequency factor for
the steam-carbon gasification reaction;

E_1 = 146 kJ/gmol, the Arrhenius activation energy for
the reaction;

R = 8.314 J/(gmol.K);

X = the fractional carbon conversion of char.

The best statistical fit to the measured kinetic data is displayed by Model 2, the volumetric model with an Arrhenius rate constant. Table 4.8 contains the statistical information relevant to the kinetic models.

Model	Sum of Squares	Variance
Johnson	$0,3439 \times 10^{-2}$	$5,3744 \times 10^{-5}$
Model 1	$0,2454 \times 10^{-2}$	$3,8963 \times 10^{-5}$
Model 2	$0,1583 \times 10^{-2}$	$2,5120 \times 10^{-5}$

TABLE 4.8 Statistical information for kinetic models.

(4.37)

The value of $E_2 = 146$ kJ/gmol, obtained with Model 2, is identical to the average value of the activation energies reported by Feldkirchner and Linden (1963), Feldkirchner and Herber (1965), Johnson (1974) and Jensen (1975) for the steam-char reaction, and compares favourably with the activation energies reported by other investigators at temperatures below 1000°C (van Heek and Muhlen, 1985; Linares-Solano et al., 1986; Kasaoka et al., 1985, and Chin et al., 1983). This result indicates that the kinetics measured in this study were controlled by the rates of the chemical reactions.

CHAPTER 5.

THE APPLICATION OF THE MEASURED KINETIC DATA FOR CHAR-STEAM GASIFICATION TO THE SIMULATION OF THE JUDD CIRCULATING FLUIDISED BED COAL GASIFIER.

5.1 INTRODUCTION.

The chemical engineering design of the Judd gasifier involves the development of a set of equations which suitably describes the material and energy balances of the gasifier. The derivation of these equations is based on the assumptions which are made concerning, inter alia, the gas-solids contacting patterns and the temperature and species concentration profiles which prevail in the gasifier. The assumptions which are made are intended to describe the real operation of the gasifier as accurately as possible, though frequently less accurate assumptions have been made in order to simplify the form of the mathematics involved. In this chapter a one-dimensional compartmental model of the gasifier is presented.

5.2 ZONAL SEPERATION OF THE REACTOR VOLUME.

The configuration of the Judd circulating fluidised bed gasifier is shown in Figure 1. An inherent feature of the configuration of this gasifier is the physical division of the volume of the reactor into two coaxial zones which are linked above and below. This division is caused by the presence of an open-ended, central draft

(5.2)

tube which allows the reactor to be divided into two separate reaction zones when the fluidising gases which are supplied to the two regions are the separate reactant gases of the reactor (i.e. air and steam). In practise the char combustion reactions (i.e. the char-air gasification reactions) occur within the draft tube region, and the char-steam gasification reactions occur in the annular region which surrounds the draft tube. The reasons for this orientation of the reaction zones shall be given later. These two regions of the reactor shall be referred to, in this text, as 'the draft tube' and 'the annulus' respectively.

5.3 CIRCULATION OF THE SOLID MATERIAL WITHIN THE REACTOR.

The zonal separation in the reactor also allows one to simultaneously operate the draft tube as a slugging bed and the annulus close to incipient fluidising conditions. This causes the circulation of solids around the draft tube-annulus loop (solids move up the draft tube and down the annulus). Circulation of the solid material within the reactor provides the mechanism of energy transfer from the combustion zone to the steam gasification zone. The bulk of the solids inventory of the reactor (about 80% - 90% by mass with d_p of about 0,75mm) is silica sand which is selected for the following reasons :

- coal is dispersed by the sand, which prevents the coal from sintering and/or agglomerating;
- circulation of solids in the reactor is not sensitive to coal particle size or density;

(5.3)

- the sand has a high thermal inertia, which aids the transfer of energy between reaction zones;
- silica sand has a relatively high melting point (approximately 1300°C) which provides a reasonable upper limit to the temperature of operation of the gasifier;
- the sand is chemically inert; and
- the sand is able to flow easily.

The partition of the fluidising gas between the draft tube and the annulus is determined by the difference in the separate pressure drops across these two paths. The phenomenon of a reactant gas flowing in the reverse direction to which it is intended is defined in this text as 'crossflow'. By arbitrary convention, 'negative crossflow' refers to the crossflow of steam, and 'positive crossflow' refers to the crossflow of air in the reactor. A pressure balance in which a nett crossflow of zero occurs is achieved by combinations of suitable reactor geometries and of appropriate operating conditions. Separation of the product gases leaving the reactor is achieved by the presence of a suitable hood over the draft tube, without interrupting the circulation of solids in the reactor.

The nature of the solids circulation pattern which occurs in the reactor is such that solid material moves down the annulus in slip-stick fashion, whilst solid material is propelled up the draft tube by gas at relatively high interstitial velocities. It is

therefore assumed in this model that the annulus behaves as a plug flow reactor with countercurrent flow of the gas and solid phases (assumption 1, A1).

In a recent study of the hydrodynamic behaviour of the reactor, Pillay (1986) has observed that the predominant form of slug which occurs in the draft tube during circulation is the wall-slug. This form of slugging involves considerable back-mixing of the solid phase as it is transported up the draft tube, and is distinct from the case in which square-nosed slugging occurs. The latter case involves the transportation of discrete plugs of solid material up the draft tube. It is therefore assumed in this model that the draft tube contains the solid phase in mixed flow and the gas phase in plug flow (A2). The relative direction of flow of the phases in the draft tube is co-current.

A principal feature of the nature of the circulation of solids in the reactor is that the elutriation rate of fine coal-char particles from the reactor is relatively low (Judd and Meihack, 1983). This arises because of the entrainment of coal into the downward flowing solid material in the annulus, and because plugs of solid material which reach the top of the draft tube expand in the shape of mushrooms which collapse gently into the annulus region. This plug eruption behavior has been found to be typical for the range of fluidising gas velocities employed in the draft tube (Rudolph, 1983; Pillay, 1986), and is unlike that which would occur if the draft tube were to be operated as a bubbling or vigorously

slugging fluidised bed. The solids circulation pattern therefore affords a high residence time in the reactor to fine char particles which allows such particles to reach a much higher level of conversion, compared to conventional fluidised beds (Judd et al., 1983).

The orientation of the reaction zones in the gasifier, with the annulus as the char-steam gasification zone, has been selected for the following reasons :

- the kinetics of the char-steam gasification reactions are known to be controlled by the rates of the chemical reactions at temperatures of up to about 1000°C, whereas
- the kinetics of the char combustion reactions are sensitive to the rates of mass transfer of gaseous species to or from the char at temperatures above about 500°C. The high dense phase interstitial gas velocity in the draft tube provides very good contact between gas and solids.
- the reaction rates of char-steam gasification are typically 2 to 3 orders of magnitude lower than the rates of char combustion, below 1000°C. This may be compensated to some extent by hosting the char-steam gasification reactions in the annulus, since the geometry of this reactor is such that the volume of the annulus is approximately ten times greater than the volume of the draft tube.

5.4 FURTHER SUB-DIVISION OF THE REACTOR VOLUME ACCORDING TO PROCESS CONDITIONS.

In this model of the gasifier it is assumed that the chemical reactions occur only once the relevant gas and solid reactants have been heated to the various local temperatures of the reactor inventory (A3). It is also assumed that these temperatures are sufficiently high for the reactions to occur spontaneously (A4). The annulus and draft tube regions of the gasifier may therefore be regarded as comprising various sub-regions/compartments in which different physico-chemical processes occur. Figure 13 is a sectional front view of the gasifier which shows the relative locations of these sub-regions in the reactor.

Before a discussion of the various sub-regions is given, the fate of the coal and the reactant gases in the gasifier shall be discussed briefly.

Coal is fed to the gasifier below the surface of the solid material in the annulus, slightly above the position of the steam spargers. On entering the gasifier, coal is rapidly pyrolysed (i.e. devolatilised) as it contacts the hot solid material in the annulus. The resultant coal-char then moves downward in the annulus until it is drawn into the draft tube entry region. Combustion of the char (i.e. air-char gasification) then occurs as the solid material is transported by the air stream up the draft tube. During steady state operation of the gasifier the oxygen

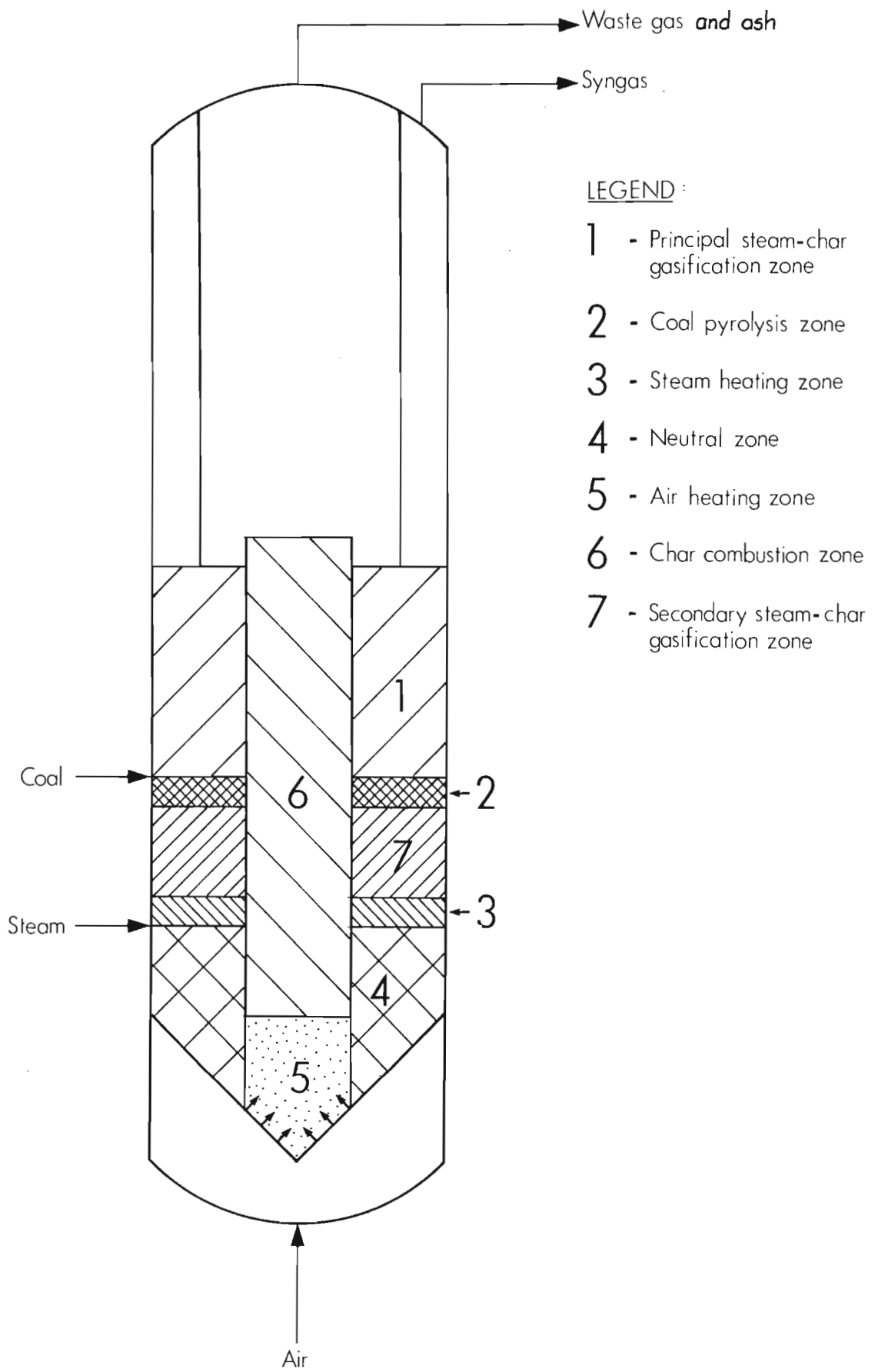


FIGURE 13 Locations of internal zones of the coal gasifier

(5.7)

content of the air supplied to the draft tube is completely consumed in the char combustion reactions. The carbon inventory of the gasifier is therefore maintained in excess of the stoichiometric amount required in the combustion reactions, and steam gasification of the excess char proceeds in the region above the steam spargers in the annulus. It may occur that some char is not fully converted in one pass of the steam gasification zone, in which case it will recycle between the annulus and draft tube regions until it is completely consumed.

Steam enters the reactor through spargers which are located in the annulus, beneath the position of the coal feeders. The direction of flow of steam in the annulus is upwards. On entering the gasifier steam is heated to the temperature of the reactor by contact with hot solids in the annulus. The superheated steam then reacts with the char in the annulus. The required steam flowrate to the gasifier is dictated by the geometry of the reactor and the particle size and density of the solid inventory in the sense that steam and the products of char-steam gasification are required to operate the annulus region at close to incipient fluidising conditions in order to sustain the circulation of solid material in the reactor. (Some flexibility, of the order of $0,6u_{mf}$ to $1,0u_{mf}$, exists in this specification without interrupting solids circulation in the reactor). It is likely, therefore, that an excess of steam exists in the product stream from the annulus. The extent of conversion of steam in the gasifier is dependent on the kinetics of the char-steam gasification reactions and on the space time of the reactor.

(5.8)

Air enters the reactor through a distributor plate located at the base of the reactor. On entering the reactor the air is heated to the temperature of the reactor by contact with hot solids in the draft tube entry region of the gasifier. The air then reacts with the char as it transports solid material up the draft tube.

The steam-char gasification reactions occur in zone 1, which occupies the bulk of the annulus volume. The base of zone 1 coincides with the position of the coal feeders of the gasifier. The design of the gasifier includes multiple, equally spaced feeder points in order to distribute the coal in the annulus. (The number of feeder points depends on the scale of operation of the plant).

Assuming that coal is distributed uniformly in the annulus by the coal feeders (A5), one may identify zone 2 as that in which coal carbonisation/pyrolysis/devolatilisation occurs and in which steam gasification of recycled char occurs. Zone 3 comprises the region of the annulus immediately above the steam spargers in which superheating of the steam occurs. Zone 4 lies between zone 3 and the draft tube entry region. This zone hosts reactions which may occur as a result of crossflow of either of the reactant gases.

Heating of the air stream occurs in zone 5, the draft tube inlet region. The air-char gasification reactions are accommodated in zone 6, the draft tube region of the reactor (A6).

(5.9)

Figure 13 also shows zone 7, which behaves like zone 1, between zone 2 and zone 3. This is to account for char-steam gasification following rapid heating of the reactants, and depends on the separation of the coal feeder and steam sparger positions.

A summary of the assumptions made in the development of the gasifier model thus far is given in Table 5.1, below.

TABLE 5.1 A summary of the assumptions made in the initial development of the gasifier model.

A1.	The annulus behaves as a plug flow reactor with countercurrent flow of the gas and solid phases.
A2.	The draft tube contains solids in mixed flow and gases in plug flow with a co-current relative direction of flow.
A3.	Reactions occur only after all the reactants have been heated to the temperature of the reactor.
A4.	The temperature of the reactor is sufficiently high for the reactions to occur spontaneously.
A5.	Coal is distributed uniformly in the annulus by the coal feeders.
A6.	The gasifier comprises six distinct zones in which different physico-chemical processes occur.

(5.11)

The derivation of the material and energy balance equations for the one-dimensional compartment model of the Judd gasifier described above are contained in Appendix E. These equations have been combined in the form of a computer program, written in the Fortran 77 language, which is designed to simulate the operation of the Judd gasifier. The computer code, which is suitable for use on a personal computer, is contained in Appendix G. A brief discussion of the structure of the program is given in Appendix F.

It is considered appropriate to include at this stage a discussion of an additional assumption made in the derivation of the equations of the model. The heat capacities of substances involved in the energy balances of the gasifier were assumed to be independent of temperature, yet were computed at the arithmetic average temperature of the reactor. Although it is accepted that this assumption is not true, it was employed for the following reasons :

- The order of magnitude of the terms containing heat capacities in the general form of the energy balance is significantly less than the heat of reaction term (See eqn. [E.29]). Therefore the heat of reaction term is more significant in determining the temperature profiles of the gasifier. For this reason, the effect of temperature on the heats of reaction were included in the derivation of the computer algorithm.
- The species with the most temperature-sensitive heat capacity is H_2O . The average change in the heat capacity of steam per $100^\circ C$ in the range $600^\circ C$ to $1000^\circ C$ is only 2.86%.

(5.12)

- The form of the mathematical expressions of the energy balances is conveniently simplified by the assumption of temperature-insensitive heat capacities.
- Many other authors of one-dimensional models have employed the same assumption regarding heat capacities (see section 2.5 of Chapter 2.).

CHAPTER 6.

RESULTS OF GASIFICATION EXPERIMENTS WITH BOSJESSPRUIT COAL USING THE MINI-PILOT SCALE JUDD GASIFIER AND OF CASE STUDIES OF COMPUTER SIMULATIONS OF THE JUDD GASIFIER.

6.1 MINI-PILOT SCALE COAL GASIFICATION EXPERIMENTS.

The experimental results reported in Chapter 4 show that the order of magnitude of the reaction rates of steam gasification of Bosjesspruit coal-char is generally much lower than the order of magnitude of typical char combustion reaction rates. Because the residence time of solid material is higher in the annulus region than in the draft tube region of the Judd gasifier and in view of the relative magnitudes of the reaction rates of char gasification and combustion, the annulus region is considered to be the most suitable location for the steam-char gasification reactions.

Three coal gasification experiments have recently been conducted using the air-steam blown mini-pilot scale Judd gasifier, the configuration of which is shown in Figure 1. These experiments were conducted with the assistance of Prof. M.R. Judd and Messrs V.L. Pillay and W. Bernhardt. The prime objective of these experiments was to test the feasibility of the production of a synthesis gas stream when steam is supplied to the annulus and air is supplied to the draft tube of the gasifier. Previous experiments with this reactor were conducted with the reverse direction of the

(6.2)

separate steam and air streams, ie. steam and air were supplied to the draft tube and annulus regions of the gasifier, respectively.

The key function of the apparatus employed in these experiments is to provide a facility with which the technology of the Judd gasifier may be progressively developed. The experimental apparatus is not designed for continuous operation. Instead, the design of the apparatus is such that modifications to the reactor are able to be performed easily and at a relatively low cost. The process is manually controlled during operation.

The general technique employed during an air-steam blown coal gasification experiment is to preheat the reactor to a particular temperature (about 900°C) by supplying air to both the draft tube and the annulus regions whilst feeding coal to the annulus, thus causing char combustion to occur throughout the reactor (combustion mode). Initially an electrical air heater is employed to preheat the air supply to the reactor, which in turn preheats the reactor, prior to the occurrence of spontaneous combustion of the char in the gasifier.

Once the reactor is heated to the desired temperature and steady circulation of the solid material is established, one then replaces the air supply to the annulus with an appropriate supply of steam to commence gasification (gasification mode). One may then either maintain the operation of the gasifier in the gasification mode or

alternate between combustion and gasification modes. The duration of a typical air-steam blown coal gasification experiment is approximately 24 hours.

The principal dimensions of the gasifier for each experiment were as follows :

Run #	G 12	G 13	G 14
Draft tube length / m	1.5	1.5	2.5
Draft tube diameter / m	0.15	0.15	0.18
Annulus diameter / m	0.5	0.5	0.5

TABLE 6.1 Principal dimensions of the gasifier for each experiment.

In order to separate the product gas streams during each of the experiments conducted, the gasifier was installed with a cylindrical 'hood' of diameter 0.35m which extended from the top of the reactor to an elevation of 0.2m below the top of the draft tube. During operation, the compositions of the dry product gases from the annulus and the draft tube were intermittantly sampled by vacuum and analysed by an on-line infra-red gas analysis system. Each of the two gas sampling streams passes through a total condenser located at the respective sampling points in order to separate any moisture from the product gas samples. Unfortunately, however, no accurate

(6.4)

measurements were made during the experiments to determine the moisture contents of the product gas streams.

At conditions of steady-state operation (with respect to gasifier temperature profile, product gas composition, and reactant flowrates) duplicate samples of the product gas stream from the annulus region were withdrawn by gas syringe and analysed by G.C. using the same technique employed in the kinetic studies (Chapter 4).

During Run G12 two steady-state conditions were established in the gasification mode of the reactor. These conditions were maintained for about 20 minutes each.

(6.5)

The process conditions and product compositions for Run G12 are shown in Table 6.2, below.

STEADY CONDITION #		1	2
COAL / STEAM RATIO		1 : 1	1 : 1
AIR FLOWRATE / Nm ³ /min		1.29	1.47
MEAN REACTOR TEMPERATURE / °C		830	920
ANNULUS PRODUCT GAS COMPOSITION (DRY) / mol percent	H ₂	31.1	34.9
	CO	13.4	14.2
	CO ₂	17.4	18.5
	CH ₄	2.5	2.0
	N ₂	35.6	30.4
ANNULUS PRODUCT GAS COMPSN (DRY, EXCLUDING CONTAMINANTS ⁺⁺) / mol percent	H ₂	56.6	56.7
	CO	24.4	23.1
	CO ₂	14.5	16.9
	CH ₄	4.5	3.3
DRAFT TUBE PRODUCT GAS COMPOSITION / mol percent	CO	0.0	0.0
	CO ₂	21.0	21.0
	N ₂	79.0	79.0

TABLE 6.2 Experimental conditions of Run G 12.

⁺⁺ ie. N₂ and CO₂ which may be present in the annulus as a result of crossflow.

The absolute values of all of the reactant flowrates employed in the experiments conducted are purposefully not disclosed in this text in order to protect the commercial interests of the various parties involved in the development of the Judd gasifier.

The relatively high N_2 content of the dry annulus product gas compositions for each of the two steady conditions of Run G12 indicates that positive crossflow (ie. air flowing into the annulus) occurred during the experiment. This result may be attributed to the combined effects of the reactor geometry and the fluidising gas velocities on crossflow; (a relatively low pressure drop existed across the annulus because of the relatively low annulus bed depth employed in this experiment).

The dry annulus product gas compositions (excluding the N_2 and CO_2 which originate as air which crossflows from the draft tube) are contained in Table 6.2 in order to indicate the quality of the annulus product gas stream under the condition of no crossflow in the reactor. These results show that the gasifier would produce a synthesis gas stream when no crossflow occurs in the reactor. During the operation of the gasifier, however, some degree of crossflow is likely to occur, albeit a relatively small quantity of gas. Consequently, in order to maintain a steady supply of synthesis gas from the gasifier, one should arrange the operating conditions of the gasifier in such a way as to enable the occurrence of a low degree of negative crossflow (ie. allow some steam to flow up the draft tube).

It is interesting to note that the product gas compositions for each of the steady conditions were almost identical, despite the difference in the mean reactor temperature (830°C and 920°C). The independence of the gas compositions on the temperature of the reactor and the actual product gas compositions agree well with the results of the kinetic studies of the steam gasification of Bosjesspruit coal-char; (cf. 49% H₂, 32% CO, 17% CO₂, 2% CH₄). The slightly higher H₂ : CO ratio observed during Run G 12, compared to that of the products of gasification during the kinetic studies is suspected to be as a result of the contribution of the volatile matter to the gas composition in the gasifier.

Having successfully demonstrated the capability of the Judd gasifier in the production of a H₂/CO rich gas stream in Run G12, a further experiment (Run G13) was conducted in order to replicate the conditions of Run G12.

Soon after the reactor had been heated to about 900°C during Run G13, however, the rate of circulation of solid material in the reactor decreased significantly. This resulted the falling of the mean reactor temperature because of the restriction of the amount of coal which was able to be fed into the reactor. (It was discovered after Run G13 that the draft tube support system had failed, thus preventing normal circulation of sand in the reactor).

Although Run G13 was not able to yield any steady-state results because of the retardation of the circulation rate of the solids,

(6.8)

two measurements were made in the gasification mode whilst the temperature of the reactor was falling. The air supply to the draft tube was interrupted during these measurements in order to reduce the N_2 content of the annulus product gas stream.

The compositions of the annulus product gas stream at the two conditions of Run G13 are shown in Table 6.3, below.

CONDITION #	1	2	
COAL / STEAM RATIO	1 : 1	1 : 1	
AIR FLOWRATE / Nm ³ /min	nominally 1.5, (unsteady)		
MEAN REACTOR TEMPERATURE / °C	860	830	
ANNULUS PRODUCT GAS COMPOSITION (DRY) / mol percent	H ₂	42.2	40.8
	CO	19.9	11.4
	CO ₂	16.6	20.4
	CH ₄	1.7	1.5
	N ₂	19.5	25.9
ANNULUS PRODUCT GAS COMPSN (DRY, EXCLUDING CONTAMINANTS) / mol percent	H ₂	56.1	60.7
	CO	26.5	17.0
	CO ₂	15.2	20.1
	CH ₄	2.2	2.2

TABLE 6.3 Experimental conditions of Run G 13.

The N₂ contents of the dry annulus product gas compositions during Run G13 are thought to be as a result of the de-gasing of residual N₂ in the reactor. The hypothetical N₂-free, dry annulus product gas composition of condition #1 of Run G13 (at T = 860°C) compares very well with the compositions measured in Run G12. The composition of the annulus gas at the second condition of Run G13 (T = 830°C) reflects a higher H₂/CO ratio than for condition #1, however. This result may have been influenced in some way by the

depletion in the char concentration of the reactor and is not regarded as being suitable for comparison with the results of Run G12.

After having measured similar annulus product gas compositions in Runs G12 and G13, it was decided to conduct an experiment in which the coal feedrate to the gasifier was higher than that employed in the previous experiments and which was maintained at a sufficiently high flowrate in order to ensure that the carbon concentration within the gasifier was carbon-rich, relative to the oxygen content of the air stream supplied to the draft tube.

Consequently, the gasifier was installed with a draft tube of a larger diameter than was previously employed (0.18m vs 0.15m). This action was taken in order to accommodate a greater air flowrate to the draft tube than was previously employed, whilst maintaining the fluidising velocity in the draft tube in the range 6 to $9u_{mf}$ (as required for the circulation of solids). The increase in the air flowrate to the combustion zone allows a corresponding increase in the amount of energy generated by char combustion, which in turn enables a greater quantity of char to be gasified in the annulus.

A further modification to the geometry of the reactor in preparation for Run G14 was that of increasing the length of the draft tube to 2.5m. This action was taken in order to increase the bed volume of the annulus region (and hence the capacity for steam-char gasification) and also to increase the gas pressure drop across the

annulus during operation. The anticipated effect of increasing the gas pressure drop across the annulus was that negative crossflow would occur during operation.

During Run G14 the gasifier was equipped with a solids flowmeter which is designed to indicate the axial velocity of solid material in the annulus (the flowmeter was designed by Mr W. Bernhardt, a colleague of the author). The circulation rate of solid material in the gasifier during Run G14 was observed to be relatively high, corresponding to an axial solids velocity of about 10mm per second. The frequency of the fluctuation in the gas pressure drop across the draft tube during Run G14 was greater than the frequencies which were observed during Runs G12 and G13, which indicates that the circulation rate of solids in the gasifier during Run G14 was greater than that which occurred in either of the former experiments. These results are attributed to the deeper annulus bed depth during Run G14, which provides a greater driving force for the circulation of solids in the gasifier.

The composition of the draft tube product gas stream was measured in the combustion mode during Run G14 and was found to be approximately 10% CO, 15% CO₂ and 75% N₂. This result indicates that under the carbon-rich condition which prevailed in the reactor during Run G14, partial char combustion (or oxy-gasification of char) occurred in the combustion zone of the reactor. The significance of this result is that the draft tube product gas stream of the gasifier represents a source of gas of low calorific value. This result should be

(6.12)

seriously considered in the utilization of the Judd gasifier in order to ensure that the potential chemical energy content of the 'waste' gas stream is efficiently employed.

After having heated the reactor to about 900°C in Run G14, steam was introduced into the annulus in order to commence gasification. Before a steady-state condition was established, however, it was observed that the temperatures of the freeboard region and of the top of the reactor in general, were higher than 1000°C. (Heat sensitive paint, which coated the outside of the reactor, responded to the high temperatures). In view of the potentially hazardous condition of the reactor, it was decided to abort the run. The material of construction of the reactor limited the safe operation of the reactor to temperatures of below 1000°C. The reason for the high temperatures observed at the top of the reactor in gasification mode is undoubtedly that a significant degree of negative crossflow occurred in the reactor. This caused steam gasification of char to occur in the region of the annulus below the steam spargers and in the draft tube, which led to combustion of the H₂ and CO products of gasification in the draft tube, thus increasing the local temperature of the reactor.

Unfortunately no samples were taken of the annulus product gas stream in the gasification mode of Run G14.

6.2 CASE STUDIES OF COMPUTER SIMULATIONS OF THE JUDD GASIFIER.

Seventeen case studies have been conducted using the algorithm of the one dimensional simulation model of the Judd gasifier (hereafter referred to as the gasifier simulator), the development of which is discussed in Appendix F. The principal objectives of the case studies were as follows :

- (1) To compare the predictions of the gasifier simulator with the results of Runs G12 to G14,
- (2) To investigate the effects of changes in operating conditions and reactor geometry on the performance of the gasifier, and
- (3) To employ the gasifier simulator in the designing of a pilot plant gasifier on a larger scale than that which was tested at the University of Natal. The objective of designing a new pilot scale gasifier is to provide an experimental facility which is capable of continuous operation. This pilot plant is to be used to thoroughly investigate the performance of the Judd gasifier under various operating conditions in order to enable the process to be evaluated.

The results of two classes of case studies, Classes A and B, are presented in this thesis. The case studies in Class A were conducted using the mean reactor geometry employed in Runs G12 to G14 of the mini-pilot scale gasifier and using a range of operating conditions about the mean values employed in the experimental program.

The case studies in Class B were employed in the design of a larger pilot scale gasifier scheduled to operate at a pressure of 5 bar gauge.

The general conditions which are common to all Class A case studies are listed below :

- Pressure of operation = atmospheric
- Air flowrate = 1.3 Nm³/minute
- Air inlet temperature = 350°C
- Steam inlet temperature = 110°C
- Minimum fluidising velocity
of air at 850°C = 0.4730 m/s
- Minimum fluidising velocity
of steam at 850°C = 0.4960 m/s
- Gasification stoichiometric
parameter (see eqn E.11) = 1.35
- Combustion stoichiometric
parameter (see eqn E.59) = 0.6
- Silica sand particle size = 750 microns
- Draft tube length = 2.0 m
- Draft tube diameter = 0.18 m
- Annulus diameter = 0.5 m
- Level of hood below top of d/tube = 0.2 m
- Level of coal feeders " = 1.5 m
- Level of steam spargers " = 1.8 m
- Axial solids velocity in annulus = 8.0 mm/sec (downwards)

The value of the gasification stoichiometric parameter, α , was selected as being 1.35 in order to simulate the product gas composition measured during the kinetic studies on the steam gasification of Bosjesspruit coal-char. Class A case studies were also conducted with a value of the combustion stoichiometric parameter, β , equal to 0.6. This value was employed to simulate the composition of the wastegas stream of Run G14 which was caused by the partial combustion of char in the draft tube.

Because of the sensitivity of the circulation of the solids inventory of the Judd gasifier to the velocities of both of the fluidising gases (air and steam), it was decided to simulate the effects of varying ratios of coal/air flowrates and of coal/steam flowrates in the gasifier by selecting a constant air/steam flow ratio (for which adequate circulation of solids occurs in the reactor) and by varying the coal feedrate, during all cases considered.

The coal : steam flow ratios simulated in the ten case studies of Class A are tabulated below :

CASE NUMBER	COAL : STEAM FLOW RATIO
A1	1.125
A2	1.10
A3	1.0625
A4	1.025
A5	1.00
A6	0.975
A7	0.95
A8	0.925
A9	0.90
A10	0.875

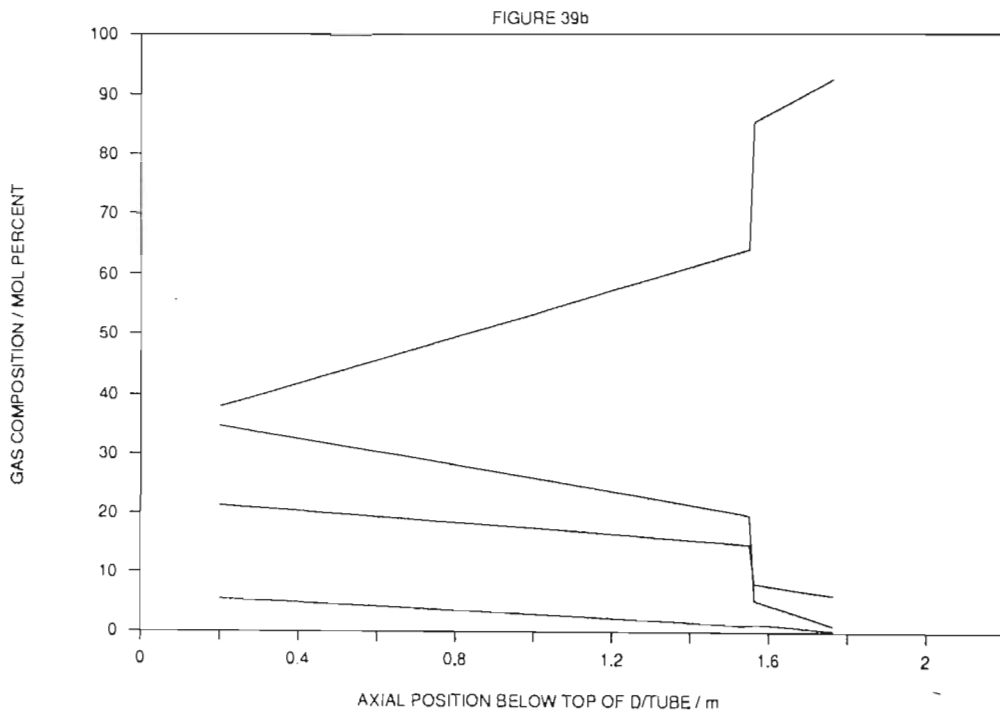
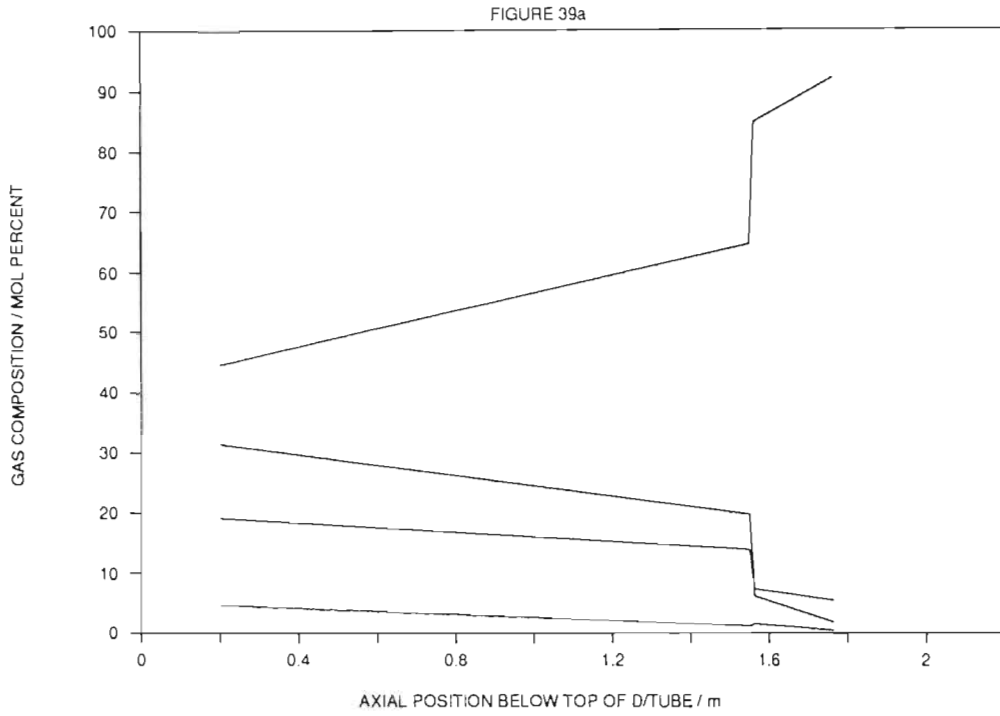
Table 6.4 Values of coal:steam flow ratios for Class A cases.

The coal : steam flow ratio of case A5 (ie. unity) is identical to that employed in Run G12. Case A5 is therefore considered a direct simulation of Run G12. The detailed results of cases A5 and A3 are shown in Figures 39a to 43b. These results are presented together in order to highlight the effects of increasing the coal feedrate to the gasifier by 6.25%, as in case A3.

Note that in Cases A5 and A3, the top of zone 1 in the annulus region is located at the axial position of the base of the product gas separating hood, ie. 0.2m below the top of the draft tube.

Figures 39a and 39b show the axial profiles of the gas compositions between the top of zone 1 and the position of the steam spargers in the annulus, for Cases A5 and A3 respectively. Note that the gasifier simulator assumes that no crossflow occurs in the reactor. Figure 39b shows that the effect of increasing the coal feedrate to the gasifier, without altering the air and steam flowrates, is to increase the concentration of the products of gasification in the syngas stream (product gas stream from the annulus). This effect arises since the amount of carbon consumed by combustion is limited by the air flowrate and the balance of the carbon in the reactor is gasified by steam in the annulus. The step change in the gas compositions, which appears in both figures 39a and 39b, occurs as a result of the step change in the global carbon concentration at the base of zone 2 in the annulus, where the coal-char which originates as coal fed to the reactor becomes available for steam gasification.

The composition of the dry syngas stream for Cases A5 and A3 is 56.5% H₂, 34.3% CO, 8.4% CO₂, 0.6% N₂ and 0.1% H₂S, which compares favourably with the dry syngas compositions measured during Runs G12 to G14 (cf. Tables 6.2 and 6.3).



Figures 39a and 39b. Axial profiles of the annulus gas compositions for Case A5(Fig. 39a) and Case A3(Fig. 39b).

(6.18)

The axial product gas velocities under the simulated conditions of both Cases A5 and A3, expressed as multiples of the minimum fluidising velocities for steam(annulus side) and air(draft tube side) at 850°C, are as follows :

	Case A5	Case A3
Annulus velocity :	7.40	7.02
Draft tube vel. :	0.66	0.67

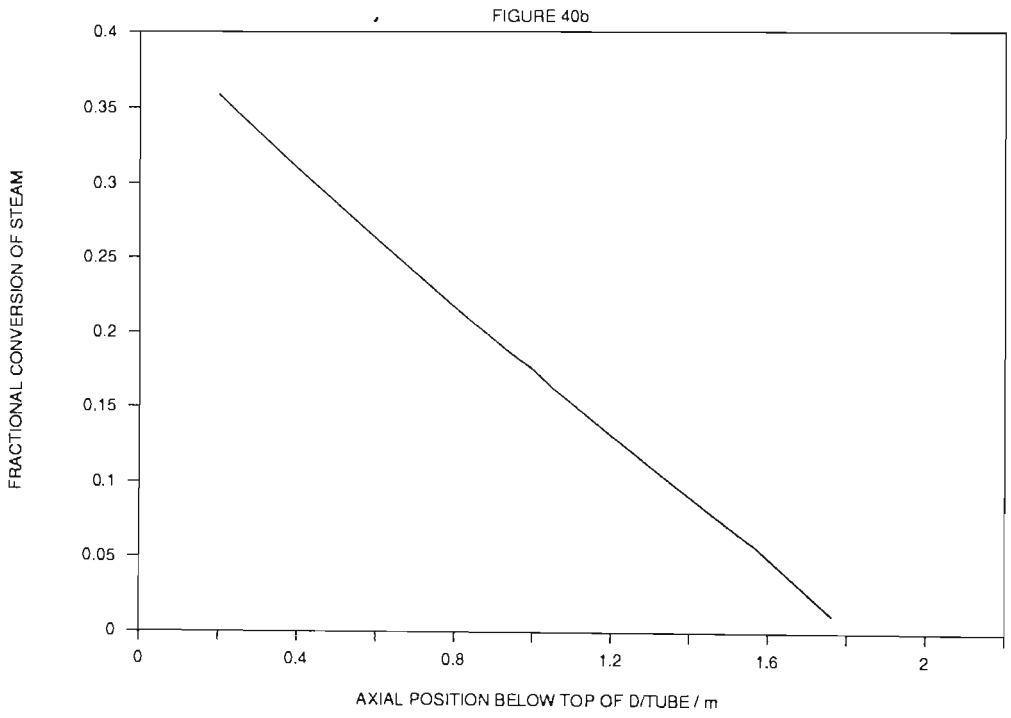
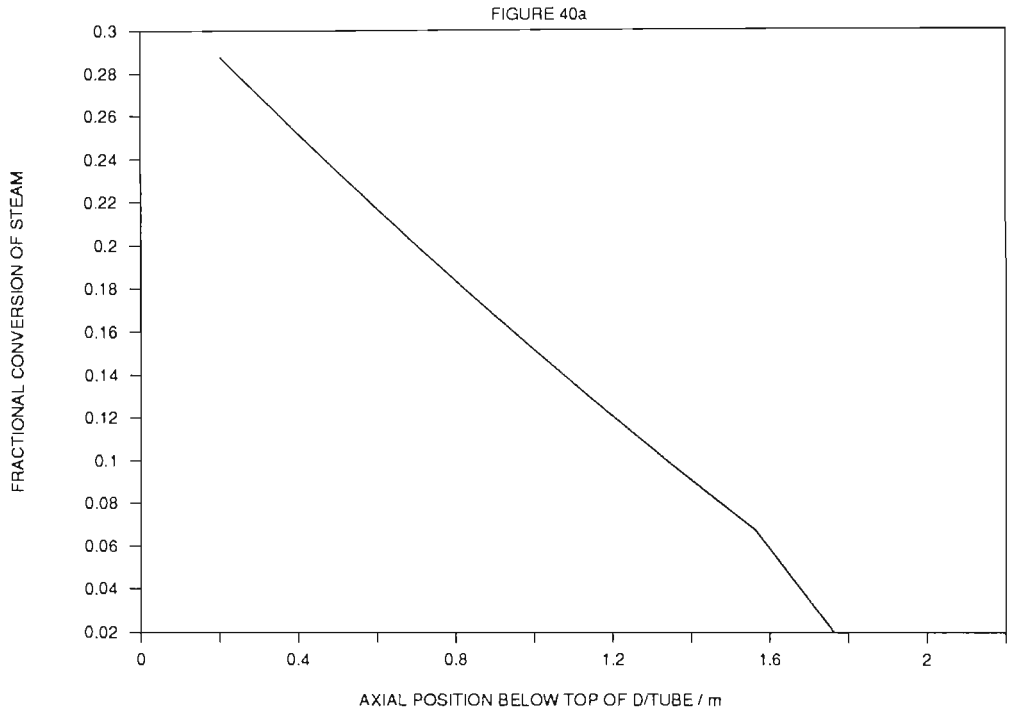
These values are within the ranges of fluidising gas velocities for which stable circulation of the solid material in the reactor is known to occur (0.5 to 1.0 u_{mf} in the draft tube; 6.0 to 9.0 u_{mf} in the annulus).

Figures 39a and 39b show that the steam concentration of the annulus gas atmosphere ranges from 40% to 100% by volume, whereas the steam-char gasification kinetic data employed by the gasifier simulator were measured in a pure steam environment. The significance of this result is that the predictions of the model become less accurate in the regions of relatively low steam concentration. Although the effect of a mixed gas atmosphere on the gasification kinetics of South African coal-chars is not quantitatively known, it is reported by Johnson (1974) that the rates of steam-char gasification are retarded when the reaction is conducted in an environment which contains a significant quantity of the products of gasification (compared to the rates of reaction in pure steam). In order to improve the accuracy of the gasifier simulator one should employ kinetic data valid for the local gas

environments of the gasifier. In the event of proceeding with kinetic studies of steam-char gasification in mixed gas environments, the predictions of the compositions of the local gas environments of the gasifier may be estimated by employing the existing gasifier simulator.

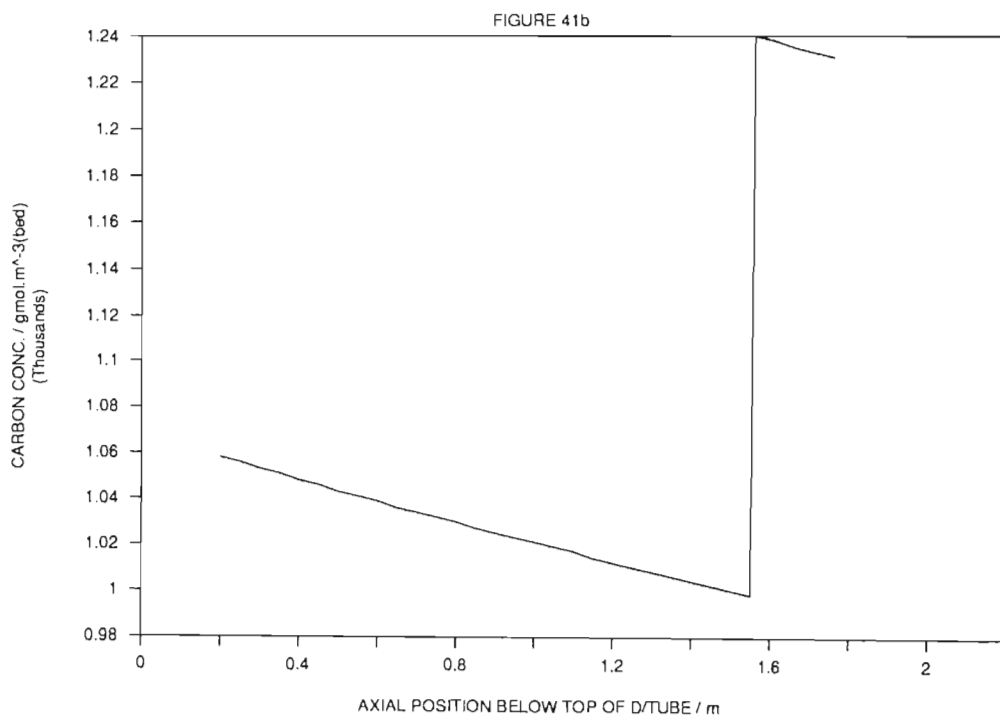
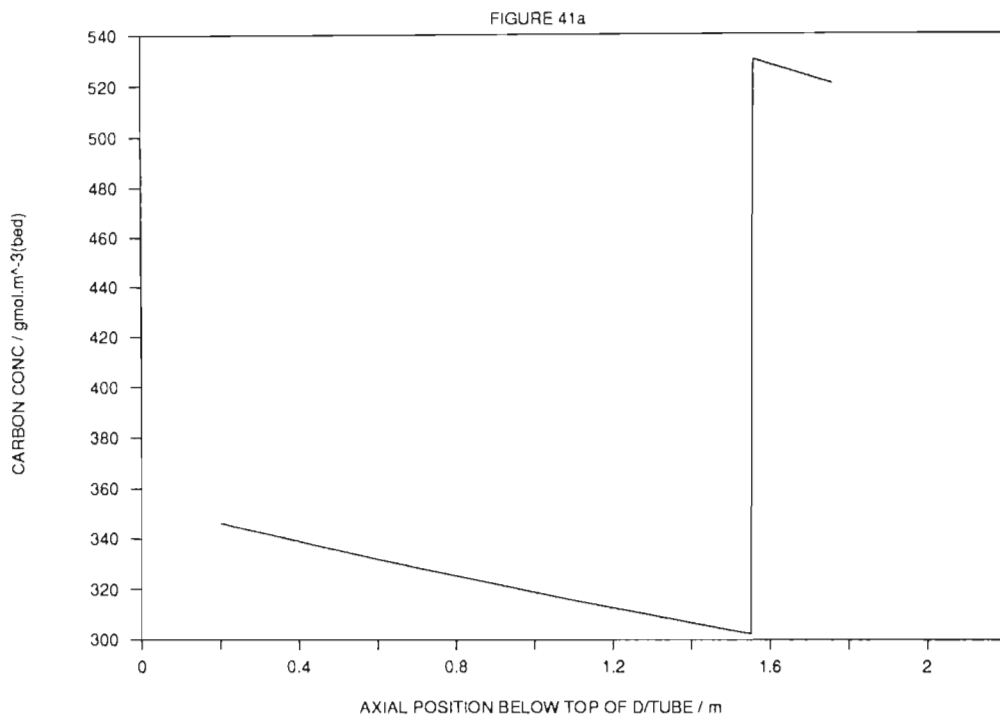
Figures 40a and 40b show the axial profiles of the fractional conversion of steam in the annulus for Cases A5 and A3, respectively. Note that the overall fractional conversion of steam in the gasifier (at $z = 0.2\text{m}$, the top of zone 1) is higher for Case A3 than for Case A5. This is attributed to the increase in the amount of carbon which gasifies in Case A3, which is associated with a corresponding increase in the amount of steam consumed by gasification.

Figures 41a and 41b illustrate the axial profiles of the global carbon concentration in the annulus for Cases A5 and A3, respectively. Note that the global concentration in the gasifier is predicted to be significantly higher (about triple) for Case A3 than for Case A5. This result occurs in order that the magnitude of the rate of steam-char gasification in Case A3 be sufficiently high to allow the gasification of the additional load of carbon in the reactor. (Note that although the carbon feedrate to the gasifier is increased by 6.25% in Case A3, 74.6% of the carbon fed to the gasifier in Case A5 combusts, so that the effective increase in the amount of carbon which gasifies in Case A3 is about 25%). The step increase in the global carbon concentration in the gasifier, shown



Figures 40a and 40b.

Axial profiles of the fractional conversion of steam in the annulus for Case A5(Fig. 40a) and Case A3(Fig. 40b).



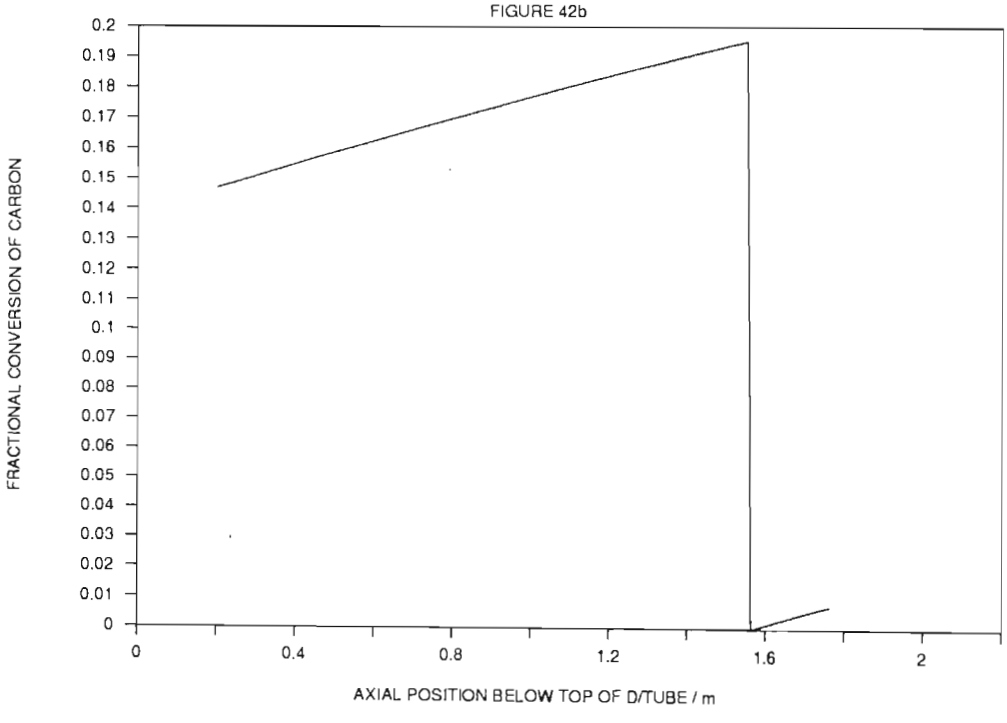
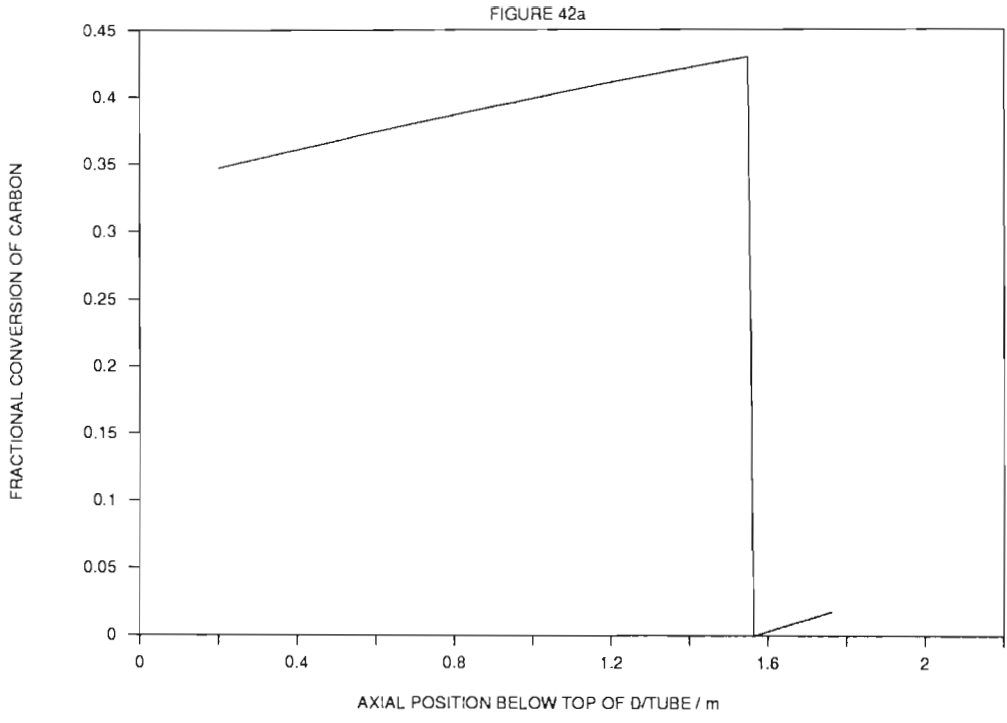
Figures 41a and 41b.

Axial profiles of the global carbon concentration in the annulus for Case A5(Fig. 41a) and Case A3(Fig. 41b).

in Figures 41a and 41b corresponds to the base of zone 2 where char which originates from the coal feed stream becomes available for gasification.

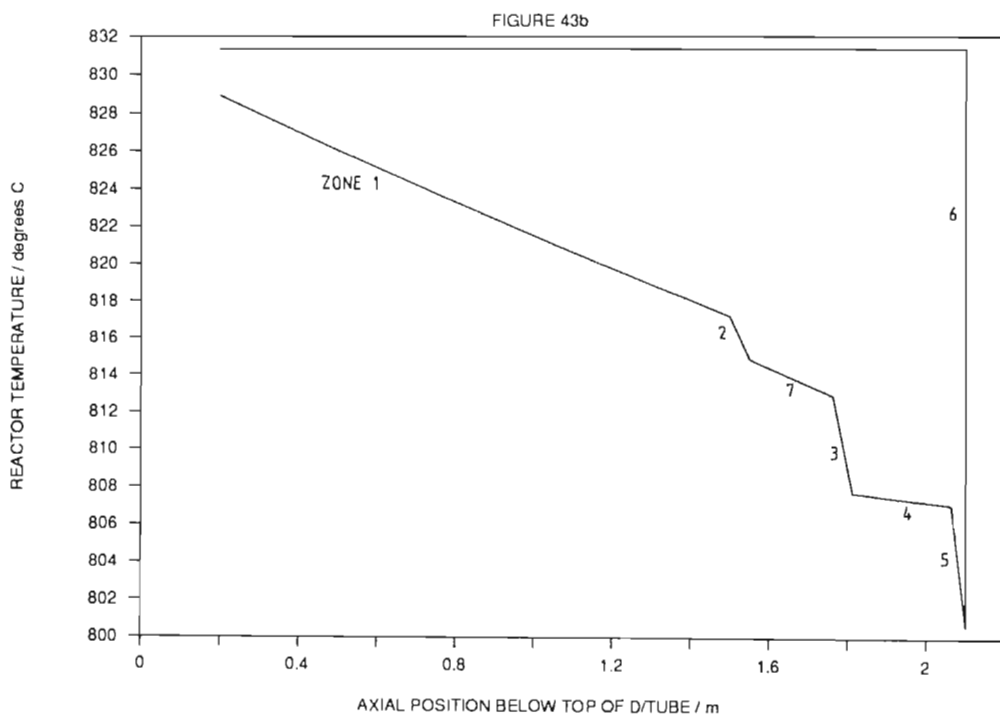
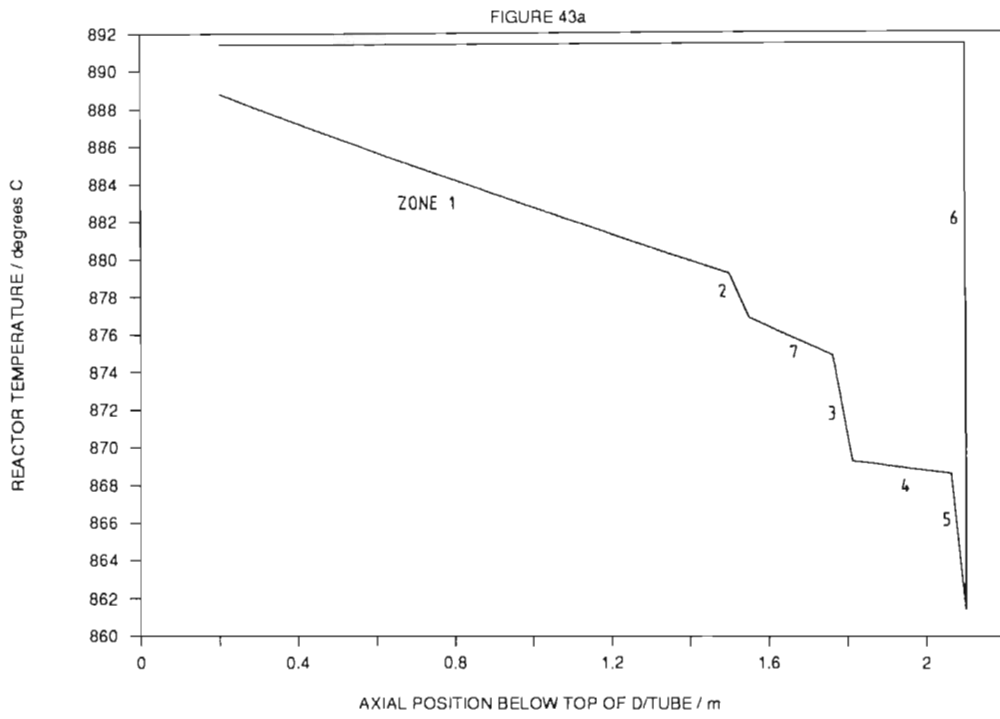
Figures 42a and 42b show the axial profiles of the fractional conversion of carbon in the annulus for Cases A5 and A3, respectively. (The fractional conversion of carbon in the gasifier is defined in the context of the gasifier simulator as the difference between the concentration of carbon at the base of zone 2 and the local carbon concentration, relative to the concentration of carbon at the base of zone 2, at which point the carbon concentration in the reactor is highest). Note that the magnitude of the fractional conversions of carbon in the gasifier are lower in Case A3 than in Case A5 on account of the higher concentration of carbon in the reactor in Case A3.

Figures 43a and 43b show the axial profiles of the temperature of the annulus for Cases A5 and A3, respectively. Each of these Figures is annotated with the respective zone numbers of the gasifier which are employed in the gasifier simulator. Note that neither of the temperature-height profiles close. This occurs because the gasifier simulator allows a 1% tolerance on the overall energy balance of the system. Figure 43a shows that the temperature at the top of the annulus is approximately 890°C and that of the bottom of the secondary gasification zone (zone 7) is about 875°C, for Case A5. The overall temperature difference across the annulus in Case A5 is shown to be about 15°C. This result compares



Figures 42a and 42b.

Axial profiles of the fractional conversion of carbon in the annulus for Case A5(Fig. 42a) and Case A3(Fig. 42b).



Figures 43a and 43b.

Axial profiles of the temperature of the annulus for Case A5(Fig. 43a) and Case A3(Fig. 43b).

(6.21)

favourably with the difference in temperature across the annulus during Runs G12 and G13 (about 15°C).

Figure 43b shows that the magnitudes of the temperatures of the gasifier are lower for Case A3 than for Case A5. This result occurs because of the increased quantity of carbon which gasifies in Case A3, which is associated with an increased quantity of energy demanded by the steam-char gasification reactions. The difference in temperature across the gasification zones of the annulus (between the top of zone 1 and the base of zone 7) is also higher in Case A3 than in Case A5 (17°C vs 15°C).

The overall effect of the increased coal feedrate in Case A3 is described by the difference in the cold gas efficiencies** of the gasifier for Cases A5 and A3. The cold gas efficiency of the gasifier increases by 4.2% to 45.4% in Case A3.

** The cold gas efficiency is defined in this text as the gross calorific value (GCV) of the cold syngas stream relative to the net calorific value (NCV) of the coal fed to the gasifier. The overall cold gas efficiency is defined as the GCV of the combined cold product gas streams relative to the NCV of the coal fed to the gasifier.

The Judd gasifier is somewhat limited in its scale-up capability in that a high risk is associated with maintaining steady circulation of solid material within the reactor as one increases the diameter

of the reactor (circulation of solids in the reactor is essential to the successful operation of the gasifier). Consequently, in view of this limitation and of the encouraging results obtained during Runs G12 to G14 with the mini-pilot scale gasifier, Prof. Judd has recently addressed the matter of the scaling up of the capacity of the Judd gasifier to a level which is suitable for commercial application. As a result, Prof. Judd has proposed a novel gasifier design which employs the same principles of operation as the current Judd gasifier and which is able to be scaled up to commercial capacity, without introducing any significant risk in the operability of the process. Furthermore, the new gasifier design allows a high margin of turndown in the capacity of the plant. Unfortunately no details of this design are able to be disclosed at this stage, since the design has not yet been patented. It is, however, encouraging to report that Prof. Judd has recently succeeded in demonstrating that the new version of the reactor is capable of a range of stable solids circulation rates at which very low levels of crossflow of fluidising gases occur. These results were obtained at 20°C with a full scale 'module' of a proposed pilot scale reactor (see Class B case studies).

The design of the new version of the Judd gasifier also allows the operation of the gasifier to be simulated by the gasifier simulator developed in Chapter 5.

(6.23)

Seven 'Class B' case studies have been conducted as part of the design phase of a pilot-scale Judd gasifier which is scheduled to be constructed in mid 1990. The general conditions which are common to all Class B case studies are listed below :

- Pressure of operation = 5 bar gauge
- Air flowrate = 4.89 Nm³/minute
- Air inlet temperature = 350°C
- Steam inlet temperature = 350°C
- Minimum fluidising velocity
of air at 850°C = 0.1863 m/s
- Minimum fluidising velocity
of steam at 850°C = 0.1984 m/s
- Gasification stoichiometric
parameter (see eqn E.11) = 1.35
- Combustion stoichiometric
parameter (see eqn E.59) = 0.6
- Silica sand particle size = 750 microns
- Draft tube length = 0.75 m
- Draft tube diameter = 0.27 m
- Annulus diameter = 0.55 m
- Level of hood below top of d/tube = 0.05 m
- Level of coal feeders " = 0.5 m
- Level of steam spargers " = 0.7 m

Note that the geometry of the gasifier considered in Class B is typical of the new version of the Judd gasifier.

(6.24)

The coal : steam flow ratios simulated in the seven case studies of Class B are tabulated below :

CASE NUMBER	COAL : STEAM FLOW RATIO
B1	1.60
B2	1.56
B3	1.52
B4	1.48
B5	1.44
B6	1.36
B7	1.28

The detailed results of case B5 are presented graphically in Figures 44 to 48. The general observations made concerning the results of Cases A5 and A3 are also valid for Case B5. The following observations are, however, specific to Case B5 :

- (1) Figures 44 shows that the concentration of gasification products in the gas atmosphere throughout the annulus is considerably higher for Case B5 than for Cases A5 and A3. This result is attributed to the higher coal/steam ratio for Case B5 than those for Cases A5 and A3. Figure 44 suggests that one should ideally employ gasification kinetic data for gas environments which contain as little as 15% steam, for accurate simulations.

- (2) Figure 45 indicates that the overall fractional conversions of steam in the gasifier for Case B5 is approximately 0.62. This result shows that the reactant steam is relatively efficiently converted in the gasifier in this case.
- (3) Figure 46 shows that the gasifier operates with a relatively high carbon content throughout. Note that the concentration of coal at the feeder position of the gasifier for Case B5 is merely 1.8 percent by mass. This relatively low concentration is desirable in order to allow the coal-char to be well dispersed by the solid allothermal agent in order to enable energy transfer to occur between the char and the allothermal agent in both the gasification and combustion zones of the gasifier.
- (4) Figure 48 shows that the overall reduction in the temperature of the solid material in the gasifier between the top of zone 1 and the exit of zone 5 is approximately 90°C for Case B5. The magnitude of the temperature drop across the gasifier is proportional to the quantity of carbon which gasifies in the reactor. Note that in order to sustain steady operation of the gasifier the temperature at the exit of zone 5 should not fall below about 600°C in order to allow the spontaneous combustion of char to occur in zone 6. This temperature limitation imposes what may be termed as the 'allothermal constraint' on the gasification capacity of the reactor in that the temperature at the exit of zone 5 is proportional to

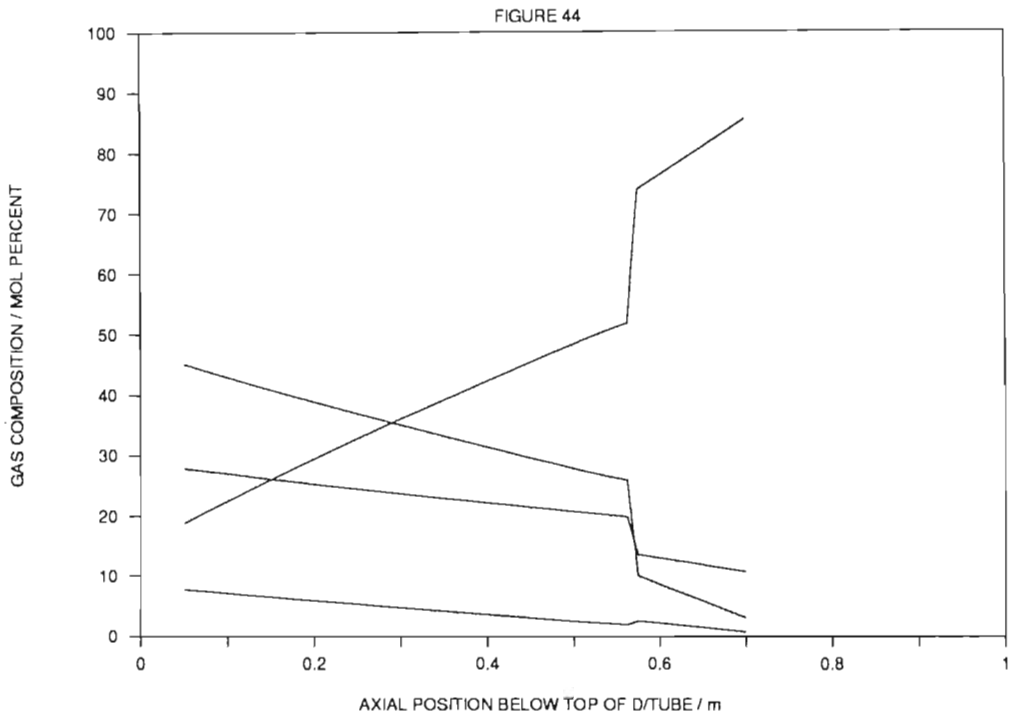


Figure 44. Axial profiles of the annulus gas compositions for Case B5.

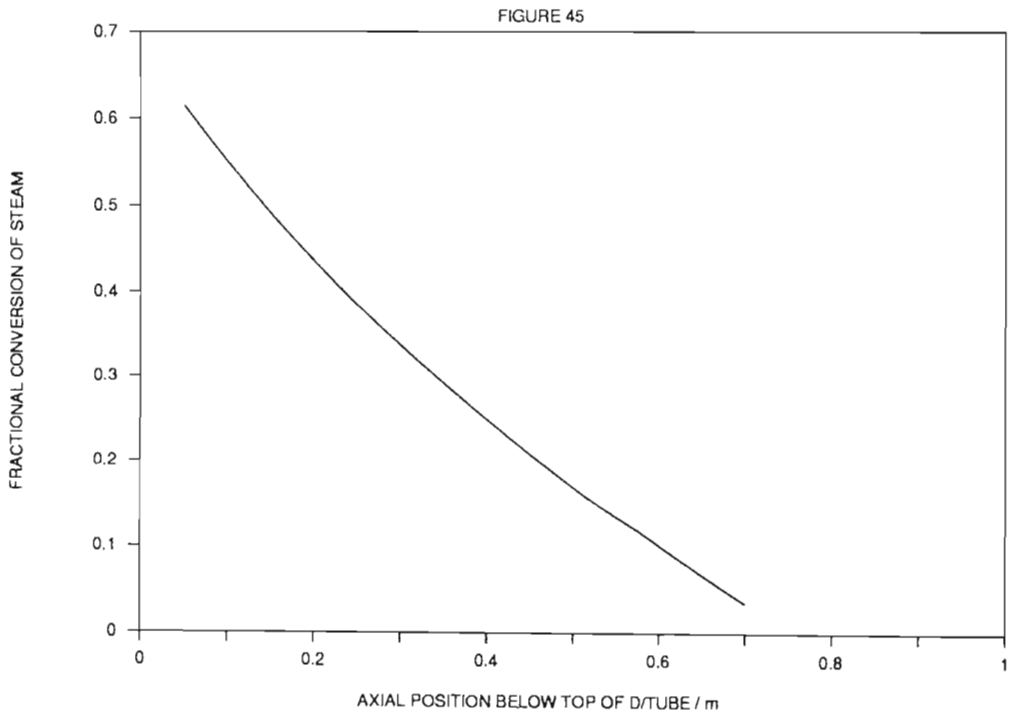


Figure 45. Axial profiles of the fractional conversion of steam in the annulus for Case B5.

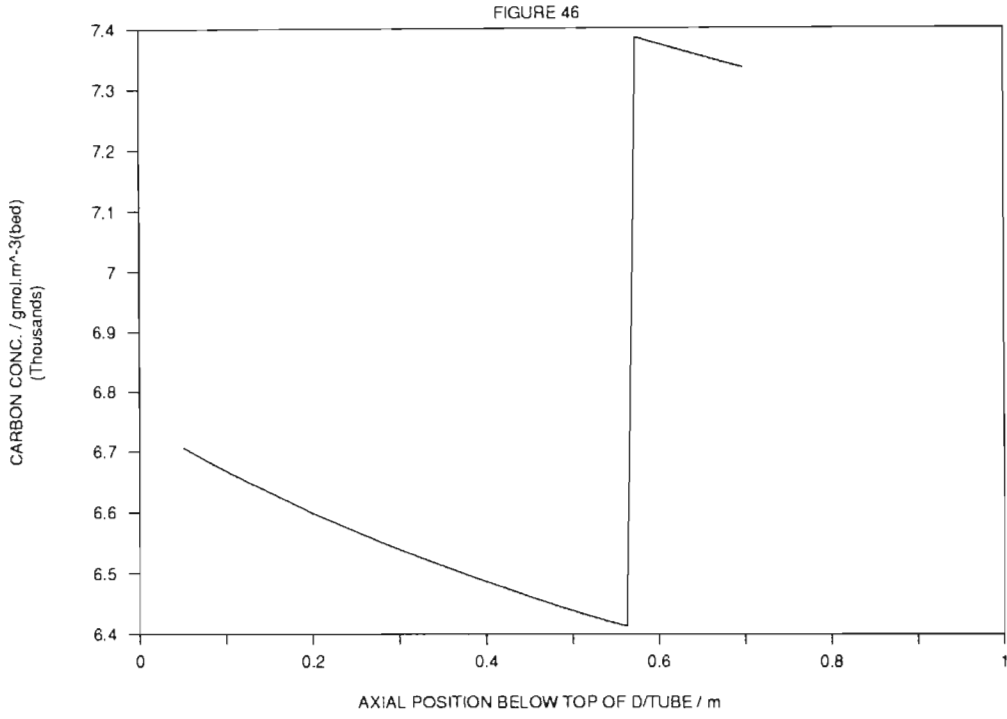


Figure 46. Axial profiles of the global carbon concentration in the annulus for Case B5.

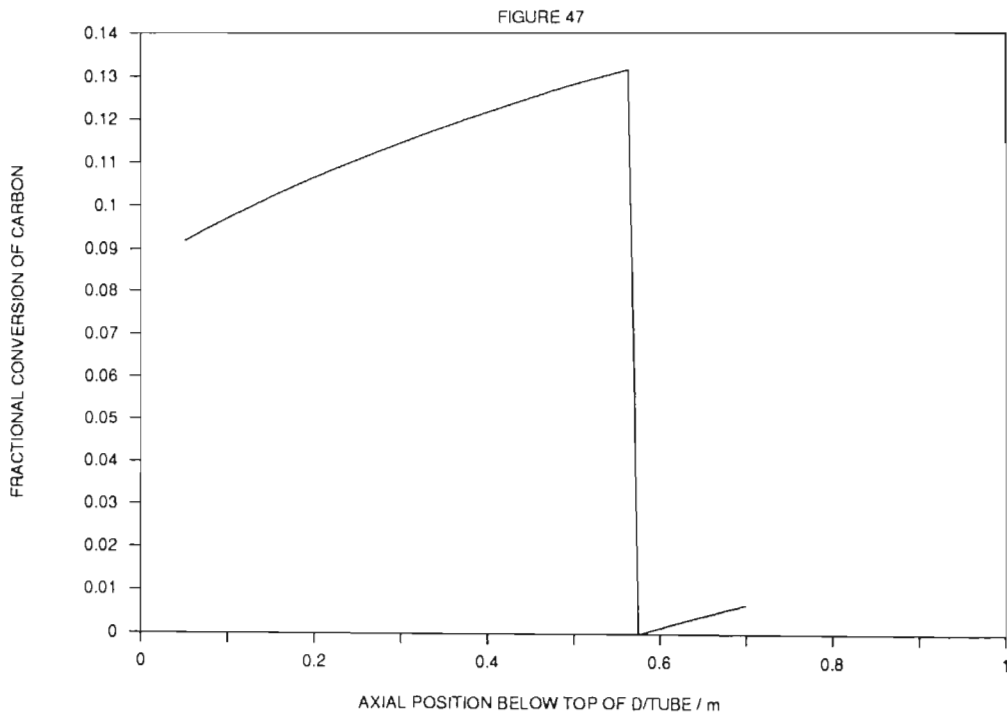


Figure 47. Axial profiles of the fractional conversion of carbon in the annulus for Case B5.

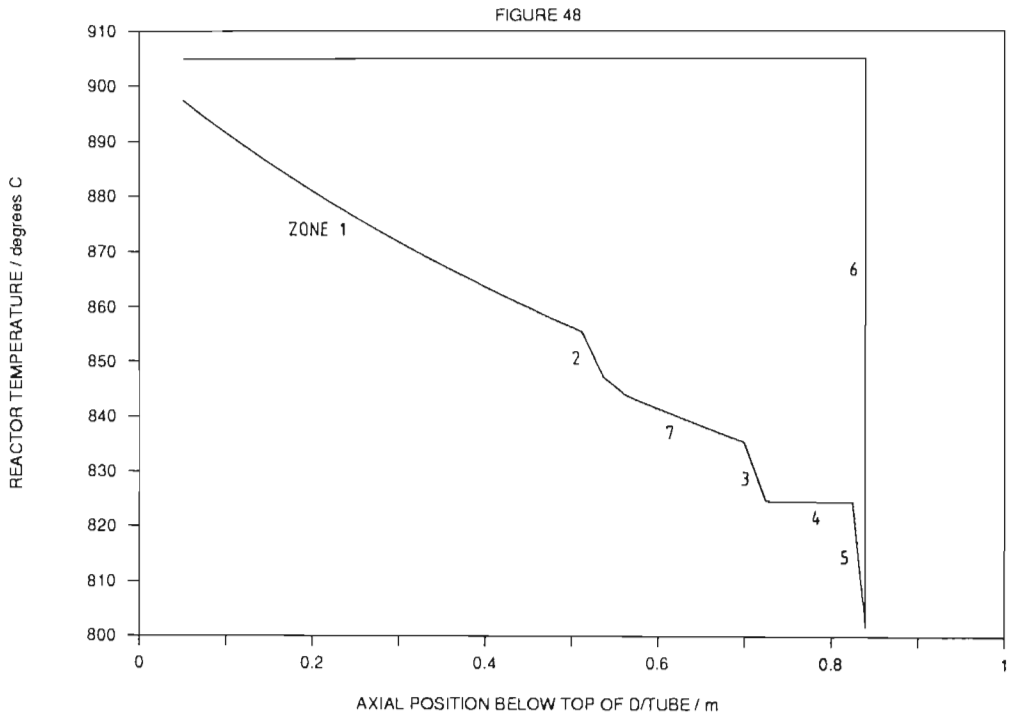


Figure 48. Axial profiles of the temperature of the annulus for Case B5.

the amount of carbon which is gasified. Because the energy demanded by the carbon gasification reactions in the gasifier is supplied by the allothermal agent, the relationship between the temperature at the exit of zone 5 and the carbon gasification capacity of the reactor is a function of the heat capacity of the allothermal agent. It is therefore desirable that the allothermal agent of the gasifier have a relatively high heat capacity. Note that silica sand has been employed in this study for the reasons listed in Chapter 1. Figure 48 suggests, however, that the carbon gasification capacity of the Judd gasifier is significantly constrained by the use of silica as the allothermal agent.

A further consideration regarding the allothermal agent which has not been addressed in any detail in the development of the gasifier simulator is that of the rate at which energy is able to be transferred to the allothermal agent in the combustion zone. It is anticipated that the energy transfer mechanism in zone 6 is that of radiant heat transfer between the surfaces of the char and the allothermal agent, followed by conduction heat transfer through the volume of the allothermal agent. Of these two paths, the conductive path is likely to offer the most resistance to the transfer of energy in zone 6. Consequently, a desirable property of the allothermal agent of the gasifier is that of a relatively high thermal conductivity. In view of the very low thermal conductivity of silica, it is the opinion of the author that one should

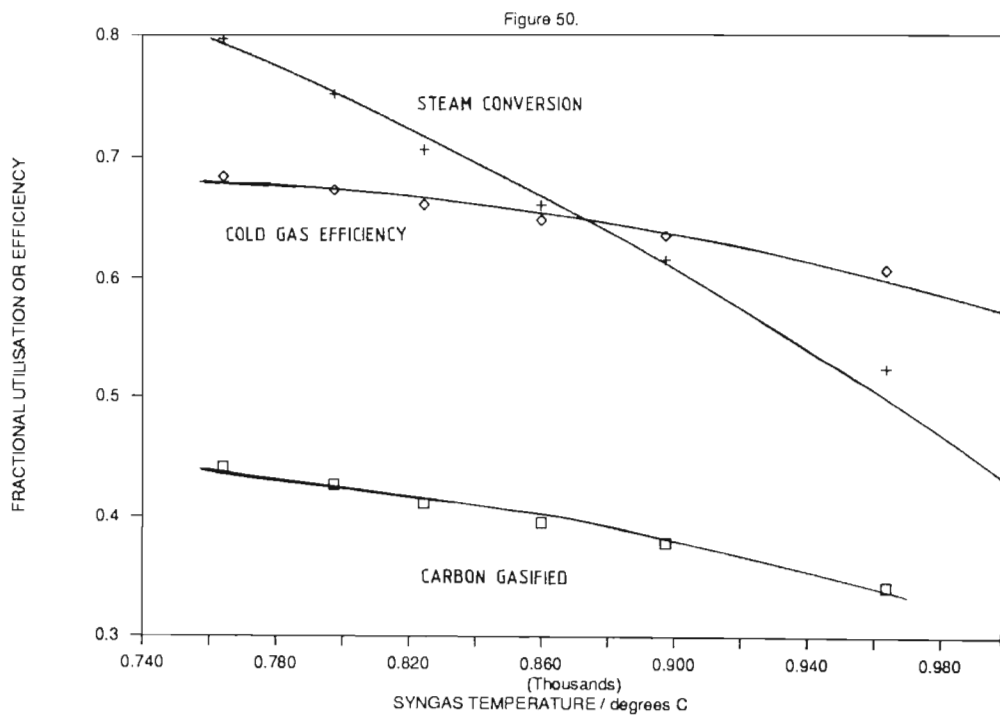
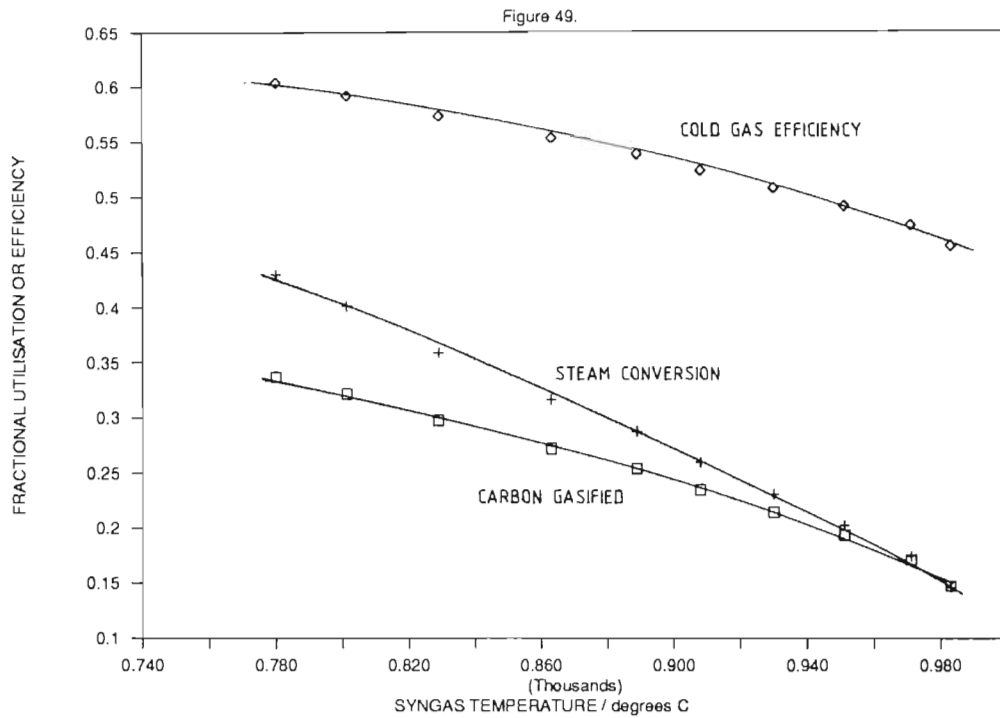
(6.27)

consider an alternative allothermal agent for the Judd gasifier which has similar fluidising properties to that of silica, eg. aluminium spheres; (the density of aluminium is very similar to that of silica).

The effects of varying the coal feedrate to the gasifier are summarised in Figures 49 and 50 for all of the cases of Class A and B, respectively. These graphs indicate the overall cold gas efficiency (ie. including the energy content of the waste gas stream) and the fractions of the carbon feed and of the steam supply which are consumed by gasification, relative to the corresponding syngas temperature, for each case study in both Classes A and B.

The following principal observations may be made with reference to Figures 49 and 50 :

- In general, the overall thermal efficiency of the gasifier (or overall cold gas efficiency) improves with increasing the coal feedrate at constant air and steam flowrates. This trend is accompanied by general improvements in the fraction of carbon gasified and by increased conversions of steam in the gasifier at increased coal feedrates. These results are to be expected, since the gasifier operates with an excess carbon content than that which is stoichiometrically required for combustion and all carbon in excess of this amount is consumed by steam gasification.



Effects of the gasifier operating temperature on the utilisation of carbon and of steam by gasification and on the cold gas efficiency of the gasifier for cases of Class A(Fig.49) and of Class B(Fig.50).

- The temperatures of the gasifier in general are found to decrease with increasing coal feedrates. This result is consistent with the fact that an increased coal feedrate is effectively consumed only by the endothermic gasification reactions.
- The higher steam conversions recorded for the case studies of Class B, when compared with the cases of Class A, may be attributed to the higher coal : steam flow ratios employed in Class B.
- The comparable carbon-gasification utilisation and thermal efficiency curves for Classes A and B are somewhat misleading in that because of the different pressures of operation and the slightly different reactor geometries considered in the two Classes, different air : steam flow ratios were required for steady circulation of the solids. Thus, since Class B required a larger air : steam flow ratio than Class A, the higher coal : steam ratios of Class B resulted in similar utilisations and efficiencies, even though the operating conditions were different. Nevertheless, the general characteristics discussed above are valid for both Classes of case study.

Note that although the performance of the gasifier is obviously improved with increasing coal feedrate, one should be cautious not to operate the reactor at too low a temperature, because of the risk of spontaneous combustion not being sustained.

CHAPTER 7.

CONCLUSIONS AND RECOMMENDATIONS.

7.1 CONCLUSIONS.

The numerical values of the results of the kinetic studies conducted and the high degree of reproducibility thereof demonstrate that the experimental apparatus and technique which were developed in this study are suitable for the determination of the steam gasification kinetics of coal chars.

The following conclusions regarding the steam gasification of Bosjesspruit coal-char may be drawn :

- The rate of steam-char gasification is very sensitive to variations in the temperature of reaction in the range 840°C to 920°C.
- Neither the rate of steam-char gasification nor the product gas composition are affected by the steam partial pressure in the range 1.8 to 4.8 bar absolute;
- During carbon-steam gasification ($C + H_2O = CO + H_2$) hydrogen is rapidly produced by the homogeneous water gas shift reaction ($H_2O + CO = H_2 + CO_2$), whilst carbon dioxide is gradually consumed in the production of carbon monoxide by the Boudouard reaction ($C + CO_2 = 2CO$), which proceeds relatively slowly (The carbon-steam reaction is essentially the sum of the latter two reactions). Furthermore, the methane formation

(7.2)

reaction is promoted at a rapid rate during gasification. These conclusions are justified by the rapid approach of the concentrations of the H_2 and CH_4 components of the product gas to their respective equilibrium compositions, whereas the concentrations of CO and CO_2 gradually approach their respective equilibrium compositions, during gasification. The rate of increase of the CO concentration during gasification is twice the rate of decrease of the CO_2 concentration, which is typical of the Boudouard reaction.

- The average product gas composition is independent of the temperature of reaction in the range $840^\circ C$ to $920^\circ C$ and is approximately 49% H_2 , 32% CO , 17% CO_2 and 2% CH_4 on a molar basis;
- The steam gasification kinetic data are well described by a fundamental Arrhenius-type volumetric reaction model at temperatures of up to $920^\circ C$. The value of the activation energy for the reaction is 146 kJ/gmol, which indicates that the gasification kinetics are controlled by the rates of the chemical reactions (ie. $C + H_2O = CO + H_2$ and $C + CO_2 = 2CO$) at temperatures up to $920^\circ C$;
- There are no major differences between the kinetics measured for Bosjesspruit coal-char and those reported in the literature for foreign coal-chars.

The experimental results obtained for the steam gasification of char derived from Transvaal Navigation coal show that the product gas stream contains very high concentrations of H_2 and CO and relatively

(7.3)

low concentrations of CO_2 and CH_4 (approximately 50% H_2 , 42% CO , 6.5% CO_2 and 1.5% CH_4 on a N_2 free basis at a carbon conversion of $X=0.5$) at both 850°C and 920°C. The levels of both the H_2 and the CH_4 concentrations rapidly attain their respective equilibrium values and remain approximately constant throughout gasification, whereas the concentrations of CO and CO_2 gradually approach their respective equilibrium values during the course of gasification and almost attain equilibrium concentrations as the conversion of carbon nears completion. The rate of steam gasification of this char is therefore also controlled by the rate of the Boudouard reaction.

The magnitudes of the steam gasification kinetics of Transvaal Navigation coal-char are comparable with those of Bosjesspruit coal-char; this may be attributed to the fact that the rate of gasification of each char is controlled by the rate of the Boudouard reaction, despite the fact that the steam-carbon reaction is promoted at a slightly lower rate during the gasification of Bosjesspruit char, as is evident from the differing product gas spectrums of the two chars. It is strongly suspected, however, that the differing reaction rates displayed by the carbon-steam reaction for each of the two chars investigated in this study were as a result of the catalytic effects of certain inherent components of the chars, although no specific tests of this nature were conducted.

The following conclusions may be drawn from the results of the steam gasification experiments conducted with Bosjesspruit coal using the mini-pilot scale, air-steam blown circulating fluidised bed gasifier

(the Judd gasifier) :

- A product gas stream which is rich in hydrogen and carbon monoxide (about 35% H₂, 15% CO, 18% CO₂, 2% CH₄, 30% N₂, on a dry molar basis) is readily produced when steam and air are supplied to the annulus and the draft tube regions of the gasifier, respectively. In principle, the extent of crossflow of reactant gases in the gasifier is able to be reduced to a very low value, in which case the composition of the product gas stream would be about 55% H₂, 25% CO, 18% CO₂, 2% CH₄ (dry, molar basis);
- The product gas stream from the draft tube contains about 10% CO as a result of the partial combustion of char within the draft tube region.

The following conclusions may be drawn from the results of the case studies conducted using the computer simulator based on the one-dimensional model of the Judd gasifier, which was developed in this study :

- The predictions of the gasifier simulator compare favourably with the few experimental results obtained with the mini-pilot scale gasifier. The simulator is therefore viewed as a useful means by which to investigate the effects of different operating conditions.
- The concentration of steam in the gas atmosphere towards the top of the annulus approaches 15% by volume under typical commercial scale operating conditions of the gasifier. The significance of this result is that the accuracy of the

simulator may deteriorate under these conditions, since the gasification kinetic data which are employed were measured in a pure steam environment;

- The thermal efficiency of the Judd gasifier increases as the coal feedrate is increased relative to the flowrates of air and steam, although this is accompanied by a general decrease in the temperatures of the reactor. The autothermal nature of the gasifier dictates that the exit temperature from the annulus region should be sufficiently high to sustain spontaneous combustion in the draft tube. This criterion limits the thermal efficiency of the Judd gasifier to about 70%.
- The use of silica sand as the fluidised solid in the gasifier imposes a relatively low limit (allothermal constraint) on the coal processing capacity of the gasifier in that the energy demanded by the gasification may reduce the temperature of the reactor to below that at which spontaneous char combustion occurs.

7.2 RECOMMENDATIONS.

The following recommendations with respect to future gasification kinetic studies using a microreactor are made by the author :

- (1) It is proposed that the steam gasification kinetics of additional local coal-chars be investigated under the same conditions described in this thesis. It is also suggested that one investigates the kinetics of steam gasification of a

(7.6)

popular foreign coal-char, eg. Illinois #6.

- (2) It is also proposed that char gasification experiments be conducted in mixed gas environments using the existing apparatus with a suitable modification in order to generate the reactant gas stream (eg. a heated, pressurised humidifier). This exercise will establish the effect of a mixed gas environment on the reaction kinetics.
- (3) Ultimately, it is proposed that one conducts experiments at higher temperatures than 920°C in order to establish the temperature at which the rates of mass transfer became significant in the determination of the overall kinetics of gasification. It is also proposed that experiments are conducted at higher pressures than the upper limit employed in this study (4.8 bar absolute).

With respect to the development of the Judd air-steam blown circulating fluidised bed gasifier, it is strongly recommended that a pilot scale module (capable of processing 5 tons of coal per day) of the new version of the gasifier be commissioned as soon as possible in order to conduct experiments on a continuous basis under typical operating conditions (5 bar gauge pressure and temperatures up to 1000°C). This phase of the development of the gasifier is regarded by the author as vital in that valuable operating experience will be gained which will add to our present knowledge of the process and will highlight aspects of the gasifier which require further research.

(7.7)

Finally, the author proposes that calculations be conducted to determine the limitations imposed by the properties of refractory silica as the allothermal agent of the Judd gasifier on the intensity of combustion in the gasifier (ie. the quantity of energy liberated per unit volume in combustion zone of the gasifier). It is the opinion of the author that, in view of the relatively low thermal conductivity of silica, this material is not ideally suited as the allothermal agent of the Judd gasifier and that the selection of a more thermally conductive material should be considered.

REFERENCES.

- Ashu, J. T., Nsakala, M. Ya., Mahajan, Om. P., Walker, P. L. Jr.,
'Enhancement of char reactivity by rapid heating of precursor
coal', Fuel, 57, (1978) 250.
- Bastick, M., Perrot, J. -M., and Weber, J., 'General Characteristics
of Coal Gasification', J. Int. Chem. Eng., vol 26(2),
(Apr 1986) 243.
- Bhattacharya, A., Salam, L., Dudukovic, M. P., and Joseph, B.,
'Experimental and Modelling Studies in Fixed-Bed Char
Gasification', IEC Process Des. Dev., 25(4), (1986) 991.
- Chen, W. J., Sheu, F. R., and Savage, R. L., 'Catalytic activity of
Coal Ash on Steam Methane Reforming and Water-Gas shift
Reactions', Fuel Processing Technology, 16, (1987) 279-288.
- Chin, G., Kimura, S., Tone, S. and Otake, T., 'Gasification of coal
char with steam (part 2). Pore structure and reactivity.',
Int. Chem. Eng., 23(1), (Jan. 1983).
- Cho, Y., and Joseph, B., 'Heterogeneous model for Moving-Bed Coal
Gasification', IEC Process Des. Dev., 20(2), (1981) 314.
- Clark, W. N. and Shorter, V. R., 'Cool Water : Mid-term performance
assessment', 6th Annual EPRI Coal Gasification Contractor's
conference', Palo Alto, California, Oct 15-16, 1986.
- Doraiswamy, L. K. and Sharma, M. M., 'Chapter 19: Gas-solid
Noncatalytic Reactions : Analysis and Modelling, in
Heterogeneous Reactions', Wiley, (1985) 453.

- Draft White Paper on the Energy Policy of the Republic of South Africa, Department of Mineral and Energy Affairs, Pretoria, (1985).
- Ergun, S. and Mentser, M., Chem. Phys. Carbon, 1, (1965) 203
- Feldkirchner, H. L. and Heuler, J., IEC Proc. Des. Dev., 4, (1965) 134.
- Feldkirchner, H. L. and Linden, H. R., IEC Process Des. Dev., 2, (1965) 153.
- Froment, G. F., 'Fixed Bed Catalytic Reactors - Current Design Status', Ind. Eng. Chem., 59(2), (Feb 1967) 19
- Gluckman, M. J., Spencer, D. F., Watts, D. H. and Shorter, V. R., 'A reconciliation of the Cool Water IGCC plant performance and cost data with equivalent projections for a mature 360 MW commercial IGCC facility', EPRI Report nr C915MJG6-1, October, 1987.
- Grover, R. W., Page, G. C., Wetherold, R. G. and Wevill, S. L., 'Preliminary environmental monitoring results for the Cool Water Coal Gasification Program', Proc. of 6th Annual EPRI Conf. on Coal Gasification, Palo Alto, California, October 15-16, 1986.
- Guo, C. -t. and Chang, L. -m., 'Kinetics of coal char gasification at elevated pressures.', Fuel, 65, (Oct. 1986) 1364.
- Hill, C. G., Jr, 'An Introduction to Chemical Engineering Kinetics and Reactor Design', Wiley, New York, 1977, p 484-521.
- Howard, J. B., Peters, W. A., and Serio, M. A., 'Coal devolatilization information for reactor modelling; assesment of data and apparatus with recommendations for research', A.P. 1803 EPRI, 1981.

- Huttinger, K. J., Masling, B., and Minges, R.,
'Catalytic activity of carbon supported potassium in the
carbon monoxide shift reaction.', *Fuel*, 65, (July 1986) 932.
- Jensen, G. A., *Ind. Eng. Chem Process Des. Dev.*, 14, (1975) 314.
- Johnson, J. L., *Advances in Chemistry Series, American Chemical
Society, Washington, D.C.*, 131, (1974) 145-178.
- Johnson, J. L., 'Relationship between the gasification reactivities
of coal char and the physical and chemical properties of coal
and coal chars', *Am. Chem. Soc. Div. Fuel Chem. Prepr.*, 20,
(1975) 85.
- Johnson, J. L., 'Kinetics of Coal Gasification.' - A Compilation of
Research, John Wiley, (1979) 148.
- Judd, M. R. et al., 'Solids circulation and Gasification
experiments in a Fluidised Bed with a Draught Tube.', *Proc.
Int. Fluidisation IV. Conference, Kashikojima, JAPAN*, (1983)
663.
- Juntgen, H., 'Reactivities of carbon to steam and hydrogen and
applications to technical gasification processes - A review',
Carbon, 19 (1981) 167.
- Kasaoka, S. et al., 'The development of rate expressions and the
evaluation of reactivity for gasification of various coal
chars with steam and oxygen.', *Int. Chem. Eng.*, 23(3),
(July 1983) 477.
- Kasaoka, S. et al., 'Kinetic evaluation of the reactivity of
various coal chars for gasification with carbon dioxide in
comparison with steam.', *Int. Chem. Eng.*, 25(1),
(Jan. 1985) 160.

- Kayembe, N. and Pulsifer, A. H., *Fuel*, 55, (1976) 211.
- Klei, H. E., Sahagian, J. and Sundstrom, D.W., *IEC Process Des. Dev.*, 14, (1975) 470.
- Knizia, K. and Weinzierl, K., 'Coal combined cycle plants with integrated coal gasification : VEW coal conversion process', lecture for conf. of Benelux Association of Energy Economists, The Hague, April 22, 1987.
- Kyle, B. G., 'Chemical and Process Thermodynamics.', Prentice-Hall, (1984) 495.
- Laurendeau, N., 'Heterogeneous kinetics of char gasification and combustion', *Prog. Energy Combustion Science*, 4, 221-270.
- Linares-Solano, A. et al., 'Catalytic activity of calcium for lignite char gasification in various atmospheres.', *Fuel*, 65, (June 1986) 776.
- Liu, Z.-l. and Zhu, H.-h., 'Steam gasification of coal char using alkali and alkaline-earth metal catalysts.', *Fuel*, 65, (Oct. 1986) 1334.
- Meihack, W., 'Combustion studies using a high pressure circulating fluidised bed gasifier.', M.Sc. Thesis, University of Natal, (1983).
- Muir, K. et al., 'Steam gasification of carbon.', *Fuel*, 65, (March 1986) 407.
- Penner, S. S. and Wiesenbahn, D. F., 'Use of Catalysts during Gasification', *Energy*, 12(8-9), Ch 7, (1987) 747.
- Pillay, V. L., 'Analysis of hydrodynamic phenomena and engineering development of a circulating fluidised bed for coal gasification.', M.Sc. Thesis, University of Natal, (1986).

- Radovic, L. R., Steczko, K., Walker, P. L. Jr., and Jenkins, R. G., 'Combined effects of inorganic constituents and pyrolysis conditions on the gasification reactivity of coal chars', *Fuel Process. Technol.*, 10, (1985) 311-326.
- Radovic, L. R., Walker, P. L., and Jenkins, R. G., 'Importance of carbon active sites in the gasification of coal chars', *Fuel*, 62, (1983) 849.
- Schmal, M., Monteiro, J. L. F., and Castellan, J. L., 'Kinetics of Coal Gasification.', *Ind. Eng. Chem. Process Des. Dev.*, 21, (1982) 256-266.
- Schilling, H.D., Bonn, B. and Krauss, U., 'Coal Gasification', Graham and Trotman, London (1981).
- Smith, I. W., *Fuel*, 57, (1978) 409.
- Smith, J. M. and Van Ness, H. C., 'Introduction to Chemical Engineering Thermodynamics', Third edition, McGraw-Hill, Kogakusha, 1975, 389-391.
- Smoot, L. D. and Smith, P. J., 'Modelling of Coal Processes', Ch. 7 of 'Coal Combustion and Gasification', Plenum, (1985) 163.
- Solomon, P. R. and Beer, J. M., 'Fundamentals of Coal conversion and relation to coal properties', *Energy*, 12(8-9), Ch. 12, (Sep 1987) 837.
- Takarada, T., Tamai, Y. and Tomita, A., *Fuel*, 64, (1985) 1438
- van Heek, K. H. and Muhlen, H. J., 'Aspects of coal properties and constitution important for gasification.', *Fuel*, 64, (Oct. 1985) 1405.
- van Heek, K. H. and Muhlen, H. J., 'Heterogene Reaktionen bei der Verbrennung von Kohle', *Brennst. Wärme Kraft*, 37, (1985) 20.

- van Heek, K. H. and Muhlen, H. J., 'Effect of coal and char properties on gasification', Fuel Proc. Technol., 15, (1987) 113-133.
- Vogel, A. I., 'A Textbook of quantitative Inorganic analysis.', Longmans, third edition, (1961) 584.
- Wakao, N. and Kaguei, S., 'Heat and Mass Transfer in Packed Beds', Gordon and Breach, (1982) 162.
- Walker, P. L., Jr. Rusinko, F., Jr., and Austin, L. G., Advances in Catalysis, 11, Academic Press, N. Y., (1959) 133.
- Walker, P. L., Jr., Mahajan, O. P., and Yarzab, R., Am. Chem. Soc., Div. Fuel Chem. Prepr. 20(1), (1977) 7-11.
- Wen, C. Y., 'Optimization of Coal Gasification Processes', R & D Res. Rep. 66, vol 1, Ch. 4, (1972) 74.
- Wen, C. Y. and Dutta, S., 'Rates of Coal Pyrolysis and Gasification Reactions', in 'Coal Conversion Technology', Addison-Wesley, Ch. 2, (1979) 57.
- Westerterp, K. R., van Swaaij, W. P. M. and Beenackers, A. A. C. M., 'Chemical Reactor Design and Operation', Wiley, (1984) 642.
- Wiggin, H. and Company Ltd., 'Iconel Alloy 600.', Publication # 3269, Holmer Rd, Hereford, England, (1971).
- Yoon, H., Wei, J. and Denn, M. M., 'A Model for Moving-Bed Coal Gasification Reactors', AIChE Jrnl, 24(5), (Sept 1978) 885.

(A.1)

APPENDIX A

THE TECHNIQUE OF OPERATION OF THE EXPERIMENTAL APPARATUS FOR THE MEASUREMENT OF THE KINETICS OF STEAM-CHAR GASIFICATION.

APPENDIX A1.

A PRACTICAL DISCUSSION OF THE PROCESS FLOW DIAGRAM.

This discussion is intended to assist the operator of the experimental apparatus in identifying the components of the process flow diagram (Figure 2) and in understanding the functions of the various components of the apparatus.

A1.1 THE STEAM ROUTE

Steam is isolated from the microreactor by the blue-handled ball valve on the main steam line. When directed to the microreactor, steam is able to flow in either one of two directions, depending on the position of the 3-way ball valve on the control panel upstream of the reactor. This valve directs steam to either bypass the reactor and flow into the condenser C1, or to flow into the preheater tube of the reactor. The purpose of the reactor bypass line for the steam is to provide a path for steam whilst the reactor is heating up. This steam stream is required to initially flush out any condensate present in the steam lines, and to heat the steam lines to the control panel before the experiment begins.

(A.2)

The flowrate of steam which bypasses the reactor during start-up is dictated by the position of the needle valve downstream of the 3-way ball valve. A position of about 2 turns open provides an adequate steam flowrate during start-up.

The steam pressure required during an experiment is set during the start-up stage by adjusting the top nut of the steam pressure regulator on the boiler and monitoring the steam pressure gauge on the control panel.

Two identical steam condensers are employed on the apparatus. Condenser C1 is used to condense steam which bypasses the reactor during start-up. The cooling water supply is common to both condensers and controlled by a 'Saunders' valve below the condensers. This valve should be fully open during operation.

During the operation of the condensers, condensate is removed from the condensate collectors which are located below each condenser. This is achieved by adjusting the valves on the outlet lines from the collectors to positions which maintain steady levels of condensate in the collectors.

It is important to note that one should not allow the condensate collectors to drain empty, as this results in the loss of the liquid seal of the vapour phase (eg. product gases) and requires some effort to re-establish.

A1.2. THE PRODUCT ROUTE.

The product gas stream from the microreactor comprises the products of the steam-char gasification reaction and excess steam. This stream exits at the base of the reactor, at which point its temperature is measured by T6, and flows upwards through the electrically-heated product line to the product condenser C2, on the extreme right of the control panel. The flowrate of the product stream is dictated by the position of the product flow control valve, Vp. The position of Vp is set such that the flowrate of steam admitted through the microreactor is able to be heated to the reaction temperature in the preheater tube. These valve settings are learned by experience. Vp has a vernier scale installed on its handle to enable the position of the valve to be precisely recorded. During steam char gasification, the products should always be directed to the product condenser, C2. This implies that the product to relief-line ball valve should be closed. An isolating ball valve exists immediately upstream of the product condenser. This should be open during an experiment.

The product condenser is designed to totally condense the steam content of the product stream. During an experiment, once steady state has been reached, one should adjust the condensate collector drain valve to a position which maintains a steady level in the collector.

The products of gasification flow out of the product steam condenser

(A.4)

and then through an oil trap and drier, respectively. The product gases are then directed to the gas sampling system. The product drier comprises a packed bed of magnesium perchlorate. The drier is used to remove the moisture content of the product gases at saturation in the condenser. The drier has the capacity of removing approximately 20 g of water. The drier is initially to be loaded with approximately 10g anhydrous magnesium perchlorate. The total mass of the drier is to be monitored after each run in order to check the progress of the absorption of moisture. Typically, fresh drying agent should be loaded after about 10 runs.

A1.3. PRODUCT GAS SAMPLING SYSTEM.

The product gas stream is directed to either the product rotameter or to the gas sampling valve, depending on the position of the 3-way ball valve, upstream. During an experiment, one alternately selects the rotameter and gas sampling paths for the process products. The frequency of switching and duration of the valve in either position depends on the overall rate of reaction; average conditions are as follows :

- normally maintain the valve in the rotameter position;
- switch to the sampling position at 4 minute intervals;
- Hold the valve in the sampling position for 30 seconds to enable the gas to fill a sample loop, before returning to the rotameter position.

To sample the product gas, switch the 3-way valve to the sampling position, allow 30 seconds for the gas to fill the

(A.5)

currently-selected sample loop, then press STEP on the sample loop position controller to advance the position to the next loop. This will cause the current sample to be sealed into the previous loop. Thereafter switch the 3-way valve back to the rotameter position.

Downstream of the rotameter, the product gases, are directed to an instrument, which is sensitive to inflammable gases. This instrument is used to detect the presence of the first products of the experiment and to check the presence of other such products during the run. The instrument is activated when required.

A.1.4. NITROGEN START-UP STREAM.

Nitrogen is used to provide an inert atmosphere in which to heat the char sample contained in the reactor as close to the desired reaction temperature. Two nitrogen bottles are provided for this purpose in the bulk gas storage rack. The N_2 is supplied to the inlet of the gas preheater tube via a 4-way ball valve, which is used to select N_2 bottles, and ultimately via an isolating ball valve (green handle) at the top of the reactor.

During start-up, a N_2 stream flows continuously through the tube-side of the reactor and out of the reactor via the product gas line. During start-up one allows the N_2 to escape to the relief line. This condition requires that the product relief valve is open. Towards the end of the start-up procedure, one normally

(A.6)

closes the relief valve and allows N_2 to flow to the product rotameter.

The same N_2 supply is used to cool the reacted char sample to room temperature in an inert atmosphere at the end of the experiment. One uses the green N_2 isolating valve at the top of the reactor to locally interrupt or demand N_2 .

A1.5. PRESURISATION OF THE OUTER VESSEL.

N_2 is also used to pressurise the outer vessel of the microreactor. This N_2 supply contained in only one bottle on the gas supply rack, and the pressure of the contents of this bottle should therefore be checked before an experiment. This N_2 is supplied directly to the base of the outer vessel. A low flowrate of N_2 is maintained through the outer vessel during a run in order to remove any condensate which may collect in the vessel as a result of steam escaping through the pressure equalisation hole in the reactor tubes. This feature has been included in the design to prevent the development of a large pressure difference across the reactor tubes during operation.

The vessel N_2 stream leaves the reactor via the vessel N_2 flow control valve. The pressure of the outer vessel is indicated on the vessel pressure gauge, immediately upstream of this valve. The N_2 flow control valve is normally just cracked open to allow a small quantity of N_2 to escape the vessel.

(A.8)

APPENDIX A2.

OPERATION OF THE GENERAL ELECTRICAL CIRCUITRY OF THE MICROREACTOR,
INCLUDING THE TEMPERATURE CONTROL SYSTEM.

The temperature of the reaction in the microreactor is controlled by a Eurotherm 070 PID temperature controller. The ID settings of the 070 controller are not adjustable. The proportional settings which are found to be suitable for this operation are as follows :

(These are adjusted on the lower front, left panel).

L : set vertically upwards

X_p : set on 8 (scale 1 - 10)

P : 50%

The temperature setpoint of the 070 is adjusted by turning the thumb wheel on the front panel, and is indicated by the lower needle on the scale. The controlled temperature, T4, is indicated by the upper needle on the same scale. The power to the 070 should be kept on at all times.

The reactor is designed to interrupt the electricity supply to the heater in the event of T3 rising above a preset temperature limit or failing to operate. This is achieved by the inclusion of a

(A.9)

Eurotherm 106 alarm temp. controller in the electrical circuit. The 106 has a thumbwheel adjusted set-point, which is normally set at about 1000°C. The status of T3 relative to the 106 set point is indicated by three L.E.Ds on the 106. The output of the 106 controls the position of a set of contacts in the adjacent relay box. These contacts carry the electrical supply to the reactor heater.

The electrical supply to the reactor heater is delivered via the transformer located beneath a protective, grounded aluminium cover. The output from the transformer is to be maintained at the 80 V position at all times. This is to ensure that no more than 25 A pass through the electrical circuit; this limitation is introduced by the capacity of the thyristors of the 070 controller.

The main power switch of the electrical circuit of the microreactor is located behind the perspex control panel of the reactor, and is accessed from the left hand side. This switch is to be turned on only for the duration of an experiment. The power is switched on when the green lever is in the down position. This status is indicated by the red light on the transformer.

The electrical supply to the process is drawn from the distribution board in the passage outside the lab. The main power supply is directed through a 40 A circuit breaker (No. 2).

The power supply to the plug sockets behind the reactor is directed

(A.10)

through a 15 A circuit breaker (No. 13)

These circuit breakers should be on (up position) at all times.

The experimental apparatus has 3 sets of electrical heating tapes. The first is used to heat the steam line from the boiler to the reactor. The others are used to heat the product line from the reactor to condenser C2.

The heating tapes are powered via independent variable transformers. These transformers are to be maintained at the respective set points, which are shown on each transformer. (Indicated by koki marks).

The heating tape transformers are to be switched on only during an experiment. The switches are on the right hand side of the reactor, between the condensers.

APPENDIX A3.

OPERATION OF THE BOILER.

Water is supplied to the boiler by an electrically driven multi-stage pump. During the operation of the boiler, the body of this pump is cooled by a continuous flow of water through the pump. This water cooling is achieved by just opening the red handled globe valve connected to the tee-piece immediately downstream of the pump, thus allowing a low flowrate of water to be pumped to the drain at all times. The boiler feed water isolating valve (black handled 'Sanders' valve) upstream of the pump is normally maintained in the open position.

To commission the boiler, the following activities should be executed:

- (1) Crack open the small, red globe valve at the pump to allow the pump to be cooled during operation.
- (2) Check that the ball valve on the drain line of the boiler is closed.
- (3) Check that the ball valve upstream of the level control valve is open.
- (4) Check that the globe valve on the steam outlet line (insulated, red handle) is closed.
- (5) Check that the ball valve (blue handle) on the steam supply line to the reactor is closed.

(A.12)

- (6) Turn on the power supply to the boiler. There are 2 power switches: 1 at the wall; 1 on the local control box. Check that both of these are on.
- (7) Press the green button on the control box to start the pump.
- (8) Check that a reasonable flow of water is reporting to the drain down the $\frac{1}{4}$ " copper line. Adjust the small globe valve at the pump if necessary.
- (9) Check that the boiler water level reaches a steady position about one-third of the way up the sight glass.
- (10) Check that the temperature thermostat is off.
- (11) Turn on the heater at the control box, using the relevant green button.
- (12) Adjust the thermostat setting to about 275°C.
- (13) Wait for steam pressure to develop in the boiler, as indicated by the boiler pressure gauge [NOTE: The boiler relief valve is set to lift at about 100 psi (= 7 bar gauge). This corresponds to a thermostat setting of about 300°C].
- (14) Check that the needle valve (yellow handle) on the drain line is closed.
- (15) Open the main steam isolating valve fully (insulated red handle).
- (16) Check that the regulated pressure, downstream of the steam pressure regulator, is about 1,5 bar. Adjust if necessary by turning the top nut on the regulator (clockwise for higher pressures).
- (17) Crack open the yellow needle valve on the drain line to allow a low flowrate of steam to escape to the drain. Check that

(A.13)

steam is flowing to the drain (outside) after about 10 mins. This practice ensures that the steam/condensate drain line is free from blockage and able to be used in the case of an emergency.

The following procedure should be employed to shutdown and blowdown the boiler :

- (1) Switch off the heater thermostat.
- (2) Turn the heaters off at the control panel.
- (3) Open the yellow needle valve on the drain line fully, until the boiler pressure has dropped to 20 Psi.
- (4) Close the yellow needle valve.
- (5) Close the main steam isolating valve (red handle).
- (6) Close the water supply ball valve (green handle).
- (7) Open the boiler drain ball valve (green handle).
- (8) Allow the steam pressure to reduce to zero and the water level in the boiler to drop fully.

(NOTE: The manual lifting of the boiler relief valve at this stage assists in dropping the boiler water level).
- (9) Close the drain ball valve.
- (10) Open the water feed ball valve to allow the water level in the boiler to rise to a steady level.
- (11) If the water appears to be very dirty, then repeat steps (6) to (10). Repeat operation up to 3 times.
- (12) Turn off the pump motor at the control panel.
- (13) Turn off the local power switch at the control panel.
- (14) Stop the pump cooling water stream by closing the small red

(A. 14)

handled globe valve at the pump.

(A.15)

APPENDIX A4

NOTES ON THE OPERATION OF THE VARIAN 4720 INTEGRATOR.

- (1) The local power switch of the integrator is located on the back right hand panel.
- (2) On initially supplying power to the unit one is prompted for the current date. Respond by using the format : month/day/year, followed by pressing the 'ENTER' key.
- (3) Thereafter one is prompted for the current time, on a 24 hour basis. One should respond with hr : min : sec ENTER.
- (4) In order to advance the paper of the integrator, simply press the ENTER key
- (5) The integrator prints the current time of day in response to one's pressing the TIME key.
- (6) In order to set the attenuation of the integrator, one should press the ATTEN key and then respond to the prompt 'AT =' by entering the desired attenuation.

APPENDIX A5

THE TECHNIQUE OF OPERATION OF THE VARIAN 3300 G.C.

- (1) The main power supply to the GC is to be maintained in the 'on' position at all times.
- (2) A local power switch exists behind the GC. This is also normally on.
- (3) The operation of the GC is controlled from the front panel of the instrument which comprises a series of soft-touch keys, status lights and an electronic visual display window. The display provides the facility of visual communication of information to the operator.

On pressing the STATUS key, one is informed of the general status of the GC, ie. column, detector and injector temperatures. When the STATUS light flashes, one is expected to press the STATUS key to receive a message concerning the status of the GC. One pressing the RESET key, the STATUS light will remain on as an indication of the acceptance of the current status of the GC. The steady STATUS conditions of the GC during normal operation are as follows :

Column temperature = 35°C;
Injector temperature = 100°C;
Detector temperature = 240°C;

- (4) The GC is installed with two sets of injectors and detectors, namely A and B. Our application employs detector A, which is a TCD. During normal operation of the GC, a steady flowrate of carrier gas flows across the filaments of TCD A whilst the filaments are heated by the passage of a steady electrical current.

Carrier gas is supplied to the analytical filaments by adjusting the flow control valve labelled 'injector A'. The normal position of this valve during operation of the GC, as indicated by a decimal scale ranging from 0,00 to 99,99, is 34,0. This valve position corresponds to a carrier gas flowrate of 30ml/min through the analytical column, column A. It is recommended that the position of this valve be adjusted to a value of 15,0 overnight in order to conserve carrier gas.

Carrier gas is supplied to the reference filaments by adjusting the REFERENCE valve, which has a green handle. The normal set-point of this valve is approximately 9 full turns open. The handle of the valve has a white mark at the top when in the fully closed position. The flowrate of the carrier gas stream across the reference filaments is measured by a soap-bubble flowmeter downstream of the TCD. The ultimate position of the REFERENCE valve is set in the vicinity of 9 turns open such that the measured flowrate of the carrier gas is 30ml/min. The position of this valve is adjusted to 6 turns open overnight in order to conserve

(A.18)

carrier gas.

Note that the carrier gas is supplied upstream of the flow control valves at a steady regulated pressure of 550kPa g.

(5) The following procedure is adopted to supply power to the TCD A filaments :

- check that the carrier gas is flowing across both analytical and reference filaments;
- check that the positions of the peripheral valves of the gas analysis system are such that carrier gas is directed through column A. Figure 12 shows the positions of these 3-way ball valves during the sampling of the product gas stream from the microreactor. This combination of valve positions directs carrier gas to bypass the gas sampling valve and flow through the analytical column and then across the analytical filaments of the TCD. The reference carrier gas stream is permanently connected to the TCD;
- press the MODIFY key on the GC control panel;
- then press the DETECTOR key;
- press 240 ENTER to set the temperature of the detector block to 240°C;
- then press MODIFY, COLUMN, 35 ENTER to set the initial temperature of the analytical column;
- press MODIFY, INJECTOR, 100 ENTER to specify the temperature of the A port injector;

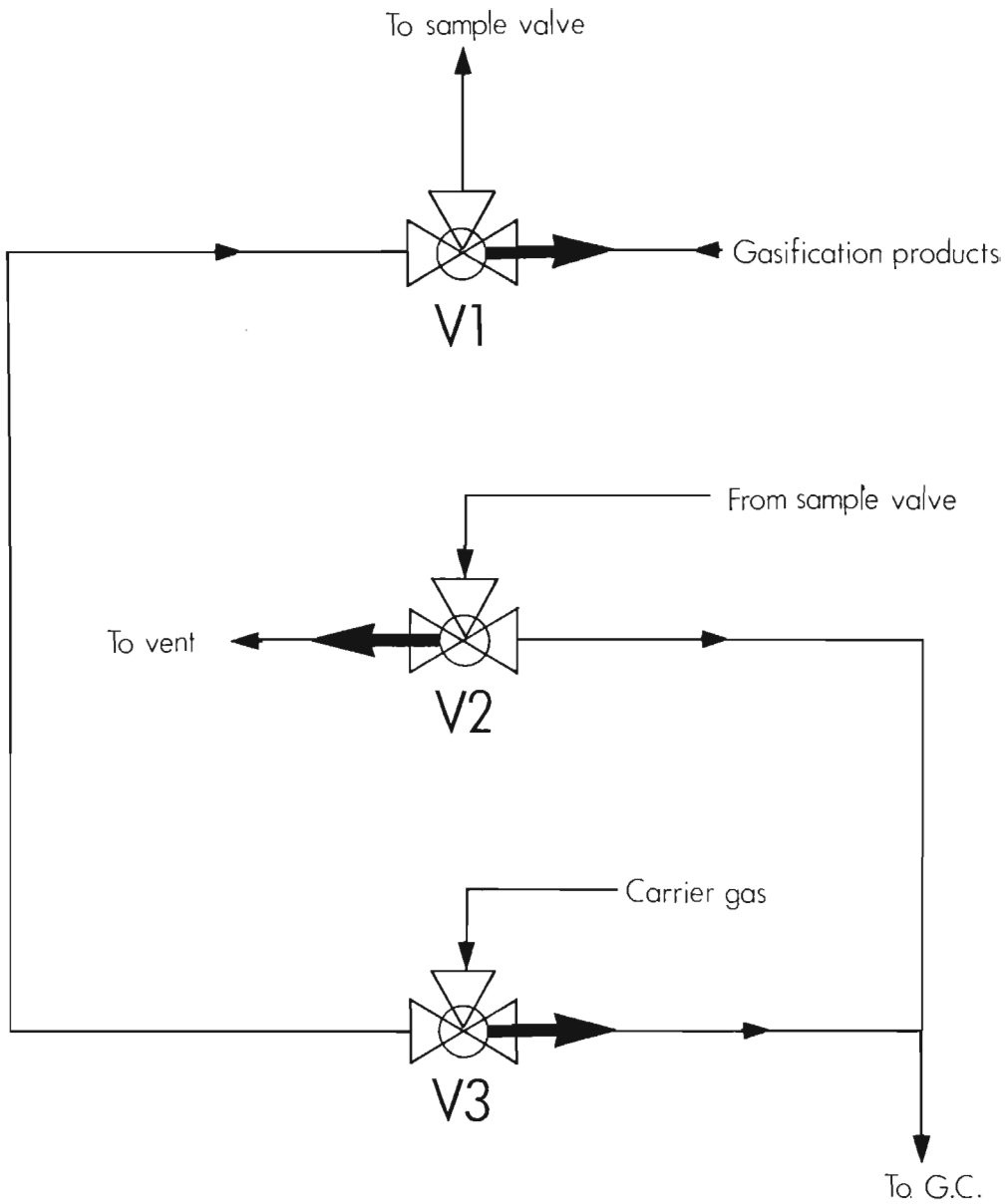


FIGURE 12 Peripheral valve positions of gas analysis system during sampling

(A.19)

- then press STATUS and wait for the above three temperatures to reach the specified set-points;

(A.20)

- when the status of the GC is approved, press MODIFY, DETECTOR;

- thereafter one is able to edit the detector program by using the left or right arrow keys and the ENTER key to select the relevant variables of the program. The normal set-points of the detector program are as follows :
 - (1) DET. TEMP = 240°C
 - (2) DET. A or B : A
 - (3) TCD A INITIAL ATTENUATION = 8
 - (4) TCD A INITIAL RANGE = 0.50 mV
 - (5) TCD A AUTOZERO ON : NO
 - (6) TCD A FILAMENT TEMP. = 280°C, and OFF during shutdown
 - (7) TCD A POLARITY POSITIVE : YES
 - (8) PROGRAM TCD A TIME IN MINUTES : 4.00
 - (9) PROGRAM TCD A ATTEN. = 8
 - (10) PROGRAM TCD A RANGE = 0.50 mV
 - (11) PROGRAM TCD A AUTOZERO ON : NO
 - (12) PROGRAM TCD A POLARITY POSITIVE : NO
 - (13) ADD NEXT TCD A PROGRAM : NO

- Note that power is supplied to the TCD by specifying the temperature of the filaments. It is imperative that the temperature of the detector body be at a steady value of 240°C before one sets the temperature of the filaments, since the current supplied to the filaments is a function of the specified filament temperature and the detector temperature. The above conditions require that a current of 136mA passes

(A.21)

through the filaments.

- (6) The temperature program of the analytical column (column A) of the GC is modified by pressing the MODIFY and COLUMN keys, after which one employs the ENTER key to advance through the program. Variables in the program are edited by altering the value of the variable before pressing the ENTER key. The following column temperature program is employed during analyses of the products of gasification :

- (1) INITIAL COLUMN TEMP. = 35(°C)
- (2) INITIAL COLUMN HOLD TIME = 7.00 (minutes)
- (3) PROGRAM 1 FINAL COL. TEMP. = 225 (°C)
- (4) PROGRAM 1 COLUMN RATE = 32.0 (°C/minute)
- (5) PROGRAM 1 COL. HOLD TIME = 10.0 (minutes)
- (6) ADD NEXT COL. PROGRAM : NO

- Note that one is able to modify a column temperature program during the progress of the program on the GC.

- (7) A further activity to be conducted before being able to proceed with gas analyses is the electronic balancing of the TCD. This activity typically follows the collection of product gas samples during an experiment after which the positions of the peripheral valves of the gas analysis system are as shown in Figure 12. The following procedure is to be executed in preparation for gas sample analyses :

- Advance the position of the gas sampling valve to loop number 1 by pressing HOME on the remote valve position control

(A.22)

box;

- Reverse the position of V1 (to the opposite of that shown in Figure 12);
- Open the main isolating valve of the helium flush gas bottle in the gas storage rack. Check that the regulated pressure is 2kPa;
- Flush the contents of the inlet line to the sampling valve, loop #1, and the outlet line with He by opening the local He flush isolating ball valve at the GC
- After about 15 seconds, reverse the position of valve V2; close the local He flush isolating valve immediately thereafter and then reverse the position of valve V3. The positions of valves C1, V2 and V3 should then be opposite to those shown in Figure 14;
- Set the carrier gas flowrates at 30ml/min at this stage, with column A at 35°C, the upstream pressure of column A will be 40psi;
- Check that the normal detector program is installed (See (5) above);
- Modify element (5) of the temperature program of column A to set the holding time of program 1 to 60.0minutes;
- Press the START key to begin running the GC with the modified column program. This activity is designed to purge the column by holding it at 225°C for 1 hour, and is practised before proceeding with a set of gas analyses. Whilst the GC is running one usually presses the STATUS and COLUMN keys to

(A.23)

monitor the temperature of the column. On the completion of the column temperature program, the GC automatically returns the temperature of the column to the initial vlaue;

- Modify element (5) of the detector program by responding YES to the prompt : TCD A autozero on?;
- Check the value of the baseline of the integrator by pressing the LEVEL key of the integrator. This should read approximately 1000;
- Press the STATUS, DETECTOR and right arrow keys of the GC to view the value of the baseline of the GC (mV). This value should ideally be 0.00mV. Adjust the baseline to as close as possible to zero by unclipping the top cover of the GC and carefully adjusting the TCD A BALANCE dial on the TCD printed circuit board. Replace the top cover after adjustment. Note that the value of the baseline of the integrator should still be 1000;
- Restore the detector program to normal;
- Restore the column temperature program to normal;
- Press the RESET key of the GC;
- Press PT EVAL on the integrator. This causes the integrator to monitor the baseline signal received from the GC. After about 1 minute, the integrator reports the value of the variable termed the 'peak threshold'. The minimum value of this variable is 12, which indicates a very stable baseline signal. Should the value of the peak threshold be greater than 50, it is suggested that one checks the carrier gas

(A.24)

flowrates and the electronic zero of the GC;

After the above procedure, the GC should be ready for gas analyses.

(8) The analysis of product gas samples contained in the loops of the gas sampling valve proceeds as follows :

- To inject the first sample into the analytical carrier gas stream, advance the position of the gas sampling valve to loop #2 by pressing STEP once on the valve position controller;
- As soon as the digit '2' appears on the valve position display, press START on the GC to begin the analysis, and immediately thereafter, press INJ A on the integrator to begin integrating the OUTPUT from the GC;
- During an analysis, the flashing of the red L.E.D. next to the RUN A key of the integrator indicates that the baseline is being plotted. When a peak is detected, this light remains illuminated until the peak has passed;
- After the CO₂ peak has been recorded by the integrator, press INJ A to terminate the integration of the GC signal. The integrator then proceeds to print a report of the details of the chromatogram. The characteristic retention times for the various gas components present in a typical gas sample are as follows :

Component	Retention time/minutes
H ₂	1.37
O ₂	6.41
N ₂	7.22
CO	8.97

(A.25)

CH ₄	12.41
CO ₂	14.65

- Note that one may abort a chromatogram at any stage by pressing ABORT A;

 - When the GC has completed the entire column of temperature program, one is required to RESET the GC before proceeding with the analysis of the following sample. Note that one may abort a GC program at any stage by pressing RESET;

 - Proceed in the manner discussed above to sequentially analyse the remaining product gas samples.
- (9) On the completion of the product gas analyses, one should reverse the positions of the peripheral valves of the gas analysis system to conform with the positions shown in Figure 12. It is important that the valves be reversed in the following order :
- (1) V3
 - (2) V2
 - (3) V1.
- (10) The following procedure should be adopted in order to change the carrier gas supply to the GC :
- Switch off the power to the GC filaments by setting the filament temperature to OFF in the detector program;

 - Close the main isolating valve of the current carrier gas

bottle;

- Open the carrier gas flow control valves widely to allow the residual 5,5 bar in the carrier gas line to the GC to drop to below 1 bar;
 - Disconnect the regulator from carrier gas bottle and connect it to the fresh bottle. Remember that this regulator has a left-hand thread;

 - Close the carrier gas flow control valves on the GC;
 - Open the main isolating valve on the new carrier gas bottle;
 - Check that the regulated carrier gas pressure is 5,5 bar;
 - Allow 48 hrs. for the stabilisation of the pressure to the gas flow controllers before using the GC for analysis.
 - Before supplying power to the filaments, allow carrier gas to flow across the filaments for at least 30 minutes to prevent the risk of oxidation of the filaments.
- (11) The GC is calibrated by analysing a range of volumes of each of the separate components of the product gas stream (eg. 0.05, 0.10, 0.15, 0.20, 0.25, 0.30, 0.40 ml) using the same analytical column and temperature program employed for the analysis of the products of gasification. Two gas syringes are employed in this exercise (one of 0.25 ml capacity and the other of 0.5 ml capacity) to inject the gas samples into the injector port for column A of the GC. The principle of this technique of calibration is that the integrated response of the chromatogram for each component may be correlated with the

(A.27)

amount of that component present in the sample. Because the response of a TCD is typically linear, linear correlations are employed in this study. The calibration factors for the respective gas components for each of the carrier gas supplies employed in this study are contained in Appendix B2.

(A.28)

APPENDIX A6

PREPARATION FOR AN EXPERIMENT.

The following activities should be performed in preparation for an experiment :

- (1) Check that at least two cylinders, containing at least half-full capacity of N_2 , are available.
- (2) Check that an ample supply of carrier gas is available for the GC, i.e. at least 2000 kPa g. This gas is a nominal 10% H_2 in Helium mixture and should be ordered at least 3 weeks in advance of the demand. It is suggested that a new bottle be ordered when the pressure drops to 4000 kPa g.
- (3) Check that one has a supply of upper and lower gaskets for the sample basket.
- (4) Check that one has a supply of magnesium perchlorate for the product gas drier.
- (5) Check that one has spare roll of paper for the integrator.

(A.29)

APPENDIX A7.

REACTOR STARTUP CHECKLIST.

- (1) Mains water, electricity and compressed air supplies are available.
- (2) GC carrier bypassing sample valve and GC idling.
- (3) Sample valve in position #2.
- (4) N₂ bottles ready.
- (5) Boiler on; bleed steam stream flowing to drain.
- (6) Char loaded; top gasket installed in sample basket.
- (7) Reactor sealed.
- (8) Thermocouples connected; check TC4 is operating.
- (9) Ensure positions of valves on control panel are correct.
- (10) N₂ supplied to reactor tube side and outer vessel.
- (11) Cooling water supplied to condensers and reactor jacket.
- (12) Heating tapes on.
- (13) Cooling air transformer on.

APPENDIX A8.

MICROREACTOR START-UP PROCEDURE.

The following activities are to be sequentially executed in order to begin an experiment :

- (1) Check that the mains water supply, electricity and compressed air are available.
- (2) Commission the boiler with a thermostat setting of 275°C. When a steady steam pressure has developed in the boiler, open the main steam-isolating valve fully and set the steam pressure regulator to deliver about 1,5 bar immediately downstream. Then crack open the steam-drain valve to allow a low flowrate of steam to clear the drain line.
- (3) Whilst the boiler is heating up, check that the GC is ready (ie. filaments on, carrier gas flowrates at normal operating values) and that the carrier gas is bypassing the gas sampling valve. (This condition is recognised by the positions of the peripheral valves and by the pressure of column A being above 40 psi).
- (4) Check that the sample valve is in position # 2. This loop will contain the first sample to be taken.
- (5) Compare the current total mass of the product gas drier to the initial total mass with anhydrous magnesium perchlorate

(A.31)

present. Renew m.p. if necessary (one usually renews m.p. after about 5 g of moisture have been collected).

- (6) Load the char sample into the reactor, and seal the reactor. This operation involves the following activities:
- clean the sample basket with tissue and compressed air; occasionally use the sharp metal instrument to remove any residue from the fine mesh stainless-steel disc inside the bottom of the basket; also use this instrument to remove any gasket residue from the upper and lower surfaces of the basket;
 - record the mass of the empty sample basket to 2 decimal places on the Mettler electronic balance in the main laboratory;
 - transfer about 3 g of char sample into the basket; record the total mass of the basket;
 - install a lower gasket onto the sample basket;
 - inspect the lower end of the preheater tube and remove any high spots gently with emery paper;
 - wipe the preheater tube with tissue;
 - clean the inside of the outer reactor tube with the cloth attached to the 1/8" tube shaft; pay particular attention to cleaning the top surface of the product gas cooler tube, which supports the sample basket on the lower gasket;
 - check the condition of the inside of the reactor with a torch;
 - wipe the top stainless flange of the reactor with tissue;
 - attach the sample basket to the loading instrument without

(A.32)

excessive force;

- whilst standing at the level of the wooden platform, lower the basket carefully into the reactor; a koki mark on the loading tool indicates the position at which the basket will have seated;
- twist the tool firstly in the clockwise direction and lift the basket slightly in order to centralise the basket;
- then twist the tool in the anti-clockwise direction in order to release the pins in the basket;
- raise the tool slowly, whilst detecting whether the basket has been released by the change in mass of the tool;
- if it is suspected that the basket is released, raise the tool carefully out of the reactor; if the basket has not been released, repeat the loading procedure;
- Centralise and drop a top sample basket gasket into the reactor. Check that the gasket has seated correctly in the top of the basket, using a torch. If not, use the hook instrument to correctly position the gasket.
- lower the preheater tube carefully into the reactor, paying particular attention to protecting the leading edge of the tube as it enters;
- remember to nudge the 6.35mm connecting tubes aside as the top flange assembly lowers into position, and to push back the counterweight cable as the weight passes the obstructing product line;
- when the top flange is about 10 cm from seating, insert guide

(A.33)

- pins # 2 and # 4 through all four top flanges of the reactor to guide the lower end of the tube into the basket;
- finally, lower the top flanges completely; pay attention during the last 2 cm, when the reactor tube enters the basket; if this does not occur, the basket may be located off-centre and will need to be re-located using the loading tool; some perseverance with gentle manipulation of the two guide pins often helps to avoid having to re-locate the basket;
 - Note that at this stage some clearance exists between the top flanges, which will be taken up by compressing the sample basket gaskets when the flange assembly is tightened;
 - insert bolts through holes # 1 and # 3; finger tighten; then tighten about $1/8$ turn with spanners;
 - remove pins # 2 and # 4; replace with bolts; tighten about $1/4$ turn with spanners;
 - sequentially tighten diagonally-opposite bolts until the flange assembly is tight;
 - attach the quickfit connector on the steam line to the steam inlet tube of the top flange assembly;
 - seal the relief line and N_2 inlet connections to the top assembly; be careful not to cross-thread the connections.
- (7) Carefully connect the male and female plugs of thermocouples T3 and T4.
- (8) Turn on the heating tapes (3 power switches);

(A.34)

- (9) Adjust the positions of the valves on the rig as follows:
- ensure that the reactor steam isolating valve (blue handle) is closed;
 - open the N₂ isolating valve (green handle);
 - select the relevant N₂ bottle for start-up ;
 - Select the 'steam to bypass reactor' position of the steam route selection valve;
 - open the steam bypass flow control valve by 2 turns;
 - open the relief valve on the product line;
 - set the product flow control valve at 25/25 turns open (using the vernier scale);
 - open the product isolating valve immediately upstream of C2 (green handle);
 - crack open the vessel N₂ flow control valve;
 - select the rotameter route for the process gas stream at the gas sampling system;
- (10) Check that the heating tapes are functioning by sensing the temperature of the heated lines;
- (11) Open fully the cooling water supplies to the condensers and to the reactor jacket;
- (12) When the boiler is ready and the heating tapes have been on for about 15 minutes, direct steam to by-pass the reactor as follows:
- open the reactor steam isolating valve (blue handle)

(A.35)

- It is suggested that immediately after one opens the main steam valve (blue), one should open the steam bypass flow control valve to a position of about 4 turns open for a short while to allow the initial condensate held in the steam line, to surge to the condenser. Thereafter, return the valve to about 2 turns open.
 - wait for the condensate level in the accumulator of C1 to rise; then open the accumulator's drain valve to maintain a fairly steady level of condensate in the accumulator;
 - collect the drained condensate in the large measuring cylinder; discard condensate when the cylinder approaches full capacity.
- (13) Direct N_2 to the tube-side of the reactor by opening the main valve on the relevant startup N_2 bottle, and by adjusting the regulated pressure from the bottle to slightly above the intended operating pressure of the experiment (e.g. about 120 kPa for a 100 kPa run).
- (14) Direct N_2 to the vessel by opening the main valve on the N_2 bottle linked to the outer vessel, and by adjusting the regulated pressure to the same value as for the tube-side N_2 stream.
- (15) Note that the tube and vessel-side pressures of the reactor will be indicated on the control panel;

(A.36)

- (16) At this stage, listen for any major gas leaks out of the reactor. If a leak is suspected, it may help to temporarily turn off the pump motor to allow confirmation of the leak. In the event of a gas leak, either rectify the leak in situ or abort the run and mend the leak. Generally, leaks around probes through the reactor are easily rectified by tightening the packing of the seals or turning off the N_2 and re-packing the seals.
- (17) Turn on the compressed cooling air supply for the main power transformer. This is done by fully opening the lower large Saunders valve (black handle) on the right-hand side of the door; check that the clear air tube under the transformer does not become dislodged.

APPENDIX A9

STEAM-CHAR GASIFICATION EXPERIMENTAL PROCEDURE.

- (1) Adjust the set point of the sample temperature controller (Eurotherm 070) to 200°C.
- (2) Select channel # 1 on the digital thermometer in order to monitor the external wall temperature of the outer reactor tube.
- (3) Begin the run by switching on the main power supply to the reactor heater, at the green switch behind the control panel. Record the time of this event and start the cumulative elapsed time stopwatch for the experiment from time zero.
- (4) Record the time-temperature profile during the heating of the reactor by noting the T4 set-point, T4, and T1, and the corresponding run times at reasonable increments of T4 (e.g. 50°C). A typical set of time-temperature profiles during the reactor heating stage is shown in Figure 13.
- (5) When T4 reaches 25°C below its set-point, increase the set point to 200°C above the previous set point. Note that the objective of the initial heating phase of the microreactor is to raise the temperature of the char sample to the desired temperature of reaction. Experience with the microreactor has shown that the rate of heat transfer from the outer reactor

(A.38)

tube to the sample basket during the initial heating in a pure N_2 atmosphere is lower than that which occurs during the gasification experiment in a pure steam atmosphere. This is not surprising in view of the greater susceptibility of steam to radiative heating. The result of this phenomenon is that one observes a temperature difference of about 100°C between T1 and T4 during the initial heating. Therefore, in order to arrive at the desired set-point of T4 for an experiment, one controls the set-point of T4 during initial heating in such a way as to allow T1 to approach 25°C above the desired reaction temperature. One then switches to steam as the reactant gas, and adjusts the T4 set-point to precisely the desired reaction temperature. T4 then rapidly approaches the set-point.

(A.39)

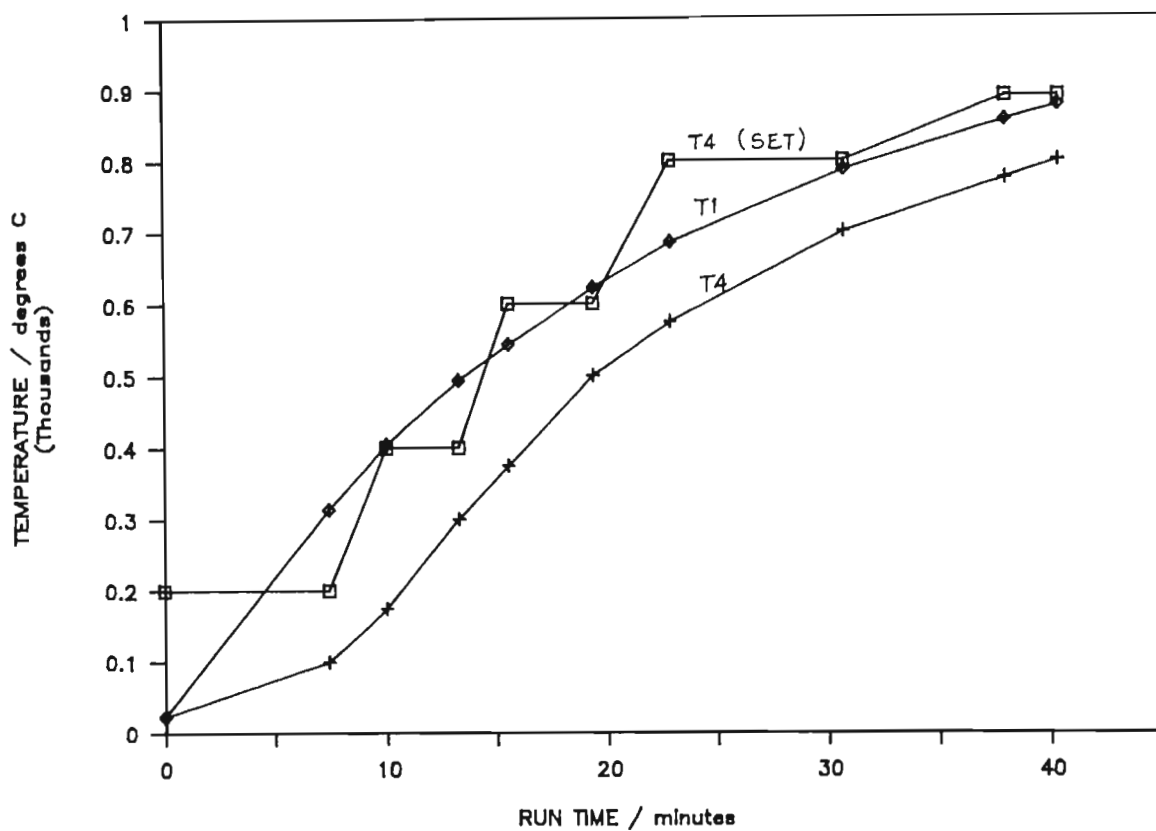


FIGURE 38 A typical set of reactor temperature-time profiles during the initial heating phase of the microreactor.

(A.40)

- (6) Repeat step (5) until T1 approaches 25°C above the desired reaction temperature of the experiment. This criterion should be tested just before the T4 set point is adjusted. It is normally necessary to decrease the final increment in the T4 set point to lower than 200°C in order to achieve this condition.

- (7) As time elapses after the final major T4 set point adjustment has been made, T4 continues to approach T1 because of the temperature difference which exists, and so it may be necessary to increase the T4 set point during this time to match the temperature of T4 in order to prevent the heater from cutting out.

- (8) Before directing steam to the reactor, assess the status of all other systems and make corrections where necessary.

- (9) Direct steam to the reactor to commence the gasification experiment by executing the following activities in fairly rapid succession :
 - adjust the T4 set point to that of the desired reaction temperature;
 - close the N₂ isolating valve on the tube-side (green);
 - reverse the position of the steam route selection valve to direct steam to the reactor. Do not be alarmed at an initial sudden surge when this occurs, which may be as a result of some condensate entering the reactor from the steam line to

(A.41)

the reactor.

NOTE: Adjust the position of the product flow control valve to 15/25 turns open (this valve may be changed whilst developing steady state conditions).

- (10) Select channel # 6 on the digital thermometer to monitor T6 the product temperature immediately downstream of the reactor. The value of T6 serves as a very good indication of the stability of the experiment. Experience has shown that, during steady operation, T6 never drops below 110°C, and that the actual value of T6 is a function of the pressure of operation. (For 100 kPa g steam pressure, T6 = 118°C).
- (11) Monitor T6 once T6 reaches above 100°C, close the product to relief line ball valve, and continue to monitor T6.
- (12) Experience has shown that the rapid opening to about 50/25 turns open and returning back to about 15/25 turns open of the product flow control valve assists in the development of a steady steam flow through the reactor. Occasionally, it has been found that the opening of the products to relief line valve has the same effect as the above.
- (13) The response of T6 to rise above 100°C usually occurs about 30-45 seconds after switching to steam.

(A.42)

- (14) If necessary, adjust the position of the product flow control valve to establish a steady steam flowrate through the reactor. (NOTE: Too high a value of the product flow control valve position will allow more steam through the reactor than is able to be heated to reaction temperature by the preheater; too low a value of the valve position will prevent any steam from flowing). The steady state operation of the microreactor is essentially managed by the sample temperature controller, within a narrow range of positions of the product flow control valve.

- (15) Check the sample temperature on the 070 controller, to see that T4 is approaching the reaction temperature set-point. Because of the sudden load on the preheater caused by the introduction of steam, the approach of T4 to the set-point is somewhat delayed, and T4 usually only reaches set-point about 5 minutes after switching to steam. It is recommended not to adjust the main temperature controller once steam has been introduced, unless the run is to be aborted.

- (16) Crack open the product condensate accumulator drain valve and control the level in the accumulator at a known graduation level throughout the run by adjusting the position of the drain valve.

- (17) Turn on the Warnex gas alarm and read the deflection of the needle.

- (18) Note the run time at which the Warnex alarm needle first deflects steadily to the off-scale position (condition red). This event corresponds to the time at which the first products of the reaction reach the sampling system
- (19) Record the flowrate of products and the corresponding run-time for each changing value of the product flowrate.
- (20) Every 4 minutes or so, collect a sample of the product gas by reversing the position of the product gas route selection valve to direct products to the sampling valve. Pause for 30 seconds whilst the gas flows through the current sample loop. Then press STEP on the loop position controller, and simultaneously record the run time at which the sample was taken. Immediately thereafter, direct the products to the rotameter.
- (21) When the product flowrate drops below 0.5 on the rotameter scale, the run is considered complete.
- (22) Once the run has started and the product condensate accumulator level has been steadily maintained, begin collecting the condensate in an empty measuring cylinder. Time the cumulative flowrate of the condensate on a separate stopwatch. Stop this measurement just before the end of the run.

(A.44)

(23) During the run, monitor the following conditions as regularly as possible, taking relevant action where necessary :

1. T6 : steady
2. T4 : steady at set point
3. Product condensate accumulator level : steady near graduation
4. Warnex alarm signal : offscale (red)
5. Boiler operation : steady steam pressure supply of about 5 bar.
- boiler pump : cool
6. Outer vessel pressure : check that this pressure is slightly below the steam inlet pressure. This is to prevent much N₂ crossing from the vessel into the reactor tube. Note, therefore, that some steam will enter the vessel which will condense and be carried out of the vessel by the N₂ flowing through the vessel. Occasionally, T1 has been noted to drop suddenly below the reaction temperature, and this is attributed to the contact of steam which enters the vessel with T1. If this happens, adjust the pressure balance to be less severe. This is best achieved by adjusting the position of the vessel N₂ flow control valve.

APPENDIX A10.

SHUTDOWN PROCEDURE FOR THE MICROREACTOR.

At the end of a run, the following procedure should be employed to shutdown the reactor :

- (1) Immediately after the last product gas sample has been taken, reverse the position of the steam route selection valve to bypass the reactor.
- (2) Open the isolating valve of the N₂ supply to the tubeside of the reactor.
- (3) Switch off the power supply to the reactor heater.
- (4) Return the set point of the temperature controller to zero.
- (5) Close the main steam supply isolating valve.
- (6) Close the product condensate accumulator drain valve.
- (7) Turn off the transformer cooling air.
- (8) Switch off all heating tapes.
- (9) Open the product to relief line valve.
- (10) Set the position of the product flow control valve to 10/25 turns open.
- (11) Close the isolating valve on the product line to the condenser.
- (12) Shut down the boiler.
- (13) Select channel #1 on the digital thermometer in order to monitor the progress of the cooling of the reactor.
- (14) De-pressurise the reactor sequentially (tube and vessel side) once T1 has dropped below about 400°C. It is important to maintain a flow of N₂ through the tube-side of the reactor to

(A.46)

ensure that the char remains in an inert atmosphere whilst cooling.

- (15) Turn off the condenser cooling water.
- (16) Once the reactor has cooled to below 500°C, turn off the reactor cooling water.

APPENDIX A11.

POST-EXPERIMENT PROCEDURE.

- (1) After the reactor has cooled to room temperature, disconnect T3 and T4, and disconnect the steam, N₂ and relief lines from the upper flange assembly of the reactor.
- (2) Remove the 4 bolts from the upper flange assembly.
- (3) Gently lift the preheater tube out of the reactor, anticipating that the sample basket may be attached by friction to the lower end of the preheater tube.
- (4) If the sample basket is attached to the top of tube, attempt to recover the lower gasket of the sample basket as the basket appears.
- (5) If the basket remains in the reactor on removal of the top tube, use the loading tool to carefully remove the basket.
- (6) It is imperative that the lower gasket of the basket be removed from the reactor, either with the basket or afterward, using a torch and a thin hooked tube.
- (7) It is good practice to occasionally disconnect the product outlet line from the reactor and to blow compressed air upwards through the reactor to remove any loose particles.
- (9) On removing the sample basket, carefully remove and discard the upper and lower gaskets of the basket.
- (10) Then dry the sample in the basket by placing the basket contained in a beaker in the WRC oven at 105°C for 1 hour.
- (11) Cool the basket in the dessicator.
- (12) Finally weigh the mass of the basket and sample residue.

(A.48)

- (13) Retain the sample residue in a labelled bottle for future reference.

(B.1)

APPENDIX B.

B1 EXPERIMENTAL INPUT DATA SET REQUIRED BY THE PROGRAM 'RATES'
FOR THE COMPUTATION OF THE KINETIC RESULTS OF RUN # 42 :

The Input data below correspond to the following list of conditions :

Date of Run, Run number, reaction temperature, sample description, fixed carbon content of char, ash content of char, mass of sample loaded into microreactor, mass of residue, barometric mercury level during run, barometric temperature, steam pressure, product pressure, vessel pressure, volume of condensate collected during run, duration of collection of condnsate, lab. temperature, Run-time of first detection of products, number of gas samples collected, important comment, integrator run number of first sample, the number of general flowrate data points, the number of steady product flowrate data points :

"28/02/87", "042", 880, "CH3/800", 3.04, 1.12, .1784007, 754, 22.2, 400, 360, 385, 359, .2539, 25.6, .5426, 11, "", "20", 42, 8

The following data represent the areas reported by the integrator for H₂, O₂, N₂, CO, CH₄ and CO₂, respectively for each gas sample collected, together with the run-times at which each sample was collected :

(B.2)

1: 32268,59486,587277,619310,32574,502292,.5539
2: 37354,20749,207455,693712,77988,577863,.5911
3: 41754,8725,49236,786884,50626,622793,1.0322
4: 37324,11166,52820,779006,46422,569694,1.0522
5: 40554,4241,46916,822772,51181,588827,1.0829
6: 40504,4234,39714,844635,47190,560541,1.113
7: 40182,4745,36802,850555,47922,541026,1.144
8: 36936,5683,44988,816813,61075,517385,1.1749
9: 35610,5820,65768,803975,59282,497471,1.2057
10: 37106,3977,61862,782371,40847,494753,1.2414
11: 35852,10073,92593,811621,59682,503192,1.2734

The run-times and the corresponding rotameter levels for the general product flowrate data follow below :

.5633,5.6
.5735,5.8
.593,4.5
1.0016,4.7
1.0103,5
1.0123,5.1
1.0209,5.2
1.0355,4.6
1.0406,4.7
1.0427,4.8
1.0627,4.1
1.0724,4.2

(B.3)

1.0928,3.7
1.0948,3.85
1.0955,3.9
1.1011,4
1.103,4.05
1.1227,3.65
1.1241,3.7
1.1257,3.75
1.1313,3.8
1.1341,3.85
1.1458,3.25
1.1509,3.35
1.1521,3.4
1.1549,3.55
1.1609,3.6
1.1638,3.65
1.1902,3
1.1917,3.05
1.1952,3.1
1.214,2.45
1.2154,2.5
1.2235,2.65
1.2307,2.7
1.2319,2.75
1.2506,2.4
1.2513,2.45
1.2521,2.5

(B.4)

1.2537,2.55

1.2605,2.6

1.264,2.65

The run-times and the corresponding rotameter levels for the steady product flowrate conditions are listed below :

1.0427,4.8

1.0724,4.2

1.103,4.05

1.1341,3.85

1.1638,3.65

1.1952,3.1

1.2319,2.75

1.264,2.65

(B.5)

B2. GC Calibration factors.

The following calibration factors were employed in this study in linear correlations of the form :

$$\text{Amount of species} = m_i * \text{corresponding chromatogram area} + c_i$$

Carrier gas # :		1		2	
species	m_i	c_i	m_i	c_i	
H ₂	2.286E-10	3.106E-6	2.312E-10	3.387E-6	
O ₂	1.132E-11	0	1.030E-11	0	
N ₂	8.843E-12	0	1.027E-11	0	
CO	9.697E-12	0	9.774E-12	0	
CH ₄	1.189E-11	0	1.071E-11	0	
CO ₂	7.777E-12	0	6.78E-12	0	

(C.1)

APPENDIX C.

PROGRAM LISTING OF THE 'RATES' CODE.

```
000 REM -----
010 REM ==PROGRAM TO COMPUTE RATES OF GASIFICATION, WRITTEN BY R. RILEY FROM
020 REM -----
030 CLS : PRINT "THIS PROGRAM COMPUTES GASIFICATION KINETICS FROM EXPERIMENTAL
040 PRINT : PRINT "GATHERED FROM A MICROREACTOR."
050 PRINT :PRINT "CHECK THAT THE CORRECT VERSION OF 'RATES' HAS BEEN LOADED ! "
060 PRINT :PRINT "'RATES1' SHOULD BE USED UP TO AND INCL. RUN 031, AFTER WHICH"
070 PRINT :PRINT "'RATES2' BE USED. (THE TWO VERSIONS DIFFER IN THEIR G.C.
080 PRINT : INPUT "INSERT THE RELEVANT DATA DISC, AND ENTER 'G' ";Q2$
090 IF Q2$ = "G" THEN 1110
100 GOTO 1080
110 DIM A1(15),A2(15),A3(15),A4(15),A5(15),A6(15),TS(15),R1(50),
120 DIM C1(15),C2(15),C3(15),C4(15),C5(15),C6(15),M(6),C(6)
130 DIM LC(95),FC(95),TC(25),DC(25),TF(50),RL(50),DX(50)
140 DIM T1(50),T2(50),T3(50),T4(50),T5(50),X(95),Y(95),D(95),F(95),G(95),H(95)
150 DIM N1(15),N2(15),N3(15),N4(15),N5(15),N6(15),NT(15),V(50),W(50),J(95),XC(50),
160 DIM M1(50),M2(50),M3(50),M4(50),M5(50),M6(50),V1(50),V2(50),V3(50),
170 DIM ST(50),S1(50),S4(50),S5(50),S6(50),HC(50)
180 PRINT : PRINT "WOULD YOU LIKE <C>OMPUTATIONS TO BE PERFORMED,"
190 PRINT : PRINT "OR A <P>RINTOUT OF PREVIOUS RESULTS ?"
200 PRINT : INPUT "ENTER 'C' OR 'P'";Q3$
210 IF Q3$ = "C" THEN 1440
220 PRINT : INPUT "ENTER THE RUN NUMBER : ";RN$
230 TITLE$ = "GASIFICATION KINETICS PROJECT"
240 RP$ = "REPRT"
250 PR$=".PRN"
260 F6$ = RP$ + RN$+PR$
270 OPEN F6$ FOR INPUT AS #1
```

(C.2)

```

D INPUT#1,TITLE$
D INPUT#1,RN$,DD$,TR,MS(1),MS(2),PS,PP,PV,FS,TL,N,NF,NP
D INPUT#1,CMM$
D FOR K = 1 TO NP
D INPUT#1,XP(K),TP(K),R1(K),R2(K),R3(K),R4(K),R5(K),R6(K),R7(K),M1(K),M2(K)
D INPUT#1,M3(K),M4(K),M5(K),M6(K),DX(K),TU(K),XU(K),S1(K),S4(K),S5(K)
D INPUT#1,S6(K),HC(K)
D NEXT K
D CLOSE #1
D GOTO 6700
D REM -----
D REM ==INITIALIZATION==
D REM -----
D REM ==NOMENCLATURE CONVENTION USED : 1=H2, 2=O2, 3=N2, 4=CO, 5=CH4, 6=CO2,
TOTAL CARBON==
D REM ==R=RATE OF APPEARANCE/DISAPPEARANCE, AREAS, M=GMOLECULAR WT./G/GMOL;
A4(5)-> AREA OF CO OF 5TH SAMPLE.==
D REM -----
D PRINT : PRINT : PRINT "INITIALIZING..."
D RESTORE
D TITLE$ = "GASIFICATION KINETICS PROJECT"
D RP$ = "REPRT"
D R$ = "RATES"
D C$ = "CMPSN"
D I$ = "INPUT"
D PR$=".PRN"
D G = 9.7935102#
D GC = 8.314
D T0 = 273.15
D M1 = 2.02
D M2 = 32!
D M3 = 28.02
D M4 = 28.01
D M5 = 16.05
D M6 = 44.01
D M7 = 12.01
D DA = .001201
D REM -----
```

(C.3)

```
1640 REM ==GC CALIBRATION FACTORS : LINEAR PARAMETERS -> M=SLOPE; C=Y-INTERCEPT;
CALIBRATION DATA OF 30/05/86, FOR CARRIER GAS #1 (USED UP TO RUN 031).==
1650 REM -----
1660 FOR I = 1 TO 6
1670 READ M(I),C(I)
1680 NEXT I
1690 DATA 2.96998E-10,2.929E-6,1.34501E-11,0.0,1.06124E-11,0.0
1700 DATA 9.54575E-12,0.0,1.18918E-11,0.0,7.18497E-12,0.0
1710 REM -----
1720 REM ==ROTAMETER CALIBRATION DATA :SK 1/8 15-G-5; DATA READ AS X,Y; X=FLOAT
LEVEL, Y=AIR FLOWRATE/ SCCPM.==
1730 REM -----
1740 FOR I = 1 TO 94
1750 READ LC(I),FC(I)
1760 NEXT I
1770 DATA 0.0,0.0,0.5,5,0.9,10,1.0,12,1.1,14,1.2,16,1.3,18.5,1.4,21
,1.5,24,1.6,27,1.7,30,1.8,33.5,1.9,36.5,2.0,40.0,2.1,44
1780 DATA 2.2,48,2.3,52,2.4,56.5,2.5,61,2.6,66,2.7,71,2.8,76,2.9,
81,3.0,86.5,3.1,92,3.2,98,3.3,103.5,3.4,109,3.5,115,3.6,122,3.7,128.5,3.8,135,3.9,
141.5,4,148,4.1,155.5,4.2,163,4.3,170,4.4,178
1790 DATA 4.5,186,4.6,194,4.7,202,4.8,210,4.9,218,5,226,5.1,
235,5.2,244,5.3,252,5.4,261,5.5,270,5.6,279,5.7,288,5.8,297,5.9,
306,6,315,6.1,324,6.2,333
1800 DATA 6.3,342,6.4,351,6.5,360,6.6,370,6.7,380,6.8,390,6.9,400,7,
410,7.1,420,7.2,430,7.3,440,7.4,450,7.5,460,7.6,470,7.7,480,7.8,490,7.9,500,8,509,8.
1,518
1810 DATA 8.2,528,8.3,537.5,8.4,547.5,8.5,557,8.6,567,8.7,577,8.8,587,8.9,596.5
1820 DATA 9,606,9.1,616,9.2,626,9.3,636,9.4,645,9.5,655,9.6,665,9.7,
675,9.8,685,9.9,695,10,705
1830 FOR I = 1 TO 21 :REM ==MERCURY DENSITY vs. TEMP DATA==
1840 READ TC(I),DC(I)
1850 NEXT I
1860 DATA 10,13.5708,11,13.5684,12,13.5659,13,13.5634,14,13.5610,
15,13.5585,16,13.5561,17,13.5536,18,13.5512,19,13.5487
1870 DATA 20,13.5462,21,13.5438,22,13.5413,23,13.5389,24,13.5364,
25,13.5340,26,13.5315,27,13.5291,28,13.5266,29,13.5242,30,13.52
1880 REM -----
1890 REM ==INPUT==
```


(C.4)

```
1900 REM -----
1910 PRINT : PRINT : PRINT "ARE EXPERIMENTAL DATA TO BE ENTERED <M>ANUALLY, OR READ
FROM <D>ISC ?"
1920 PRINT : INPUT "ENTER 'M' OR 'D' ";Q1$
1930 IF Q1$ = "M" THEN 2240
1940 PRINT : INPUT "FOR WHICH RUN WOULD YOU LIKE INPUT DATA TO BE RETRIEVED ? ";RN$
1950 F9$ = I$ + RN$+PR$
1960 OPEN F9$ FOR INPUT AS #1
1970
INPUT#1,DD$,RN$,TR,SAMPLE$,MS(1),MS(2),CO,PA,TA,PS,PP,PV,VC,TC,TL,TP,N,CMM$,IN$,NF,
NP
1980 FOR L = 1 TO N
1990 INPUT#1,A1(L),A2(L),A3(L),A4(L),A5(L),A6(L),TS(L)
2000 NEXT L
2010 FOR M = 1 TO NF
2020 INPUT#1,TF(M),RL(M)
2030 NEXT M
2040 FOR J=1 TO NP
2050 INPUT #1,TP(J),RP(J)
2060 NEXT J
2070 CLOSE#1
2080 PRINT:INPUT "WOULD YOU LIKE TO APPLY ANY CORRECTIONS TO THE INPUT DATA ?
(Y/N)";ID$
2090 IF ID$="N" GOTO 3020 :REM ==BEGIN CALCS.==
2100 CLS:PRINT "THIS STAGE ALLOWS CORRECTIONS TO BE APPLIED TO THE INPUT DATA. SUCH
CORRECTIONS SHOULD ONLY BE APPLIED ONCE INPUT DATA HAS BEEN EXAMINED ";
2110 PRINT "USING THE 'FILE IMPORT' FACILITY OF LOTUS-2, AND ONCE THE USER IS ";
2120 PRINT "FULLY FAMILIAR WITH THE VARIABLE NAMES ASSOCIATED WITH THE INPUT DATA ";
2130 PRINT "(SEE PROGRAM LISTING). THE CORRECTION PROCEDURE INVOLVES INTERRUPTING
";
2140 PRINT "THE PROGRAM AT THIS STAGE AND DIRECTLY ASSIGNING CORRECT VALUES TO
VARIABLES ";
2150 PRINT "FROM THE KEYBOARD, eg. A1(1)=34562. ";
2160 PRINT :PRINT "ONCE ALL CORRECTIONS HAVE BEEN APPLIED, ONE SHOULD ENTER THE
COMMAND ";
2170 PRINT "'CONT', WHICH WILL CAUSE THE PROGRAM TO RESUME OPERATION AT THE POINT ";
2180 PRINT "OF INTERRUPTION."
2190 PRINT :INPUT "ENTER 'Y' TO APPLY CORRECTIONS.";CR$
```

(C.5)

```
2200 IF CR$="Y" GOTO 2220
2210 GOTO 2190
2220 STOP
2230 GOTO 2860
2240 CLS
2250 PRINT : INPUT "DATE OF RUN / DD/MM/YR : ? ";DD$
2260 PRINT : INPUT "RUN NUMBER : ? ";RN$
2270 PRINT : INPUT "REACTION TEMPERATURE /deg. C = ? ";TR
2280 PRINT : INPUT "SAMPLE DESCRIPTION : ";SAMPLE$
2290 PRINT : PRINT "ENTER THE COMPOSITION OF THE CHAR SAMPLE : "
2300 PRINT : INPUT "% FC (CH-1: 70.94 -2: 67.76 -3: 70.48 -4:      ) = ? ";FC
2310 PRINT : INPUT "% ASH (CH-1: 29.06 -2: 32.24 -3: 29.52 -4:      ) = ? ";AS
2320 PRINT : INPUT "MASS OF SAMPLE LOADED INTO REACTOR /g = ? ";MS(1)
2330 PRINT : INPUT "MASS OF RESIDUE /g = ? ";MS(2)
2340 PRINT : INPUT "BAROMETRIC LEVEL /mm Hg = ? ";PA
2350 PRINT : INPUT "BAROMETRIC TEMPERATURE /deg. C = ? ";TA
2360 PRINT : INPUT "STEAM PRESSURE /KPaG = ? ";PS
2370 PRINT : INPUT "PRODUCT PRESSURE /KPaG = ? ";PP
2380 PRINT : INPUT "VESSEL PRESSURE /KPaG = ? ";PV
2390 PRINT :PRINT "STEADY STEAM FLOWRATE :": PRINT
2400 PRINT : INPUT "VOLUME OF CONDENSATE COLLECTED /ml. =? ";VC
2410 PRINT : INPUT "DURATION OF COLLECTION OF CONDENSATE / HR.MMSS = ? ";TC
2420 PRINT : INPUT "LAB. TEMP. DURING RUN /deg C =? ";TL
2430 PRINT : INPUT "RUN TIME OF FIRST DETECTION OF PRODUCTS / HR.MMSS =? ";TP
2440 PRINT : INPUT "NUMBER OF GAS SAMPLES COLLECTED = ? ";N
2450 PRINT :INPUT "IMPORTANT COMMENT INVITED : ? ";CMM$
2460 CLS : PRINT "ENTER THE AREAS FROM THE RELEVANT CHROMATOGRAM FOR EACH
COMPONENT"
2470 PRINT : PRINT "OF EACH SAMPLE AS PROMPTED, BEGINNING WITH THE FIRST SAMPLE"
2480 PRINT : PRINT "AND PROCEEDING SEQUENTIALLY TO THE LAST."
2490 PRINT : PRINT : PRINT "ALSO ENTER THE RUN TIME AT WHICH EACH SAMPLE WAS TAKEN
/ (HR.MMSS)"
2500 PRINT :PRINT :PRINT "CAUTION : ERRORS IN INPUT ARE NOT ABLE TO BE CORRECTED!"
2510 PRINT : PRINT : PRINT : INPUT "ENTER THE INTEGRATOR RUN # OF SAMPLE 1 :? ";IN$
2520 FOR L = 1 TO N
2530 PRINT : PRINT "SAMPLE NO.: ";L
2540 PRINT " _____ "
2550 PRINT : INPUT "H2 AREA = ?";A1(L)
```

(C.6)

```
2560 PRINT : INPUT "O2 AREA = ?";A2(L)
2570 PRINT : INPUT "N2 AREA = ?";A3(L)
2580 PRINT : INPUT "CO AREA = ?";A4(L)
2590 PRINT : INPUT "CH4 AREA = ?";A5(L)
2600 PRINT : INPUT "CO2 AREA = ?";A6(L)
2610 PRINT : INPUT "RUN TIME OF SAMPLE /HR.MMSS ?";TS(L)
2620 NEXT L
2630 CLS : PRINT "GENERAL FLOWRATE INPUT DATA :"
2640 PRINT : PRINT "ENTER THE RUN TIMES (IN HR.MMSS), AND THE CORRESPONDING
ROTAMETER LEVELS"
2650 PRINT : PRINT "WHEN PROMPTED."
2660 PRINT : PRINT : INPUT "FIRSTLY, ENTER THE NUMBER OF GENERAL FLOWRATE DATA
POINTS : ";NF
2670 FOR I = 1 TO NF
2680 PRINT : PRINT "GENERAL FLOWRATE NO. : ";I
2690 PRINT " _____"
2700 PRINT : INPUT "RUN TIME / HR.MMSS = ? ";TF(I)
2710 PRINT : INPUT "ROTAMETER LEVEL = ? ";RL(I)
2720 NEXT I
2730 PRINT :PRINT :PRINT "NOW ENTER THE STEADY PRODUCT FLOWRATE DATA :"
2740 PRINT :INPUT "ENTER THE NUMBER OF STEADY PRODUCT FLOWRATE DATA POINTS :";NP
2750 FOR J=1 TO NP
2760 PRINT :PRINT "STEADY PRODUCT FLOWRATE NO. : ";J
2770 PRINT " _____"
2780 PRINT :INPUT "RUN TIME / HR.MMSS = ? ";TP(J)
2790 PRINT :INPUT "ROTAMETER LEVEL = ? ";RP(J)
2800 NEXT J
2810 C0 = FC / 100 * MS(1)
2820 C0 = C0 / 12.01
2830 REM _____
2840 REM ==FILE 9 : INPUTRN$.PRN==
2850 REM _____
2860 F9$ = I$ + RN$+PR$
2870 OPEN F9$ FOR OUTPUT AS #1
2880
WRITE#1,DD$,RN$,TR,SAMPLE$,MS(1),MS(2),C0,PA,TA,PS,PP,PV,VC,TC,TL,TP,N,CMM$,IN$,NF,N
P
2890 FOR L = 1 TO N
```

(C.7)

```
2900 WRITE#1,A1(L),A2(L),A3(L),A4(L),A5(L),A6(L),TS(L)
2910 NEXT L
2920 FOR M = 1 TO NF
2930 WRITE#1,TF(M),RL(M)
2940 NEXT M
2950 FOR J=1 TO NP
2960 WRITE#1,TP(J),RP(J)
2970 NEXT J
2980 CLOSE#1
2990 REM -----
3000 REM ==CALCULATIONS==
3010 REM -----
3020 REM ==CONVERT TIMES FROM HR.MMSS TO MINUTES==
3030 REM ==TP; TP= TIME OF DETECTION OF FIRST PRODUCTS ==
3040 CLS : PRINT "PLEASE WAIT FOR ABOUT 2 MINUTES..."
3050 T = 1
3060 T1(1) = TP
3070 GOSUB 7310
3080 TP = T5(1)
3090 T1(1) = TC : REM == CONDENSATE TIME ==
3100 GOSUB 7310
3110 TC = T5(1)
3120 REM ==TS(J);          SAMPLE TIMES ==
3130 T = N
3140 FOR J = 1 TO N
3150 T1(J) = TS(J)
3160 NEXT J
3170 GOSUB 7310
3180 FOR J = 1 TO N
3190 TS(J) = T5(J)
3200 NEXT J
3210 REM ==TF(J);          GENERAL PRODUCT FLOWRATE TIMES ==
3220 T = NF
3230 FOR J = 1 TO NF
3240 T1(J) = TF(J)
3250 NEXT J
3260 GOSUB 7310
3270 FOR J = 1 TO NF
```

(C.8)

```
3280 TF(J) = T5(J)
3290 NEXT J
3300 REM ==TP(J);          STEADY PRODUCT FLOWRATE TIMES ==
3310 T=NP
3320 FOR J=1 TO NP
3330 T1(J)=TP(J)
3340 NEXT J
3350 GOSUB 7310
3360 FOR J=1 TO NP
3370 TP(J)=T5(J)
3380 NEXT J
3390 REM ==CONVERT RUN TIMES (MINUTES) TO GASIFICATION TIMES (MINS.)==
3400 FOR I = 1 TO N
3410 TS(I) = TS(I) - TP
3420 NEXT I
3430 FOR J = 1 TO NF
3440 TF(J) = TF(J) - TP
3450 NEXT J
3460 FOR J=1 TO NP
3470 TP(J)=TP(J)-TP
3480 NEXT J
3490 REM ==CALC STEAM FLOWRATE==
3500 FS = VC / TC
3510 REM ==CALCULATE COMPOSITIONS OF EACH SAMPLE USING CALIBRATIONS; UNITS : AMOUNT
OF COMPONENT / GMOLS. = MCOMP.*(AREA FROM CHROMATOGRAM)+ CCOMP.==
3520 REM ==N(I(J))=AMOUNT OF ITH COMPONENT IN JTH SAMPLE.==
3530 FOR I = 1 TO N
3540 N1(I) = M(1) * A1(I) + C(1)
3550 N2(I) = M(2) * A2(I) + C(2)
3560 N3(I) = M(3) * A3(I) + C(3)
3570 N4(I) = M(4) * A4(I) + C(4)
3580 N5(I) = M(5) * A5(I) + C(5)
3590 N6(I) = M(6) * A6(I) + C(6)
3600 NT(I) = N1(I) + N2(I) + N3(I) + N4(I) + N5(I) + N6(I)
3610 NT(I) = NT(I) / 100
3620 C1(I) = N1(I) / NT(I)
3630 C2(I) = N2(I) / NT(I)
3640 C3(I) = N3(I) / NT(I)          : REM == MOL % ==
```

(C.9)

```
3650 C4(I) = N4(I) / NT(I)
3660 C5(I) = N5(I) / NT(I)
3670 C6(I) = N6(I) / NT(I)
3680 NEXT I
3690 REM ==INTERPOLATE ON COMPOSITION DATA==
3700 REM ==ADDRESS SPLINE FIT WITH X,Y COMPOSITION DATA==
3710 REM ==HYDROGEN==
3720 P = N
3730 FOR R = 1 TO N
3740 X(R) = TS(R)
3750 Y(R) = C1(R)
3760 NEXT R
3770 GOSUB 7410: REM ==CALCULATES PARABOLIC COEFFICIENTS==
3780 GOSUB 4570 :REM ==COMPUTE GAS COMPOSITION (MOL%) AT GENERAL FLOWRATE
TIMES.==
3790 FOR S = 1 TO NF
3800 M1(S) = V(S)
3810 NEXT S
3820 GOSUB 4620
3830 FOR T=1 TO NP
3840 P1(T)=V(T)
3850 NEXT T
3860 REM ==OXYGEN==
3870 FOR R = 1 TO N
3880 X(R) = TS(R)
3890 Y(R) = C2(R)
3900 NEXT R
3910 GOSUB 7410
3920 GOSUB 4570
3930 FOR S = 1 TO NF
3940 M2(S) = V(S)
3950 NEXT S
3960 GOSUB 4620
3970 FOR T=1 TO NP
3980 P2(T)=V(T)
3990 NEXT T
4000 REM ==NITROGEN==
4010 FOR R = 1 TO N
```

(C.10)

```
4020 X(R) = TS(R)
4030 Y(R) = C3(R)
4040 NEXT R
4050 GOSUB 7410
4060 GOSUB 4570
4070 FOR S = 1 TO NF
4080 M3(S) = V(S)
4090 NEXT S
4100 GOSUB 4620
4110 FOR T=1 TO NP
4120 P3(T)=V(T)
4130 NEXT T
4140 REM ==CARBON MONOXIDE==
4150 FOR R = 1 TO N
4160 X(R) = TS(R)
4170 Y(R) = C4(R)
4180 NEXT R
4190 GOSUB 7410
4200 GOSUB 4570
4210 FOR S = 1 TO NF
4220 M4(S) = V(S)
4230 NEXT S
4240 GOSUB 4620
4250 FOR T=1 TO NP
4260 P4(T)=V(T)
4270 NEXT T
4280 REM ==METHANE==
4290 FOR R = 1 TO N
4300 X(R) = TS(R)
4310 Y(R) = C5(R)
4320 NEXT R
4330 GOSUB 7410
4340 GOSUB 4570
4350 FOR S = 1 TO NF
4360 M5(S) = V(S)
4370 NEXT S
4380 GOSUB 4620
4390 FOR T=1 TO NP
```

(C.11)

```
4400 P5(T)=V(T)
4410 NEXT T
4420 REM ==CARBON DIOXIDE==
4430 FOR R = 1 TO N
4440 X(R) = TS(R)
4450 Y(R) = C6(R)
4460 NEXT R
4470 GOSUB 7410
4480 GOSUB 4570
4490 FOR S = 1 TO NF
4500 M6(S) = V(S)
4510 NEXT S
4520 GOSUB 4620
4530 FOR T=1 TO NP
4540 P6(T)=V(T)
4550 NEXT T
4560 GOTO 4670
4570 FOR S = 1 TO NF
4580 J(S) = TF(S)
4590 GOSUB 7540: REM ==CALCULATES Y(X)==
4600 NEXT S
4610 RETURN
4620 FOR S=1 TO NP
4630 J(S)=TP(S)
4640 GOSUB 7540:REM ==COMPUTES Y(X)==
4650 NEXT S
4660 RETURN
4670 FOR I=1 TO NP :REM ==COMPUTE CONCENTRATION OF GASIFICATION PRODUCTS IN PRODUCT
STREAM AT STEADY FLOWRATE TIMES.==
4680 ST(I)=(P1(I)+P4(I)+P5(I)+P6(I))/100
4690 S1(I)=P1(I)/ST(I)
4700 S4(I)=P4(I)/ST(I)
4710 S5(I)=P5(I)/ST(I)
4720 S6(I)=P6(I)/ST(I)
4730 REM == COMPUTE H2/CO RATIO IN PRODUCT GAS AT STEADY STATE.==
4740 HC(I)=S1(I)/S4(I)
4750 NEXT I
4760 REM ==ADDRESS SPLINE FIT WITH X,Y FLOWRATE DATA==
```


(C.12)

```
4770 REM ==X=ROTAM. LEVEL; Y=AIR FLOWRATE /SCCPM; P=NO. OF DATA POINTS==
4780 P = 94
4790 FOR R = 1 TO P
4800 X(R) = LC(R)
4810 Y(R) = FC(R)
4820 NEXT R
4830 GOSUB 7410
4840 FOR S = 1 TO NF :REM == AIR FLOWRATES AT MEASURED GENERAL FLOW LEVELS==
4850 J(S) = RL(S)
4860 GOSUB 7540
4870 NEXT S
4880 FOR S = 1 TO NF
4890 RF(S) = V(S)
4900 NEXT S
4910 FOR S=1 TO NP :REM == COMPUTES AIR FLOWRATES AT STEADY PROD. FLOW LEVELS==
4920 J(S)=RP(S)
4930 GOSUB 7540
4940 NEXT S
4950 FOR S=1 TO NP
4960 PF(S)=V(S)
4970 NEXT S
4980 REM ==ADDRESS SPLINE FIT WITH HG DENSITY DATA FOR ATM PRESS. CALC.==
4990 P = 21
5000 FOR R = 1 TO P
5010 X(R) = TC(R)
5020 Y(R) = DC(R)
5030 NEXT R
5040 GOSUB 7410
5050 S = 1
5060 J(1) = TA
5070 GOSUB 7540
5080 DM = V(1)
5090 REM ==CALC ATM. PRESS./PA==
5100 PA = PA * DM * G
5110 REM ==LAB TEMP/K==
5120 TL = TL + T0
5130 REM ==COMPUTE CONVERSION AT GENERAL FLOW MEAS. LEVELS==
5140 Z = NF
```

(C.13)

```
5150 FOR I = 1 TO NF
5160 FV(I) = RF(I)           : REM == VOL.AIR FLOWRATES AT FLOW TIMES ==
5170 NEXT I
5180 GOSUB 5710
5190 XC(1) = R7(1) * TF(1) / C0
5200 FOR S = 2 TO NF
5210 XC(S) = XC(S - 1) + R7(S) * (TF(S) - TF(S - 1)) / C0
5220 NEXT S
5230 P=NF           :REM ==USE CUBIC SPLINE INTERPOLN TO READ CONVERSION AT STEADY
PRODUCT FLOW POINTS.==
5240 FOR I=1 TO NF
5250 X(I)=TF(I)
5260 Y(I)=XC(I)
5270 NEXT I
5280 GOSUB 7410
5290 FOR S=1 TO NP
5300 J(S)=TP(S)
5310 GOSUB 7540
5320 NEXT S
5330 FOR K=1 TO NP
5340 XP(K)=V(K)
5350 NEXT K
5360 Z=NP :REM ==COMPUTE RATES AT STEADY PRODUCT FLOW TIMES ==
5370 FOR I=1 TO NP
5380 FV(I)=PF(I)
5390 M1(I)=P1(I)
5400 M2(I)=P2(I)
5410 M3(I)=P3(I)
5420 M4(I)=P4(I)
5430 M5(I)=P5(I)
5440 M6(I)=P6(I)
5450 NEXT I
5460 GOSUB 5710
5470 REM ==CONVERT RATES FROM ABS., TO GMOLS.MIN^-1.(GMOL C IN FEED COAL CHAR)^-1==
5480 FOR I = 1 TO NP
5490 R1(I) = R1(I) / C0
5500 R2(I) = R2(I) / C0
5510 R3(I) = R3(I) / C0
```

(C.14)

```
5520 R4(I) = R4(I) / C0
5530 R5(I) = R5(I) / C0
5540 R6(I) = R6(I) / C0
5550 R7(I) = R7(I) / C0
5560 NEXT I
5570 TL = TL - T0
5580 REM == CALC TIME TAKEN TO REACH X=0.5 ==
5590 IF XC(NF)<=.5 GOTO 6040
5600 FOR I=1 TO NF
5610 X(I)=XC(I)
5620 Y(I)=TF(I)
5630 NEXT I
5640 GOSUB 7410
5650 S=1
5660 J(1)=.5
5670 GOSUB 7540
5680 TX=V(1)
5690 GOTO 5950
5700 REM ==CALC AVG MOLECULAR WEIGHTS, MW(S)==
5710 FOR S = 1 TO Z
5720 MW(S) = (M1(S) * M1 + M2(S) * M2 + M3(S) * M3 + M4(S) * M4 + M5(S) * M5 + M6(S)
* M6) / 100
5730 REM == CALC GAS DENSITIES / g.ml-1 ==
5740 DP(S) = (MW(S) * PA) / (GC * TL * 10 ^ 6)
5750 REM == CALC PRODUCT GAS FLOWRATES / ml.min-1 ==
5760 FV(S) = FV(S) * (DA / DP(S)) ^ .5
5770 REM == CALC VOLUMETRIC COMPONENT FLOWS / ml.min-1 ==
5780 V1(S) = M1(S) / 100 * FV(S)
5790 V2(S) = M2(S) / 100 * FV(S)
5800 V3(S) = M3(S) / 100 * FV(S)
5810 V4(S) = M4(S) / 100 * FV(S)
5820 V5(S) = M5(S) / 100 * FV(S)
5830 V6(S) = M6(S) / 100 * FV(S)
5840 REM ==CALC MOLAR COMPONENT FLOWS, RC(S)/GMOL.MIN-1==
5850 R1(S) = (PA * V1(S)) / (GC * TL * 10 ^ 6)
5860 R2(S) = (PA * V2(S)) / (GC * TL * 10 ^ 6)
5870 R3(S) = (PA * V3(S)) / (GC * TL * 10 ^ 6)
5880 R4(S) = (PA * V4(S)) / (GC * TL * 10 ^ 6)
```

(C.15)

```
5890 R5(S) = (PA * V5(S)) / (GC * TL * 10 ^ 6)
5900 R6(S) = (PA * V6(S)) / (GC * TL * 10 ^ 6)
5910 REM ==CALC MOLAR CARBON FLOWRATE/ GMOL C.MIN^-1==
5920 R7(S) = R4(S) + R5(S) + R6(S)
5930 NEXT S
5940 RETURN
5950 REM ==WALKER MODEL.==
5960 UA=.375
5970 UB=.276
5980 UC=-.148
5990 FOR I=1 TO NP
6000 TU(I)=TP(I)/TX
6010 XU(I)=UA*TU(I)+UB*TU(I)^2+UC*TU(I)^3
6020 NEXT I
6030 GOTO 6050
6040 PRINT :PRINT :PRINT "FINAL CHAR CONVERSION LOWER THAN 0.5 ."
6050 REM ==JOHNSON MODEL.==
6060 TR=TR+T0
6070 PR=(PP+PS)/200*.986923+PA/101325!
6080 KT=EXP(9.020099-12910/TR)/((1+EXP(-22.216+24882/TR))*(1/PR))^2)
6090 FOR I=1 TO NP
6100 DX(I)=KT*(1-XP(I))^(2/3)
6110 NEXT I
6120 TR=TR-T0
6130 PRINT : INPUT "WOULD YOU LIKE THE RESULTS TO BE SAVED ON DISC ? (Y/N) ";Q3$
6140 IF Q3$ = "N" THEN 6640
6150 REM -----
6160 REM ==OUTPUT==
6170 REM -----
6180 REM -----
6190 REM ==FILE 6 : REPRTRN$.PRN==
6200 REM -----
6210 F6$ = RP$ + RN$+PR$
6220 OPEN F6$ FOR OUTPUT AS #1
6230 WRITE#1,TITLE$
6240 WRITE#1,RN$,DD$,TR,MS(1),MS(2),PS,PP,PV,FS,TL,N,NF,NP
6250 WRITE#1,CMM$
6260 FOR K = 1 TO NP
```

```

6270 WRITE#1,XP(K),TP(K),R1(K),R2(K),R3(K),R4(K),R5(K),R6(K),R7(K),M1(K),M2(K)
6280 WRITE#1,M3(K),M4(K),M5(K),M6(K),DX(K),TU(K),XU(K),S1(K),S4(K),S5(K)
6290 WRITE#1,S6(K),HC(K)
6300 NEXT K
6310 CLOSE#1
6320 REM -----
6330 REM ==FILE 7 : RATESRN$.PRN==
6340 REM -----
6350 F7$ = R$ + RN$+PR$
6360 OPEN F7$ FOR OUTPUT AS #1
6370 WRITE#1,RN$,TR,N,NP
6380 FOR J = 1 TO NP
6390 WRITE#1,XP(J),DX(J),R1(J),R2(J),R3(J),R4(J),R5(J),R6(J),R7(J)
6400 NEXT J
6410 CLOSE #1
6420 REM -----
6430 REM ==FILE 8 : CMPSNRN$.PRN==
6440 REM -----
6450 F8$ = C$ + RN$+PR$
6460 OPEN F8$ FOR OUTPUT AS #1
6470 WRITE#1,RN$,TR,N,NP
6480 FOR L = 1 TO NP
6490
WRITE#1,XP(L),M1(L),M2(L),M3(L),M4(L),M5(L),M6(L),S1(L),S4(L),S5(L),S6(L),HC(L)
6500 NEXT L
6510 CLOSE #1
6520 REM -----
6530 REM ==FILE U : UNIFNRN$.PRN==
6540 REM -----
6550 U$="UNIFN"
6560 FU$ = U$ + RN$+PR$
6570 OPEN FU$ FOR OUTPUT AS #1
6580 WRITE#1,RN$,DD$,TR,N,NP
6590 FOR I = 1 TO NP
6600 WRITE#1,TU(I),XP(I),XU(I)
6610 NEXT I
6620 CLOSE#1
6630 PRINT : PRINT "ALL DATA HAS BEEN SAVED."

```

(C.17)

```
6640 PRINT : PRINT "WOULD YOU LIKE A PRINTOUT OF THE RESULTS ?"
6650 PRINT : INPUT "ENTER <Y>ES OR <N>O :";Q4$
6660 IF Q4$ = "N" THEN 7240
6670 REM -----
6680 REM ==PRINTOUT OF REPORT==
6690 REM -----
6700 PRINT : PRINT "CHECK THAT THE PRINTER IS READY."
6710 PRINT : INPUT "THEN ENTER 'R' ";Q6$
6720 IF Q6$ = "R" THEN 6740
6730 GOTO 6700
6740 LPRINT CHR$(12)
6750 LPRINT CHR$(14);TITLE$
6760 LPRINT CHR$(14);"-----"
6770 WIDTH "LPT1:",132 : LPRINT CHR$(15)
6780 LPRINT : LPRINT "RESULTS OF RUN NUMBER ";RN$
6790 LPRINT : LPRINT "DATE OF RUN / DD/MM/YR : ";DD$
6800 LPRINT : LPRINT "REACTION TEMPERATURE /deg. C = ";TR
6810 LPRINT : LPRINT "MASS OF SAMPLE LOADED INTO REACTOR /g = ";MS(1)
6820 LPRINT : LPRINT "MASS OF RESIDUE /g = ";MS(2)
6830 LPRINT : LPRINT "STEAM PRESSURE /KPaG = ";PS
6840 LPRINT : LPRINT "PRODUCT PRESSURE /KPaG = ";PP
6850 LPRINT : LPRINT "VESSEL PRESSURE /KPaG = ";PV
6860 LPRINT : LPRINT "STEADY STEAM FLOWRATE / ml/min = ";FS
6870 LPRINT : LPRINT "LAB. TEMP. DURING RUN /deg C = ";TL
6880 LPRINT : LPRINT "IMPORTANT COMMENT : ";CMM$
6890 LPRINT CHR$(12)
6900 LPRINT "RESULTS OF RUN NO. ";RN$
6910 LPRINT : LPRINT "FRACTIONAL"; TAB( 25);"RATES OF DISAPPEARANCE OR APPEARANCE
";
6920 LPRINT "OF SPECIES DURING GASIFICATION / gmol.(gmol original C)^-1.(min)^-1"
6930 LPRINT "CONVERSION";TAB(13);"RUN"; TAB( 25);"TOTAL"; TAB( 40);"H2 :"; TAB(
55);"O2 :"; TAB( 70);"N2 :"; TAB(85);"CO :"; TAB(100);"CH4 :"; TAB(115);"CO2 :
6940 LPRINT "OF SAMPLE";TAB(13);"TIME/ min"; TAB( 25);"CARBON"
6950 FOR I = 1 TO NP
6960 LPRINT : LPRINT XP(I);TAB(15);TP(I); TAB(25);R7(I); TAB(40);R1(I);
TAB(55);R2(I); TAB(70);R3(I); TAB(85);R4(I); TAB(100);R5(I); TAB(115);R6(I)
6970 NEXT I
6980 LPRINT CHR$(12)
```

(C.18)

```
6990 LPRINT "RESULTS OF RUN NO. ";RN$
7000 LPRINT : LPRINT : LPRINT "FRACTIONAL"; TAB( 45);"COMPOSITION OF PRODUCT GAS
STREAM / mol %"
7010 LPRINT "CONVERSION"; TAB( 40);"H2 :"; TAB( 55);"O2 :"; TAB( 70);"N2 :"; TAB(
85);"CO :"; TAB(100);"CH4 :"; TAB(115);"CO2 :"
7020 LPRINT "OF SAMPLE"
7030 FOR I = 1 TO NP
7040 LPRINT : LPRINT XP(I); TAB(40);M1(I); TAB(55);M2(I); TAB(70);M3(I);
TAB(85);M4(I); TAB(100);M5(I); TAB(115);M6(I)
7050 NEXT I
7060 LPRINT CHR$(12)
7070 LPRINT "RESULTS OF RUN NO. ";RN$
7080 LPRINT : LPRINT : LPRINT "FRACTIONAL"; TAB( 40);"COMPOSITION OF PRODUCTS OF
GASIFICATION / mol %"
7090 LPRINT "CONVERSION"; TAB( 35);"H2 :"; TAB( 50);"CO :"; TAB( 65);"CH4 :"; TAB(
80);"CO2 :";TAB(95);"H2/CO RATIO"
7100 LPRINT "OF SAMPLE"
7110 FOR I = 1 TO NP
7120 LPRINT : LPRINT XP(I); TAB(35);S1(I); TAB(50);S4(I); TAB(65);S5(I);
TAB(80);S6(I);TAB(95);HC(I)
7130 NEXT I
7140 LPRINT CHR$(12)
7150 LPRINT "RESULTS OF RUN NO. ";RN$
7160 LPRINT : LPRINT : LPRINT "RUN
TIME";TAB(20);"FRACTIONAL";TAB(40);"DIMENSIONLESS";TAB(60);"CONVERSION";TAB(80);"CAR
BON GASIFICATION"
7170 LPRINT "
(t)";TAB(20);"CONVERSION";TAB(40);"TIME";TAB(60);"(AFTER";TAB(80);"RATE"
7180 LPRINT " / min";TAB(24);"(X)";TAB(40);"t/t(X=0.5)";TAB(60);"
WALKER)";TAB(80);"(JOHNSON)"
7190 FOR I=1 TO NP
7200 LPRINT :LPRINT TP(I);TAB(20);XP(I);TAB(40);TU(I);TAB(60);XU(I);TAB(80);DX(I)
7210 NEXT I
7220 LPRINT CHR$(12):LPRINT CHR$(12)
7230 LPRINT CHR$(18):LPRINT CHR$(13)
7240 PRINT : INPUT "ANOTHER RUN OF 'RATES'?(Y/N)";Q5$
7250 IF Q5$ = "Y" THEN 1180
7260 GOTO 7990
```

```

7270 REM -----
7280 REM ==ROUTINE TIME==
7290 REM -----
7300 REM   : CONVERT TIME TO BE EXPRESSED IN MINUTES; INPUT TIME AS T1(I)=?HR.MMSS.
7310 FOR I = 1 TO T
7320 T2(I) = T1(I) - INT (T1(I))
7330 T3(I) = T2(I) * 100
7340 T4(I) = T3(I) - INT (T3(I))
7350 T5(I) = INT (T1(I)) * 60 + T4(I) * 100 / 60 + INT (T3(I))
7360 NEXT I
7370 RETURN
7380 REM -----
7390 REM ==CUBIC SPLINE INTERPOLATION ROUTINE==
7400 REM -----
7410 REM
7420 REM -----
7430 REM ==INPUT DATA : P=NO. OF DATA POINTS; X(R),Y(R)= COORDINATES OF DATA.==
7440 REM -----
7450 REM ==COMPUTE DERIVATIVE==
7460 REM -----
7470 GOSUB 7630
7480 REM -----
7490 REM ==COMPUTE CUBIC SPLINE COEFFICIENTS==
7500 REM -----
7510 GOSUB 7850
7520 RETURN : REM ==TO MAIN PROGRAM==
7530 REM ==FIND PROPER INTERVAL==
7540 FOR K = 2 TO P
7550 IF J(S) < X(K) THEN 7570
7560 NEXT K
7570 K = K - 1
7580 GOSUB 7950
7590 RETURN
7600 REM -----
7610 REM ==ROUTINE : DERIVATIVE==
7620 REM -----
7630 J = 2
7640 GOSUB 7760

```


(C.20)

```
7650 D(1) = 2 * A * X(1) + B
7660 D(2) = 2 * A * X(2) + B
7670 FOR J = 3 TO P - 1
7680 GOSUB 7760
7690 D(J) = 2 * A * X(J) + B
7700 NEXT J
7710 D(P) = 2 * A * X(P) + B
7720 RETURN
7730 REM -----
7740 REM ==ROUTINE : COEFFICIENTS OF PARABOLA==
7750 REM -----
7760 A = (Y(J - 1) - Y(J)) / (X(J - 1) - X(J))
7770 A = A - (Y(J) - Y(J + 1)) / (X(J) - X(J + 1))
7780 A = A / (X(J - 1) - X(J + 1))
7790 B = (Y(J - 1) - Y(J)) / (X(J - 1) - X(J))
7800 B = B - A * (X(J - 1) + X(J))
7810 RETURN
7820 REM -----
7830 REM ==ROUTINE : CUBIC SPLINE COEFFICIENTS==
7840 REM -----
7850 FOR J = 1 TO P - 1
7860 F(J) = D(J) * (X(J + 1) - X(J))
7870 G(J) = 3 * Y(J + 1) - D(J + 1) * (X(J + 1) - X(J))
7880 G(J) = G(J) - 3 * Y(J) - 2 * F(J)
7890 H(J) = Y(J + 1) - Y(J) - F(J) - G(J)
7900 NEXT J
7910 RETURN
7920 REM -----
7930 REM ==EVALUATE POLYNOMIAL==
7940 REM -----
7950 W(S) = (J(S) - X(K)) / (X(K + 1) - X(K))
7960 V(S) = Y(K) + F(K) * W(S) + G(K) * W(S) * W(S) + H(K) * W(S) * W(S) * W(S)
7970 PRINT ". ";
7980 RETURN
7990 END
```

(D.1)

APPENDIX D.

THEMODYNAMIC ANALYSIS OF PRODUCT GAS COMPOSITIONS.

If one assumes that the only gaseous species present in a steam coal-char gasification process are H_2O , H_2 , CO , CO_2 and CH_4 , then the composition of the resultant gas phase will be dictated by the following set of three independent reactions :

(a) THE BOUDOUARD REACTION



(b) THE WATER-GAS SHIFT REACTION



(c) THE METHANE FORMATION REACTION



Note that the steam-carbon gasification reaction, $C + H_2O = CO + H_2$ is derived by combining equations [D.1] and [D.2].

(D.2)

The thermodynamic characteristics of equations [D.1] to [D.3] are reported in Table D.1, below :

Reaction	ΔH_{298}° (J/gmol)	ΔG_{298}° (J/gmol)	Expression for eqm constant
[D.1]	+172 576	+120 144	$K_{PB} = \frac{y_{CO}^2 P_t}{y_{CO_2}}$
[D.2]	-41 186	-28 646	$K_{PW} = \frac{y_{CO_2} y_{H_2}}{y_{CO} y_{H_2O}}$
[D.3]	-74 898	-50 828	$K_{PM} = \frac{y_{CH_4}}{y_{H_2}^2 P_t}$

Table D.1 Thermodynamic characteristics of gasification reactions.

The rate of change of the equilibrium constant of a reaction with respect to temperature is dictated by the Van't Hoff equation.

Thus,

$$\frac{d \ln K}{dT} = \frac{\Delta H_T^{\circ}}{RT^2}$$
$$\Rightarrow \ln K = \frac{1}{R} \int_0^T \frac{\Delta H_T^{\circ}}{T^2} dT + I \quad [D.4]$$

The term 'I' in equation [D.4] is a constant of integration.

(D.3)

The effect of temperature on the standard heat of a reaction may be expressed as follows (Smith and Van Ness, 1975),

$$\Delta H_T^{\circ} = \Delta H_0 + \int_0^T \Delta C_P^{\circ} dT \quad [D.5]$$

Here,
$$\Delta C_P^{\circ} = \sum_{\text{Products}} n C_P^{\circ} - \sum_{\text{Reactants}} n C_P^{\circ}$$

If the heat capacities of the various gaseous species in a gasifier are expressed as functions of temperature by equations of the form

$$C_P^{\circ} = a + bT + cT^2 + dT^3 + e/T^2 \quad [D.6]$$

(in which a, b, c, d and e are constants specific to each gas species, as shown in Table D.2 below), then,

$$\Delta C_P^{\circ} = \Delta a + \Delta bT + \Delta cT^2 + \Delta dT^3 + \Delta e/T^2 \quad [D.7]$$

wherein
$$\Delta a = \sum_{\text{Products}} n a - \sum_{\text{Reactants}} n a$$

with similar definitions for Δb , Δc , Δd and Δe .

Substance	a	b x 10 ²	c x 10 ⁵	d x 10 ⁹	e
O ₂	8.27	0.0258	0.0	0.0	-187 700
H ₂ O	7.700	0.04594	0.2521	-0.8587	0.0
H ₂	6.952	-0.04576	0.09563	-0.2079	0.0
CH ₄	3.381	1.8044	-0.43	0.0	0.0
CO	6.726	0.04001	0.1283	-0.5307	0.0
CO ₂	4.316	1.4285	-0.8362	1.784	0.0

Table D.2 Coefficients for correlation of heat capacity data according to eqn [D.6]; units of C_p : cal/(gmol.K).

(D.4)

The substitution of equation [D.7] into equation [D.5] and the subsequent integration of equation [D.5] yields :

$$\Delta H_T^{\circ} = \Delta H_0 + \Delta aT + \frac{\Delta b}{2} T^2 + \frac{\Delta c}{3} T^3 + \frac{\Delta d}{4} T^4 - \frac{\Delta e}{T} \quad [D.8]$$

The term ΔH_0 in equation [D.8] is also a constant of integration which may be calculated from a knowledge of ΔH° at $T = 298K$.

Equation [D.4] may be integrated with respect to T after the substitution of equation [D.8] to yield the following result :

$$\ln K = -\frac{\Delta H_0}{RT} + \frac{\Delta a}{R} \ln T + \frac{\Delta b}{2R} T + \frac{\Delta c}{6R} T^2 + \frac{\Delta d}{12R} T^3 + \frac{\Delta e}{2RT^2} + I \quad [D.9]$$

The law of mass action dictates that

$$\Delta G^{\circ} = -RT \ln K_P$$

or
$$\ln K_P = -\frac{\Delta G^{\circ}}{RT} \quad [D.10]$$

With a knowledge of ΔG° at $T = 298K$, equation [D.10] may be substituted into equation [D.9] which may then be solved for the integration constant "I". The intermediate results in the calculation of ΔH_0 and I for each reaction are tabulated below :

Reaction	$\int_0^T \Delta C_P dT$	ΔH_0	$\int_0^T \frac{\Delta H_T}{RT^2} dT$	I
[D.1]	910.11	40 309	-50.31	1.87
[D.2]	-458.35	-9 379	7.67	3.88
[D.3]	-3 654.18	-14 235	-12.30	32.79

Table D.3 Intermediate results in the calculation of ΔH_0 and I.

Equations [D.8] and [D.9] may be employed to calculate the values of the equilibrium constants for each reaction at any particular temperature. The equilibrium constants for each of the reactions considered at the reaction temperatures employed in this study are tabulated below :

Reaction	Temperature / °C				
	800	840	850	880	920
[D.1]	9.4780	19.0385	22.49	36.40	66.55
[D.2]	0.7874	0.6777	0.6539	0.5899	0.5187
[D.3]	0.0489	0.0340	0.0312	0.0242	0.0176

Table D.4 Equilibrium constants of gasification reactions.

The computation of the equilibrium compositions of the gas phase during steam-char gasification under the various conditions of the experimental program of this study was performed by using a trial and error approach on a 'Lotus-123' spreadsheet. This technique involved the adjustment of the mole fractions of the various components of the gas phase until the following criteria were satisfied :

- Chemical equilibrium of reactions [D.1], [D.2] and [D.3], according to the relationships shown in Table D.1 ;

- Specification of the reactant gas composition as pure steam by means of elemental material balances for H_2 and O_2 as follows :

$$H_2 : 4 n_{CH_4} + 2 n_{H_2O} + 2 n_{H_2} = 2$$

$$O_2 : n_{H_2O} + n_{CO} + 2 n_{CO_2} = 1 ,$$

in which n_i represents the number of gmols of species i present in the gas phase;

- The sum of the mole fractions of the components of the gas phase equals one.

The equilibrium compositions of the gas phase during steam-char gasification under the conditions of this study are tabulated below :

Temp./ °C	Equilibrium composition of gas phase / mol frac.				
	y_{CO}	y_{CO_2}	y_{H_2}	y_{H_2O}	y_{CH_4}
800	0.4285	0.0345	0.4615	0.0472	0.0185
840	0.4666	0.0204	0.4805	0.0309	0.0140
850	0.4737	0.0178	0.4828	0.0277	0.0129
880	0.4892	0.0117	0.4935	0.0200	0.0105
920	0.5014	0.0067	0.4972	0.0129	0.0078

Table D.5 Equilibrium compositions at $P = 1.78$ Bar abs.

(D.7)

Temp./ °C	Equilibrium composition of gas phase / mol frac.				
	y_{CO}	y_{CO_2}	y_{H_2}	$y_{\text{H}_2\text{O}}$	y_{CH_4}
800	0.4068	0.0551	0.4521	0.0779	0.0316
840	0.4500	0.0336	0.4682	0.0516	0.0236
850	0.4535	0.0289	0.4699	0.0458	0.0218
880	0.4764	0.0197	0.4798	0.0336	0.0176
920	0.4931	0.0115	0.4879	0.0220	0.0133

Table D.6 Equilibrium compositions at P = 3.16 Bar abs.

Temp./ °C	Equilibrium composition of gas phase / mol frac.				
	y_{CO}	y_{CO_2}	y_{H_2}	$y_{\text{H}_2\text{O}}$	y_{CH_4}
800	0.3662	0.0676	0.4196	0.0984	0.0412
840	0.4150	0.0432	0.4412	0.0678	0.0316
850	0.4250	0.0384	0.4458	0.0616	0.0296
880	0.4485	0.0264	0.4563	0.0456	0.0241
920	0.4802	0.0166	0.4739	0.0315	0.0189

Table D.7 Equilibrium compositions at P = 4.78 Bar abs.

APPENDIX E.

THE DERIVATION OF THE MATERIAL AND ENERGY BALANCE EQUATIONS FOR THE SIMULATION MODEL OF THE JUDD CIRCULATING FLUIDISED BED COAL GASIFIER.

The nature of this model is one-dimensional in that species concentrations and reactor temperatures are assumed to vary in the axial direction only. This type of model is frequently used in preliminary design calculations because it provides a good approximation to the real situation and can be used to investigate the effect of changes in design parameters and operating conditions on product conditions (Hill,1977). The division of the reactor volume into separate axial zones in the initial development of this reactor model is consistent with the one-dimensional model concept. In this model, energy transfer from the reactor in the radial direction is therefore considered to be localised to a thin boundary layer adjacent to the wall, and is accounted for by an effective radial heat transfer coefficient which is based on the difference in temperature between the inventory of the reactor and the wall.

E.1 MATERIAL BALANCE FOR ZONE 1, THE PRINCIPAL STEAM-CHAR GASIFICATION ZONE.

Carbon shall be regarded as the key reactant for the purpose of

(E.2)

developing material balances in the reactor. This convention is consistent with the expression of the steam-char gasification reaction kinetics in terms of the amount of carbon which reacts.

Consider an element of the volume of the annulus, as is shown in Figure 14, below :

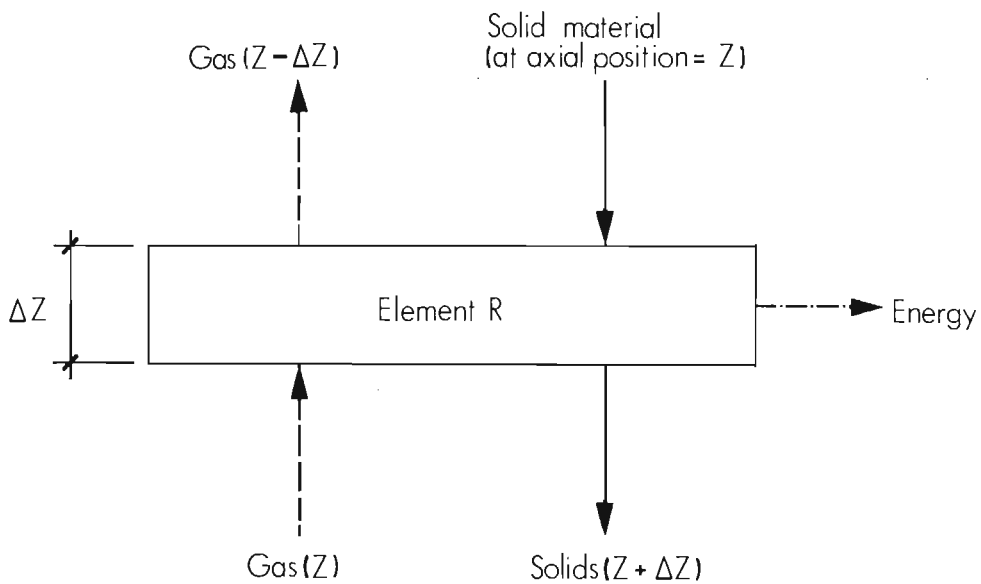


FIGURE 14 Directions of flow of material and energy through a differential element of the annulus region

(E.3)

Note that in Figure 14, z is the axial co-ordinate of the reactor and the independent variable in the equations which follow. z is defined as being positive in the downward direction in the annulus, which is consistent with the level of conversion of the char increasing in this direction.

A steady state carbon material balance for a volume element in zone 1 during a time period of Δt is such that :

$$\text{Input} = \text{Output} + \text{Disappearance by reaction} \quad [\text{E.1}]$$

Here,

$$\text{Input} = \left[\frac{\pi}{4} (D^2 - d^2) u_{s,a} c_{C,s} \right]_z \Delta t \quad [\text{E.2}]$$

$$\text{Output} = \left[\frac{\pi}{4} (D^2 - d^2) u_{s,a} c_{C,s} \right]_{z + \Delta z} \Delta t \quad [\text{E.3}]$$

$$\text{and Disappearance} = \frac{\pi}{4} (D^2 - d^2) \Delta z \Delta t (-r_{l,v}) \quad [\text{E.4}]$$

where :

D = outer diameter of the annular region ; m

d = diameter of draft tube ; m

$u_{s,a}$ = average axial velocity of solids in the zone 1 ; m/min

$c_{C,s}$ = concentration of carbon in the solid phase ; gmol/m³(bed)

$-r_{l,v}$ = rate of disappearance of carbon in char by char-steam gasification, (a positive quantity) ; gmol/(m³(bed).min)

$$(E.4)$$

It is to be noted that $c_{C,s}$ and $-r_{l,v}$ are global properties in that they are expressed in terms of the total annulus volume. On combining equations [E.2], [E.3] and [E.4] and dividing the result by $\frac{\pi}{4} (D^2 - d^2) \Delta t$, one obtains :

$$(u_{s,a} c_{C,s})_z = (u_{s,a} c_{C,s})_{z + \Delta z} + \Delta z (-r_{l,v})$$

so that

$$\frac{(u_{s,a} c_{C,s})_{z + \Delta z} - (u_{s,a} c_{C,s})_z}{\Delta z} = r_{l,v} \quad [E.5]$$

Note: $r_{l,v}$ is intrinsically negative.

The left hand side of equation [E.5] represents the first finite difference of $(u_{s,a} c_{C,s})$ with respect to z as $z \rightarrow 0$. Therefore,

$$\frac{d(u_{s,a} c_{C,s})}{dz} = r_{l,v} \quad [E.6]$$

The char content of the solid material in the gasifier is typically in the region of 5% by mass. Hence the change in $c_{C,s}$ across zone 1 is not expected to significantly affect $u_{s,a}$. Therefore one may simplify equation [E.6] as follows :

$$u_{s,a} \frac{d(c_{C,s})}{dz} = r_{l,v} , \text{ or}$$

$$\frac{d(c_{C,s})}{dz} = \frac{r_{l,v}}{u_{s,a}} \quad [E.7]$$

At this stage in the development of the model, one may relate the

(E.5)

expression for the specific rate of steam gasification of Bosjesspruit coal-char, which was derived in chapter 4, to the global rate of steam gasification of carbon in the simulated gasifier. The specific rate of carbon gasification may be written as follows :

$$-r_C = k_1 \exp(-E_1/RT_z) (1 - X_{C_z})$$

Where $k_1 = 183\,707$ gmol carbon gasified / (gmol carbon initially present.min), the frequency factor for the reaction;

$E_1 = 146$ kJ/gmol, the Arrhenius activation energy for the reaction;

$R = 8.314$ J/(gmol.K);

$T_z =$ the local reaction temperature at an axial position of z in the reactor; K

$X_{C_z} =$ the local fractional carbon conversion of char at an axial position of z in the reactor

now
$$X_{C_z} = 1 - c_{C_z} / c_{C_z}^0 \quad [E.8]$$

Where $c_{C_z} =$ the current global fixed carbon concentration at position z in the reactor; gmol/(m³ (bed).min)

$c_{C_z}^0 =$ the initial global fixed carbon concentration at position z in the reactor (ie. before reaction); gmol/(m³ (bed).min)

Therefore,
$$1 - X_{C_z} = c_{C_z} / c_{C_z}^0 \quad [E.9]$$

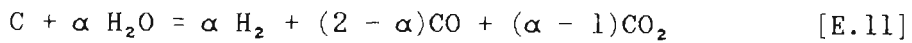
(E.6)

On substituting equation [E.9] into equation and multiplying by $c_{C_z}^0$, since $(-r_{1,V}) = (-r_C * c_{C_z}^0)$, one obtains the following expression for the rate of steam gasification of Bosjesspruit coal char on a global reactor volume basis :

$$-r_{1,V} = k_1 \exp(-E_1/RT_z) c_{C_z} ; \text{ gmol}/(\text{m}^3 (\text{bed}).\text{min}) \quad [\text{E.10}]$$

The general stoichiometry of a system in which steam-char gasification occurs may be represented by the equation which follows. This equation is derived from a linear combination of the carbon-steam gasification reaction and the water-gas shift reaction, and excludes methane formation (which is valid at relatively low pressures).

Thus,



The standard heat of this reaction is therefore given as :

$$\Delta H_{1,T_0}^0 = (2 - \alpha) \Delta H_{f,\text{CO}}^0 + (\alpha - 1) \Delta H_{f,\text{CO}_2}^0 - \alpha \Delta H_{f,\text{H}_2\text{O}}^0$$

Where $\Delta H_{f,i}^0$ = the standard heats of formation of species i at T_0 ; kJ/gmol

and $T_0 = 298.15 \text{ K}$; the reference temperature used for the evaluation of thermodynamic properties.

Now $\Delta H_{f,\text{CO}}^0 = -110.6 \text{ kJ/gmol}$

$$\Delta H_{f,\text{CO}_2}^0 = -393.7 \text{ kJ/gmol}$$

and $\Delta H_{f,\text{H}_2\text{O}}^0 = -286.0 \text{ kJ/gmol}$

(E.7)

So that $\Delta H_{1,T_0}^{\circ} = (2 - \alpha)(-110.6) + (\alpha-1)(-393.7) - \alpha(-286.0)$
or $\Delta H_{1,T_0}^{\circ} = 172.5 + 2.9\alpha$; kJ/gmol [E.12]

Furthermore, the standard heat of reaction [E.11] may be expressed as a function of temperature as follows (Smith and Van Ness, 1975) :

$$\Delta H_{1,T}^{\circ} = \Delta H_{1,T_0}^{\circ} + \int_{T_0}^T \Delta C_P^{\circ} dT \quad [E.13]$$

where $\Delta C_P^{\circ} = \sum_{\text{Products}} C_P^{\circ} - \sum_{\text{Reactants}} C_P^{\circ}$

If one expresses the effect of temperature on C_P° as follows :

$$C_P^{\circ} = a + bT + cT^2 + dT^3$$

then $\Delta C_P^{\circ} = \Delta a + \Delta bT + \Delta cT^2 + \Delta dT^3$ [E.14]

in which $\Delta a = \sum_{\text{All Prods}} a - \sum_{\text{All Reacts}} a$

and Δb , Δc , and Δd are defined in a similar fashion to Δa .

On substituting equation [E.14] into equation [E.13], one obtains

$$\Delta H_{1,T}^{\circ} = \Delta H_{1,T_0}^{\circ} + \int_{T_0}^T (\Delta a + \Delta b T + \Delta c T^2 + \Delta d T^3) dT$$

$\Rightarrow \Delta H_{1,T}^{\circ} = \Delta H_{1,T_0}^{\circ} + \Delta a(T-T_0) + \frac{\Delta b}{2}(T^2-T_0^2) + \frac{\Delta c}{3}(T^3-T_0^3) + \frac{\Delta d}{4}(T^4-T_0^4)$
[E.15]

(E.8)

E.2 ENERGY BALANCE FOR ZONE 1.

Because of the relatively low difference in temperatures which is observed in practise between the draft tube and the annulus zones of the gasifier, it is assumed in this model that the draft tube operates adiabatically. This condition implies that no energy is transferred in the radial direction from the draft tube to the annulus. With reference again to Figure 14, one may write the steady state energy balance for a volume element in zone 1 during a time period Δt as follows :

$$\begin{aligned} \text{Input} &= \text{Output} + \text{Energy demand by steam-char gasification} \\ &+ \text{Losses} \end{aligned} \quad [\text{E.16}]$$

Here,

$$\text{Input} = \left[G_{s,a} A_a \int_{T_0}^T C_{p,s} dT \right]_z \Delta t + \left[G_{g,a} A_a \int_{T_0}^T C_{p,g} dT \right]_z \Delta t \quad [\text{E.17}]$$

Output =

$$\left[G_{s,a} A_a \int_{T_0}^T C_{p,s} dT \right]_{z+\Delta z} \Delta t + \left[G_{g,a} A_a \int_{T_0}^T C_{p,g} dT \right]_{z-\Delta z} \Delta t \quad [\text{E.18}]$$

Energy demand by steam-char gasification =

$$(-r_{1,v}) \Delta H_{1,T}^0 A_a \Delta z \Delta t \quad [\text{E.19}]$$

and,

$$\text{Losses} = U \pi D \Delta z (T - T_{\text{amb}}) \Delta t \quad [\text{E.20}]$$

(E.9)

The following nomenclature has been used above :

$G_{s,a}$ = superficial mass flowrate of solid material in the annulus
; $\text{kg}/(\text{m}^2.\text{s})$

$A_a = \frac{\pi}{4} (D^2 - d^2)$ = cross sectional area of the annulus ; m^2

$C_{P,s}$ = heat capacity of the solid material at the local
temperature of zone 1 ; $\text{J}/(\text{kg.K})$

T = local temperature of the annulus at an axial position of
 z ; K

$T_o = 298.15 \text{ K}$

$G_{g,a}$ = superficial mass flowrate of gas phase in the annulus at
position z ; $\text{kg}/(\text{m}^2.\text{K})$

$C_{P,g}$ = heat capacity of the gas phase at the local temperature of
zone 1 ; $\text{J}/(\text{kg.K})$

$\Delta H_{1,T}^o$ = standard heat of steam-char gasification reaction at
temperature T ; $\text{J}/(\text{gmol})$

U = overall heat transfer coefficient ; $\text{J}/(\text{min.m}^2.\text{K})$

T_{amb} = ambient temperature of environment surrounding the reactor
; K

Because of the relatively insignificant effects of C_p , compared with that of ΔH , on the ultimate temperature profile in the gasifier and because of the relatively small changes in the C_p data in the range of typical operating temperatures of the gasifier, the C_p data employed here are assumed to be constant values, calculated at the average reactor temperature.

(E.10)

One may therefore approximate the integrals which contain C_P terms as follows :

$$\int_{T_0}^T C_{P,i} dT = \bar{C}_{P,i} (T - T_0) \quad [E.21]$$

On combining equations [E.17], [E.18], [E.19],[E.20] and [E.21] according to equation [E.16], and on dividing the result by $\Delta t \Delta z$ and rearranging, one obtains :

$$\begin{aligned} & \frac{[G_{g,a} A_a \bar{C}_{P,g} (T - T_0)]_z - [G_{g,a} A_a \bar{C}_{P,g} (T - T_0)]_{z - \Delta z}}{\Delta z} \\ & = \frac{[G_{s,a} A_a \bar{C}_{P,s} (T - T_0)]_{z + \Delta z} - [G_{s,a} A_a \bar{C}_{P,s} (T - T_0)]_z}{\Delta z} \\ & \quad - r_{l,v} \Delta \bar{H}_1^0 A_a + U \pi D (T - T_{amb}) \end{aligned} \quad [E.22]$$

in which $\Delta \bar{H}_1^0 = \Delta H_{1,T}^0$ evaluated at the arithmetic mean temperature of the reactor.

In the limiting case of an infinitesimally thin volume element, as $\Delta z \rightarrow 0$, the terms in equation [E.22] which contain T_0 cancel, and the two quotients become first finite differences with respect to z . One then obtains :

$$\begin{aligned} \frac{d(G_{g,a} A_a \bar{C}_{P,g} T)}{dz} & = \frac{d(G_{s,a} A_a \bar{C}_{P,s} T)}{dz} - r_{l,v} \Delta \bar{H}_1^0 A_a \\ & \quad + U \pi D (T - T_{amb}) \end{aligned} \quad [E.23]$$

(E.11)

On dividing equation [E.23] by A_a , which equals $\frac{\pi}{4} (D^2 - d^2)$, and by defining $\delta = \frac{D^2 - d^2}{D}$, one obtains :

$$\begin{aligned} \bar{C}_{P,g} \frac{d(G_{g,a} T)}{dz} &= G_{s,a} \bar{C}_{P,s} \frac{dT}{dz} - r_{l,v} \Delta \bar{H}_1^0 \\ &+ 4 U \frac{1}{\delta} (T - T_{amb}) \end{aligned} \quad [E.25]$$

in which it is assumed that $G_{s,a}$ is not significantly affected by the steam-char reaction, because of the large excess of allothermal agent, and therefore remains effectively constant.

The left hand side of equation [E.25] may be expanded as follows, by employing the product rule of differential calculus :

$$\begin{aligned} \bar{C}_{P,g} \frac{d(G_{g,a} T)}{dz} &= \bar{C}_{P,g} (G_{g,a} \frac{dT}{dz} + T \frac{dG_{g,a}}{dz}) \\ &= \bar{C}_{P,g} G_{g,a} \frac{dT}{dz} + \bar{C}_{P,g} T \frac{dG_{g,a}}{dz} \end{aligned} \quad [E.26]$$

Equation [E.25] may then be written as :

$$\begin{aligned} \bar{C}_{P,g} G_{g,a} \left[\frac{dT}{dz} \right] + \bar{C}_{P,g} T \frac{dG_{g,a}}{dz} &= \\ \bar{C}_{P,s} G_{s,a} \left[\frac{dT}{dz} \right] - r_{l,v} \Delta \bar{H}_1^0 + 4 U \frac{1}{\delta} (T - T_{amb}) \end{aligned} \quad [E.27]$$

Factorising equation [E.27] with respect to $\frac{dT}{dz}$ yields :

$$(\bar{C}_{P,s} G_{s,a} - \bar{C}_{P,g} G_{g,a}) \frac{dT}{dz} =$$

(E.12)

$$\bar{C}_{P,g} T \frac{dG_{g,a}}{dz} + r_{l,v} \Delta \bar{H}_l^0 - 4 U \frac{1}{\delta} (T - T_{amb}) \quad [E.28]$$

If one defines the function $F(C_P G) = (\bar{C}_{P,s} G_{s,a} - \bar{C}_{P,g} G_{g,a})$, then the energy balance for zone 1 of the gasifier may be written as follows :

$$\frac{dT}{dz} = \frac{1}{F(C_P G)} \left[T \bar{C}_{P,g} \left[\frac{dG_{g,a}}{dz} \right] + r_{l,v} \Delta \bar{H}_l^0 - 4 U \frac{1}{\delta} (T - T_{amb}) \right] \quad [E.29]$$

Equation [E.29] contains the term $\frac{d(G_{g,a})}{dz}$ which may be related to the carbon material balance by considering the overall material balance across an element of zone 1 (refer to Figure 14). The overall material balance dictates that :

Material into an element = Material out of the element

Since the mass of the silica allothermal agent is common to both input and output terms, one may write that during the period Δt :

$$\begin{aligned} \text{Input} &= \frac{C_{mm}}{1000} \left[\frac{\pi}{4} (D^2 - d^2) u_{s,a} c_{C,s} \right]_z \Delta t \\ &+ \left[\frac{\pi}{4} (D^2 - d^2) G_{g,a} \right]_z \Delta t \quad ; \text{ kg} \end{aligned} \quad [E.30]$$

and that,

(E.13)

$$\begin{aligned} \text{Output} = & \frac{C_{\text{mm}}}{1000} \left[\frac{\pi}{4} (D^2 - d^2) u_{s,a} c_{C,s} \right]_{z + \Delta z} \Delta t \\ & + \left[\frac{\pi}{4} (D^2 - d^2) G_{g,a} \right]_{z - \Delta z} \Delta t \quad ; \text{ kg} \quad [\text{E.31}] \end{aligned}$$

in which C_{mm} represents the molecular mass of carbon (g/gmol).

On dividing equations [E.30] and [E.31] by $\frac{\pi}{4} (D^2 - d^2) \Delta t$ and re-arranging terms, one obtains :

$$(G_{g,a})_{z} - (G_{g,a})_{z - \Delta z} =$$

$$\frac{C_{\text{mm}}}{1000} \left[(u_{s,a} c_{C,s})_{z + \Delta z} - (u_{s,a} c_{C,s})_{z} \right] \quad [\text{E.32}]$$

In the limit as $\Delta z \rightarrow 0$, and since $u_{s,a}$ is approximately constant, equation [E.32] becomes :

$$\frac{d(G_{g,a})}{dz} = \frac{C_{\text{mm}}}{1000} u_{s,a} \left[\frac{d(c_{C,s})}{dz} \right] \quad [\text{E.33}]$$

By incorporating the carbon material balance (equation [E.7]) one obtains :

$$\frac{d(G_{g,a})}{dz} = \frac{C_{\text{mm}}}{1000} r_{1,v} \quad [\text{E.34}]$$

The final form of the energy balance for zone 1 is therefore :

$$\frac{dT}{dz} = \frac{1}{F(C_p G)} \left[\frac{C_{\text{mm}}}{1000} T \bar{C}_{P,g} r_{1,v} + r_{1,v} \Delta \bar{H}_1^0 - 4 U \frac{1}{\delta} (T - T_{\text{amb}}) \right]$$

which factorises to :

(E.14)

$$\frac{dT}{dz} = \frac{l}{F(C_p G)} \left[r_{l,v} \left[\frac{C_{mm}}{1000} T \bar{C}_{p,g} + \Delta \bar{H}_l^0 \right] - 4 U \frac{l}{\delta} (T - T_{amb}) \right] \quad [E.35]$$

E.3 MATERIAL BALANCES FOR ZONE 2, THE COAL PYROLYSIS ZONE.

The material balance which describes the steam gasification of carbon in this zone is identical to equation [E.7]. This equation applies to carbon which has entered zone 2 from zone 1. It is assumed, however, that the coal-char generated by the input of coal to zone 2 is not available for gasification in zone 2 and that the carbon concentration of the reactor is incremented at the base of zone 2 by the amount of fixed carbon fed to the gasifier. This step change in carbon concentration is given as follows :

$$(c_{C,s})_{z + \Delta z} = (c_{C,s})_z + c^0_{C,s} \quad [E.36]$$

where z = the axial position of the base zone 2; m

$c^0_{C,s}$ = the global concentration of fixed carbon fed to
to reactor; gmol/(m³(bed)min)

The mass flowrate of fixed carbon fed to the reactor is given by the following expression :

$$m_C^0 = C_{char}^0 (1 - v_{m,coal}) m_{coal} \quad ; \quad \text{kg/min}$$

where C_{char}^0 = the mass fraction of fixed carbon in the freshly
pyrolysed char, and

$v_{m,coal}$ = the mass fraction of volatile matter in the coal
feed

(E.15)

$c_{C,s}^0$ is therefore given by :

$$c_{C,s}^0 = m_C^0 * 1000 / (C_{mm} u_{s,a} A_a) \quad [E.37]$$

E.4 ENERGY BALANCE FOR ZONE 2.

It is assumed in this model that the coal fed to zone 2 is well distributed across the cross sectional area of the annulus and that the global concentration of coal at the feeder position is relatively low (in the region of 5% by mass). It is also assumed that the energy is transferred to the coal-char predominantly by radiation from the surrounding silica material. In order to estimate the quantity of energy transferred to the coal-char it is assumed that the char comprises spherical particles of mean diameter dp_c .

Then, the specific surface area of the char

$$= \frac{6}{dp_c} \quad ; \quad \left[\frac{m^2}{m^3} \right]$$

and the external area of char exposed to the bed is given by :

$$A_c = \frac{m_{coal}}{\rho_{coal}} * \frac{6}{dp_c} \quad ; \quad \left[\frac{m^2}{m} \right] \quad [E.38]$$

The external area of char added to zone 2 during a time period Δt is therefore given by :

$$A_z = \frac{A_c}{u_{s,a}} \quad ; \quad \left[\frac{m^2}{m} \right] \quad [E.39]$$

(E.16)

where $u_{s,a}$ = the average axial velocity of solid material in zone 2; m/min

The quantity of energy transferred to coal-char in an element of zone 2 of depth Δz during a time period Δt may therefore be written as follows :

$$q_c = h_{R_z} (A_z \Delta z) (T_z - T_{c_z}) \Delta t \quad [E.40]$$

where h_{R_z} = the radiative heat transfer coefficient (silica-char); J/(min.m².K)

T_z = the local temperature of the reactor; K

T_{c_z} = the local temperature of char in the reactor; K

The steady state overall energy balance for zone 2 is given by :

$$\begin{aligned} \text{Input} &= \text{Output} + (\text{Energy demanded by steam-char gasification}) \\ &+ \text{Losses} + \text{Energy gained by coal-char} \end{aligned} \quad [E.41]$$

This equation is an extension of equation [E.16] which was developed into the form of equation [E.35]. It may be shown that by following a procedure which analagous to that employed for zone 1 and by incorporating equation [E.40] into equation [E.41] one obtains the following energy balance for zone 2 :

$$\frac{dT}{dz} = \frac{1}{F(C_p G)} \left[r_{1,v} \left[\frac{C_{mm}}{1000} T \bar{C}_{P,g} + \Delta \bar{H}_1^{\circ} \right] - 4 U \frac{1}{\delta} (T - T_{amb}) \right]$$

(E.17)

$$- h_R \frac{A_c}{u_{s,a} A_a} (T - T_c) \quad [E.42]$$

Note that the energy transferred to the coal-char in the differential element of zone 2 considered above results in an increase in the temperature of the char according to the following expression :

$$q_c = m_{\text{coal}} C_{\text{pyro}} (T_{c,z + \Delta z} - T_{c,z}) \quad [E.43]$$

where C_{pyro} = the 'pyro' heat capacity of the coal as reported by Johnson (1974); J/(kg.K)

On equating equation[E.40] with equation [E.43] and in the limit, as $\Delta z \rightarrow 0$, one obtains the following expression for the axial temperature profile of the coal-char in zone 2 :

$$\frac{dT_c}{dz} = \frac{h_R A_c (T - T_c)}{u_{s,a} m_{\text{coal}} C_{\text{pyro}}} \quad [E.44]$$

E.5 THE MATERIAL AND ENERGY BALANCES FOR ZONE 7. (THE SECONDARY STEAM-CHAR GASIFICATION ZONE).

The existence of zone 7 in the reactor is dictated by the physical geometry and the capacity of the gasifier. In essence, zone 7 exists between the base of zone 2 and the top of zone 3.

The equations which describe the material and energy balances in

(E.18)

zone 7 are identical to equations [E.7] and [E.35] respectively.

E.6 THE ENERGY BALANCE FOR ZONE 3, THE STEAM HEATING ZONE.

Although zone 3 has been represented as having a finite volume in Figure 13, it is assumed in this model that the heating of the steam to the temperature of the reactor occurs instantaneously in an infinitesimally thin element of the annulus at the position of the steam spargers. This assumption is based on the comment made by Rase (1976), that very rapid gas heating rates are typical of gas-solid fluidised beds. It is assumed here that this phenomenon applies to zone 3 of the annulus which operates at close to incipient fluidising conditions.

The steady state energy balance for zone 3 is as follows :

$$\Delta E_{\text{solids},3} = \Delta E_{\text{steam},3} \quad [\text{E.45}]$$

where

$\Delta E_{\text{solids},3}$ = energy lost by the solid material in zone 3; J/min

$\Delta E_{\text{steam},3}$ = energy gained by the steam in zone 3; J/min

now,

$$\Delta E_{\text{solids},3} = G_{s,a} A_a \int_{T_{z3}}^{T_{z3} - \Delta z} C_{P,s} dT * \text{conv}_{\text{SiO}_2} \quad [\text{E.46}]$$

and,

$$\Delta E_{\text{steam},3} = m_{\text{stm}} \int_{T_{\text{stm}}}^{T_{z3}} C_{P,\text{stm}} dT * \text{conv}_{\text{H}_2\text{O}} \quad [\text{E.47}]$$

(E.19)

where z_3 = the axial position of zone 3 in the reactor; m
 T_{z_3} = the temperature of zone 3; K
 $T_{z_3-\Delta z}$ = the temperature at the base of zone 7; K
 T_{stm} = the steam inlet temperature; K
 $C_{P,s}$ = the heat capacity of the solid material;
cal/(gmol.K)
 $C_{p,stm}$ = the heat capacity of steam; J/(kg.K)
 m_{stm} = the flowrate of steam to zone 3; kg/min
 $conv_i$ = a factor which converts the mass flowrate of
species i into a molar flowrate and the units of
energy from calories to joules;
 $conv_i = 4.1868 \times 1000 / mm_i$, where
 mm_i = molecular mass of species i; g/gmol

(E.20)

In this model, correlations in the form of polynomial functions of temperature have been employed for the heat capacity terms which appear in the energy balances of the various zones.

The following data, which are taken from Kyle(1984), Perry(1973) and Smith and Van Ness(1975), have been employed in this model in correlations for molar heat capacities of the form :

$$C_p = a + bT + cT^2 + dT^3 + e/T^2; \text{ cal}/(\text{gmol.K}) \quad [\text{E.48}]$$

Substance	a	b x 10 ²	c x 10 ⁵	d x 10 ⁹	e
SiO ₂	10.95	0.550	0.0	0.0	0.0
H ₂ O	7.700	0.04594	0.2521	-0.8587	0.0
N ₂	6.903	-0.03753	0.1930	-0.6861	0.0
O ₂	8.27	0.0258	0.0	0.0	-187 700
Air	6.713	0.04697	0.1147	-0.4696	0.0
H ₂	6.952	-0.04576	0.09563	-0.2079	0.0
C(gr)	2.673	0.2617	0.0	0.0	-116 900
CH ₄	3.381	1.8044	-0.43	0.0	0.0
CO	6.726	0.04001	0.1283	-0.5307	0.0
CO ₂	4.316	1.4285	-0.8362	1.784	0.0
H ₂ S	7.070	0.3128	0.1364	-0.7867	0.0

On integrating equation [E.46], one obtains :

$$\Delta E_{\text{solids},3} = G_{s,a} A_a \left[a_{\text{SiO}_2} (T_{z3} - \Delta z - T_{z3}) + \frac{b_{\text{SiO}_2}}{2} (T_{z3}^2 - \Delta z - T_{z3}^2) \right] \text{conv}_{\text{SiO}_2} \quad [\text{E.49}]$$

and integration of equation [E.47] yields,

(E.21)

$$\Delta E_{stm,3} = m_{stm} \left[a_{H_2O} (T_{z3} - T_{stm}) + \frac{b_{H_2O}}{2} (T_{z3}^2 - T_{stm}^2) + \frac{c_{H_2O}}{3} (T_{z3}^3 - T_{stm}^3) + \frac{d_{H_2O}}{4} (T_{z3}^4 - T_{stm}^4) \right] conv_{H_2O} \quad [E.50]$$

The temperature of zone 3, T_{z3} in equations [E.49] and [E.50], may be computed by employing an appropriate root solving technique for equation [E.45].

E.7 THE ENERGY BALANCE FOR ZONE 4, THE NEUTRAL ZONE.

In this model it is assumed that no crossflow of the reactant gases (air and steam) occurs between the draft tube and annulus regions of the reactor. Zone 4 therefore behaves as a moving bed of solid material in the absence of a gas stream and without the occurrence of any chemical reactions. The carbon material balance for zone 4 is therefore trivial, with the global carbon concentration in zone 4 being maintained at the constant value of the concentration at the exit of zone 3.

The energy balance for zone 4 is developed in the same way as for zone 1, with exclusion of terms which contain $G_{g,a}$ and $-r_{1,v}$.

Simplification of equation [E.35] yields the following energy balance for zone 4 :

$$\frac{dT}{dz} = \frac{1}{F(C_p G)} \left[-4 U \frac{1}{\delta} (T - T_{amb}) \right] \quad [E.51]$$

(E.22)

where $F(C_p G) = \bar{C}_{P,s} G_{s,a}$ [E.52]

E.8 THE ENERGY BALANCE FOR ZONE 5, THE AIR HEATING ZONE.

As for zone 3, zone 5 is also assumed to occupy an infinitesimally small volume of the reactor within which very rapid heating of the air feed stream occurs.

The steady state energy balance for zone 5 is as follows :

$$\Delta E_{\text{solids},5} = \Delta E_{\text{air},5} \quad [\text{E.53}]$$

where

$\Delta E_{\text{solids},5}$ = energy lost by the solid material in zone 5; J/min

$\Delta E_{\text{air},5}$ = energy gained by the air in zone 5; J/min

now,

$$\Delta E_{\text{solids},5} = G_{s,d} A_d \int_{T_{z5}}^{T_{z5 - \Delta z}} C_{P,s} dT * \text{conv}_{\text{SiO}_2} \quad [\text{E.54}]$$

and,

$$\Delta E_{\text{air},5} = m_{\text{air}} \int_{T_{\text{air}}}^{T_{z5}} C_{P,\text{air}} dT * \text{conv}_{\text{air}} \quad [\text{E.55}]$$

where z_5 = the axial position of zone 5 in the reactor; m

T_{z5} = the temperature of zone 5; K

$T_{z5-\Delta z}$ = the temperature at the base of zone 4; K

T_{air} = the air inlet temperature; K

$G_{s,d} = G_{s,a} [A_a/A_d]$ the superficial mass flowrate of

(E.23)

- solid material in the draft tube; $\text{kg}/(\text{m}_2 \cdot \text{min})$
- A_d = the cross sectional area of the draft tube; m_2
- $C_{p,\text{air}}$ = the heat capacity of air; $\text{J}/(\text{kg} \cdot \text{K})$
- m_{air} = the mass flowrate of air to the reactor; kg/min

Integration of equation [E.54] yields :

$$\Delta E_{\text{solids},5} = G_{s,d} A_d \left[a_{\text{SiO}_2} (T_{z5} - \Delta z - T_{z5}) + \frac{b_{\text{SiO}_2}}{2} (T_{z5}^2 - \Delta z - T_{z5}^2) \right] \text{conv}_{\text{SiO}_2} \quad [\text{E.56}]$$

and integration of equation [E.55] yields,

$$\Delta E_{\text{air},5} = m_{\text{air}} \left[a_{\text{air}} (T_{z5} - T_{\text{air}}) + \frac{b_{\text{air}}}{2} (T_{z5}^2 - T_{\text{air}}^2) + \frac{c_{\text{air}}}{3} (T_{z5}^3 - T_{\text{air}}^3) + \frac{d_{\text{air}}}{4} (T_{z5}^4 - T_{\text{air}}^4) \right] \text{conv}_{\text{air}} \quad [\text{E.57}]$$

The temperature of zone 5, T_{z5} in equations [E.56] and [E.57] may be computed using the same approach that would be adopted for computing T_{z3} .

Note that no chemical reaction is assumed to occur in zone 5 which implies that the global carbon concentration in zone 5 is identical to that for zone 4.

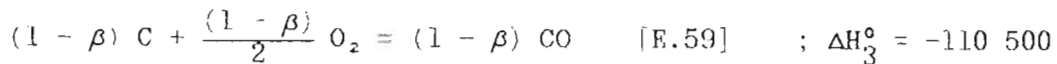
E.9 THE MATERIAL BALANCES FOR ZONE 6, THE CHAR COMBUSTION ZONE.

This model assumes that the oxygen content of the air stream to the

(E.24)

gasifier is completely consumed in the combustion of a stoichiometrically equivalent quantity of carbon in zone 6. The partial combustion of carbon to carbon monoxide in this zone is accommodated by the introduction of a stoichiometric factor β , where β represents the fraction of the carbon which combusts to completion (ie. to CO_2) relative to the total quantity of carbon which participates in the combustion reactions. The rates of the carbon combustion reactions in zone 6 are assumed in this model to occur instantaneously.

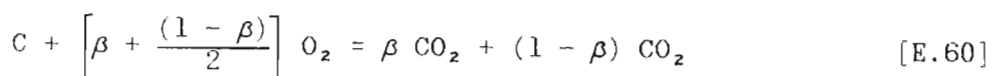
The stoichiometry of the carbon combustion reactions is as follows :



where ΔH_2° = the standard heat of reaction [E.58], the complete combustion of carbon; J/gmol

and ΔH_3° = the standard heat of reaction [E.59], the partial combustion of carbon; J/gmol

On combining reactions [E.58] and [E.59] one obtains the following general expression for the stoichiometry of the combustion of carbon in zone 6



(E.25)

With reference to equation [E.60], if one defines

$$f(\beta) = \left[\beta + \frac{(1-\beta)}{2} \right] \quad [E.61]$$

and one assumes that the air stream directed to the reactor contains 79.0 mol % nitrogen, one may express the molar flowrates of nitrogen, carbon dioxide and carbon monoxide in the product gas stream from zone 6 (ie. the waste gas stream of the gasifier) as follows :

$$\text{mol}_{N_2} = 0.79/0.21 \text{ mol}_{O_2} \quad [E.62]$$

$$\text{mol}_{CO_2} = \beta/f(\beta) \text{ mol}_{O_2} \quad [E.63]$$

$$\text{mol}_{CO} = (1-\beta)/f(\beta) \text{ mol}_{O_2} \quad [E.64]$$

where mol_{O_2} = the molar flowrate of oxygen contained in the air supply to the gasifier; gmol/min

The total molar flowrate of the waste gas stream from the gasifier is therefore :

$$\text{mol}_{\text{waste}} = [1/f(\beta) + 0.79/0.21] \text{ mol}_{O_2} \quad [E.65]$$

The fractional molar compositions of nitrogen, carbon dioxide and carbon monoxide in the waste gas stream are as follows :

$$\text{comp}_{N_2,w} = \frac{0.79/0.21}{[1/f(\beta) + 0.79/0.21]} \quad [E.66]$$

$$\text{comp}_{CO_2,w} = \frac{\beta/f(\beta)}{[1/f(\beta) + 0.79/0.21]} \quad [E.67]$$

$$\text{comp}_{CO,w} = \frac{(1-\beta)/f(\beta)}{[1/f(\beta) + 0.79/0.21]} \quad [E.68]$$

With reference to equation [E.63], one may express the amount of carbon which combusts as follows :

(E.26)

$$\text{mol}_C^{\text{comb}} = 1/f(\beta) \text{ mol}_{O_2} \quad [\text{E.69}]$$

In this model, zone 6 is regarded as containing solid material in mixed flow and gas in plug flow in the upward direction through the draft tube.

It is therefore assumed that zone 6 operates at a uniform global carbon concentration and a uniform temperature, which are dictated by the following material and energy balances, respectively.

The steady state carbon material balance for zone 6 is as follows :

$$\begin{aligned} \text{Carbon input} &= \text{Carbon output} + \text{Carbon} \\ &\quad \text{consumed by combustion reaction} \end{aligned} \quad [\text{E.70}]$$

When expressed symbolically, equation [E.70] may be written as :

$$c_{C,s,5} u_{s,d} A_d = c_{C,s,6} u_{s,d} A_d + \frac{1}{f(\beta)} \text{ mol}_{O_2} \quad [\text{E.71}]$$

where $c_{C,s,5}$ = the global carbon concentration of the solid material in zone 5; gmol/m^3 (bed)
 $c_{C,s,6}$ = the global carbon concentration of the solid material in zone 6; gmol/m^3 (bed)

The global carbon concentration in zone 6 may be derived from equation [E.71] as follows :

$$c_{C,s,6} = c_{C,s,5} - \frac{1}{f(\beta)} \text{ mol}_{O_2} / (u_{s,d} A_d) \quad [\text{E.72}]$$

(E.27)

E.10 THE ENERGY BALANCE FOR ZONE 6.

The steady state energy balance for zone 6 is as follows :

$$\text{Energy input} = \text{Energy output} \quad [\text{E.73}]$$

now,

$$\begin{aligned} \text{Energy input} &= \text{Energy generated by the combustion of char} + \\ &\quad \text{Energy contained in the air stream from zone 5} + \\ &\quad \text{Energy contained in the solid material stream} \\ &\quad \text{from zone 5} \end{aligned} \quad [\text{E.74}]$$

and,

$$\begin{aligned} \text{Energy output} &= \text{Energy contained in the product gas stream from} \\ &\quad \text{zone 6} + \text{Energy contained in the solid material} \\ &\quad \text{stream leaving zone 6} \end{aligned} \quad [\text{E.75}]$$

The energy balance for zone 6 may be expressed symbolically as follows :

$$E_{\text{comb}} + E_{\text{air},5} + E_{\text{solids},5} = E_{\text{wst}} + E_{\text{solids},6} \quad [\text{E.76}]$$

By rearranging equation [E.76], one obtains :

$$\begin{aligned} E_{\text{comb}} &= [E_{\text{solids},6} - E_{\text{solids},5}] + E_{\text{wst}} - E_{\text{air},5} \\ \Rightarrow E_{\text{comb}} &= \Delta E_{\text{solids},6} + E_{\text{wst}} - E_{\text{air},5} \end{aligned} \quad [\text{E.77}]$$

The four components of equation [E.77] may be expanded as follows :

$$\begin{aligned} (1) \quad E_{\text{comb}} &= [(\beta/f(\beta)) * (-\Delta\bar{H}_2) + \\ &\quad ((1-\beta)/f(\beta)) * (-\Delta\bar{H}_3)] \text{ mol}_{\text{O}_2} \end{aligned} \quad [\text{E.78}]$$

$$(2) \quad \Delta E_{\text{solids},6} = G_{\text{s,d}} A_{\text{d}} [a_{\text{SiO}_2} (T_{z6} - T_{z5}) +$$

(E.28)

$$\frac{b_{\text{SiO}_2}}{2} (T_{z6}^2 - T_{z5}^2) \text{ conv}_{\text{SiO}_2} \quad [\text{E.79}]$$

In which T_{z6} = the steady state uniform temperature of zone 6; K

$$(3) \quad E_{\text{wst}} = E_{\text{N}_2, \text{w}} + E_{\text{CO}_2, \text{w}} + E_{\text{CO}, \text{w}} \quad [\text{E.80}]$$

where,

$$E_{i, \text{w}} = \text{comp}_{i, \text{w}} \int_{298}^{T_{z6}} C_{P, i} dT * 4.1868 \quad [\text{E.81}]$$

in which i represents each of the three components of the waste gas, namely N_2 , CO_2 and CO . Note that the units of $E_{i, \text{w}}$ are joules/min.

Integration of equation [E.81] yields

$$E_{i, \text{w}} = \text{comp}_{i, \text{w}} \text{ mol}_{\text{waste}} \left[a_i (T_{z6} - 298) + \frac{b_i}{2} (T_{z6}^2 - 298^2) + \frac{c_i}{3} (T_{z6}^3 - 298^3) + \frac{d_i}{4} (T_{z6}^4 - 298^4) \right] * 4.1868 \quad [\text{E.82}]$$

Finally,

$$E_{\text{air}, 5} = \text{mol}_{\text{O}_2} / 0.21 \left[a_{\text{air}} (T_{z5} - 298) + \frac{b_{\text{air}}}{2} (T_{z5}^2 - 298^2) + \frac{c_{\text{air}}}{3} (T_{z6}^3 - 298^3) + \frac{d_{\text{air}}}{4} (T_{z6}^4 - 298^4) \right] * 4.1868 \quad [\text{E.83}]$$

Note that the arbitrary reference temperature of 298 K has been employed in the above equations to determine the enthalpies of

(E.29)

zone 6.

A similar root solving approach to that adopted for zones 3 and 5 may be employed to compute the temperature of zone 6, T_{z6} , which satisfies equations [E.77] to [E.83].

E.11 THE OVERALL MATERIAL AND ENERGY BALANCES OF THE GASIFIER.

E.11.1 CARBON MATERIAL BALANCE.

The steady state, overall carbon material balance in the gasifier is as follows :

$$\text{Input} = \text{Amount gasified} + \text{Amount combusted} \quad [\text{E.84}]$$

$$\Rightarrow \text{Amount gasified} = \text{Input} - \text{Amount combusted}$$

$$\text{Now} \quad \text{Carbon input} = c_{C,s}^0 u_{s,a} A_a \quad [\text{E.85}]$$

$$\text{and} \quad \text{Carbon combusted} = 1/f(\beta) \text{ mol}_{O_2} \quad [\text{E.86}]$$

$$\begin{aligned} \Rightarrow \text{Carbon gasified} &= c_{C,s}^0 u_{s,a} A_a - 1/f(\beta) \text{ mol}_{O_2} \\ &= \text{mol}_C^{\text{gas}} \quad [\text{E.87}] \end{aligned}$$

During the implementation of this model in the form of a computer algorithm, an iterative strategy is employed to simultaneously solve the overall material and energy balances of the gasifier.

(E.30)

The overall carbon material balance of the gasifier during each iteration may be expressed as follows :

$$C_{\text{bal}} = (C_{\text{fed}} - C_{\text{comb}} - C_{\text{gas}}) / C_{\text{fed}} \quad [\text{E.88}]$$

Where, $C_{\text{fed}} = c_{\text{C,s}}^0 u_{\text{s,a}} A_a$

$$C_{\text{comb}} = 1/f(\beta) \text{ mol}_{\text{O}_2}$$

and $C_{\text{gas}} = r_{\text{C}}^{\text{gas}}$, the total cumulative amount of carbon gasified in the reactor as computed by the model (ie. dependant of the initial conditions) ;
gmol/min

When the conditions of the simulated gasifier are such that the steady state overall carbon material balance is true (equation [E.84]) then the value of C_{bal} in equation [E.88] will be zero.

In view of the circulating nature of the solid inventory of the gasifier and the fact that, during steady state operation, the reactor operates with a finite residual fixed carbon content throughout (ie. carbon-rich operation), one may regard the gasifier as a standard recycle reactor with the carbon feed being realised at the base of the coal pyrolysis zone. The maximum global carbon concentration in the reactor is therefore to be found at this point (R = F7).

The fractional fixed carbon conversion of char at any position in the gasifier may therefore be defined as follows :

(E.31)

$$X_{C,s}^{(R)} = \frac{c_{C,s}^{(F7)} - c_{C,s}^{(R)}}{c_{C,s}^{(F7)}} \quad [E.89]$$

Where $c_{C,s}^{(F7)}$ = the global carbon concentration of the solid material in the final element of zone 2 ;
gmol/m³(bed)

$c_{C,s}^{(R)}$ = the global carbon concentration of the solid material in element R of the annulus region ;
gmol/m³(bed)

E.11.2 THE OVERALL ENERGY BALANCE.

The steady state overall energy balance of the gasifier is as follows :

$$\text{Energy input} = \text{Energy output} \quad [E.90]$$

Now,

$$\begin{aligned} \text{Energy input} = & \text{Energy generated by the combustion of char} \\ & + \text{Enthalpy input of steam} + \text{Enthalpy input} \\ & \text{of air} \end{aligned} \quad [E.91]$$

and,

$$\begin{aligned} \text{Energy output} = & \text{Energy demanded by steam-char gasification} \\ & + \text{Enthalpy output of syngas} \\ & + \text{Enthalpy output of wastegas} \\ & + \text{Enthalpy output of ash stream} \\ & + \text{Energy demanded by coal pyrolysis} \\ & + \text{Energy lost to the surroundings} \end{aligned} \quad [E.92]$$

Equation [E.91] may be expressed as :

(E.32)

$$E_{in} = E_{comb} + E_{stm} + E_{air} \quad [E.93]$$

and equation [E.92] as :

$$E_{out} = E_{gas} + E_{syn} + E_{wst} + E_{ash} + E_{pyrol} + E_{loss} \quad [E.94]$$

The definition of the components of equations [E.93] and [E.94] relative to 298K are as follows :

E_{comb} is defined by equation [E.78]

$$E_{stm} = m_{stm} \left[a_{H_2O} (T_{stm} - 298) + \frac{b_{H_2O}}{2} (T_{stm}^2 - 298^2) + \frac{c_{H_2O}}{3} (T_{stm}^3 - 298^3) + \frac{d_{H_2O}}{4} (T_{stm}^4 - 298^4) \right] * conv_{H_2O} \quad [E.95]$$

$$E_{air} = mol_{O_2} / 0.21 \left[a_{air} (T_{air} - 298) + \frac{b_{air}}{2} (T_{air}^2 - 298^2) + \frac{c_{air}}{3} (T_{air}^3 - 298^3) + \frac{d_{air}}{4} (T_{air}^4 - 298^4) \right] * 4.1868 \quad [E.96]$$

$$E_{gas} = C_{gas} * \Delta H_l \quad [E.97]$$

$$E_{syn} = \sum E_{i,syn} \quad [E.98]$$

Where $i = H_2, CO, CO_2, H_2O, N_2, H_2S$, the components of the synthesis gas

and

$$E_{i,syn} = \left[a_i (T(1) - 298) + \frac{b_i}{2} (T(1)^2 - 298^2) + \frac{c_i}{3} (T(1)^3 - 298^3) \right]$$

(E.33)

$$+ \frac{d_i}{4} (T(1)^4 - 298^4) \Big] * 4.1868 * \text{wet}_i(1)/100 * \text{mol}_{\text{syn}} \quad [\text{E.99}]$$

in which,

$E_{i,\text{syn}}$ = the enthalpy of the i th component of the syngas, relative to 298K; J/min

$T(1)$ = the temperature of the syngas and of the first element in zone 1; K

$\text{wet}_i(1)$ = the molar composition of the i th component of the syngas yet to be defined; mol percent

mol_{syn} = the molar flowrate of the syngas stream yet to be defined; gmol/min

E_{wst} is defined by equation [E.80]

$$E_{\text{ash}} = m_{\text{ash}} \left[a_{\text{SiO}_2} (T_{z6} - 298) + \frac{b_{\text{SiO}_2}}{2} (T_{z6}^2 - 298^2) \right] \text{conv}_{\text{SiO}_2} \quad [\text{E.100}]$$

$$E_{\text{pyro}} = \sum_{z = z(F2)}^{z(F3 - 1)} q_{C_z} \quad [\text{E.101}]$$

in which,

q_{C_z} = the energy required to pyrolyse the fresh char-coal in the element of zone 2 which is located at the axial position of z , as defined in equation [E.43]; J/min

$$E_{\text{loss}} = \sum_{z = z1}^{z = RH} \pi U D (T_2 - T_{\text{amb}}) dz \quad [\text{E.102}]$$

(E.34)

in which, z_1 = the axial position of the top of zone 1 of the reactor; m
 RH = the equivalent reactor height, which is defined in Appendix C5; m
 T_z = the local temperature at an axial position of z in the annulus; K
 dz = the depth of an incremental element of the annulus; m

During the computerised implementation of this model one may define the fractional error in the energy balance, E_{bal} , where

$$E_{bal} = (E_{in} - E_{out})/E_{in} \quad [E.103]$$

When the overall energy balance of the simulated gasifier is satisfied (equation [E.90]), then the value of E_{bal} will be zero.

E.11.3 THE MOLAR FLOWRATES OF GAS WHICH ORIGINATES AS VOLATILE MATTER OF THE COAL.

The molecular mass of the gas stream which originates as volatile matter of the coal feed and is evolved from the pyrolysis zone of the gasifier may be expressed as follows :

$$\begin{aligned} vol_{mm} = & vm_{H_2} * H_{2mm} + vm_{CO} * CO_{mm} + vm_{H_2O} * H_2)_{mm} \\ & + vm_{N_2} * N_{2mm} + vm_{H_2S} * H_2S_{mm} \end{aligned} \quad [E.104]$$

where, vm_i = the mass fraction of component i in the gas which

(E.35)

originates from volatile matter in the coal feed.

i = the gaseous components of the abovementioned gas,
ie. H_2 , CO , H_2O , N_2 and H_2S

i_{mm} = the molecular mass of component i of the
abovementioned gas; g/gmol

The molar flowrate of each component, i , of the gas which originates as the volatile matter content of the coal feed is therefore as follows :

$$vol_i = v_{m_i} (v_{m_{coal}} m_{coal} * 1000) / v_{m_{mm}} \quad [E.105]$$

where, $v_{m_{coal}}$ = the mass fraction of volatile matter in the coal
feed stream

E.11.4 STEAM MATERIAL BALANCE.

The steady state, overall material balance for steam in the gasifier is as follows :

$$\text{Input} = \text{Output} + \text{Amount consumed by} \\ \text{steam-char gasification} \quad [E.106]$$

The overall extent steam conversion in the gasifier may be written as follows :

$$X_{stm}(1) = (\text{Quantity of steam consumed}) / \text{Steam input} \quad [E.107]$$

$$\Rightarrow X_{stm}(1) = \alpha (\text{Quantity of carbon gasified}) \\ / \text{Steam input} \quad [E.108]$$

(E.36)

By incorporating equation [E.87] one obtains :

$$X_{stm}(1) = \alpha (c_{C,s}^o u_{s,a} A_a - 1/f(\beta) \text{mol}_{O_2}) / \text{mol}_{stm} \quad [E.109]$$

where, $X_{stm}(1)$ = the fractional conversion of steam at the top of zone 1, ie in the syngas stream

α = the stoichiometric parameter of the general steam-carbon gasification reaction, equation [E.11]

E.11.5 THE COMPOSITION OF THE SYNGAS STREAM.

In accordance with the notation which is employed in this model, the properties of the synthesis gas stream op the gasifier are synonymous with those of the gas phase leaving the first element of the annulus region, were $R = 1$. The component gases of the syngas stream arise from two different sources, namely the steam gasification of char and the pyrolysis of coal. The amount of steam which is consumed in the gasification of char is given by :

$$Stm_{gas} = X_{stm}(1) \text{mol}_{stm} \quad [E.110]$$

where, $X_{stm}(1)$ = the overall fractional conversion of steam in the gasifier, as defined by equation [E.108]

mol_{stm} = the molar flowrate of steam fed to the gasifier;
gmol/min

The general stoichiometry of steam-carbon gasification (equation [E.11]) dictates that the total molar flowrates of the components

(E.37)

of the syngas are therefore as follows :

$$\begin{aligned}H_2O(l) &= (1 - X_{stm}(l)) \text{ mol}_{stm} + \text{vol}_{H_2O} \\H_2(l) &= \text{stm}_{gas} + \text{vol}_{H_2} \\CO(l) &= ((2 - \alpha)/\alpha) \text{ stm}_{gas} + \text{vol}_{CO} \\CO_2(l) &= ((\alpha - 1)/\alpha) \text{ stm}_{gas} + \text{vol}_{CO_2} \\N_2(l) &= \text{vol}_{N_2} \\H_2S(l) &= \text{vol}_{H_2S}\end{aligned}\tag{E.111}$$

The total molar flowrate of the syngas stream is therefore :

$$\begin{aligned}\text{mol}_{gas}(l) &= H_2O(l) + H_2(l) + CO(l) + CO_2(l) + \\&N_2(l) + H_2S(l)\end{aligned}\tag{E.112}$$

The molar percentage composition of each component, i , of the syngas stream (including H_2O) is given by :

$$\text{wet}_i(l) = i(l) * 100/\text{mol}_{gas}(l)\tag{E.113}$$

The mean molecular mass of the syngas stream is therefore given by :

$$\text{gas}_{mm}(l) = \frac{\sum \text{all } i (\text{wet}_i(l) * i_{mm})}{100}\tag{E.114}$$

The superficial mass flowrate of syngas is therefore defined as follows :

$$G_{g,a}(l) = \text{mol}_{gas}(l) * \text{gas}_{mm}(l)/(1000 * A_a)\tag{E.115}$$

The molar flowrate of the dry syngas stream is given by :

$$\text{prods}(l) = H_2(l) + CO(l) + CO_2(l) + N_2(l) + H_2S(l)\tag{E.116}$$

(E.38)

and the molar percentage composition of each component of the dry syngas is given by :

$$\text{dry}_i(l) = i(l) * 100/\text{prods}(l) ; \text{ all } i \text{ except } \text{H}_2\text{O} \quad [\text{E.117}]$$

E.11.6 MATERIAL BALANCE FOR THE ALLOTHERMAL AGENT (SILICA SAND).

In this model it is assumed that the allothermal agent of the gasifier circulates between the combustion and gasification zones at a steady mass flowrate. It is also assumed that the ash content of the coal fed to the gasifier is elutriated from zone 6 by the waste gas stream.

The mass flowrate of ash fed to the gasifier is as follows :

$$m_{\text{ash}} (1 - C_{\text{char}})(1 - \text{vm}_{\text{coal}}) m_{\text{coal}} \quad [\text{E.118}]$$

where, C_{char} = the mass fraction of fixed carbon of freshly pyrolysed char,

and, vm_{coal} = the mass fraction of volatile matter contained in the coal feed.

The superficial mass flowrate of ash in the annulus is therefore :

$$G_{\text{ash}} = m_{\text{ash}}/A_a \quad [\text{E.119}]$$

The superficial mass flowrate of allothermal agent in zone 1 of the gasifier may be expressed as follows :

$$G_{s,a}(l) = (1 - e) u_{s,a}(l) \rho_s \quad [\text{E.120}]$$

(E.39)

where, e = the voidage of annulus

$u_{s,a}(1)$ = the linear axial velocity of solid material in zone 1
of the annulus; m/min

ρ = the particle density of the allothermal agent; kg/m³

The superficial mass flowrate of solid material in zone 2 is assumed to be as follows :

$$G_{s,a}(2) = G_{s,a}(1) + G_{ash} \quad [E.121]$$

Note that, in view of the relatively low concentration of char in the solid phase of the gasifier (below 5% by mass), the contribution to $G_{s,a}$ by the fixed carbon of the char has been neglected in this model.

Therefore : $u_{s,a}(2) = G_{s,a}(2)/((1 - e)\rho_s)$ [E.122]

The superficial mass flowrates and axial, linear velocities of solid material in zones 7, 3 and 4 of the gasifier are assumed to be identical to those of zone 2.

The steady state material balance for the allothermal agent in the gasifier dicatates that :

$$G_{s,d} = G_{s,a}(2) A_a/A_d \quad [E.123]$$

If one assumes that the voidage of the annulus region is identical to that of the draft tube region, then :

$$u_{s,d} = u_{s,a}(2) A_a/A_d \quad [E.124]$$

(F.1)

APPENDIX F

DISCUSSION OF THE COMPUTER ALGORITHM FOR THE ONE-DIMENSIONAL SIMULATION MODEL OF THE GASIFIER.

A computer algorithm has been written in the FORTRAN 77 language to simultaneously solve the material and energy balances of the Judd gasifier, the development of which are contained in Appendix E. The program is designed to run on a personal computer, which allows it to be employed during on-line simulation of the gasifier.

The design of the Judd gasifier includes a recycle stream of coal-char, which complicates the simultaneous solution of the overall material and energy balances of the gasifier. A principal feature of the structure of the computer algorithm is that the starting point of the computations corresponds with the top of zone 1 of the reactor. This philosophy allows the subsequent computation of the properties of each of the remaining zones in the reactor according to the equations of the model, after which the status of the simultaneous overall material and energy balances of the reactor may be tested. The computer program of the Judd gasifier model is capable of solving the overall material and energy balances of the gasifier to a tolerance of 1% in about 15 minutes when run on a PC with a 10 Mhz microprocessor.

(F.2)

The assumed plug flow nature of material in the annular region of the reactor has led to the development of a set of first order differential equations which describe the material and energy balances in a one-dimensional model of the region. Consequently the standard Runge-kutta technique is conveniently employed by program to simultaneously solve the relevant material and energy balances of the annulus region at the axial intervals of 12.5mm in each zone. This selection of axial interval provides for the axial resolution of the annulus region into 80 distinct elements per metre of annulus depth.

The following features of the program are of special interest :

- The program iterates to a solution, at which the tolerance levels of the overall material and energy balances are satisfied, by adjusting the estimates of the properties at the top of zone 1 of the gasifier.
- The overall energy balance and the energy balances of zones 3, 5 and 6 account for the effects of temperature on the heat capacities of the various species (ie. enthalpy balances are considered).
- Only in the energy balances for zones 1, 2 and 4 are species heat capacities evaluated at the arithmetic mean temperature of the reactor, for the reasons mentioned in Chapter 5.
- The effects of temperature on the heats of reaction are considered throughout the program.

(G.1)

APPENDIX G.

LISTING OF GASIFIER SIMULATOR CODE.

* VARIABLES DIRECTORY : *

NOTE THAT S.I. UNITS ARE EMPLOYED IN THIS PROGRAM, WITH THE EXCEPTION
OF THAT OF TIME, FOR WHICH MINUTES ARE USED.

A1=ARRHENIUS FREQUENCY FACTOR FOR CHAR-STEAM GASIFICATION REACTION,
GMOL CARBON GASIFIED/(GMOL C INITIALLY PRESENT.MIN).

ACHAR=EXTERNAL SURFACE AREA EXPOSED BY A PARTICLE OF COAL-CHAR
\$ TO THE SURROUNDING BED MATERIAL IN ZONE 2, SQ.M.

AIR1,AIR2,AIR3,AIR4=COEFFICIENTS IN A POLYNOMIAL CORRELATION FOR THE
\$ SPECIFIC HEAT OF AIR AS A FUNCTION OF TEMPERATURE

AIRMM=MOLECULAR MASS OF AIR, G/GMOL (NOTE UNITS - CONVERSION TO KG
\$ IS DONE LATER).

ALPHA=STOICHIOMETRIC PARAMETER IN CHAR-STEAM GASIFICATION REACTION :
\$ $C + (\text{ALPHA})\text{H}_2\text{O} = (\text{ALPHA})\text{H}_2 + (2 - \text{ALPHA})\text{CO} + (\text{ALPHA} - 1)\text{CO}_2$.

AREAAN=CROSS SECTIONAL AREA OF THE ANNULUS REGION, SQ.M.

AREADT=CROSS SECTIONAL AREA OF THE DRAFT TUBE, SQ.M.

CALTOJ=FACTOR FOR CONVERSION OF UNITS FROM CALORIES TO J, J/CAL.

CCHAR=MASS FRACTION OF CHAR WHICH COMPRISES FIXED CARBON, -.

CCSV0=FIXED-CARBON CONCENTRATION OF INITIAL ELEMENT OF CHAR PREPARED
\$ IN THE REACTOR, EXPRESSED IN PSEUDO-HOMOGENEOUS UNITS,
\$ GMOL/CU.M(TOTAL REACTOR VOLUME).

CCSVF=THE ESTIMATE OF CCSV(F7) WHICH IS USED AS THE REFERENCE
CARBON CONCENTRATION FOR COMPUTING XCSV(R) IN THE REACTOR.

CCSV(R)=FIXED-CARBON CONCENTRATION OF CHAR IN ELEMENT R OF THE
\$ REACTOR, EXPRESSED IN PSEUDO-HOMOGENEOUS UNITS, GMOL/CU.M
\$ (TOTAL REACTOR VOLUME).

CCSV5=FIXED-CARBON CONCENTRATION OF CHAR IN ZONE 5 OF THE REACTOR
\$ EXPRESSED IN PSEUDO-HOMOGENEOUS UNITS, GMOL/CU.M
\$ (TOTAL REACTOR VOLUME).

CCSV6=FIXED-CARBON CONCENTRATION OF CHAR IN ZONE 6 OF THE REACTOR
\$ EXPRESSED IN PSEUDO-HOMOGENEOUS UNITS, GMOL/CU.M

(G.2)

C \$ (TOTAL REACTOR VOLUME).

C CMM=MOLECULAR MASS OF CARBON, G/GMOL.

C COMM=MOLECULAR MASS OF CARBON MONOXIDE, G/GMOL.

C CO2MM=MOLECULAR MASS OF CARBON DIOXIDE, G/GMOL.

C CM1,CM2,CM3,CM4=COEFFICIENTS IN A POLYNOMIAL CORRELATION FOR THE

C \$ SPECIFIC HEAT OF CO AS A FUNCTION OF TEMPERATURE.

C CO(R)=MOLAR FLOWRATE OF CO THROUGH ELEMENT R, GMOL/MIN.

C CO2(R)=MOLAR FLOWRATE OF CO2 THROUGH ELEMENT R, GMOL/MIN.

C CO21,CO22,CO23,CO24=COEFFICIENTS IN A POLYNOMIAL CORRELATION FOR THE

C \$ SPECIFIC HEAT OF CO2 AS A FUNCTION OF TEMPERATURE

C CAPGAS(TM)=STATEMENT FUNCTION DEFINITIONS OF THE SPECIFIC HEATS OF 'GAS' SPECIES

IN THE REACTOR AT TEMPERATURE TM, J/(GMOL.K)

('GAS' SPECIES CONSIDERED ARE AIR, CO, CO2, H2, H2S, H2O, N2, O2).

C DELH1=HEAT OF THE CHAR-STEAM GASIFICATION REACTION, J/GMOL.

C DELH2=HEAT OF THE CHAR COMBUSTION REACTION, J/GMOL.

C DELH3=HEAT OF THE PARTIAL COMBUSTION OF CHAR REACTION, J/GMOL.

C DENSCL=PARTICLE DENSITY OF THE COAL FEED, KG/CU.M.

C DENSOL=PARTICLE DENSITY OF THE SILICA SAND, KG/CU.M.

C DIAMAN=OUTER DIAMETER OF THE ANNULUS REGION, IE. INSIDE DIAMETER

C \$ OF THE REACTOR VESSEL, M.

C DIAMDT=NOMINAL DIAMETER OF THE DRAFT TUBE, M.

C DINV=REAL FUNCTION OF ABOVEMENTIONED DIAMETERS, DEFINED IN INITIAL

C \$ VARIABLE ASSIGNMENT STATEMENT, 1/M.

C DPCOAL=D50 MEAN PARTICLE DIAMETER OF THE COAL FEED, M.

C DPSAND=D50 MEAN PARTICLE DIAMETER OF THE SAND, M.

C DRYH2(R)=MOISTURE-FREE HYDROGEN COMPOSITION OF GAS IN ELEMENT R

C \$ OF THE ANNULAR REGION OF THE GASIFIER, MOL %.

C DRYCO(R)=ANALAGOUS TO DRYH2(R), BUT FOR CARBON MONOXIDE, MOL %.

C DRYCO2(R)=ANALAGOUS TO DRYH2(R), BUT FOR CARBON DIOXIDE, MOL %.

C DRYN2(R)=ANALAGOUS TO DRYH2(R), BUT FOR NITROGEN, MOL %.

C DRYH2S(R)=ANALAGOUS TO DRYH2(R), BUT FOR HYDROGEN SULPHIDE, MOL %.

C DZ=DEPTH OF INCREMENTAL ELEMENT OF THE REACTOR, M.

C E1=ARRHENIUS ACTIVATION ENERGY FOR THE CHAR-STEAM GASIFICATION

C \$ REACTION, J/GMOL.

C EMISS=EMISSIVITY OF THE SOLID MATERIAL IN THE REACTOR. -.

C F1=1, THE NUMBER OF THE DIFFERENTIAL ELEMENT AT THE TOP OF ZONE 1.

C F2=THE NUMBER OF THE DIFFERENTIAL ELEMENT AT THE TOP OF ZONE 2.

C F3=THE NUMBER OF THE DIFFERENTIAL ELEMENT AT THE TOP OF ZONE 3.

(G.3)

C F4=THE NUMBER OF THE DIFFERENTIAL ELEMENT AT THE TOP OF ZONE 4.
C F5=THE NUMBER ASSOCIATED WITH ZONE 5.
C F6=THE NUMBER ASSOCIATED WITH ZONE 6.
C F7=THE NUMBER OF THE DIFFERENTIAL ELEMENT AT THE TOP OF ZONE 7.
C GASH=SUPERFICIAL MASS FLOWRATE OF ASH IN ZONES 3,4 AND 7,
C GASMM1=THE MOLECULAR MASS OF GAS AT THE TOP OF ZONE 1, G/GMOL.
C \$ KG/(SQ.M.MIN.)
C GGANN(R)=SUPERFICIAL MASS FLOWRATE OF GAS THROUGH ELEMENT R
C \$ OF THE REACTOR, KG/SQ.M.MIN.
C GGDTZ5=STEADY SUPERFICIAL MASS FLOWRATE OF GAS IN ZONE 5,
C \$ KG/(SQ.M.MIN.)
C GGDTZ6=STEADY AVERAGE SUPERFICIAL MASS FLOWRATE OF GAS IN ZONE 6,
C \$ KG/(SQ.M.MIN.)
C GSANN(Z), Z=1,2,3,4,7 =STEADY SUPERFICIAL MASS FLOWRATE OF SOLID
C \$ MATERIAL IN ZONES 1,2,3,4,7 RESPECTIVELY, KG/(SQ.M.MIN.)
C GSDT=STEADY SUPERFICIAL MASS FLOWRATE OF SOLID MATERIAL IN THE
C \$ DRAFT TUBE, KG/(SQ.M.MIN.)
C GSTEAM=STEADY SUPERFICIAL MASS FLOWRATE OF STEAM IN THE ANNULUS,
C \$ KG/(SQ.M.MIN.)
C Z=THE POSITION FROM THE TOP ALONG THE VERTICAL AXIS OF THE REACTOR, M.
C HCYL=HEIGHT OF THE CYLINDER OF DIAMETER=DIAMAN, AND VOLUME=VBASE,
C \$ M.
C H21,H22,H23,H24=COEFFICIENTS IN A POLYNOMIAL CORRELATION FOR THE
C \$ SPECIFIC HEAT OF H2 AS A FUNCTION OF TEMPERATURE.
C H2MM=MOLECULAR MASS OF HYDROGEN, G/GMOL.
C H2OMM=MOLECULAR MASS OF STEAM, G/GMOL.
C H2SMM=MOLECULAR MASS OF HYDROGEN SULPHIDE, G/GMOL.
C H2(R)=MOLAR FLOWRATE OF H2 THROUGH ELEMENT R, GMOL/MIN.
C H2O(R)=MOLAR FLOWRATE OF H2O THROUGH ELEMENT R, GMOL/MIN.
C H2S(R)=MOLAR FLOWRATE OF H2S THROUGH ELEMENT R, GMOL/MIN.
C H2O1,H2O2,H2O3,H2O4=COEFFICIENTS IN A POLYNOMIAL CORRELATION FOR THE
C \$ SPECIFIC HEAT OF H2O AS A FUNCTION OF TEMPERATURE
C H2S1,H2S2=COEFFICIENTS IN A POLYNOMIAL CORRELATION FOR THE
C \$ SPECIFIC HEAT OF H2S AS A FUNCTION OF TEMPERATURE.
C HRAD(R)=RADIANT HEAT TRANSFER COEFFICIENT BETWEEN SOLID MATERIAL
C \$ AND CHAR UNDERGOING PYROLYSIS IN ZONE 2, J/(MIN.SQ.M.K)
C ICOUNT=VARIABLE USED TO MONITOR THE NUMBER OF ITERATIONS OF THE
C \$ MAIN PROGRAM.

(G.4)

C K1(R)=ARRHENIUS RATE CONSTANT FOR THE CHAR-STEAM GASIFICATION
C \$ GASIFICATION REACTION IN ELEMENT R,
C \$ GMOL C REACTED/(GMOL CO.MIN).
C LENDT=LENGTH OF DRAFT TUBE, M.
C MAIR=STEADY MASS FLOWRATE OF AIR TO THE REACTOR, KG/MIN.
C MASH=STEADY MASS FLOWRATE OF ASH INTO THE REACTOR, KG/MIN.
C MCOAL=STEADY COAL FEEDRATE TO THE GASIFIER, KG/MIN.
C MSTEAM=STEADY STEAM FLOWRATE TO THE GASIFIER, KG/MIN.
C MOLGAS(1)=MOLAR FLOWRATE OF THE ENTIRE PRODUCT GAS STREAM FROM
C \$ THE ANNULUS (INCL. H2O), GMOL/MIN.
C MOLGAS(R)=MOLAR FLOWRATE OF THE PRODUCT GAS STREAM (INCL. H2O)
C \$ AT ELEMENT R OF THE ANNULUS, GMOL/MIN.
C MOLC5=THE AMOUNT OF FIXED-CARBON LEAVING ZONE 5, GMOL/MIN.
C MOLO2=THE AMOUNT OF OXYGEN CONTAINED IN THE INLET AIR STREAM,
C GMOL/MIN.
C MOLSTM=STEADY MOLAR FLOWRATE OF STEAM TO THE REACTOR, GMOL/MIN.
C N2(R)=MOLAR FLOWRATE OF N2 THROUGH ELEMENT R, GMOL/MIN.
C N21,N22,N23,N24=COEFFICIENTS IN A POLYNOMIAL CORRELATION FOR THE
C \$ SPECIFIC HEAT OF N2 AS A FUNCTION OF TEMPERATURE.
C N2MM=MOLECULAR MASS OF NITROGEN, G/GMOL.
C O21,O22,O23=COEFFICIENTS IN A POLYNOMIAL CORRELATION FOR THE
C \$ SPECIFIC HEAT OF O2 AS A FUNCTION OF TEMPERATURE.
C O2MM=MOLECULAR MASS OF OXYGEN, G/GMOL.
C PI=FUNDAMENTAL TRIGONOMETRIC CONSTANT=RATIO (CIRCLE CIRCUMFERENCE/
C DIAMETER).
C PRESS=NOMINAL PRESSURE OF OPERATION OF THE REACTOR, PA.
C PRODS(R)=MOLAR FLOWRATE OF DRY PRODUCT GASES AT ELEMENT R OF THE
C \$ ANNULUS, GMOL.MIN.
C R=INTEGER VARIABLE USED TO INDICATE THE CHRONOLOGICAL POSITION OF
C \$ THE CURRENT DIFFERENTIAL ELEMENT OF THE REACTOR, THE TOP ELEMENT
C \$ IN ZONE 1 CORRESPONDING TO R=1.
C RIMOL(R)=THE RATE OF STEAM GASIFICATION OF CHAR IN ELEMENT R
C \$ OF THE REACTOR, GMOL C REACTED/(GMOL CO.MIN).
C RIVOL(R)=THE RATE OF STEAM GASIFICATION OF CHAR IN ELEMENT R
C \$ OF THE REACTOR, GMOL C REACTED/(CU.M REACTOR VOLUME.MIN).
C RC(R)=RATE OF STEAM GASIFICATION OF CARBON IN ELEMENT R OF THE
C \$ REACTOR, GMOL/MIN.
C RCZ1=CUMULATIVE RATE OF GASIFICATION OF CARBON IN ELEMENTS 1 TO R

(G.5)

C \$ OF ZONE 1, GMOL/MIN.
C RCZ2=CUMULATIVE RATE OF GASIFICATION OF CARBON IN ELEMENTS 1 TO R
C \$ OF ZONE 2, GMOL/MIN.
C RCZ7=CUMULATIVE RATE OF GASIFICATION OF CARBON IN ELEMENTS 1 TO R
C \$ OF ZONE 7, GMOL/MIN.
C RH2(R)=RATE OF PRODUCTION OF HYDROGEN IN ELEMENT R OF THE REACTOR,
C \$ GMOL/MIN.
C RH2Z1=CUMULATIVE RATE OF PRODUCTION OF HYDROGEN IN ELEMENTS 1 TO R
C \$ OF ZONE 1, GMOL/MIN.
C RH2Z2=CUMULATIVE RATE OF PRODUCTION OF HYDROGEN IN ELEMENTS 1 TO R
C \$ OF ZONE 2, GMOL/MIN.
C RH2Z7=CUMULATIVE RATE OF PRODUCTION OF HYDROGEN IN ELEMENTS 1 TO R
C \$ OF ZONE 7, GMOL/MIN.
C RCO(R)=RATE OF PRODUCTION OF 'CO' IN ELEMENT R OF THE REACTOR,
C \$ GMOL/MIN.
C RCOZ1=CUMULATIVE RATE OF PRODUCTION OF 'CO' IN ELEMENTS 1 TO R
C \$ OF ZONE 1, GMOL/MIN.
C RCOZ2=CUMULATIVE RATE OF PRODUCTION OF 'CO' IN ELEMENTS 1 TO R
C \$ OF ZONE 2, GMOL/MIN.
C RCOZ7=CUMULATIVE RATE OF PRODUCTION OF 'CO' IN ELEMENTS 1 TO R
C \$ OF ZONE 7, GMOL/MIN.
C RCO2(R)=RATE OF PRODUCTION OF 'CO2' IN ELEMENT R OF THE REACTOR,
C \$ GMOL/MIN.
C RCO2Z1=CUMULATIVE RATE OF PRODUCTION OF 'CO2' IN ELEMENTS 1 TO R
C \$ OF ZONE 1, GMOL/MIN.
C RCO2Z2=CUMULATIVE RATE OF PRODUCTION OF 'CO2' IN ELEMENTS 1 TO R
C \$ OF ZONE 2, GMOL/MIN.
C RCO2Z7=CUMULATIVE RATE OF PRODUCTION OF 'CO2' IN ELEMENTS 1 TO R
C \$ OF ZONE 7, GMOL/MIN.
C RGAS=IDEAL GAS CONSTANT=8.314 J/GMOL.K.
C RH=EQUIVALENT HEIGHT OF THE REACTOR, ASSUMING THE TAPER TO THE
C \$ DISTRIBUTOR TO BE AT 45 DEGREES, AND THE DIAMETER OF THE
C \$ BASE OF THE DISTRIBUTOR TO BE THAT OF THE DRAFT TUBE.
C \$ (NOTE THAT THIS HEIGHT REFERS TO THE DISTANCE BETWEEN THE
C \$ TOP OF THE DRAFT TUBE AND THE BASE OF THE REACTOR.), M.
C SB=SPECIFIC SURFACE OF THE REACTOR, IE. SURFACE AREA OF SOLID
C MATERIAL PER UNIT VOLUME OF BED, SQ.M/CU.M
C SIO2MM=MOLECULAR MASS OF 'SILICA', G/GMOL.

(G.6)

C SIZE=INTEGER VARIABLE INDICATING THE DIMENSION OF THE ARRAYS USED
C \$ FOR STORAGE OF THE PROPERTIES OF EACH ELEMENT OF THE REACTOR.
C SOL1, SOL2 =COEFFICIENTS IN A POLYNOMIAL CORRELATION FOR THE
C \$ SPECIFIC HEAT OF SILICA AS A FUNCTION OF TEMPERATURE.
C T(R)=LOCAL TEMPERATURE OF THE REACTOR IN ELEMENT R, KELVIN.
C T(1)=ESTIMATED TEMPERATURE OF ELEMENT 1, AT THE TOP OF ZONE 1, K.
C TAIRIN=AIR INLET TEMPERATURE TO THE REACTOR, K.
C TAIR(R)=AIR TEMPERATURE IN ELEMENT R OF ZONE 5, K.
C TABS0=273.15K, USED TO CONVERT TEMPERATURES FROM C TO K, K.
C TAMB=AMBIENT TEMPERATURE OF SURROUNDINGS, K.
C TCHAR(R)=THE LOCAL TEMPERATURE OF CHAR IN ELEMENT R OF ZONE 2,
C \$ KELVIN.
C TCOAL=TEMPERATURE OF THE COAL FEED TO THE REACTOR, K.
C TCRT=THE ACCEPTABLE PERCENTAGE DIFFERENCE BETWEEN TWO ESTIMATES
C \$ OF A PARTICULAR TEMPERATURE IN THE REACTOR AT STEADY STATE
C \$ SOLUTION, K.
C TGAS(R)=THE LOCAL TEMPERATURE OF THE COMBUSTION PRODUCTS IN ELEMENT
C \$ R OF ZONE 6, K.
C TM=THE ARITHMETIC AVERAGE TEMPERATURE OF THE GASIFIER, K.
C TMAX=THE MAXIMUM TEMPERATURE LIMIT FOR THE REACTOR, ABOVE WHICH
C \$ THE PROGRAM TERMINATES, K.
C TMIN=THE MINIMUM TEMPERATURE LIMIT FOR THE REACTOR, BELOW WHICH
C \$ THE PROGRAM TERMINATES, K.
C TREF=THE REFERENCE TEMPERATURE (298.15K) FOR THE CALCULATION OF THE
C \$ ENTHALPY OF THE GAS IN ZONE 6, K.
C TSTMIN=TEMPERATURE OF THE STEAM SUPPLY TO THE REACTOR, K.
C TSTEAM(R)=THE LOCAL TEMPERATURE OF STEAM IN ELEMENT R OF ZONE 3,
C \$ K.
C TZ5=THE TEMPERATURE OF ZONE 5 OF THE REACTOR, K.
C TZ6=THE TEMPERATURE OF ZONE 6 OF THE REACTOR, K.
C U=OVERALL HEAT TRANSFER COEFFICIENT FOR HEAT TRANSFER FROM MATERIAL
C \$ IN THE ANNULUS TO THE REACTOR SURROUNDINGS, J/(MIN.SQ.M.K).
C USANN(1)=LINEAR AXIAL SOLIDS VELOCITY IN ZONE 1, M/MIN.
C USANN(2)=LINEAR AXIAL SOLIDS VELOCITY IN ZONE 2, M/MIN.
C USDT=LINEAR AXIAL SOLIDS VELOCITY IN THE DRAFT TUBE, M/MIN.
C VBASE=VOLUME OF THE TRUNCATED CONICAL REGION OF THE BASE OF THE
C \$ REACTOR, CU.M.
C VMCOAL=THE FRACTION OF THE FEED COAL WHICH COMPRISES VOLATILE MATTER.

C VMH2=THE MOL FRACTION OF THE VOLATILE MATTER WHICH COMPRISES 'H2'.
 C VMCO=THE MOL FRACTION OF THE VOLATILE MATTER WHICH COMPRISES 'CO'.
 C VMH2O=THE MOL FRACTION OF THE VOLATILE MATTER WHICH COMPRISES 'H2O'.
 C VMH2S=THE MOL FRACTION OF THE VOLATILE MATTER WHICH COMPRISES 'H2S'.
 C VMN2=THE MOL FRACTION OF THE VOLATILE MATTER WHICH COMPRISES 'N2'.
 C VOID=THE VOIDAGE OF THE ANNULAR REGION OF THE REACTOR, -.
 C VOLMM=THE MOLECULAR MASS OF THE VOLATILE MATTER PRODUCED IN
 C ZONE 2, G/GMOL.
 C VOLH2=THE MOLAR FLOWRATE OF 'H2' PRODUCED BY PYROLYSIS OF THE
 C COAL IN ZONE 2, GMOL/MIN.
 C VOLCO=THE MOLAR FLOWRATE OF 'CO' PRODUCED BY PYROLYSIS OF THE
 C COAL IN ZONE 2, GMOL/MIN.
 C VOLH2O=THE MOLAR FLOWRATE OF 'H2O' PRODUCED BY PYROLYSIS OF THE
 C COAL IN ZONE 2, GMOL/MIN.
 C VOLN2=THE MOLAR FLOWRATE OF 'N2' PRODUCED BY PYROLYSIS OF THE
 C COAL IN ZONE 2, GMOL/MIN.
 C VOLH2S=THE MOLAR FLOWRATE OF 'H2S' PRODUCED BY PYROLYSIS OF THE
 C COAL IN ZONE 2, GMOL/MIN.
 C VOLAIR=STEADY VOLUMETRIC AIR FLOWRATE TO THE REACTOR, NML CU.M/MIN.
 C VOLGAS=THE ACTUAL VOLUMETRIC FLOWRATE OF GAS (INCL. H2O) FROM
 C \$ THE ANNULUS, CU.M/MIN.
 C VOLWST=THE ACTUAL VOLUMETRIC FLOWRATE OF WASTE GAS FROM THE
 C \$ DRAFT TUBE, CU.M/MIN.
 C WASTMM=MOLECULAR MASS OF WASTE GAS, G/GMOL.
 C WETH2(R)=OVERALL HYDROGEN COMPOSITION (INCL. H2O) OF GAS IN ELEMENT
 C \$ R OF THE ANNULUS, MOL %.
 C WETCO(R)=OVERALL 'CO' COMPOSITION (INCL. H2O) OF GAS IN ELEMENT R
 C \$ OF THE ANNULUS, MOL %.
 C WETCO2(R)=OVERALL 'CO2' COMPOSITION (INCL. H2O) OF GAS IN ELEMENT R
 C \$ OF THE ANNULUS, MOL %.
 C WETH2O(R)=OVERALL 'H2O' COMPOSITION (INCL. H2O) OF GAS IN ELEMENT R
 C \$ OF THE ANNULUS, MOL %.
 C WETN2(R)=OVERALL 'N2' COMPOSITION (INCL. H2O) OF GAS IN ELEMENT R
 C \$ OF THE ANNULUS, MOL %.
 C WETH2S(R)=OVERALL 'H2S' COMPOSITION (INCL. H2O) OF GAS IN ELEMENT R
 C \$ OF THE ANNULUS, MOL %.
 C XCSV(R)=FRACTIONAL CONVERSION OF CARBON CONTENT OF CHAR AT ELEMENT
 C \$ R OF THE REACTOR, -.

(G.8)

C XCSV(1)=ESTIMATED FRACTIONAL CONVERSION OF CARBON CONTENT OF CHAR AT
C \$ ELEMENT F1, THE TOP OF ZONE 1.
C XCSV5=FRACTIONAL CONVERSION OF CARBON CONTENT OF CHAR IN ZONE 5, -.
C XCSV6=FRACTIONAL CONVERSION OF CARBON CONTENT OF CHAR IN ZONE 6, -.
C XSTM(R)=FRACTIONAL CONVERSION OF STEAM AT ELEMENT R IN THE ANNULUS.
C Z(R)=AXIAL POSITION OF ELEMENT R OF THE REACTOR, M.
C \$ (Z=0 AT THE TOP OF THE DRAFT TUBE).
C Z0=0.0 AT THE TOP OF THE DRAFT TUBE, THE REFERENCE FOR AXIAL
C \$ POSITIONS IN THE REACTOR.
C Z1=THE AXIAL POSITION OF F1, THE FIRST ELEMENT IN ZONE 1, M.
C Z2=THE AXIAL POSITION OF F2, THE FIRST ELEMENT IN ZONE 2, M.
C Z3=THE AXIAL POSITION OF F3, THE FIRST ELEMENT IN ZONE 3, M.
C Z4=THE AXIAL POSITION OF F4, THE FIRST ELEMENT IN ZONE 4, M.
C Z5=THE AXIAL POSITION OF F5, THE FIRST ELEMENT IN ZONE 5, M.
C Z6=THE AXIAL POSITION OF F6, THE FIRST ELEMENT IN ZONE 6, M.
C Z7=THE AXIAL POSITION OF F7, THE FIRST ELEMENT IN ZONE 7, M.
C ZCOAL=AXIAL POSITION OF THE COAL FEED POINT IN THE REACTOR,
C \$ IE. TOP OF ZONE 2, M.
C ZDT=THE AXIAL POSITION IN ZONES 5 AND 6 ABOVE THE BASE OF THE
C \$ DRAFT TUBE, M.
C ZSPARG=THE AXIAL POSITION OF THE STEAM SPARGERS IN THE REACTOR, M.
C ZTEST=AXIAL POSITION TEST CRITERION, M.

```

D Line# 1      7                                Microsoft FORTRAN77 V3.20 02/84
  1      PROGRAM RILEY
  2 C *****
  3 C *
  4 C * A STEADY STATE, ONE-DIMENSIONAL SIMULATION MODEL OF THE JUDD *
  5 C * CIRCULATING FLUIDISED BED GASIFIER. *
  6 C *
  7 C * WRITTEN BY R.K. RILEY, NOVEMBER 1989. *
  8 C *
  9 C *****
 10 C
 11 C INITIALISATION :
 12 C -----
 13      INTEGER F1, F2, F3, F4, F5, F6, F7, R, SIZE
 14 C -----
 15      PARAMETER (SIZE=200)
 16 C -----
 17      REAL K1, KZ5, KZ6, LENDT, MAIR, MASH, MCOAL, MSTEAM, MOLGAS, MOLWST,
 18      $MOLC5, MOLCOM, MOLO2, MOLSTM, N2, NZZ1, NZZ2, NZZ3, NZZ7, N21, N22,
 19      $N23, N24, N2MM
 20 C -----
 21      DIMENSION CCSV(SIZE), CO(SIZE), CO2(SIZE), CPGANN(SIZE),
 22      $DCCSV1(SIZE), DCCSV2(SIZE), DGGAN1(SIZE), DGGAN2(SIZE),
 23      $DT1(SIZE), DT2(SIZE), DT4(SIZE), DTCHAR(SIZE),
 24      $DRYH2(SIZE), DRYCO(SIZE), DRYCO2(SIZE), DRYN2(SIZE),
 25      $DRYH2S(SIZE), ENLOS1(SIZE), ENLOS2(SIZE), ENLOS7(SIZE),
 26      $ENLOS4(SIZE), ENPYRO(SIZE), FCPG(SIZE), GGANN(SIZE), GSANN(7),
 27      $GASMM(SIZE), H2O(SIZE), H2S(SIZE), HRAD(SIZE), H2(SIZE),
 28      $K1(SIZE), MOLGAS(SIZE), N2(SIZE),
 29      $PRODS(SIZE), RC(SIZE), RH2(SIZE), RCO(SIZE),
 30      $RCO2(SIZE), RCGAS(SIZE), T(SIZE), TCHAR(SIZE), USANN(7),
 31      $WETH2(SIZE), WETCO(SIZE), WETCO2(SIZE), WETH2O(SIZE),
 32      $WETN2(SIZE), WETH2S(SIZE), XCSV(SIZE), XSTM(SIZE), Z(SIZE)
 33 C -----
 34 C UNITS OF TAMB, TMAX, TMIN IN DATA FOLLOWING ARE DEGREES C :
 35      DATA A1, AIRMM, AIR1, AIR2, AIR3, AIR4, ALPHA, CALTOJ, CCHAR,
 36      $CMM, COMM, CO2MM, CM1, CM2, CM3, CM4, CO21, CO22, CO23, CO24, CV,
 37      $DELH1, DELH2, DELH3, DENSCL, DA2, DB2, DC2, DD2, DE2, DA3, DB3, DC3, DD3, DE3,

```

```

38  $DENSOL,DIAMAN,DIAMDT,DPCOAL,DPSAND,E1,EMISS,H21,H22,H23,H24,
39  $H2MM,H2OMM,H2SMM,H2O1,H2O2,H2O3,H2O4,H2S1,H2S2,H2S3,H2S4/
40  $183707.0,28.8503,6.713,0.04697E-02,0.1147E-05,-0.4696E-09,
41  $1.35,4.1868,0.7183,12.01115,
42  $28.0106,44.0100,6.726,0.04001E-02,0.1283E-05,-0.5307E-09,
43  $5.316,1.4285E-02,-0.8362E-05,1.784E-09,31.0E+06,172500.0,
44  $-393700.0,-110600.0,1300.0,
45  $-6.6270,1.1410E-02,-0.8362E-05,1.784E-09,304600.0,
46  $-0.0820,-0.2346E-02,0.1283E-05,-0.5307E-09,210750.0,
47  $2600.0,0.50,0.18,2.0E-03,675.0E-06,
48  $145760.0,0.85,6.952,-0.04576E-02,0.09563E-05,-0.2079E-09,
49  $2.0158,18.0152,34.0798,
50  $7.70,0.04594E-02,0.2521E-05,-0.8587E-09,
51  $7.07,0.3128E-02,0.1364E-05,-0.7867E-09/
52  DATA N21,N22,N23,N24,N2MM,O21,O22,O23,O24,O2MM,RGAS,
53  $SOL1,SOL2,SIO2MM,TABS0,TAMB,TAPPCH,TCRIT,TMAX,TMIN,TREF,
54  $VMCOAL,VMH2,VMCO,VMH2O,VMH2S,VMN2,VOID,ZO/
55  $6.903,-0.03753E-02,0.1930E-05,-0.6861E-09,28.0134,
56  $6.085,0.3631E-02,-0.1709E-05,0.3133E-09,31.9988,
57  $8.314,10.95,5.50E-03,60.0848,273.15,25.0,0.99,2.0,1200.0,550.0,
58  $25.0,0.219,0.6315,0.3481,0.0,0.0037,0.0168,0.52,0.0/
59 C ++++++
60 C DEFINITION OF STATEMENT FUNCTIONS :
61 C
62 C STEADY STATE CARBON MATERIAL BALANCES :
63     FCCSV1(Z,T,CCSV,GGANN)=-A1*EXP(-E1/(RGAS*T))*CCSV/USANN(IZONE)
64     FGGAN1(Z,T,CCSV,GGANN)=-CMM/1000.0*A1*EXP(-E1/(RGAS*T))*CCSV
65     FCCSV2(Z,T,CCSV,GGANN,TCHAR)=
66     $-A1*EXP(-E1/(RGAS*T))*CCSV/USANN(IZONE)
67     FGGAN2(Z,T,CCSV,GGANN,TCHAR)=-CMM/1000.0*A1*
68     $EXP(-E1/(RGAS*T))*CCSV
69 C STEADY STATE ENERGY BALANCES :
70     FT1(Z,T,CCSV,GGANN)=1.0/FCPG(R)*
71     $(-A1*EXP(-E1/(RGAS*T))*CCSV*(CMM/1000.0*CPGANN(R)*T+DH1)-
72     $4.0*U*DINV*(T-TAMB))
73     FT2(Z,T,CCSV,GGANN,TCHAR)=1.0/FCPG(R)*
74     $(-A1*EXP(-E1/(RGAS*T))*CCSV*(CMM/1000.0*CPGANN(R)*T+DH1)-
75     $4.0*U*DINV*(T-TAMB))-

```

(G.11)

76 $\$(5.672E-08*60.0*EMISS*(T**4-TCHAR**4)/(T-TCHAR))*$
77 $\$ACHAR/(USANN(IZONE)*AREAAN)*(T-TCHAR)$
78 $FTCHAR(Z,T,CCSV,GGANN,TCHAR)=5.672E-08*60.0*EMISS*$
79 $\$(T**4-TCHAR**4.0)/(T-TCHAR)*ACHAR*$
80 $\$(T-TCHAR)/(USANN(IZONE)*MCOAL*(0.174+1.98E-04*(T-TABS0)+$
81 $\$(0.33+5.49E-04*(T-TABS0))*VMCOAL*CALTOJ*1000.0))$
82 $FT4(Z,T)=-4.0*U*DINV*(T-TAMB)/FCPG(R)$
83 C
84 C ENERGY BALANCE FOR ZONE 3 :
85 C
86 $HSOL3(T,TZ3)=(SOL1*(T-TZ3)+SOL2/2.0*(T**2-TZ3**2))*$
87 $\$CALTOJ*1000.0/SIO2MM*GSANN(3)*AREAAN$
88 $ESTM3(TZ3)=(H2O1*(TZ3-TSTMIN)+H2O2/2.0*(TZ3**2-TSTMIN**2)+$
89 $\$H2O3/3.0*(TZ3**3-TSTMIN**3)+H2O4/4.0*(TZ3**$
90 $\$4.0-TSTMIN**4))*CALTOJ*MOLSTM$
91 C
92 C ENERGY BALANCE FOR ZONE 5 :
93 C
94 $EAIR5(TZ5)=(AIR1*(TZ5-TAIRIN)+AIR2/2.0*(TZ5**2-TAIRIN**2)+$
95 $\$AIR3/3.0*(TZ5**3-TAIRIN**3)+AIR4/4.0*(TZ5**4-TAIRIN**4))$
96 $\$*CALTOJ*MOLO2/0.21$
97 $HSOL5(T,TZ5)=(SOL1*(T-TZ5)+SOL2/2.0*(T**2-TZ5**2))*$
98 $\$CALTOJ*1000.0/SIO2MM*GSDT*AREADT$
99 C
100 C ENERGY BALANCE FOR ZONE 6 :
101 C
102 C ENTHALPY OF THE WASTE GAS PRODUCTS, J/MIN :
103 $ECOW(TZ6)=(CM1*(TZ6-TREF)+(CM2/2.0)*(TZ6**2-TREF**2)+$
104 $\$(CM3/3.0)*(TZ6**3-TREF**3)+(CM4/4.0)*(TZ6**4-TREF**4))$
105 $\$*CALTOJ*CMPCO/100.0*MOLWST$
106 $ECO2W(TZ6)=(CO21*(TZ6-TREF)+(CO22/2.0)*(TZ6**2-TREF**2)+$
107 $\$(CO23/3.0)*(TZ6**3-TREF**3)+(CO24/4.0)*(TZ6**4-TREF**4))$
108 $\$*CALTOJ*CMPCO2/100.0*MOLWST$
109 $EN2W(TZ6)=(N21*(TZ6-TREF)+(N22/2.0)*(TZ6**2-TREF**2)+$
110 $\$(N23/3.0)*(TZ6**3-TREF**3)+(CN2/4.0)*(TZ6**4-TREF**4))$
111 $\$*CALTOJ*CMPN2/100.0*MOLWST$
112 C ENTHALPY OF THE AIR STREAM TO ZONE 6, J/MIN :
113 $EAIR6I(TZ5)=(AIR1*(TZ5-TREF)+(AIR2/2.0)*(TZ5**2-TREF**2)+$

114 $\$(AIR3/3.0)*(TZ5^{**3}-TREF^{**3})+(AIR4/4.0)*(TZ5^{**4}-TREF^{**4})$
 115 $\$*CALTOJ*MOL02/0.21$
 116 C ENTHALPY CHANGE OF THE SOLID MATERIAL IN ZONE 6, J/MIN. :
 117 $HSOL6(TZ5, TZ6)=(SOL1*(TZ6-TZ5)+SOL2/2.0*(TZ6^{**2}-TZ5^{**2}))*$
 118 $\$CALTOJ*1000.0/SIO2MM*GSDT*AREADT$
 119 C
 120 C THE ENERGY LOST TO THE SURROUNDINGS FROM AN ELEMENT OF DEPTH DZ :
 121 $ENLOS(T)=U*PI*DIAMAN*DZ*(T-TAMB)$
 122 C THE ENERGY REQUIRED TO PYROLISE THE COAL :
 123 $EPYROL(TCH1, TCH2)=MCOAL*(0.174+1.98E-04*(TCH2-TABS0)+$
 124 $\$(0.33+5.49E-04*(TCH2-TABS0))*VMCOAL*CALTOJ*1000.0)*(TCH2-TCH1)$
 125 C ENTHALPY OF THE ASH STREAM, RELATIVE TO 298 K :
 126 $ENASH(TZ6)=(SOL1*(TZ6-TREF)+SOL2/2.0*(TZ6^{**2}-TREF^{**2}))$
 127 $\$*CALTOJ*1000.0/SIO2MM*MASH$
 128 C (THE ENTHALPIES OF THE GAS REACTANTS AND PRODUCTS ARE COMPUTED
 129 C RELATIVE TO 298 K. THIS CONVENTION HAS BEEN EMPLOYED TO PREVENT
 130 C HAVING TO COMPUTE THE ENTHALPY OF THE VOLATILE MATTER CONTENT OF THE
 131 C COAL, SINCE IT IS ASSUMED THAT THE COAL INLET TEMPERATURE IS 298 K.)
 132 C
 133 C ENTHALPY OF THE PRODUCT GASES RELATIVE TO 298 K :
 134 C
 135 C SYNGAS PRODUCTS, J/MIN :
 136 C -----
 137 $EH2P(T)=(H21*(T-TREF)+H22/2.0*(T^{**2}-TREF^{**2})+$
 138 $\$H23/3.0*(T^{**3}-TREF^{**3})+H24/4.0*(T^{**4}-TREF^{**4}))*$
 139 $\$CALTOJ*WETH2(1)/100.0*MOLGAS(1)$
 140 $ECOP(T)=(CM1*(T-TREF)+CM2/2.0*(T^{**2}-TREF^{**2})+$
 141 $\$CM3/3.0*(T^{**3}-TREF^{**3})+CM4/4.0*(T^{**4}-TREF^{**4}))*$
 142 $\$CALTOJ*WETCO(1)/100.0*MOLGAS(1)$
 143 $ECO2P(T)=(CO21*(T-TREF)+CO22/2.0*(T^{**2}-TREF^{**2})+$
 144 $\$CO23/3.0*(T^{**3}-TREF^{**3})+CO24/4.0*(T^{**4}-TREF^{**4}))*$
 145 $\$CALTOJ*WETCO2(1)/100.0*MOLGAS(1)$
 146 $EH2OP(T)=(H2O1*(T-TREF)+H2O2/2.0*(T^{**2}-TREF^{**2})+$
 147 $\$H2O3/3.0*(T^{**3}-TREF^{**3})+H2O4/4.0*(T^{**4}-TREF^{**4}))*$
 148 $\$CALTOJ*WETH2O(1)/100.0*MOLGAS(1)$
 149 $EN2P(T)=(N21*(T-TREF)+N22/2.0*(T^{**2}-TREF^{**2})+$
 150 $\$N23/3.0*(T^{**3}-TREF^{**3})+N24/4.0*(T^{**4}-TREF^{**4}))*$
 151 $\$CALTOJ*WETN2(1)/100.0*MOLGAS(1)$

(G.13)

```
152      EH2SP(T)=(H2S1*(T-TREF)+H2S2/2.0*(T**2-TREF**2)+
153      $H2S3/3.0*(T**3-TREF**3)+H2S4/4.0*(T**4-TREF**4))*
154      $CALTOJ*WETH2S(1)/100.0*MOLGAS(1)
155 C
156 C WASTE GAS PRODUCTS, J/MIN : - DEFINED IN TREATMENT OF ZONE 6.
157 C -----
158 C ENTHALPY OF THE REACTANT GASES RELATIVE TO 298 K :
159 C STEAM, J/MIN :
160 C -----
161      ESTEAM(T)=(H2O1*(T-TREF)+H2O2/2.0*(T**2-TREF**2)+
162      $H2O3/3.0*(T**3-TREF**3)+H2O4/4.0*(T**4-TREF**4))
163      $*CALTOJ*MOLSTM
164 C AIR, J/MIN :
165 C -----
166      EAIR(T)=(AIR1*(T-TREF)+AIR2/2.0*(T**2-TREF**2)+
167      $AIR3/3.0*(T**3-TREF**3)+AIR4/4.0*(T**4-TREF**4))
168      $*CALTOJ*MOLO2/0.21
169 C
170 C EXPRESSIONS FOR THE HEATS OF REACTION AT TM, J/GMOL :
171 C -----
172      DHR1(TM)=(DH10+DA1*TM+(DB1/2.0)*TM*TM+(DC1/3.0)*TM**3+
173      $(DD1/4.0)*TM**4-DE1/TM)*CALTOJ
174      DHR2(TM)=(DH20+DA2*TM+(DB2/2.0)*TM*TM+(DC2/3.0)*TM**3+
175      $(DD2/4.0)*TM**4-DE2/TM)*CALTOJ
176      DHR3(TM)=(DH30+DA3*TM+(DB3/2.0)*TM*TM+(DC3/3.0)*TM**3+
177      $(DD3/4.0)*TM**4-DE3/TM)*CALTOJ
178 C
179 C EXPRESSIONS FOR THE HEAT CAPACITIES AT TM, J PER GMOL.K :
180 C -----
181      CAPH2(TM)=(H21+H22*TM+H23*TM*TM+H24*TM**3)*CALTOJ
182      CAPCO(TM)=(CM1+CM2*TM+CM3*TM*TM+CM4*TM**3)*CALTOJ
183      CAPCO2(TM)=(CO21+CO22*TM+CO23*TM*TM+CO24*TM**3)*CALTOJ
184      CAPH2O(TM)=(H2O1+H2O2*TM+H2O3*TM*TM+H2O4*TM**3)*CALTOJ
185      CAPN2(TM)=(N21+N22*TM+N23*TM*TM+N24*TM**3)*CALTOJ
186      CAPH2S(TM)=(H2S1+H2S2*TM+H2S3*TM*TM+H2S4*TM**3)*CALTOJ
187      CAPAIR(TM)=(AIR1+AIR2*TM+AIR3*TM*TM+AIR4*TM**3)*CALTOJ
188      CAPSOL(TM)=(SOL1+SOL2*TM)*CALTOJ
189 C
```

```

190 C ++++++
191
192     OPEN(UNIT=6,FILE='LPT2')
193 C
194 C READ INPUT DATA FROM THE KEYBOARD :
195     WRITE(*,8)
196     WRITE(*,9)
197     8 FORMAT(/,1X,'GASIFIER SIMULATOR INPUT DATA :')
198     9 FORMAT(1X,'-----')
199     WRITE(*,1)
200     1 FORMAT(/,1X,'DIAMETER OF ANNULUS (M) = ')
201     READ(*,*)DIAMAN
202     WRITE(*,2)
203     2 FORMAT(/,1X,'DIAMETER OF DRAFT TUBE (M) = ')
204     READ(*,*)DIAMDT
205     WRITE(*,3)
206     3 FORMAT(/,1X,'LENGTH OF DRAFT TUBE (M) = ')
207     READ(*,*)LENDT
208     WRITE(*,4)
209     4 FORMAT(/,1X,'AXIAL POSITION OF HOOD BELOW TOP OF D/T (M) = ')
210     READ(*,*)Z1
211     WRITE(*,5)
212     5 FORMAT(/,1X,'AXIAL PSN OF COAL FEEDERS BELOW TOP OF D/T (M) = ')
213     READ(*,*)ZCOAL
214     WRITE(*,6)
215     6 FORMAT(/,1X,'AXIAL PSN OF STEAM SPARGERS BELOW TOP OF D/T (M) = ')
216     READ(*,*)ZSPARG
217     WRITE(*,101)
218 101 FORMAT(/,1X,'STEADY COAL FLOWRATE TO REACTOR (KG/MIN) = ')
219     READ(*,*)MCOAL
220     WRITE(*,102)
221 102 FORMAT(/,1X,'STEADY STEAM FLOWRATE TO REACTOR (KG/MIN) = ')
222     READ(*,*)MSTEAM
223     WRITE(*,103)
224 103 FORMAT(/,1X,'STEADY AIR F/RATE TO REACTOR (N CU M./MIN) = ')
225     READ(*,*)VOLAIR
226     WRITE(*,104)
227 104 FORMAT(/,1X,'PRESSURE OF OPERATION OF REACTOR (BAR G) = ')

```

```
228     READ(*,*)PRESS
229     WRITE(*,99)
230  99  FORMAT(/,1X,'UMF OF AIR AT 850 C AND ABOVE PRESS (M/S) = ')
231     READ(*,*)UMFA
232     WRITE(*,97)
233  97  FORMAT(/,1X,'UMF OF STEAM AT 850 C AND ABOVE PRESS (M/S) = ')
234     READ(*,*)UMFS
235     WRITE(*,105)
236 105  FORMAT(/,1X,'INLET TEMP. OF STEAM (DEGREES C) = ')
237     READ(*,*)TSTMIN
238     WRITE(*,106)
239 106  FORMAT(/,1X,'INLET TEMP. OF AIR (DEGREES C) = ')
240     READ(*,*)TAIRIN
241     WRITE(*,107)
242 107  FORMAT(/,1X,'ESTIMATED VALUE OF T(1) (DEGREES C) = ')
243     READ(*,*)T(1)
244     WRITE(*,108)
245 108  FORMAT(/,1X,'T(1) ADJUSTMENT FACTOR = ')
246     READ(*,*)TADJ
247     WRITE(*,109)
248 109  FORMAT(/,1X,'CCSV(1) ADJUSTMENT FACTOR = ')
249     READ(*,*)CADJ
250     WRITE(*,111)
251 111  FORMAT(/,1X,'% TOLERANCE ALLOWED IN INTERNAL ENERGY BALANCES = ')
252     READ(*,*)ENTOL
253     WRITE(*,819)
254 819  FORMAT(/,1X,'% TOLERANCE ALLOWED IN OVERALL MTL & EN BALANCES =')
255     READ(*,*)PCTOL
256 C
257     TCOAL=25.0
258     USANN(1)=8.00
259     ALPHA=1.35
260     BETA=0.60
261     U=4.0
262 C  REFLECT PROCESS CONTROL VARIABLES TO THE PRINTER :
263     WRITE(6,140)
264     WRITE(6,141)
265     WRITE(6,275)
```



```

266      WRITE(6,150)
267      WRITE(6,160)MCOAL
268      WRITE(6,170)MSTEAM
269      WRITE(6,180)VOLAIR
270      WRITE(6,190)PRESS
271      WRITE(6,200)TCOAL
272      WRITE(6,210)TSTMIN
273      WRITE(6,220)TAIRIN
274      WRITE(6,230)USANN(1)
275      WRITE(6,240)T(1)
276      WRITE(6,290)ALPHA
277      WRITE(6,291)BETA
278      WRITE(6,292)DIAMAN
279      WRITE(6,294)DIAMDT
280      WRITE(6,296)LENDT
281      WRITE(6,298)Z1
282      WRITE(6,300)ZCOAL
283      WRITE(6,302)ZSPARG
284      WRITE(6,304)UMFA
285      WRITE(6,306)UMFS
286      WRITE(6,308)U
287      WRITE(6,51)ENTOL
288      WRITE(6,52)PCTOL
289  51  FORMAT(/,1X,'% TOLERANCE ALLOWED FOR INTERNAL ENERGY BALANCES = ',
290      $F6.4)
291  52  FORMAT(/,1X,'% TOLERANCE ALLOWED FOR OVERALL MTL & EN. BALANCES = '
292      $,1X,F6.4)
293  140 FORMAT(/,1X,'RESULTS OF THE STEADY STATE, ONE DIMENSIONAL '
294      $'SIMULATION MODEL')
295  141 FORMAT(1X,'OF THE JUDD CIRCULATING FLUIDISED BED GASIFIER')
296  150 FORMAT(/,/,1X,'REFLECTION OF THE INPUT DATA TO THE SIMULATION'
297      $' MODEL :',/)
298  160 FORMAT(/,1X,'THE STEADY COAL FLOWRATE TO THE REACTOR'
299      $' = ',F8.4,' KG/MIN.')
```

```

300  162 FORMAT(/,1X,'THE INCREMENTAL STEP SIZE IN THE REACTOR'
301      $' IS ',E12.4,' M.')
```

```

302  170 FORMAT(/,1X,'STEADY STEAM FLOWRATE TO THE REACTOR'
303      $' = ',F8.4,' KG/MIN.')
```

```

304 180  FORMAT(/,1X,'THE ESTIMATED STEADY AIR FLOWRATE TO THE REACTOR'
305      '$' = ',F8.4,' NORMAL CUBIC M./MIN.')
```

```

306 190  FORMAT(/,1X,'THE NOMINAL PRESSURE OF OPERATION OF THE REACTOR'
307      '$' = ',F6.2,' BAR GAUGE')
```

```

308 200  FORMAT(/,1X,'THE INLET TEMPERATURE OF THE COAL'
309      '$' = ',F6.2,' DEGREES C')
```

```

310 210  FORMAT(/,1X,'THE INLET TEMPERATURE OF THE STEAM'
311      '$' = ',F6.2,' DEGREES C')
```

```

312 220  FORMAT(/,1X,'THE INLET TEMPERATURE OF THE AIR'
313      '$' = ',F6.2,' DEGREES C')
```

```

314 230  FORMAT(/,1X,'THE LINEAR, AXIAL VELOCITY OF SOLID MATERIAL'
315      '$' IN THE ANNULUS = ',F6.2,' MM/SEC')
```

```

316 240  FORMAT(/,1X,'THE ESTIMATED TEMPERATURE OF THE TOP OF'
317      '$' ZONE 1 = ',F6.2,' DEGREES C')
```

```

318 290  FORMAT(/,1X,'THE STOICHIOMETRIC PARAMETER IN THE GASIFICATION'
319      '$' REACTION IS ',F4.2)
```

```

320 291  FORMAT(/,1X,'OF THE CARBON THAT COMBUSTS, THE FRACTION WHICH '
321      '$' COMBUSTS TO COMPLETION (IE. TO CO2) IS ',F6.4)
```

```

322 292  FORMAT(/,1X,'THE OUTER DIAMETER OF THE ANNULUS = ',F5.2,' M')
```

```

323 294  FORMAT(/,1X,'THE DIAMETER OF THE DRAFT TUBE = ',F5.2,' M')
```

```

324 296  FORMAT(/,1X,'THE LENGTH OF THE DRAFT TUBE = ',F5.2,' M')
```

```

325 298  FORMAT(/,1X,'THE DEPTH OF THE HOOD BELOW THE TOP OF THE'
326      '$' DRAFT TUBE = ',F4.2,' M')
```

```

327 300  FORMAT(/,1X,'THE DEPTH OF THE COAL FEEDERS BELOW THE TOP OF THE'
328      '$' DRAFT TUBE = ',F4.2,' M')
```

```

329 302  FORMAT(/,1X,'THE DEPTH OF THE STEAM SPARGERS BELOW THE TOP OF '
330      '$' THE DRAFT TUBE = ',F4.2,' M')
```

```

331 304  FORMAT(/,1X,'THE UMF OF AIR AT 850 C AND THE ABOVE PRESSURE '
332      '$' IS ',F7.4,' M/S')
```

```

333 306  FORMAT(/,1X,'THE UMF OF STEAM AT 850 C AND THE ABOVE PRESSURE '
334      '$' IS ',F7.4,' M/S')
```

```

335 308  FORMAT(/,1X,'THE OVERALL HEAT TRANSFER COEFFICIENT FOR ENERGY '
336      '$' LOST TO THE SURROUNDINGS IS ',F8.4,' W/(M**2.K)')
```

```

337 275  FORMAT(1X,'-----',
338      '$'-----')
```

```

339 280  FORMAT(1X,F10.4)
```

```

340 C  -----
341      WRITE(*,56)
```

(G.18)

```
342 56 FORMAT(/,1X'*** PLEASE WAIT - COMPUTATIONS ARE IN PROGRESS !')
```

```
343 C INITIAL VARIABLE ASSIGNMENTS :
```

```
344     R=1
```

```
345     ICOUNT=1
```

```
346 C GEOMETRICAL RELATIONSHIPS :
```

```
347     PI=4.0*ATAN(1.0)
```

```
348     AREAAN=PI/4.0*(DIAMAN*DIAMAN-DIAMDT*DIAMDT)
```

```
349     AREADT=PI/4.0*DIAMDT*DIAMDT
```

```
350     DINV=DIAMAN/(DIAMAN*DIAMAN-DIAMDT*DIAMDT)
```

```
351 C CALCULATE THE EQUIVALENT REACTOR HEIGHT, RH, ASSUMING THE BASE OF
```

```
352 C THE REACTOR TO BE CYLINDRICAL :
```

```
353     VBASE=1.0/3.0*PI*((DIAMAN/2.0)**3-(DIAMDT/2.0)**3)
```

```
354     HCYL=4.0/(PI*DIAMAN*DIAMAN)*VBASE
```

```
355     RH=LENDT+HCYL
```

```
356 C SET THE INCREMENTAL STEP SIZE IN THE REACTOR, M :
```

```
357     DZ=1.250E-02
```

```
358     WRITE(6,162)DZ
```

```
359 C -----
```

```
360 C CONVERT UNITS OF PRESSURE TO PA :
```

```
361     PRESS=(PRESS+1.01325)*1.0E+05
```

```
362 C CONVERT UNITS OF USANN(1) TO M/MIN. :
```

```
363     USANN(1)=USANN(1)*60.0/1000.0
```

```
364 C CONVERT UNITS OF TEMPERATURE OF REACTANTS TO KELVIN :
```

```
365     TAIRIN=TAIRIN+TABS0
```

```
366     TSTMIN=TSTMIN+TABS0
```

```
367     TCOAL=TCOAL+TABS0
```

```
368     T(1)=T(1)+TABS0
```

```
369     TAMB=TAMB+TABS0
```

```
370     TMAX=TMAX+TABS0
```

```
371     TMIN=TMIN+TABS0
```

```
372     TREF=TREF+TABS0
```

```
373 C INITIALISE TM, THE MEAN REACTOR TEMPERATURE, K :
```

```
374     TM=T(1)
```

```
375 C CONVERT THE UNITS OF 'U' TO J/(MIN.M**2.K) :
```

```
376     U=U*60.0
```

```
377 C ACCOUNT FOR THE ENERGY DEMAND OF THE SHIFT REACTION DURING
```

```
378 C GASIFICATION, J/GMOL :
```

```
379     DELH1=DELH1+2900.0*ALPHA
```

(G.19)

```
380 C COMPUTE ELEMENTS OF THE EXPRESSION FOR THE HEAT OF THE
381 C GASIFICATION REACTION :
382     DA1=6.463-3.158*ALPHA
383     DB1=-1.6102E-02+1.2968E-02*ALPHA
384     DC1=1.0928E-05-1.1210E-05*ALPHA
385     DD1=-2.8454E-09+2.9655E-09*ALPHA
386 C COMPUTE THE CONSTANTS, DHi0, IN THE EXPRESSIONS DHi=f(DHi0,T) :
387     DH10=DELH1/CALTOJ-(DA1*TREF+DB1/2.0*TREF*TREF+DC1/3.0*TREF**3+
388     $DD1/4.0*TREF**4)
389     DH20=DELH2/CALTOJ-(DA2*TREF+DB2/2.0*TREF*TREF+DC2/3.0*TREF**3+
390     $DD2/4.0*TREF**4-DE2/TREF)
391     DH30=DELH3/CALTOJ-(DA3*TREF+DB3/2.0*TREF*TREF+DC3/3.0*TREF**3+
392     $DD3/4.0*TREF**4-DE3/TREF)
393 C
394 C COMPUTE THE HEATS OF REACTION AT TM, J/GMOL :
395     DH1=DHR1(TM)
396     DH2=DHR2(TM)
397     DH3=DHR3(TM)
398 C
399 C CONVERT VOLAIR TO MAIR, KG PER MINUTE :
400     MAIR=(101325.0*VOLAIR*AIRMM)/(RGAS*298.15*1000.0)
401     MOLO2=0.21*MAIR*1000.0/AIRMM
402 C CONVERT MSTEAM TO MOLSTM, GMOL PER MINUTE :
403     MOLSTM=MSTEAM*1000.0/H2OMM
404 C -----
405 C COMPUTE CCSV0 :
406     CCSV0=CCHAR*(1.0-VMCOAL)*MCOAL*1000.0/(CMM*USANN(1)*AREAAN)
407 C INTRODUCE THE TERM 'FBETA' AS A FUNCTION OF BETA :
408     FBETA=(BETA+(1.0-BETA)/2.0)
409 C ESTIMATE CCSV(1) USING REACTION RATE AT T(1) :
410     CCSV(1)=(CCSV0*AREAAN*USANN(1)-1.0/FBETA*MOLO2)/(A1*EXP(-E1/(RGAS
411     $*T(1)))*AREAAN*(ZSPARG-Z1))
412 C COMPUTE XSTM(1) :
413     XSTM(1)=(ALPHA*(CCSV0*AREAAN*USANN(1)-1.0/FBETA*MOLO2))/MOLSTM
414     GSTEAM=MSTEAM/AREAAN
415     MASH=(1.0-CCHAR)*(1.0-VMCOAL)*MCOAL
416     GASH=MASH/AREAAN
417     GSANN(1)=(1.0-VOID)*USANN(1)*DENSOL
```

```

418      GSANN(2)=GSANN(1)+GASH
419      USANN(2)=GSANN(2)/((1.0-VOID)*DENSOL)
420      USANN(7)=USANN(2)
421      USANN(3)=USANN(2)
422      USANN(4)=USANN(2)
423      USDT=USANN(2)*AREAAN/AREADT
424      GSANN(7)=GSANN(2)
425      GSANN(3)=GSANN(2)
426      GSANN(4)=GSANN(2)
427      ACHAR=MCOAL/DENSCL*6.0/DPCOAL
428      SB=6.0/DPSAND*(1.0-VOID)
429 C   COPMUTE THE AMOUNT OF CARBON FED AND THE AMOUNT COMBUSTED :
430      CFED=CCSV0*USANN(2)*AREAAN
431      CCOMB=1.0/FBETA*MOLO2
432 C   COMPUTE THE STEADY MOLAR FLOWRATES OF THE COMPONENTS OF THE
433 C   VOLATILE MATTER IN ZONES 1 AND 2, GMOL/MIN. :
434      VOLMM=VMH2*H2MM+VMCO*COMM+VMH2O*H2OMM+VMN2*N2MM+VMH2S*H2SMM
435      VOLH2=VMH2*(VMCOAL*MCOAL*1000.0)/VOLMM
436      VOLCO=VMCO*(VMCOAL*MCOAL*1000.0)/VOLMM
437      VOLH2O=VMH2O*(VMCOAL*MCOAL*1000.0)/VOLMM
438      VOLN2=VMN2*(VMCOAL*MCOAL*1000.0)/VOLMM
439      VOLH2S=VMH2S*(VMCOAL*MCOAL*1000.0)/VOLMM
440 C   COMPUTE THE SYNTHESIS GAS COMPOSITION (MOL %) AND THE INITIAL
441 C   HEAT CAPACITY OF THE SYNGAS (J/KG.K.) AT THE TOP OF THE REACTOR :
442 C   MOLAR COMPONENT FLOWRATES ARE :
443      H2O(1)=(1.0-XSTM(1))*MOLSTM+VOLH2O
444      STMGAS=XSTM(1)*MOLSTM
445      H2(1)=STMGAS+VOLH2
446      CO(1)=((2.0-ALPHA))*STMGAS+VOLCO
447      CO2(1)=((ALPHA-1.0)/ALPHA)*STMGAS+VOLCO2
448      N2(1)=VOLN2
449      H2S(1)=VOLH2S
450 C   TOTAL MOLAR FLOWRATE OF SYNGAS :
451      MOLGAS(1)=H2(1)+CO(1)+CO2(1)+H2O(1)+N2(1)+H2S(1)
452 C   COMPUTE THE LOCAL OVERALL GAS COMPOSITION (INCL. H2O) IN ELEMENT 1,
453 C   MOL PERCENT :
454      WETH2(1)=H2(1)/MOLGAS(1)*100.0
455      WETCO(1)=CO(1)/MOLGAS(1)*100.0

```

(G.21)

```
456      WETCO2(1)=CO2(1)/MOLGAS(1)*100.0
457      WETH2O(1)=H2O(1)/MOLGAS(1)*100.0
458      WETN2(1)=N2(1)/MOLGAS(1)*100.0
459      WETH2S(1)=H2S(1)/MOLGAS(1)*100.0
460 C    COMPUTE THE SUPERFICIAL MASS FLOWRATE OF GAS FROM ZONE 1,KG/SQ.M.MIN
461      GASMM(1)=(WETH2(1)*H2MM+WETCO(1)*COMM+WETCO2(1)*CO2MM+WETH2O(1)*
462      $H2OMM+WETN2(1)*N2MM+WETH2S(1)*H2SMM)/100.0
463      GGANN(1)=MOLGAS(1)*GASMM(1)/(1000.0*AREEAN)
464 C    COMPUTE THE DRY PRODUCT GAS COMPOSITION IN ELEMENT 1 :
465      PRODS(1)=H2(1)+CO(1)+CO2(1)+N2(1)+H2S(1)
466      DRYH2(1)=H2(1)/PRODS(1)*100.0
467      DRYCO(1)=CO(1)/PRODS(1)*100.0
468      DRYCO2(1)=CO2(1)/PRODS(1)*100.0
469      DRYN2(1)=N2(1)/PRODS(1)*100.0
470      DRYH2S(1)=H2S(1)/PRODS(1)*100.0
471 C    COMPUTE THE HEAT CAPACITIES AT TM, J PER GMOL.K :
472      CPH2=CAPH2(TM)
473      CPCO=CAPCO(TM)
474      CPCO2=CAPCO2(TM)
475      CPH2O=CAPH2O(TM)
476      CPN2=CAPN2(TM)
477      CPH2S=CAPH2S(TM)
478      CPGANN(1)=(WETH2(1)*CAPH2(TM)+WETCO(1)*CAPCO(TM)
479      $+WETCO2(1)*CAPCO2(TM)+WETH2O(1)*CAPH2O(TM)+WETN2(1)*CAPN2(TM)
480      $+WETH2S(1)*CAPH2S(TM))/100.0
481      CPSOL=CAPSOL(TM)
482 C    CONVERT UNITS OF HEAT CAPACITIES TO J/KG.K :
483      CPGANN(1)=CPGANN(1)*1000.0/GASMM(1)
484      CPSOL=CPSOL*1000.0/SIO2MM
485 C
486 C    NOTE : THIS IS THE ENTRY POINT FOR ITERATIONS TO A SOLUTION !
487 C    -----
488 C    DEFINE A FUNCTION IN THE HEAT CAPACITY TERMS, TO BE EMPLOYED BY
489 C    THE ENERGY BALANCE ;
490 500  FCPG(1)=GSANN(1)*CPSOL-GGANN(1)*CPGANN(1)
491 C    DEFINITION OF THE ELEMENTS OF THE INITIAL MATERIAL BALANCE
492 C    FOR ZONE 1 :
493      K1(1)=A1*EXP(-E1/(RGAS*T(1)))
```

(G.22)

```
494 C LOCAL RATE OF GASIFICATION OF CARBON AND OF GAS PRODUCTION IN THE
495 C INITIAL ELEMENT, GMOLS PER MINUTE :
496     RC(1)=K1(1)*CCSV(1)*AREAAN*DZ
497 C ALPHA IS THE STOICHIOMETRIC PARAMETER IN THE GASIFICATION REACTN
498     RH2(1)=ALPHA*RC(1)
499     RCO(1)=(2.0-ALPHA)*RC(1)
500     RCO2(1)=(ALPHA-1.0)*RC(1)
501     RCGAS(ICOUNT)=RC(1)
502     ENLOS1(ICOUNT)=U*PI*DIAMAN*DZ*(T(R)-TAMB)
```

```

503 C
504 C
505 C *****
506 C * COMPUTATIONS FOR ZONE 1, THE PRIMARY STEAM-CHAR GASIFICATION ZONE *
507 C *****
508 C
509     IF( ICOUNT.GT.200)THEN
510         WRITE(6,270) ICOUNT
511 270     FORMAT(/,1X,'NO SOLUTION HAS BEEN REACHED AFTER ',I3,
512         $ ' ITERATIONS.')
```

```

513     STOP
514     END IF
515     IZONE=1
516     ENLOS1(ICOUNT)=ENLOS(T(R))
517     Z(1)=Z1
518     ZTEST=ZCOAL
519 701    IF(Z(R).LE.ZTEST)THEN
520         IF(CCSV(R).LE.0.0)THEN
521             CCSV(R)=0.0
522         END IF
523 C +-----+
524 C + SIMULTANEOUS SOLUTION OF THE MATERIAL AND ENERGY BALANCES OF ZONE1 +
525 C + BY THE RUNGE-KUTTA METHOD :                                         +
526 C +-----+
527     RK1=FT1(Z(R),T(R),CCSV(R),GGANN(R))*DZ
528     RL1=FCCSV1(Z(R),T(R),CCSV(R),GGANN(R))*DZ
529     RM1=FGGAN1(Z(R),T(R),CCSV(R),GGANN(R))*DZ
530 C
531     RK2=FT1(Z(R)+DZ/2.0,T(R)+RK1/2.0,CCSV(R)+RL1/2.0,
532     $ GGANN(R)+RM1/2.0)*DZ
533     RL2=FCCSV1(Z(R)+DZ/2.0,T(R)+RK1/2.0,CCSV(R)+RL1/2.0,
534     $ GGANN(R)+RM1/2.0)*DZ
535     RM2=FGGAN1(Z(R)+DZ/2.0,T(R)+RK1/2.0,CCSV(R)+RL1/2.0,
536     $ GGANN(R)+RM1/2.0)*DZ
537 C
538     RK3=FT1(Z(R)+DZ/2.0,T(R)+RK2/2.0,CCSV(R)+RL2/2.0,
539     $ GGANN(R)+RM2/2.0)*DZ
540     RL3=FCCSV1(Z(R)+DZ/2.0,T(R)+RK2/2.0,CCSV(R)+RL2/2.0,
```



```

541      $ GGANN(R)+RM2/2.0)*DZ
542      RM3=FGGAN1(Z(R)+DZ/2.0,T(R)+RK2/2.0,CCSV(R)+RL2/2.0,
543      $ GGANN(R)+RM2/2.0)*DZ
544 C
545      RK4=FT1(Z(R)+DZ,T(R)+RK3,CCSV(R)+RL3,GGANN(R)+RM3)*DZ
546      RL4=FCCSV1(Z(R)+DZ,T(R)+RK3,CCSV(R)+RL3,GGANN(R)+RM3)*DZ
547      RM4=FGGAN1(Z(R)+DZ,T(R)+RK3,CCSV(R)+RL3,GGANN(R)+RM3)*DZ
548 C
549      DT1(R)=1.0/6.0*(RK1+2.0*RK2+2.0*RK3+RK4)
550      DCCSV1(R)=1.0/6.0*(RL1+2.0*RL2+2.0*RL3+RL4)
551      DGGAN1(R)=1.0/6.0*(RM1+2.0*RM2+2.0*RM3+RM4)
552 C
553      T(R+1)=T(R)+DT1(R)
554      ENLOS1(ICOUNT)=ENLOS1(ICOUNT)+ENLOS(T(R))
555      CCSV(R+1)=CCSV(R)+DCCSV1(R)
556      GGANN(R+1)=GGANN(R)+DGGAN1(R)
557      Z(R+1)=Z(R)+DZ
558      R=R+1
559 C -----
560 C COMPUTE LOCAL MOLAR RATE OF GASIFICATION OF CARBON AND
561 C RATES OF GAS PRODUCTION :
562      K1(R)=A1*EXP(-E1/(RGAS*T(R)))
563      RC(R)=K1(R)*CCSV(R)*AREAAN*DZ
564      RH2(R)=ALPHA*RC(R)
565      RCO(R)=(2.0-ALPHA)*RC(R)
566      RCO2(R)=(ALPHA-1.0)*RC(R)
567      RCGAS(ICOUNT)=RCGAS(ICOUNT)+RC(R)
568 C COMPUTE LOCAL FRACTIONAL CONVERSION OF STEAM :
569      XSTM(R)=XSTM(R-1)-ALPHA*RC(R)/MOLSTM
570 C COMPUTE THE LOCAL OVERALL GAS COMPOSITIONS IN ZONE1 :
571 C MOLAR COMPONENT FLOWRATES ARE :
572      H2O(R)=H2O(R-1)+ALPHA*RC(R)
573      H2(R)=H2(R-1)-RH2(R)
574      CO(R)=CO(R-1)-RCO(R)
575      CO2(R)=CO2(R-1)-RCO2(R)
576      N2(R)=N2(R-1)
577      H2S(R)=H2S(R-1)
578 C TOTAL MOLAR FLOWRATE OF SYNGAS :

```

```

579      MOLGAS(R)=H2(R)+CO(R)+CO2(R)+H2O(R)+N2(R)+H2S(R)
580 C   COMPUTE THE LOCAL OVERALL GAS COMPOSITION (INCL. H2O), MOL PERCENT :
581      WETH2(R)=H2(R)/MOLGAS(R)*100.0
582      WETCO(R)=CO(R)/MOLGAS(R)*100.0
583      WETCO2(R)=CO2(R)/MOLGAS(R)*100.0
584      WETH2O(R)=H2O(R)/MOLGAS(R)*100.0
585      WETN2(R)=N2(R)/MOLGAS(R)*100.0
586      WETH2S(R)=H2S(R)/MOLGAS(R)*100.0
587 C   COMPUTE THE LOCAL PRODUCT GAS COMPOSITIONS, MOL PERCENT :
588      PRODS(R)=H2(R)+CO(R)+CO2(R)+N2(R)+H2S(R)
589      DRYH2(R)=H2(R)/PRODS(R)*100.0
590      DRYCO(R)=CO(R)/PRODS(R)*100.0
591      DRYCO2(R)=CO2(R)/PRODS(R)*100.0
592      DRYN2(R)=N2(R)/PRODS(R)*100.0
593      DRYH2S(R)=H2S(R)/PRODS(R)*100.0
594      GASMM(R)=(WETH2(R)*H2MM+WETCO(R)*COMM+WETCO2(R)*CO2MM+
595      $ WETH2O(R)*H2OMM+WETN2(R)*N2MM+WETH2S(R)*H2SMM)/100.0
596      CPGANN(R)=(WETH2(R)*CPH2+WETCO(R)*CPCO+WETCO2(R)*CPCO2
597      $ +WETH2O(R)*CPH2O+WETN2(R)*CPN2+WETH2S(R)*CPH2S)/100.0
598      CPGANN(R)=CPGANN(R)*1000.0/GASMM(R)
599 C   DEFINE A FUNCTION IN THE HEAT CAPACITY TERMS, TO BE EMPLOYED BY
600 C   THE ENERGY BALANCE :
601      FCPG(R)=GSANN(IZONE)*CPSOL-GGANN(R)*CPGANN(R)
602      GO TO 701
603      END IF
604      F2=R
605 C
606 C *****
607 C * COMPUTATIONS FOR ZONE 2, THE COAL CARBONISATION/PYROLYSIS ZONE *
608 C *****
609 C
610 C   SET FLAG FOR ZONE 2 :
611      IZONE=2
612      Z2=Z(R)-DZ
613      TCHAR(F2)=TCOAL
614      ENPYRO(ICOUNT)=0.0
615      ENLOS2(ICOUNT)=ENLOS(T(R))
616 C +-----+

```

```

617 C + SIMULTANEOUS SOLUTION OF THE MATERIAL AND ENERGY BALANCES OF ZONE2 +
618 C + BY THE RUNGE-KUTTA METHOD : +
619 C +-----+
620 ENLOS2(ICOUNT)=U*PI*DIAMAN*DZ*(T(R)-TAMB)
621 702 IF(ABS((T(R)-TCHAR(R))/T(R))*100.0.GT.1.00)THEN
622 IF(CCSV(R).LE.0.0)THEN
623 CCSV(R)=0.0
624 END IF
625 C
626 RK1=FT2(Z(R),T(R),CCSV(R),GGANN(R),TCHAR(R))*DZ
627 RL1=FCCSV2(Z(R),T(R),CCSV(R),GGANN(R),TCHAR(R))*DZ
628 RM1=FGGAN2(Z(R),T(R),CCSV(R),GGANN(R),TCHAR(R))*DZ
629 RN1=FTCHAR(Z(R),T(R),CCSV(R),GGANN(R),TCHAR(R))*DZ
630 C
631 RK2=FT2(Z(R)+DZ/2.0,T(R)+RK1/2.0,CCSV(R)+RL1/2.0,
632 $ GGANN(R)+RM1/2.0,TCHAR(R)+RN1/2.0)*DZ
633 RL2=FCCSV2(Z(R)+DZ/2.0,T(R)+RK1/2.0,CCSV(R)+RL1/2.0,
634 $ GGANN(R)+RM1/2.0,TCHAR(R)+RN1/2.0)*DZ
635 RM2=FGGAN2(Z(R)+DZ/2.0,T(R)+RK1/2.0,CCSV(R)+RL1/2.0,
636 $ GGANN(R)+RM1/2.0,TCHAR(R)+RN1/2.0)*DZ
637 RN2=FTCHAR(Z(R)+DZ/2.0,T(R)+RK1/2.0,CCSV(R)+RL1/2.0,
638 $ GGANN(R)+RM1/2.0,TCHAR(R)+RN1/2.0)*DZ
639 C
640 RK3=FT2(Z(R)+DZ/2.0,T(R)+RK2/2.0,CCSV(R)+RL2/2.0,
641 $ GGANN(R)+RM2/2.0,TCHAR(R)+RN2/2.0)*DZ
642 RL3=FCCSV2(Z(R)+DZ/2.0,T(R)+RK2/2.0,CCSV(R)+RL2/2.0,
643 $ GGANN(R)+RM2/2.0,TCHAR(R)+RN2/2.0)*DZ
644 RM3=FGGAN2(Z(R)+DZ/2.0,T(R)+RK2/2.0,CCSV(R)+RL2/2.0,
645 $ GGANN(R)+RM2/2.0,TCHAR(R)+RN2/2.0)*DZ
646 RN3=FTCHAR(Z(R)+DZ/2.0,T(R)+RK2/2.0,CCSV(R)+RL2/2.0,
647 $ GGANN(R)+RM2/2.0,TCHAR(R)+RN2/2.0)*DZ
648 C
649 RK4=FT2(Z(R)+DZ,T(R)+RK3,CCSV(R)+RL3,GGANN(R)+RM3,
650 $ TCHAR(R)+RN3)*DZ
651 RL4=FCCSV2(Z(R)+DZ,T(R)+RK3,CCSV(R)+RL3,GGANN(R)+RM3,
652 $ TCHAR(R)+RN3)*DZ
653 RM4=FGGAN2(Z(R)+DZ,T(R)+RK3,CCSV(R)+RL3,GGANN(R)+RM3,
654 $ TCHAR(R)+RN3)*DZ

```

(G.27)

```
655      RN4=FTCHAR(Z(R)+DZ,T(R)+RK3,CCSV(R)+RL3,GGANN(R)+RM3,
656 $ TCHAR(R)+RN3)*DZ
657 C
658      DT2(R)=1.0/6.0*(RK1+2.0*RK2+2.0*RK3+RK4)
659      DCCSV2(R)=1.0/6.0*(RL1+2.0*RL2+2.0*RL3+RL4)
660      DGGAN2(R)=1.0/6.0*(RM1+2.0*RM2+2.0*RM3+RM4)
661      DTCHAR(R)=1.0/6.0*(RN1+2.0*RN2+2.0*RN3+RN4)
662 C
663      T(R+1)=T(R)+DT2(R)
664      ENLOS2(ICOUNT)=ENLOS2(ICOUNT)+ENLOS(T(R))
665      CCSV(R+1)=CCSV(R)+DCCSV2(R)
666      GGANN(R+1)=GGANN(R)+DGGAN2(R)
667      TCHAR(R+1)=TCHAR(R)+DTCHAR(R)
668 C COMPUTE THE ENERGY REQUIRED TO PYROLISE THE COAL, J :
669      ENPYRO(ICOUNT)=ENPYRO(ICOUNT)+EPYROL(TCHAR(R),TCHAR(R+1))
670      Z(R+1)=Z(R)+DZ
671      R=R+1
672 C
673 C COMPUTE LOCAL MOLAR RATE OF GASIFICATION OF CARBON AND
674 C RATES OF GAS PRODUCTION :
675      K1(R)=A1*EXP(-E1/(RGAS*T(R)))
676      RC(R)=K1(R)*CCSV(R)*AREAAN*DZ
677      RH2(R)=ALPHA*RC(R)
678      RCO(R)=(2.0-ALPHA)*RC(R)
679      RCO2(R)=(ALPHA-1.0)*RC(R)
680      RCGAS(ICOUNT)=RCGAS(ICOUNT)+RC(R)
681      ENLOS2(ICOUNT)=ENLOS2(ICOUNT)+U*PI*DIAMAN*DZ*(T(R)-TAMB)
682 C COMPUTE LOCAL FRACTIONAL CONVERSION OF STEAM :
683      XSTM(R)=XSTM(R-1)-ALPHA*RC(R)/MOLSTM
684 C COMPUTE THE LOCAL OVERALL GAS COMPOSITIONS IN ZONE 2 :
685 C MOLAR COMPONENT FLOWRATES ARE :
686      H2O(R)=H2O(R-1)+ALPHA*RC(R)
687      H2(R)=H2(R-1)-RH2(R)
688      CO(R)=CO(R-1)-RCO(R)
689      CO2(R)=CO2(R-1)-RCO2(R)
690      N2(R)=N2(R-1)
691      H2S(R)=H2S(R-1)
692 C TOTAL MOLAR FLOWRATE OF SYNGAS :
```

```
693      MOLGAS(R)=H2(R)+CO(R)+CO2(R)+H2O(R)+N2(R)+H2S(R)
694 C  COMPUTE THE LOCAL OVERALL GAS COMPOSITION (INCL. H2O), MOL PERCENT :
695      WETH2(R)=H2(R)/MOLGAS(R)*100.0
696      WETCO(R)=CO(R)/MOLGAS(R)*100.0
697      WETCO2(R)=CO2(R)/MOLGAS(R)*100.0
698      WETH2O(R)=H2O(R)/MOLGAS(R)*100.0
699      WETN2(R)=N2(R)/MOLGAS(R)*100.0
700      WETH2S(R)=H2S(R)/MOLGAS(R)*100.0
701 C  COMPUTE THE LOCAL PRODUCT GAS COMPOSITIONS, MOL PERCENT :
702      PRODS(R)=H2(R)+CO(R)+CO2(R)+N2(R)+H2S(R)
703      DRYH2(R)=H2(R)/PRODS(R)*100.0
704      DRYCO(R)=CO(R)/PRODS(R)*100.0
705      DRYCO2(R)=CO2(R)/PRODS(R)*100.0
706      DRYN2(R)=N2(R)/PRODS(R)*100.0
707      DRYH2S(R)=H2S(R)/PRODS(R)*100.0
708      GASMM(R)=(WETH2(R)*H2MM+WETCO(R)*COMM+WETCO2(R)*CO2MM+
709  $ WETH2O(R)*H2OMM+WETN2(R)*N2MM+WETH2S(R)*H2SMM)/100.0
710      CPGANN(R)=(WETH2(R)*CPH2+WETCO(R)*CPCO+WETCO2(R)*CPCO2
711  $ +WETH2O(R)*CPH2O+WETN2(R)*CPN2+WETH2S(R)*CPH2S)/100.0
712      CPGANN(R)=CPGANN(R)*1000.0/GASMM(R)
713 C  DEFINE A FUNCTION IN THE HEAT CAPACITY TERMS, TO BE EMPLOYED BY
714 C  THE ENERGY BALANCE :
715      FCPG(R)=GSANN(IZONE)*CPSOL-GGANN(R)*CPGANN(R)
716      GO TO 702
717      END IF
718 C
719      IF(Z(R).LT.ZSPARG)THEN
720          F7=R
721      ELSE
722          GO TO 301
723      END IF
724 C
725 C*****
726 C* COMPUTATIONS FOR ZONE 7, THE SECONDARY STEAM-CHAR GASIFICATION ZONE *
727 C*****
728 C
729 C  SET FLAG FOR ZONE 7 :
730      IZONE=7
```

```

731 C INITIALISE THE ENERGY LOSS TERM IN ZONE 7 :
732     ENLOS7(ICOUNT)=ENLOS(T(R))
733 C
734 C ADJUST THE MOLAR GAS FLOWRATES BY THE RELEVANT FLOWRATES OF
735 C THE COMPONENTS RELEASED AS THE VOLATILE MATTER OF THE COAL :
736     H2O(R)=H2O(R)-VOLH2O
737     H2(R)=H2(R)--VOLH2
738     CO(R)=CO(R)-VOLCO
739     CO2(R)=CO2(R)-VOLCO2
740     N2(R)=N2(R)-VOLN2
741     H2S(R)=H2S(R)-VOLH2S
742 C TOTAL MOLAR FLOWRATE OF SYNGAS :
743     MOLGAS(R)=H2(R)+CO(R)+CO2(R)+H2O(R)+N2(R)+H2S(R)
744 C COMPUTE THE LOCAL OVERALL GAS COMPOSITION (INCL. H2O) IN
745 C ELEMENT F7, MOL PERCENT :
746     WETH2(R)=H2(R)/MOLGAS(R)*100.0
747     WETCO(R)=CO(R)/MOLGAS(R)*100.0
748     WETCO2(R)=CO2(R)/MOLGAS(R)*100.0
749     WETH2O(R)=H2O(R)/MOLGAS(R)*100.0
750     WETN2(R)=N2(R)/MOLGAS(R)*100.0
751     WETH2S(R)=H2S(R)/MOLGAS(R)*100.0
752 C COMPUTE THE SUPERFICIAL MASS FLOWRATE OF GAS AT THE TOP OF ZONE 7,
753 C KG/(SQ.M.MIN.) :
754     GASMM(R)=(WETH2(R)*H2MM+WETCO(R)*COMM+WETCO2(R)*CO2MM+WETH2O(R)
755     $*H2OMM+WETN2(R)*N2MM+WETH2S(R)*H2SMM)/100.0
756     GGANN(R)=MOLGAS(R)*GASMM(R)/(1000.0*AREAAN)
757 C COMPUTE THE HEAT CAPACITY OF THE GAS AT THE TOP OF ZONE 7, (J/KG.K) :
758     CPGANN(R)=(WETH2(R)*CPH2+WETCO(R)*CPCO+WETCO2(R)*CPCO2
759     $+WETH2O(R)*CPH2O+WETN2(R)*CPN2+WETH2S(R)*CPH2S)/100.0
760     CPGANN(R)=CPGANN(R)*1000.0/GASMM(R)
761 C DEFINE A FUNCTION IN THE HEAT CAPACITY TERMS, TO BE EMPLOYED BY
762 C THE ENERGY BALANCE :
763     FCPG(R)=GSANN(IZONE)*CPSOL-GGANN(R)*CPGANN(R)
764 C COMPUTE THE LOCAL DRY GAS COMPOSITIONS AT THE TOP OF ZONE 7 :
765     PRODS(R)=H2(R)+CO(R)+CO2(R)+N2(R)+H2S(R)
766     DRYH2(R)=H2(R)/PRODS(R)*100.0
767     DRYCO(R)=CO(R)/PRODS(R)*100.0
768     DRYCO2(R)=CO2(R)/PRODS(R)*100.0

```

```

769      DRYN2(R) = N2(R) / PRODS(R) * 100.0
770      DRYH2S(R) = H2S(R) / PRODS(R) * 100.0
771 C
772      Z7 = Z(R) - DZ
773      F7 = R
774 C INCREMENT CARBON CONCENTRATION IN ELEMENT F7 BY THE AMOUNT OF
775 C CARBON CONTAINED IN THE FRESH CHAR :
776      CCSV(F7) = CCSV(F7-1) + CCSV0
777 C +-----+
778 C + SIMULTANEOUS SOLUTION OF THE MATERIAL AND ENERGY BALANCES OF ZONE7 +
779 C + BY THE RUNGE-KUTTA METHOD : +
780 C +-----+
781      ENLOS7(ICOUNT) = U * PI * DIAMAN * DZ * (T(R) - TAMB)
782 703 IF(Z(R) .LE. ZSPARG) THEN
783      IF(CCSV(R) .LE. 0.0) THEN
784          CCSV(R) = 0.0
785      END IF
786 C
787      RK1 = FT1(Z(R), T(R), CCSV(R), GGANN(R)) * DZ
788      RL1 = FCCSV1(Z(R), T(R), CCSV(R), GGANN(R)) * DZ
789      RM1 = FGGAN1(Z(R), T(R), CCSV(R), GGANN(R)) * DZ
790 C
791      RK2 = FT1(Z(R) + DZ/2.0, T(R) + RK1/2.0, CCSV(R) + RL1/2.0,
792      $ GGANN(R) + RM1/2.0) * DZ
793      RL2 = FCCSV1(Z(R) + DZ/2.0, T(R) + RK1/2.0, CCSV(R) + RL1/2.0,
794      $ GGANN(R) + RM1/2.0) * DZ
795      RM2 = FGGAN1(Z(R) + DZ/2.0, T(R) + RK1/2.0, CCSV(R) + RL1/2.0,
796      $ GGANN(R) + RM1/2.0) * DZ
797 C
798      RK3 = FT1(Z(R) + DZ/2.0, T(R) + RK2/2.0, CCSV(R) + RL2/2.0,
799      $ GGANN(R) + RM2/2.0) * DZ
800      RL3 = FCCSV1(Z(R) + DZ/2.0, T(R) + RK2/2.0, CCSV(R) + RL2/2.0,
801      $ GGANN(R) + RM2/2.0) * DZ
802      RM3 = FGGAN1(Z(R) + DZ/2.0, T(R) + RK2/2.0, CCSV(R) + RL2/2.0,
803      $ GGANN(R) + RM2/2.0) * DZ
804 C
805      RK4 = FT1(Z(R) + DZ, T(R) + RK3, CCSV(R) + RL3, GGANN(R) + RM3) * DZ
806      RL4 = FCCSV1(Z(R) + DZ, T(R) + RK3, CCSV(R) + RL3, GGANN(R) + RM3) * DZ

```

(G,31)

```
807      RM4:=FGGANI(Z(R)+DZ,T(R)+RK3,CCSV(R)+RL3,GGANN(R)+RM3)*DZ
808 C
809      DT1(R)=1.0/6.0*(RK1+2.0*RK2+2.0*RK3+RK4)
810      DCCSV1(R)=1.0/6.0*(RL1+2.0*RL2+2.0*RL3+RL4)
811      DGGANI(R)=1.0/6.0*(RM1+2.0*RM2+2.0*RM3+RM4)
812 C
813      T(R+1)=T(R)+DT1(R)
814      ENLOS7(ICOUNT)=ENLOS7(ICOUNT)+ENLOS(T(R))
815      CCSV(R+1)=CCSV(R)+DCCSV1(R)
816      GGANN(R+1)=GGANN(R)+DGGANI(R)
817      Z(R+1)=Z(R)+DZ
818      R=R+1
819 C
820 C COMPUTE LOCAL MOLAR RATE OF GASIFICATION OF CARBON AND
821 C RATES OF GAS PRODUCTION :
822      K1(R)=A1*EXP(-E1/(RGAS*T(R)))
823      RC(R)=K1(R)*CCSV(R)*AREAAN*DZ
824      RH2(R)=ALPHA*RC(R)
825      RCO(R)=(2.0-ALPHA)*RC(R)
826      RCO2(R)=(ALPHA-1.0)*RC(R)
827      RCGAS(ICOUNT)=RCGAS(ICOUNT)+RC(R)
828      ENLOS7(ICOUNT)=ENLOS7(ICOUNT)+U*PI*DIAMAN*DZ*(T(R)-TAMB)
829 C COMPUTE LOCAL FRACTIONAL CONVERSION OF STEAM :
830      XSTM(R)=XSTM(R-1)-ALPHA*RC(R)/MOLSTM
831 C COMPUTE THE LOCAL OVERALL GAS COMPOSITIONS IN ZONE 7 :
832 C MOLAR COMPONENT FLOWRATES ARE :
833      H2O(R)=H2O(R-1)+ALPHA*RC(R)
834      H2(R)=H2(R-1)-RH2(R)
835      CO(R)=CO(R-1)-RCO(R)
836      CO2(R)=CO2(R-1)-RCO2(R)
837      N2(R)=N2(R-1)
838      H2S(R)=H2S(R-1)
839 C TOTAL MOLAR FLOWRATE OF SYNGAS :
840      MOLGAS(R)=H2(R)+CO(R)+CO2(R)+H2O(R)+N2(R)+H2S(R)
841 C COMPUTE THE LOCAL OVERALL GAS COMPOSITION (INCL. H2O), MOL PERCENT :
842      WETH2(R)=H2(R)/MOLGAS(R)*100.0
843      WETCO(R)=CO(R)/MOLGAS(R)*100.0
844      WETCO2(R)=CO2(R)/MOLGAS(R)*100.0
```



```

845      WETH2O(R)=H2O(R)/MOLGAS(R)*100.0
846      WETN2(R)=N2(R)/MOLGAS(R)*100.0
847      WETH2S(R)=H2S(R)/MOLGAS(R)*100.0
848 C    COMPUTE THE LOCAL PRODUCT GAS COMPOSITIONS, MOI. PERCENT :
849      PRODS(R)=H2(R)+CO(R)+CO2(R)+N2(R)+H2S(R)
850      DRYH2(R)=H2(R)/PRODS(R)*100.0
851      DRYCO(R)=CO(R)/PRODS(R)*100.0
852      DRYCO2(R)=CO2(R)/PRODS(R)*100.0
853      DRYN2(R)=N2(R)/PRODS(R)*100.0
854      DRYH2S(R)=H2S(R)/PRODS(R)*100.0
855      GASMM(R)=(WETH2(R)*H2MM+WETCO(R)*COMM+WETCO2(R)*CO2MM+
856 $    WETH2O(R)*H2OMM+WETN2(R)*N2MM+WETH2S(R)*H2SMM)/100.0
857      CPGANN(R)=(WETH2(R)*CPH2+WETCO(R)*CPCO+WETCO2(R)*CPCO2
858 $    +WETH2O(R)*CPH2O+WETN2(R)*CPN2+WETH2S(R)*CPH2S)/100.0
859      CPGANN(R)=CPGANN(R)*1000.0/GASMM(R)
860 C    DEFINE FCPG :
861      FCPG(R)=GSANN(IZONE)*CPSOL-GGANN(R)*CPGANN(R)
862      GO TO 703
863      END IF
864 C
865 C    *****
866 C    * COMPUTATIONS FOR ZONE 3, THE STEAM HEATING ZONE *
867 C    *****
868 C
869 301  F3=R
870      Z3=Z(R)
871      ITZ3=1
872 C    ESTIMATE THE TEMPERATURE OF ZONE 3 BY USING A SIMPLE ENERGY BALANCE :
873      TSTMAV=(T(R)+TSTMIN)/2.0
874      CPSTM3=CAPH2O(TSTMAV)
875      CPSOL3=CAPSOL(T(R))
876 C    CONVERT UNITS OF HEAT CAPACITIES TO J/KG.K :
877      CPSTM3=CPSTM3*1000.0/H2OMM
878      CPSOL3=CPSOL3*1000.0/SIO2MM
879      TZ3=(GSANN(3)*AREAAN*CPSOL3*T(R)+MSTEAM*CPSTM3*TSTMIN)/
880 $    (GSANN(3)*AREAAN*CPSOL3+MSTEAM*CPSTM3)
881 C
882 C    SOLUTION OF THE ENERGY BALANCE OF ZONE 3 :

```

```

883 C -----
884 706 ENBAL3=(HSOL3(T(R),TZ3)-ESTM3(TZ3))/ESTM3(TZ3)*100.0
885     IF(ABS(ENBAL3).GT.ENTOL)THEN
886         TZ3=TZ3+1.0*ENBAL3/100.0
887         ITZ3=ITZ3+1
888         GO TO 706
889     END IF
890     T(R)=TZ3
891 C *****
892 C * COMPUTATIONS FOR ZONE 4, THE NEUTRAL OR CROSSFLOW ZONE *
893 C *****
894     R=R+1
895     T(R)=T(R-1)
896     F4=R
897     Z(R)=Z(R-1)+DZ
898     Z4=Z(R)
899     GGANN(R)=0.0
900     CCSV(R)=CCSV(R-1)
901     FCPG(R)=GSANN(4)*CPSOL
902     ENLOS4(ICOUNT)=ENLOS(T(R))
903 C
904 C SOLUTION OF THE ENERGY BALANCE OF ZONE 4 BY THE RUNGE-KUTTA METHOD :
905 C -----
906 704 IF(Z(R).LT.RH)THEN
907     RK1=FT4(Z(R),T(R))*DZ
908     RK2=FT4(Z(R)+DZ/2.0,T(R)+RK1/2.0)*DZ
909     RK3=FT4(Z(R)+DZ/2.0,T(R)+RK2/2.0)*DZ
910     RK4=FT4(Z(R)+DZ,T(R)+RK3)*DZ
911 C
912     DT4(R)=1.0/6.0*(RK1+2.0*RK2+2.0*RK3+RK4)
913     T(R+1)=T(R)+DT4(R)
914     ENLOS4(ICOUNT)=ENLOS4(ICOUNT)+ENLOS(T(R))
915     Z(R+1)=Z(R)+DZ
916     CCSV(R+1)=CCSV(R)
917     FCPG(R+1)=FCPG(R)
918     R=R+1
919     GO TO 704
920 END IF

```

```

921 C
922 C *****
923 C * COMPUTATIONS FOR ZONE 5, THE AIR HEATING ZONE : *
924 C *****
925 C
926     F5=R
927     Z5=Z(R)
928     ZDT=0.0
929     ITZ5=1
930     GSDT=GSANN(2)*AREAA/AREADT
931     CCSV5=CCSV(R)
932 C ESTIMATE THE TEMPERATURE OF ZONE 5 BY USING A SIMPLE ENERGY BALANCE :
933     TAIRAV=(T(R)+TAIRIN)/2.0
934     CPAIR5=CAPAIR(TAIRAV)
935     CPSOL5=CAPSOL(T(R))
936 C CONVERT UNITS OF HEAT CAPACITIES TO J/KG.K :
937     CPAIR5=CPAIR5*1000.0/AIRMM
938     CPSOL5=CPSOL5*1000.0/SIO2MM
939     TZ5=(GSDT*AREADT*CPSOL5*T(R)+MAIR*CPAIR5*TAIRIN)/
940     $(GSDT*AREADT*CPSOL5+MAIR*CPAIR5)
941 C
942 C SOLUTION OF THE ENERGY BALANCE OF ZONE 5 :
943 C -----
944 551 ENBAL5=(HSOL5(T(R),TZ5)-EAIR5(TZ5))/EAIR5(TZ5)*100.0
945     IF(ABS(ENBAL5).GT.ENTOL)THEN
946         WRITE(6,552)ITZ5,TZ5,ENBAL5
947         TZ5=TZ5+1.0*ENBAL5/100.0
948         ITZ5=ITZ5+1
949 552 FORMAT(/,1X,'ITZ5 = ',I3,2X,'TZ5 = ',F8.4,'ENBAL5 = ',F7.3)
950     GO TO 551
951     END IF
952     T(R)=TZ5
953     R=R+1
954     F6=R
955     Z(R)=Z(F5)-DZ
956 C
957 C -----
958 C + SOLUTION OF THE MATERIAL AND ENERGY BALANCES FOR ZONE 6 +

```

```

959 C + OF THE REACTOR (THE CHAR COMBUSTION ZONE). +
960 C -----
961     IF(ICOUNT.EQ.1) THEN
962 C INITIALISE CONDITIONS OF ZONE 6 :
963     Z6=Z(R)
964     ITZ6=1
965     USDT=USANN(2)*AREAAN/AREADT
966     MOLO2=0.21*MAIR*1000.0/AIRMM
967 C INTRODUCE THE TERM 'FBETA' AS A FUNCTION OF BETA :
968     FBETA=(BETA+(1.0-BETA)/2.0)
969 C COMPUTE THE MOLAR PERCENTAGE COMPOSITION OF THE WASTE GAS :
970     CMPN2=0.79/(0.21*(1.0/FBETA+0.79/0.21))*100.0
971     CMPCO=(1-BETA)/(FBETA*(1/FBETA+0.79/0.21))*100.0
972     CMPCO2=BETA/(FBETA*(1/FBETA+0.79/0.21))*100.0
973 C COMPUTE THE MOLAR FLOWRATE OF WASTEGAS, GMOL/MIN. :
974     MOLWST=(BETA/FBETA+(1.0-BETA)/FBETA+0.79/0.21)*MOLO2
975     END IF
976 C ESTIMATE THE TEMPERATURE OF ZONE 6, USING A SIMPLE ENERGY BALANCE :
977 C -----
978 C COMPUTE THE QUANTITY OF ENERGY GENERATED BY THE COMBUSTION OF CHAR :
979     ENCOMB=(BETA/FBETA*(-DH2)+(1.0-BETA)/FBETA*(-DH3))*MOLO2
980 C CONVERT UNITS OF HEAT CAPACITIES TO J/KG.K :
981     CPAIR6=CPAIR(TZ5)*1000.0/AIRMM
982     CPSOL6=CAPSOL(TZ5)*1000.0/SIO2MM
983     TZ6=(ENCOMB+(GSDT*AREADT*CPSOL6+MAIR*CPAIR6)*TZ5)/
984     $(GSDT*AREADT*CPSOL6+MAIR*CPAIR6)
985     MOLC5=CCSV5*USDT*AREADT
986     IF(MOLC5.LE.1.0/FBETA*MOLO2) THEN
987         WRITE(6,350)
988 350     FORMAT(/,1X,'A CARBON-LEAN CONDITION EXISTS IN THE'
989     $ ' DRAFT TUBE. THE PROGRAM HAS THEREFORE BEEN INTERRUPTED.')
```

```

990     WRITE(6,352)T(F5)--TABS0,CCSV(F5)
991 352     FORMAT(/,1X,'T(F5) = ',F12.2,' C',3X,'CCSV(F5)=' ,F12.4)
992     STOP
993     END IF
994 C CARBON MATERIAL BALANCE :
995     CCSV6=CCSV5-(1.0/FBETA)*MOLO2/(USDT*AREADT)
996 C
```

```

997 C SOLVE THE ENERGY BALANCE OF ZONE 6 :
998 C -----
999 709 EWST=ECOW(TZ6)+ECO2W(TZ6)+EN2W(TZ6)
1000     ENBAL6=(ENCOMB+EAIR6I(TZ5)-HSOL6(TZ5,TZ6)-EWST)/
1001     $(ENCOMB+EAIR6I(TZ5))*100.0
1002     IF(ABS(ENBAL6).GT.ENTOL)THEN
1003         TZ6=TZ6+1.0*ENBAL6/25.0
1004         ITZ6=ITZ6+1
1005         GO TO 709
1006     END IF
1007 C
1008 C UPDATE TM AND ALL RELATED PROPERTIES :
1009     TM=(T(1)+TZ5)/2.0
1010 C COMPUTE THE HEATS OF REACTION AT TM, J/GMOL :
1011     DH1=DHR1(TM)
1012     DH2=DHR2(TM)
1013     DH3=DHR3(TM)
1014 C HEAT CAPACITIES AT TM, J PER GMOL.K :
1015     CPGANN(1)=(WETH2(1)*CAPH2(TM)+WETCO(1)*CAPCO(TM)
1016     $+WETCO2(1)*CAPCO2(TM)+WETH2O(1)*CAPH2O(TM)+WETN2(1)*CAPN2(TM)
1017     $+WETH2S(1)*CAPH2S(TM))/100.0
1018     CPSOL=CAPSOL(TM)
1019 C CONVERT UNITS OF HEAT CAPACITIES TO J/KG.K :
1020     CPGANN(1)=CPGANN(1)*1000.0/GASMM(1)
1021     CPSOL=CPSOL*1000.0/SIO2MM
1022 C
1023 C +-----+
1024 C + CONDUCT AN ENERGY AUDIT OF THE SYSTEM : +
1025 C +-----+
1026 C
1027 C COMPUTE THE QUANTITY OF ENERGY DEMANDED BY THE GASIFICATION OF CHAR :
1028     ENGAS=RCGAS(ICOUNT)*DH1
1029 C COMPUTE THE QUANTITY OF ENERGY LOST TO THE SURROUNDINGS, J/MIN :
1030     ENLOSS=ENLOS1(ICOUNT)+ENLOS2(ICOUNT)+ENLOS7(ICOUNT)
1031     $+ENLOS4(ICOUNT)
1032 C ENTHALPY OF SYNGAS PRODUCTS :
1033     ESYN=EH2P(T(1))+ECOP(T(1))+ECO2P(T(1))+EH2OP(T(1))+
1034     $EN2P(T(1))+EH2SP(T(1))

```

```

1035 C  ENTHALPY OF WASTE GASES :
1036      EWST=ECOW(TZ6)+ECO2W(TZ6)+EN2W(TZ6)
1037 C  SUMMARIZE ENTHALPY TERMS, J/MIN :
1038      EPRODS=ESYN+EWST
1039      EREACT=ESTEAM(TSTMIN)+EAIR(TAIRIN)
1040      ENIN=ENCOMB+EREACT
1041      ENOUT=ENGAS+EPRODS+ENPYRO(ICOUNT)+ENASH(TZ6)+ENLOSS
1042      ENBAL=(ENIN-ENOUT)/ENIN*100.0
1043 C  REPORT THE CARBON MATERIAL BALANCE IN THE REACTOR :
1044      CGAS=RCGAS(ICOUNT)
1045      CBAL=(CFED-CGAS-CCOMB)/CFED*100.0
1046      WRITE(*,400)ICOUNT,T(1)-TABS0,TZ6-TABS0,CBAL,ENBAL
1047 400  FORMAT(/,1X,'IT.#',I3,' : ',1X,'T(1)= ',F7.2,2X,'TZ6= ',F7.2,' C,'
1048      $,2X,'M. BAL.= ',F7.4,2X,'E. BAL.= ',F7.4,' %')
1049 C
1050 C  INCREMENT ITERATION COUNTER :
1051      ICOUNT=ICOUNT+1
1052      R=1
1053 C
1054 C  ITERATE TO A SOLUTION USING THE INTERVAL HALVING TECHNIQUE :
1055 C  -----
1056 C
1057      IF(ABS(ENBAL).GT.PCTOL)THEN
1058          IF(TZ6.GT.TMAX)THEN
1059              TMAXC=TMAX-TABS0
1060              WRITE(*,360)TMAXC
1061 360    FORMAT(/,1X,'THE TEMPERATURE AT THE TOP OF THE'
1062      $    ' REACTOR HAS EXCEEDED ',F10.4,' C. RE-ITERATE WITH A HIGHER'
1063      $    ' COAL FEED RATE.')

```

(G.38)

```
073      T(1)=T(1)+ENBAL*TADJ
074      GO TO 500
075      END IF
076      WRITE(*,380)
077 380  FORMAT(/,1X,'ENERGY BALANCE HAS BEEN ACHIEVED - '
078      '$'NOW DRIVING THE MATERIAL BALANCE.')
```

```
079      IF(ABS(CBAL).GT.PCTOL)THEN
080          CCSV(1)=CCSV(1)+CBAL*CADJ
081          GO TO 500
082      END IF
083 C
084 C  COMPUTE THE FRACTIONAL CONVERSIONS OF CHAR, ON SOLUTION :
085      DO 390 I=1,F5-1
086          XCSV(I)=(CCSV(F7)-CCSV(I))/CCSV(F7)
087 390  CONTINUE
088          XCSV5=(CCSV(F7)-CCSV5)/CCSV(F7)
089          XCSV6=(CCSV(F7)-CCSV6)/CCSV(F7)
090 C  COMPUTE THE VOLUMETRIC FLOWRATE OF SYNGAS, CUBIC M PER MINUTE :
091      VOLGAS=MOLGAS(1)*RGAS*T(1)/PRESS
092 C  COMPUTE THE VOLUMETRIC FLOWRATE OF WASTEGAS, CU.M/MIN :
093      VOLWST=MOLWST*RGAS*TZ6/PRESS
094 C
095      WRITE(6,801)
096 801  FORMAT(1X,'CONVERGENCE ACHIEVED !')
```

```
097 C
098 C  +-----+
099 C  + OUTPUT OF RESULTS : +
100 C  +-----+
101 C
102      ESTEAM=ESTEAM(TSTMIN)
103      EAIR=EAIR(TAIRIN)
104      HSOL6=HSOL6(TZ5,TZ6)
105      HSOLA=(SOL1*(T(1)-TZ5)+SOL2/2.0*(T(1)**2-TZ5**2))*CALTOJ
106      $*1000.0/SIO2MM*GSANN(2)*AREAAN
107 C  CONVERT TEMPS TO DEGREES C :
108      DO 1010 I=1,F5-1
109          T(I)=T(I)-TABS0
110 1010  CONTINUE
```

```

1111      DO 1012 I=F2,F3-1
1112          TCHAR(I)=TCHAR(I)-TABS0
1113 1012  CONTINUE
1114      TZ5=TZ5-TABS0
1115      TZ6=TZ6-TABS0
1116      WRITE(6,1148)
1117      WRITE(6,1149)
1118      WRITE(6,1151)CFED
1119      WRITE(6,1152)CGAS
1120      WRITE(6,1154)CCOMB
1121      WRITE(6,1155)CCOMB/CFED*100.0
1122      CONCCL=MCOAL*100.0/(MCOAL+GSANN(1)*AREAAN)
1123      WRITE(6,1156)CONCCL
1124      WRITE(6,1815)MASH
1125      WRITE(6,1810)GSDT*AREADT
1126      WRITE(6,1170)VOLGAS
1127      UANN=VOLGAS/(AREAAN*60.0*UMFS)
1128      WRITE(6,1175)UANN
1129      WRITE(6,1180)VOLWST
1130      UDT=VOLWST/(AREADT*60.0*UMFA)
1131      WRITE(6,1185)UDT
1132      WRITE(6,1200)MOIGAS(1)
1133      WRITE(6,1210)
1134      WRITE(6,1220)
1135      WRITE(6,1230)
1136      WRITE(6,1240)WETH2(1),WETCO(1),WETCO2(1),WETH2O(1),WETN2(1),
1137  $WETH2S(1)
1138      WRITE(6,1250)
1139      WRITE(6,1190)XSTM(1)
1140      WRITE(6,1260)PRODS(1)
1141      WRITE(6,1270)
1142      WRITE(6,1280)
1143      WRITE(6,1290)
1144      WRITE(6,1300)DRYH2(1),DRYCO(1),DRYCO2(1),DRYN2(1),DRYH2S(1)
1145      WRITE(6,1310)
1146      WRITE(6,1312)
1147      WRITE(6,1314)
1148      WRITE(6,1316)VOLH2,VOLCO,VOLH2O,VOLN2,VOLH2S

```



```

1149      WRITE(6,1205)MOLWST
1150      WRITE(6,1215)
1151      WRITE(6,1220)
1152      WRITE(6,1235)
1153      WRITE(6,1245)CMPCO,CMPCO2,COMP2
1154      WRITE(6,1250)
1155      WRITE(6,1625)ENCOMB
1156      ENINT:=(ENCOMB*60.0)/(LENDT*AREADT)
1157      WRITE(6,1627)ENINT
1158      WRITE(6,1655)ENBAL
1159      WRITE(6,1659)
1160      CVSYN=(WETH2(1)*285800.0+WETCO(1)*283000.0)*MOLGAS(1)/100.0
1161      CVWST=CMPCO*MOLWST*283000.0/100.0
1162      ECOLD=CVSYN/(MCOAL*CV)*100.0
1163      ECOLDO=(CVSYN+CVWST)/(MCOAL*CV)*100.0
1164      WRITE(6,1660)MCOAL*CV
1165      WRITE(6,1665)CVSYN
1166      WRITE(6,1670)CVWST
1167      WRITE(6,1675)ECOLD
1168      WRITE(6,1680)ECOLDO
1169      WRITE(6,1320)
1170      WRITE(6,1325)
1171      WRITE(6,1328)
1172      WRITE(6,1330)
1173      WRITE(6,1350)
1174      WRITE(6,1360)
1175      WRITE(6,1370)
1176      WRITE(6,1380)
1177      WRITE(6,1390)
1178      WRITE(6,1400)
1179      DO 1425 I=1,F2-1,2
1 1180          WRITE(6,1410)Z(I),T(I),XCSV(I),CCSV(I),XSTM(I)
1 1181 1425  CONTINUE
1182      WRITE(6,1373)
1183      WRITE(6,1374)
1184      DO 1426 I=1,F2-1,2
1 1185          WRITE(6,1409)Z(I),WETH2(I),WETCO(I),WETCO2(I),WETH2O(I),
1 1186          $ WETN2(I),WETH2S(I)

```

```
1 1187 1426 CONTINUE
1188 WRITE(6,1331)
1189 WRITE(6,1350)
1190 WRITE(6,1360)
1191 WRITE(6,1370)
1192 WRITE(6,1380)
1193 WRITE(6,1390)
1194 WRITE(6,1400)
1195 DO 1430 I=F2,F7-1,2
1 1196 WRITE(6,1410)Z(I),T(I),XCSV(I),CCSV(I),XSTM(I)
1 1197 1430 CONTINUE
1198 WRITE(6,1373)
1199 WRITE(6,1374)
1200 DO 1427 I=F2,F7-1,2
1 1201 WRITE(6,1409)Z(I),WETH2(I),WETCO(I),WETCO2(I),WETH2O(I),
1 1202 $ WETN2(I),WETH2S(I)
1 1203 1427 CONTINUE
1204 WRITE(6,1337)
1205 WRITE(6,1341)
1206 WRITE(6,1365)
1207 WRITE(6,1371)
1208 WRITE(6,1401)
1209 DO 1435 I=F2,F7-1,2
1 1210 WRITE(6,1411)Z(I),T(I),TCHAR(I)
1 1211 1435 CONTINUE
1212 WRITE(6,1332)
1213 WRITE(6,1350)
1214 WRITE(6,1360)
1215 WRITE(6,1370)
1216 WRITE(6,1380)
1217 WRITE(6,1390)
1218 WRITE(6,1400)
1219 DO 1440 I=F7,F3-1,2
1 1220 WRITE(6,1410)Z(I),T(I),XCSV(I),CCSV(I),XSTM(I)
1 1221 1440 CONTINUE
1222 WRITE(6,1373)
1223 WRITE(6,1374)
1224 DO 1428 I=F7,F3-1,2
```

```

1 1225      WRITE(6,1409)Z(I),WETH2(I),WETCO(I),WETCO2(I),WETH2O(I),
1 1226      $ WETN2(I),WETH2S(I)
1 1227 1428  CONTINUE
1228      WRITE(6,1333)
1229      WRITE(6,1351)T(F3)
1230      WRITE(6,1334)
1231      WRITE(6,1352)
1232      WRITE(6,1362)
1233      WRITE(6,1372)
1234      WRITE(6,1402)
1235      DO 1470 I=F4,F5-1,2
1 1236      WRITE(6,1412)Z(I),T(I)
1 1237 1470  CONTINUE
1238      WRITE(6,1335)
1239      WRITE(6,1353)TZ5
1240      WRITE(6,1336)
1241      WRITE(6,1354)TZ6
1242      WRITE(6,1364)XCSV6
1243      WRITE(6,1328)
1244 1148  FORMAT(/,1X,'CARBON MATERIAL BALANCE :')
1245 1149  FORMAT(1X,'-----')
1246 1151  FORMAT(/,1X,'AMOUNT OF CARBON FED = ',F10.4,' GMOLS/MIN.')
```

```

1247 1152  FORMAT(/,1X,'AMOUNT OF CARBON GASIFIED = ',F10.4,' GMOLS/MIN.')
```

```

1248 1154  FORMAT(/,1X,'AMOUNT OF CARBON COMBUSTED = ',F10.4,' GMOLS/MIN.')
```

```

1249 1155  FORMAT(/,1X,'% OF CARBON FED WHICH COMBUSTS = ',F8.2)
1250 1156  FORMAT(/,1X,'THE CONC. OF COAL AT THE FEEDER POSITION '
```

```

1251      $'RELATIVE TO THE TOTAL SOLIDS CONTENT IS ',
1252      $F7.4,' MASS %')
```

```

1253 1170  FORMAT(/,1X,'VOLUMETRIC FLOWRATE OF SYNGAS, INCL. STEAM, =
1254      $',F8.4,1X,'CU. M./MIN.')
```

```

1255 1175  FORMAT(/,1X,'THE SYNGAS VELOCITY IS ',F6.3,' X UMF OF STEAM'
```

```

1256      $' AT 850 C AND THE CURRENT PRESSURE OF OPERATION.')
```

```

1257 1180  FORMAT(/,1X,'VOLUMETRIC FLOWRATE OF WASTE GAS = ',F8.4,1X,
1258      $'CUBIC M./MIN.')
```

```

1259 1185  FORMAT(/,1X,'THE WASTEGAS VELOCITY IS ',F6.3,' X UMF OF AIR '
```

```

1260      $' AT 850 C AND THE CURRENT PRESSURE OF OPERATION.')
```

```

1261 1190  FORMAT(/,/,1X,'FRACTIONAL CONVERSION OF STEAM = ',F6.4,/)
1262 1200  FORMAT(/,1X,'MOLAR FLOWRATE OF ENTIRE SYNGAS STREAM'
```

```

1263      $' = ',F8.4,1X,'GMOLS/MIN. ')
1264 1205  FORMAT(/,1X,'THE MOLAR FLOWRATE OF THE WASTEGAS STREAM'
1265      $' = ',F8.4,1X,'GMOLS/MIN. ')
1266 1210  FORMAT(/,1X,'MOLAR COMPOSITION OF ENTIRE SYNGAS STREAM :')
1267 1215  FORMAT(/,1X,'MOLAR COMPOSITION OF WASTEGAS STREAM :')
1268 1220  FORMAT(/,26X,'COMPONENT :')
1269 1230  FORMAT(/,20X,'H2',5X,'CO',6X,'CO2',5X,'H2O',6X,'N2',5X,'H2S')
1270 1235  FORMAT(/,20X,'CO',6X,'CO2',5X,'N2')
1271 1240  FORMAT(/,1X,'COMPOSITION/',5X,6(F5.2,3X))
1272 1245  FORMAT(/,1X,'COMPOSITION/',5X,3(F5.2,3X))
1273 1250  FORMAT(1X,'MOL PERCENT')
1274 1260  FORMAT(/,1X,'MOLAR FLOWRATE OF DRY SYNGAS STREAM = ',F8.4,
1275      $1X,'GMOLS/MIN. ')
1276 1270  FORMAT(/,1X,'MOLAR COMPOSITION OF DRY SYNGAS STREAM :')
1277 1280  FORMAT(/,26X,'COMPONENT :')
1278 1290  FORMAT(/,20X,'H2',5X,'CO',6X,'CO2',6X,'N2',5X,'H2S')
1279 1300  FORMAT(/,1X,'COMPOSITION/',5X,5(F5.2,3X))
1280 1310  FORMAT(1X,'MOL PERCENT')
1281 1312  FORMAT(/,5X,'GAS PRESENT IN SYNGAS STREAM WHICH ORIGINATES FROM '
1282      $'VOL. MATTER OF THE COAL :')
1283 1314  FORMAT(/,1X,'FLOWRATE/',10X,'H2',10X,'CO',10X,'H2O',10X,'N2',10X,
1284      $'H2S')
1285 1316  FORMAT(/,1X,'GMOLS/MIN. :',4X,5(F8.3,3X))
1286 1320  FORMAT(/,/,,1X,'DETAILED RESULTS :')
1287 1325  FORMAT(1X,'*****')
1288 1328  FORMAT(/,1X,'(*) NOTE : THE FRACTIONAL FIXED CARBON CONVERSION '
1289      $'OF CHAR IS DEFINED RELATIVE TO THE CARBON CONCENTRATION AT '
1290      $'THE FEEDER POSITION. ')
1291 1330  FORMAT(/,/,,1X,'ZONE NUMBER 1, THE PRINCIPAL CHAR-STEAM'
1292      $' GASIFICATION REACTION ZONE :')
1293 1331  FORMAT(/,/,,1X,'ZONE NUMBER 2, THE COAL PYROLYSIS ZONE :')
1294 1332  FORMAT(/,/,,1X,'ZONE NUMBER 7, THE SECONDARY CHAR-STEAM'
1295      $' GASIFICATION REACTION ZONE :')
1296 1333  FORMAT(/,/,,1X,'ZONE NUMBER 3, THE STEAM HEATING ZONE :')
1297 1334  FORMAT(/,/,,1X,'ZONE NUMBER 4, THE NEUTRAL ZONE :')
1298 1335  FORMAT(/,/,,1X,'ZONE NUMBER 5, THE AIR HEATING ZONE :')
1299 1336  FORMAT(/,/,,1X,'ZONE NUMBER 6, THE CHAR COMBUSTION ZONE :')
1300 1337  FORMAT(/,/,,1X,'TEMPERATURE PROFILE OF CHAR IN ZONE 2 :')

```

```

1301 1341  FORMAT(/,1X,'AXIAL POSITION',5X,'LOCAL')
1302 1350  FORMAT(/,1X,'AXIAL POSITION',5X,'LOCAL',10X,'FRACTIONAL',8X,
1303      '$GLOBAL',10X,'FRACTIONAL')
1304 1351  FORMAT(/,1X,'THE TEMPERATURE OF THE STEAM HEATING ZONE IS ',
1305      '$F10.2,' C')
1306 1352  FORMAT(/,1X,'AXIAL POSITION',5X,'LOCAL')
1307 1353  FORMAT(/,1X,'THE UNIFORM TEMPERATURE OF THE AIR HEATING ZONE '
1308      '$(MFR) IS ',F10.2,' C')
1309 1354  FORMAT(/,1X,'THE UNIFORM TEMPERATURE OF THE CHAR COMBUSTION ZONE'
1310      '$(MFR) IS ',F10.2,' C')
1311 1360  FORMAT(1X,'BELOW TOP OF',7X,'REACTOR',8X,'FIXED CARBON',6X,
1312      '$CARBON',10X,'CONVERSION')
1313 1361  FORMAT(1X,'BELOW TOP OF',7X,'REACTOR',8X,'STEAM')
1314 1362  FORMAT(1X,'BELOW TOP OF',7X,'REACTOR')
1315 1363  FORMAT(1X,'BELOW TOP OF',7X,'AIR')
1316 1364  FORMAT(/,1X,'THE FRACTIONAL CONVERSION OF CHAR IN ZONE 6 (*) IS ',
1317      '$F6.4)
1318 1365  FORMAT(1X,'BELOW TOP OF',7X,'REACTOR',8X,'CHAR')
1319 1370  FORMAT(1X,'DRAFT TUBE',9X,'TEMPERATURE,',3X,'CONVERSION',8X,
1320      '$CONCENTRATION',3X,'OF STEAM')
1321 1373  FORMAT(/,/,1X,'AXIAL POSITION BELOW',15X,'MOLAR PERCENTAGE'
1322      '$ COMPOSITION OF GAS')
1323 1371  FORMAT(1X,'DRAFT TUBE',9X,'TEMPERATURE,',3X,'TEMPERATURE')
1324 1372  FORMAT(1X,'DRAFT TUBE',9X,'TEMPERATURE,')
1325 1380  FORMAT(35X,'OF CHAR(*)')
1326 1390  FORMAT(53X,'GMOL PER')
1327 1374  FORMAT(1X,'TOP OF DRAFT TUBE (M)',15X,'H2',5X,'CO',5X,'CO2',
1328      '$5X,'H2O',5X,'N2',5X,'H2S')
1329 1400  FORMAT(/,5X,'M',14X,'DEG. C',27X,'CUBIC M. ')
1330 1401  FORMAT(/,5X,'M',14X,'DEG. C',9X,'DEG. C')
1331 1402  FORMAT(/,5X,'M',14X,'DEG. C')
1332 1410  FORMAT(/,3X,F6.4,10X,F9.4,7X,F6.4,11X,E9.4,8X,F6.4)
1333 1409  FORMAT(/,3X,F6.4,25X,6(F5.2,3X))
1334 1411  FORMAT(/,3X,F6.4,10X,F9.4,6X,F9.4)
1335 1412  FORMAT(/,3X,F6.4,10X,F9.4)
1336 1415  FORMAT(1X,F6.4,1X,F9.4)
1337 1416  FORMAT(/)
1338 1420  FORMAT(1X,E9.4)

```

```
1339 1422  FORMAT(1X,6(F5.2,1X))
1340 1424  FORMAT(1X,5(F5.2,1X))
1341 1625  FORMAT(/,1X,'(1) THE TOTAL ENERGY INPUT BY THE COMBUSTION OF '
1342      $'CHAR IS (+) ',E12.6,' J/MIN')
1343 1627  FORMAT(/,1X,'      (THIS INPUT CORRESPONDS TO AN ENERGY INTENSITY'
1344      $' OF ',E12.6,' J/(M^3.HR) IN THE COMBUSTION ZONE).')
1345 1655  FORMAT(/,1X,'THE PERCENTAGE DIFFERENCE BETWEEN THE ENERGY INPUT'
1346      $' AND ENERGY OUTPUT TERMS IS ',F8.4,' %')
1347 1659  FORMAT(/,/,1X,'PROCESS EFFICIENCY :')
1348 1660  FORMAT(/,/,1X,'THE POTENTIAL CHEMICAL ENERGY INPUT TO THE '
1349      $'GASIFIER (NCV OF THE COAL) IS 'E12.6,' J/MIN')
1350 1665  FORMAT(/,1X,'THE GROSS CALORIFIC VALUE OF THE COLD SYNGAS IS '
1351      $,E12.6,' J/MIN ')
1352 1670  FORMAT(/,1X,'THE GROSS CALORIFIC VALUE OF THE COLD WASTEGAS IS '
1353      $,E12.6,' J/MIN ')
1354 1675  FORMAT(/,/,1X,'THE CONVENTIONALL COLD GAS EFFICIENCY OF THE '
1355      $'GASIFIER IS 'F8.4,' % IE.(GCV COLD SYNGAS *100/NCV COAL FED '
1356      $'TO THE GASIFIER)')
1357 1680  FORMAT(/,/,1X,'THE OVERALL COLD GAS EFFICIENCY OF THE '
1358      $'GASIFIER IS 'F8.4,' % IE.(GCV COLD SYN+WASTE GASES*100/NCV COAL'
1359      $' FED TO THE GASIFIER)')
1360 1810  FORMAT(/,1X,'CIRCULATION RATE OF SOLIDS = ',F8.4,' KG/MIN')
1361 1815  FORMAT(/,1X,'TOTAL MASS FLOWRATE OF ASH LEAVING THE REACTOR '
1362      $'(ENTRAINED IN WASTEGAS STREAM) = ',F8.4,' KG/MIN')
1363      CLOSE(UNIT=6)
1364      STOP
1365      END
```

(H.1)

APPENDIX H.

DETAILS OF THE INPUT DATA OF THE GASIFIER SIMULATION ALGORITHM.

H.1 ASSIGNMENTS TO VARIABLES IN THE 'DATA' STATEMENT.

A1 = 183 707.0 gmol carbon gasified/(gmol carbon initially
present.minute)

AIRMM = 28.8503 g/gmol

AIR1 = 6.713

AIR2 = 0.04697 E - 02

AIR3 = 0.1147 E - 05

AIR 4 = -0.4696 E - 09

ALPHA = 1.35

CALTOJ = 4.1868 J/Cal

CCHAR = 0.7183

CMM = 12.01115 g/gmol

COMM = 28.0106 g/gmol

CO2MM = 44.0100 g/gmol

CM1 = 6.726

CM2 = 0.4001 E - 02

CM3 = 0.1283 E = 05

CM4 = -0.5307 E - 09

CO21 = 5.316

CO22 = 1.4285 E - 02

CO23 = -0.8362 E - 05

CO24 = 1.784 E - 09

CV = 31.0 E + 06 J/kg

DELH1 = 172 500.0 J/gmol

DELH2 = -393 700.0 J/gmol

DELH3 = -110.600 J/gmol

DENSCL = 1300.0 kg/m³

DENSOL = 2600.0 kg/m³

DPCOAL = 2.0 E - 03 m

DPSAND = 675.0 E - 06 m

E1 = 145 760.0 J/gmol

EMISS = 0.85

H21 = 6.952

(H.2)

H22 = -0.04576 E - 02
H23 = 0.09563 E - 05
H24 = -0.2079 E - 09
H2MM = 2.0158 g/gmol
H2OMM = 18.0152 g.gmol
H2SMM = 34.0798
H2O1 = 7.70
H2O2 = 0.04594 E - 02
H2O3 = 0.2521 E - 05
H2O4 = -0.8587 E - 09
H2S1 = 7.07
H2S2 = 0.3128 E - 02
H2S3 = 0.1364 E - 05
H2S4 = -0.7869 E - 09
N21 = 6.903
N22 = -0.03753 E - 02
N23 = 0.1930 E - 05
N24 = -0.6861 E - 09
N2MM = 28.0134
O21 = 6.085
O22 = 0.3631 E - 02
O23 = -0.1709 E - 05
O24 = 0.3133 E - 09
O2MM = 31.9988
RGAS = 8.314 J/(gmol.K)
SOL1 = 10.95
SOL2 = 5.50 E -03
SIO2MM = 60.0848
TABS0 = 273.15
TAMB = 25.0
TAPPCH = 0.99
TCRIT = 2.0
TMAX = 1200.0
TMIN = 550.0
TREF = 25.0
VMCOAL = 0.219
VMH2 = 0.6315
VMCO = 0.3481

(H.3)

VMH20 = 0.0

VMH2S = 0.0037

VMN2 = 0.0168

VOID = 0.52

Z0 = 0.0

(I.4)

APPENDIX I.

GEOMETRIC RELATIONSHIPS OF THE GASIFIER.

The cross sectional areas of the annulus and draft tube regions respectively are as follows :

$$A_a = \frac{\pi}{4} (D^2 - d^2)$$

$$A_d = \frac{\pi}{4} d^2$$

where D = the nominal outer diameter of the annulus; m
 d = the nominal diameter of the draft tube; m

In this model the height of the reactor has been characterised by the dimension from the top of the draft tube to the base of the annulus zone. In reality the interface of the base of the reactor and the air plenum is formed by a truncated conical volume with a 45° hypotenuse, as is shown in Figure 1. In this model, however, the geometry at the base of the reactor has been assumed to be cylindrical with an equivalent volume to that of the truncated cone geometry. One is therefore able to calculate the equivalent height of the reactor as follows :

$$V_1 + V_2 = \frac{1}{3} \pi \frac{D^2}{4} \frac{D}{2} = \frac{1}{3} \pi \frac{D^3}{8} \quad [I.1]$$

$$V_1 = \frac{1}{3} \pi \frac{D^3}{8} \quad [I.2]$$

$$\Rightarrow V_2 = \frac{1}{3} \pi ((d/2)^3 - (d/2)^3) \quad [I.3]$$

now equating V_2 to the volume of a cylinder,

$$V_2 = \pi \frac{D^2}{4} \cdot h_{cyl} \quad [I.4]$$

$$\Rightarrow h_{cyl} = \frac{4}{\pi} \cdot \frac{1}{D^2} V_2 \quad [I.5]$$

On substituting equation [I.3] into equation [I.5], one obtains :

(I.5)

$$h_{\text{cyl}} = \frac{4}{3} \frac{1}{D^2} ((D/2)^3 - (D/2)^3) \quad [\text{I.6}]$$

The equivalent height of the reactor is therefore given by :

$$R_h = L_d + h_{\text{cyl}} \quad [\text{I.7}]$$

where L_d = the length of the draft tube; m